SANTOS BAROSSA DPD STUDIES

Sediment Dispersion Modelling

Document status

Version	Purpose of document	Authored by	Reviewed by	Approved by	Review date
Rev A	Issued for internal review	Nuala Page	David Wright	David Wright	24/06/2022
Rev 0	Issued for client review	Nuala Page	David Wright	David Wright	30/06/2022
Rev 1	Issued to address comments from peer reviewer	Nuala Page	Hemerson Tonin Ceri Morgan	David Wright	21/10/2022
Rev 2	Issued to client	Nuala Page	Ceri Morgan Peter Ivicevich Xander van Beusekom Andrew Lindsay Lachlan MacArthur	David Wright	23/02/2023

Approval for issue

David Wright   *David Wright*   23 February 2023

Prepared by:

RPS

Nuala Page
Senior Coastal Engineer

Level 2, 27-31 Troode Street
West Perth WA 6005

T   +61 8 9211 1111
E   nuala.page@rpsgroup.com

Prepared for:

Santos Limited

Lachlan MacArthur
Approvals Adviser Barossa Project

First Floor, 53 Ord Street
West Perth WA 6005

T   +61 417 250 717
E   lachlan.macarthur@santos.com

Contents

Tables

Figures

1 INTRODUCTION

1.1 Background

Santos is exploring options for the Darwin pipeline duplication (DPD) project associated with development of the Barossa gas field in northern Australia. The proposed pipeline would run from the offshore point where the Barossa gas export pipeline (GEP) reaches the existing Bayu-Undan pipeline to the Darwin LNG (DLNG) plant at Wickham Point in Darwin Harbour. Sections making up approximately 16 km of the proposed pipeline within the harbour will require trenching using dredge vessels, with the remaining sections – including the section offshore from the harbour –, laid on the seabed. Trenched material is proposed to be disposed of at an offshore disposal site adjacent to the existing INPEX spoil ground (Figure 1.1). Pipeline burial where required is proposed using quarry rock material that contains minimal fines; as such, this activity is not expected to represent a significant source of suspended sediment. Suspended sediment generated during the trenching and disposal activities has a potential to cause environmental impacts which must be identified, quantified, mitigated and managed to acceptable levels.

RPS was commissioned by Santos to undertake sediment dispersion modelling of the trenching and disposal operations associated with the Barossa DPD project in support of environmental approvals documentation and the development of the trenching and spoil disposal monitoring and management plan (TSDMMP) for the project. The sediment dispersion modelling has quantified the potential magnitude, intensity and spatial distribution of suspended sediment concentrations (SSC) and sedimentation that would be expected for the trenching and disposal operations proposed for the project. The predicted outcomes are to be used to inform the assessment of the potential for influence or impact upon water quality and benthic habitats in the region.

This technical report contains a summary of the sediment fate model inputs, methodologies and assumptions, and the model outcomes following analysis of specified threshold criteria. This report has been improved through updates made in response to a third-party expert review by the Australian Institute of Marine Science (AIMS) (AIMS, 2022; Appendix A). The review comments and subsequent changes made in response to these comments are summarised in Appendix B.

Subsequent to the sediment and spoil disposal modelling presented in this report, and in response to feedback from the Northern Territory (NT) Department of Environment Parks and Water Security (DEPWS) and an expert peer review report from AIMS (Appendix A), an additional spoil ground stability assessment study was conducted and has been presented in a separate addendum to this report (*Santos Barossa DPD Studies: Sediment Dispersion Modelling Addendum 1 - Spoil Stability Assessment*).
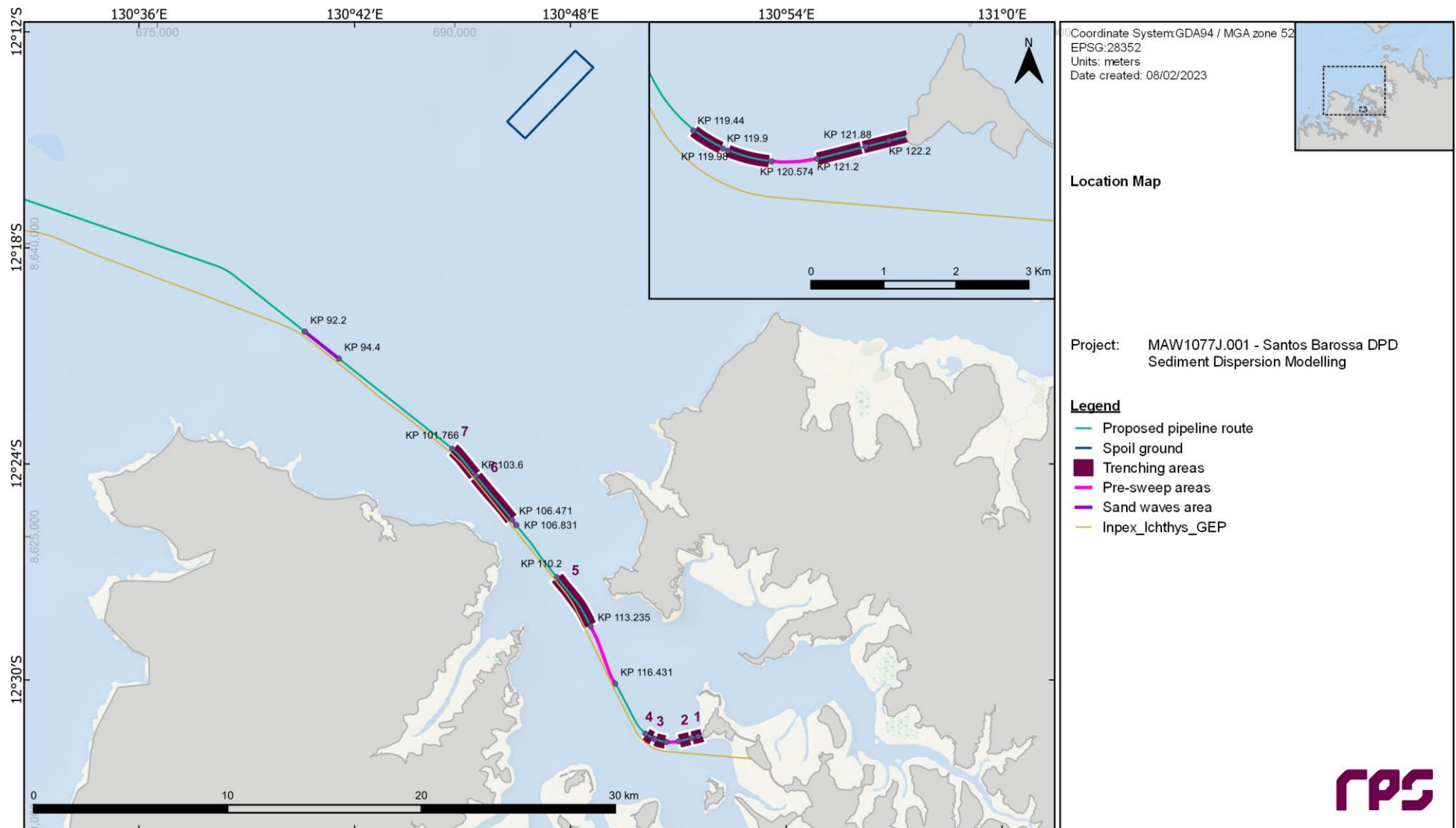
Figure 1.1 **Route of the nearshore section (KP78 to KP122.5) of the proposed DPD project pipeline in Darwin Harbour, showing trenching, pre-sweep and sand wave sections and the location of the proposed offshore spoil ground that will be utilised during disposal activities. Note the trenching area widths shown on this and other Figures in this report are exaggerated to aid visual clarity.**

1.2 Modelling Scope

RPS was commissioned to conduct sediment dispersion modelling for the following activities:

- The fate of the suspended material generated during trenching along the pipeline route.
- The fate of the material that is relocated to the nominated spoil grounds.

The scope of work required to complete the sediment dispersion modelling included:

1. Hydrodynamic and Wave Modelling.

   a. An initial assessment of the existing D-FLOW hydrodynamic and D-WAVE wave model frameworks in Darwin Harbour determined that refinements were necessary to suit the requirements of this scope of work. Reconfiguration of the models was conducted, to increase resolution within the harbour and update the model with the latest bathymetric data. This was followed by re-validation of the model predictions against available measurements of water levels, currents and waves.

   b. Two years (2019-2020) of hydrodynamic and wave simulation data was produced for use as input to the sediment dispersion model.

2. Sediment Dispersion Modelling.

   a. Inputs for the trenching program were prepared for the DREDGEMAP model, accounting for all potential concurrent sources of sediment characterised by location, intensity, particle size distribution, vertical distribution in the water column, and levels of cohesivity.

   b. Two trenching and disposal scenarios were simulated: (i) trenching commencing in winter/dry season; and (ii) trenching commencing in summer/wet season. The two scenarios simulated the ongoing sequence of all sediment-disturbing operations, along with simulation of a suitable post-trenching period to account for the fate of loosely consolidated material disturbed by the trenching and sediment placement.

   c. Simulation outputs from each separate trenching and disposal activity were post-processed, combined and analysed to determine outcomes including zones of impact and influence for each scenario based on specified threshold criteria.

   d. Key model outcomes were provided as spatial datasets in GIS shapefile format.

3. Reporting. This technical report detailing the sediment fate model inputs, methodologies, assumptions and model outcomes following analysis of specified threshold criteria was provided.

1.3 Definition of Relevant Terms and Abbreviations

BHD:

Backhoe Dredge. A pontoon equipped with a hydraulic excavator. The pontoon is stabilised and secured by three spuds. The excavator uses a large arm fitted with a bucket to excavate material from the seabed and discharge it into (typically) a split hopper barge moored alongside. BHDs are mainly used for dredging or breaking up the sedimentary rock below a layer of unconsolidated sediments, or for dredging in areas inaccessible to larger self-propelled vessels.

CSD:

Cutter Suction Dredge. A stationary (or self-propelled) vessel that is secured by a spud. The vessel is equipped with a rotating cutterhead, controlled via means of winches and anchors, that is used to cut and fragment material on the seabed. The vessel has a powerful pump system that sucks up a mixture of sediment and water and discharges it into a split hopper barge moored alongside or to a disposal zone via a pipeline. CSDs are mainly used for dredging hard soils and sedimentary rock.

Dewatering:

Draining of excess water from a split hopper barge using its drainage system.

Overflow:

Excess water and suspended solids that leave a trailing suction hopper dredge and are discharged to the water column via a weir and discharge pipe located at the base of the vessel.

Resuspension:

Removal of deposited material from the seabed to the water column as a result of natural or artificial agitation.

Sedimentation rate:

Rate of sediment accumulation on the seabed following deposition of SSC from the water column.

SHB:

Split Hopper Barge: Vessel with a large open hold used to load and transport dredged material. The unloading is performed by splitting the two halves of the hull to release the material towards the seabed.

SSC:

Suspended Solids Concentration (or Suspended Sediment Concentration). The concentration of sediment material in the water column following natural or artificial resuspension from the seabed.

TSHD:

Trailing Suction Hopper Dredge. A self-propelled vessel with one or two suction tubes/arms, equipped with dragheads that are lowered to the seabed and trailed over the bottom. The vessel has a powerful pump system that sucks up a mixture of sediment and water and discharges it in the hopper (hold) of the vessel. TSHDs are mainly used for dredging loose and soft soils such as sand, gravel, silt or clay.

2 REGIONAL METOCEAN CONDITIONS

The trenching and disposal operations for the DPD project will be conducted within Darwin Harbour and the area just offshore of the Harbour entrance, with the spoil ground located approximately 20 km to the north-east of the Harbour in Beagle Gulf (Figure 1.1). Knowledge of the metocean conditions in this region is necessary for prediction of the dispersion and sedimentation of any suspended sediment generated by the trenching and disposal operations associated with the project. Details of the regional climate and metocean conditions in the project area were outlined in the DPD Project NT EPA Referral (CDM Smith, 2022), and the following sections summarise the metocean conditions relevant to the trenching and disposal operation locations.

2.1 Climate

The project area is characterised by a tropical monsoonal climate with a distinct dry season (May to September) and wet season (October to March), separated by a relatively short transition period. The dry season is dominated by dry, cool weather with little rain, low humidity and wide-ranging temperatures. The onset and duration of the wet season varies between years; however, most rainfall in the Northern Territory is associated with monsoonal troughs and/or from isolated convective storms (BoM, 2021). High precipitation rates are commonly experienced during storm events in the wet season.

Tropical cyclones occur in the project area on average about once per year, typically occurring between November to April. The strongest winds and heaviest rainfall are associated with the passage of tropical cyclones.

2.2 Wind Climate

Synoptic winds during the dry season tend to be dominated by the south-east trade winds, while light west to north-westerlies predominate during the wet season. Sea breezes from the north-west occur on most afternoons throughout the year.

Mean afternoon wind speeds tend to be stronger than morning wind speeds all year round. Morning wind speed is typically stronger during the dry season, whereas the afternoon wind speed increases during the late dry, build-up and wet season periods which is most likely associated with the formation of mid-to-late afternoon storm cells during this time of the year. Strong wind gusts can be experienced at any time throughout the year.

2.3 Hydrodynamics: Currents and Water Levels

While oceanic currents in the region offshore of Beagle Gulf are influenced by the Indonesian Throughflow and South Equatorial Current, the Beagle Gulf is dominated by strong internal circulation and experiences only minor oceanic interaction. In the dry season there is a general south-westerly drift while wet season circulation is dominated by a north-easterly drift, generated by north-west monsoonal winds. The drift currents are often less than 0.5 knots (0.26 m/s; Smit *et al.*, 2000). Tidal ranges in this region are 6 m to 8 m (ConocoPhillips, 2019).

INPEX (2010) deployed a bottom mounted Acoustic Doppler Current Profiler (ADCP) in the vicinity of the proposed offshore spoil ground in Beagle Gulf. Measurements showed currents flowed over a tidal axis oriented approximately east-west at speeds up to 1 m/s. The data showed marginally larger variations at the surface indicating increased influence of wind forcing on the currents.

Darwin Harbour experiences regular and rapid exchange of water with Beagle Gulf as large tidal movements, and to a lesser extent winds, drive the exchange of large volumes of water between inner Darwin Harbour and the Beagle Gulf each day. The macro-tidal regime of the harbour is the dominant influence on currents which are strongly correlated with the rise and fall of the tide. Currents in the harbour can peak at speeds of up to 2-2.5 m/s (Williams *et al.*, 2006).

The macro-tidal regime of Darwin Harbour has a maximum range of 8.1 m (Harper, 2010) with predominantly semidiurnal tides (two highs and two lows per day), with a slight diurnal inequality. The mean neap tidal range is 1.9 m and mean spring tidal range is 5.5 m (NT Government, 2011).

2.4   Waves

The wave climate in Beagle Gulf exhibits a strong seasonality associated with the tropical north-west monsoon that occurs between November and March. The monsoon's north westerly winds blow over the uninterrupted fetch of the Timor Sea, increasing incident wave energy in Beagle Gulf and at the entrance to Darwin Harbour. During the months of April to October, south-easterly trade winds blow across a limited fetch and generate a low energy local wave climate, with wave heights generally below 1.0 m for 90% of the time, and peak wave energy periods of about 3-5 seconds (Nicholas *et al.*, 2019).

Darwin Harbour is well sheltered from long period tsunami and ocean swell waves by the Tiwi Islands and the harbour's orientation, shallow bathymetry and coastline configuration. The energy of long period waves entering the harbour quickly dissipates and wave heights decrease significantly. Waves within the harbour are generally of short (3-5 seconds) mean periods with heights well below 1.0 m under non-cyclone conditions (INPEX, 2010).

Tropical cyclones can cause extreme wave conditions with significant wave height of 4.5 m and mean wave period of 7.5 seconds at the harbour entrance, which reduces in height down to 0.7 m inside the harbour (Makarynska, 2019a, 2019b). Wave height measurements from Australia's Integrated Marine Observing System (IMOS) national reference station at the entrance to Darwin Harbour recorded significant wave heights exceeding 3.5 m during the passage of tropical lows in 2012 with peak periods of wave energy also increasing to between about 6-8 seconds (Nicholas *et al.*, 2019).

3   MODEL SKILL MEASURES

The predictive capabilities of the hydrodynamic and wave models under development were validated through quantitative and visual comparisons of measured and modelled data.

3.1   Statistical Analysis

To provide a quantitative measure of model performance, analyses of the Index of Agreement (IOA; Willmott, 1981) and the Mean Absolute Error (MAE; Willmott, 1982; Willmott & Matsuura, 2005) were conducted. Although other traditional error estimates – such as the correlation coefficient and the root mean square error (RMSE) – are problematic and prone to ambiguities and bias (Willmott, 1982; Willmott & Matsuura, 2005), they are presented in some instances to provide better context for the IOA and MAE estimates.

The IOA is determined using the following formula:

$$\text{IOA} = 1 - \frac{\sum |X_{\text{model}} - X_{\text{obs}}|^2}{\sum \left(|X_{\text{model}} - \overline{X_{\text{obs}}}| + |X_{\text{obs}} - \overline{X_{\text{obs}}}| \right)^2}$$

In this equation, X represents the variable being compared and $\overline{X}$ represents the mean of that variable over time.

A perfect agreement can be said to exist between field observations and model predictions if the IOA gives a measure of unity (1), while complete disagreement will produce an IOA measure of zero (Willmott, 1981). Although there are no definitive guidelines for what IOA values might represent a good agreement, Willmott *et al.* (1985) suggests that values meaningfully larger than 0.5 represent good model performance.

The MAE is simply the average of the absolute differences between observed and modelled values. As a more natural measure of average error (Willmott & Matsuura, 2005) it is more readily understood than the IOA. In common with the RMSE, a lower MAE implies better model performance.

An important point to note regarding both the IOA and MAE, and in fact most measures of model performance, is that slight phase differences between two data sets can result in a seemingly poor statistical comparison – particularly in rapidly-changing data such as tidal direction or water elevation where the tidal range is large. It is therefore always important to consider both the statistics and a visual representation of the comparison (Willmott *et al.*, 1985).

Another potential source of misleading statistical comparisons is that directional fluctuations across the 0/360° compass point can bias the skill measures of current direction. Therefore, this study has based the quantitative assessment of model skill on the separate U (east-west) and V (north-south) components of the wind or current vectors rather than on the derived products of magnitude and direction.

3.2   Time Series Analysis

In addition to bulk statistical measures, model performance for the validation periods was assessed visually with the aid of time series plots of wind speed and direction for the wind field input, water level, current speed and current direction data for the hydrodynamic model, and time series plots of wave height, wave period and wave direction for the wave model. This approach is particularly valuable for the hydrodynamic model because statistical measures of model skill can heavily penalise errors in phase (i.e. time lags) even when the dynamics of flow are broadly reproduced.

4 HYDRODYNAMIC AND WAVE MODELLING

Modelling of the potential sediment dispersion from the trenching and disposal activities associated with the Barossa DPD project required temporal and spatial representation of the hydrodynamic and wave conditions within the project area. A hydrodynamic and wave model framework of the Beagle Gulf area centred and refined in Darwin Harbour was constructed, calibrated and validated for a past marine modelling study of dredging and spoil disposal for INPEX (RPS, 2009). This model framework has been redeveloped for the Barossa DPD project scope of work and is described in the following sections.

The hydrodynamic and wave modelling for the project was conducted using the Delft3D suite of software. The Delft3D suite is a fully integrated computer software package composed of several modules (e.g. flow, waves, sediment, water quality, and ecology) grouped around a common interface. This software suite has been developed to carry out studies with a multi-disciplinary approach and multi-dimensional calculations (e.g. 2-D and 3-D) for a range of systems, such as oceanic, coastal, estuarine and river environments. It can simulate the interaction of flows, waves, sediment transport, morphological developments, water quality and aquatic ecology. Specific modules of the Delft3D suite are referenced in this report, following the convention of the software developers, with the suffix D- (e.g. D-FLOW for the Delft3D Hydrodynamics module and D-WAVE for the Delft3D Spectral Wave module).

The Delft3D suite has been developed by Deltares, an independent institute for applied research on water with over 30 years of experience in modelling aquatic systems (http://www.deltares.nl/en). The Delft3D suite of models adheres to the International Association for Hydro-Environment Engineering and Research guidelines for documenting the validity of computational modelling software, closely replicating an array of analytical, laboratory, schematic and real-world data.

The configuration of the hydrodynamic and wave models is in line with recommendations of best practice for sediment dispersion modelling as outlined by WAMSI Dredging Science Node guidance (Sun *et al.*, 2016). Inclusion of mesoscale ocean currents is recommended, as these currents have a significant influence on the net drift of suspended material over the time scales of trenching operations (days to weeks) and are therefore important to predictions of sediment transport. The use of three-dimensional current modelling with a series of interconnected grids of progressively finer resolution is also recommended, as are coupling of the hydrodynamic and wave models and validation of current predictions against measured data.

4.1 Hydrodynamic Model (D-FLOW)

4.1.1 Model Description

To simulate the hydrodynamics within Darwin Harbour, Beagle Gulf and the surrounding area, a three-dimensional model with accurate representations of the bathymetry, bottom roughness and spatially-varying wind stress was utilised for the region. The model framework was developed through the combination of a large-scale regional model with smaller refined regions, or sub-domains.

The D-FLOW model is ideally suited to represent the hydrodynamics of complex coastal waters, including regions where the tidal range creates large intertidal zones. RPS has applied the model for numerous studies in the region.

D-FLOW is a multi-dimensional (2-D or 3-D) hydrodynamic (and transport) simulation program which calculates non-steady flow and transport phenomena that result from tidal, meteorological and baroclinic forcing on a rectilinear or a curvilinear, boundary-fitted grid. In three-dimensional simulations, the vertical grid can be defined following the sigma-coordinate approach, where the local water depth is divided into a series of layers with thickness at a set proportion of the depth.

D-FLOW allows for the establishment of a series of interconnected (two-way, dynamically-nested) curvilinear grids of varying resolution; a technique referred to as "domain decomposition". This allows for the generation of a series of grids with progressively increasing spatial resolution, down to an appropriate scale for accurate resolution of the hydrodynamics associated with features such as dredged channels. The main advantage of domain decomposition over traditional one-way, or static, nesting systems is that the model domains interact seamlessly, allowing transport and feedback between the regions of different scales. The ability to dynamically couple multiple model domains offers a flexible framework for hydrodynamic model development. This modelling method was applied in this study.

Inputs to the model, as discussed in the following sections, included:

- Bathymetry of the study area, including shipping channels, islands, and adjacent features. The wetting and drying of the intertidal zones was simulated in applicable areas.

- Boundary elevation forcing data.

- Spatially-varying surface wind and pressure data.

4.1.2 Bathymetry and Domain Definition

The hydrodynamic model was established over the domain shown in Figure 4.1. Accurate bathymetry is a significant factor in development of a model framework required to resolve highly variable current conditions. The bathymetry was developed using Geoscience Australia lidar data, as well as project specific multibeam bathymetry data within Darwin Harbour provided by Santos, supplemented with GEBCO (General Bathymetric Chart of the Oceans) data (GEBCO, 2021) and the C-MAP electronic chart database in the broader area where relevant and required.

The composite bathymetric data was interpolated onto the D-FLOW Cartesian grid. The resultant bathymetry is shown in Figure 4.2. The extent and shape of the model coastline will change as water levels rise and fall with tidal movements due to the inclusion of wetting and drying within the model system.

The vertical grid of the model comprised five layers of varying thickness, depending on location, throughout the domain. Five layers were found to be enough to resolve the circulation and provide suitable bed-level currents without overly compromising model performance. As the model was set up as a proportional sigma-grid in the vertical dimension, these layers therefore represented a terrain-following arrangement with a layer thickness of 20% of the total local water depth.

To offset the computational effort required for a large, multi-layered model domain, and to achieve adequate horizontal and temporal resolution, a multiple-grid (domain-decomposition) strategy was applied using five sub-domains of varying horizontal grid cell size (Figure 4.1 and Figure 4.2). Horizontal resolutions within each sub-domain were 80 m for the Darwin Harbour area (sub-grid 4), 240 m for the region from Gunn Point to Dundee Beach (sub-grid 3), 720 m for the Beagle Gulf and Clarence Strait region (sub-grid 2), 2.2 km for the Van Diemen Gulf and Tiwi Island region (sub-grid 1), and 6.5 km for the outer domain (sub-grid 0).

Each sub-domain is an individual hydrodynamic model simulated in parallel with the others, with dynamic coupling at the shared boundaries between sub-domains. The outermost sub-domains captured large-scale oceanographic phenomena which progressively fed into the finer-resolution domains representing the area of interest. The resolution of the innermost sub-domain was specified after assessment of the requirement to adequately resolve the variation in current fields, and in turn the sediment dynamics.
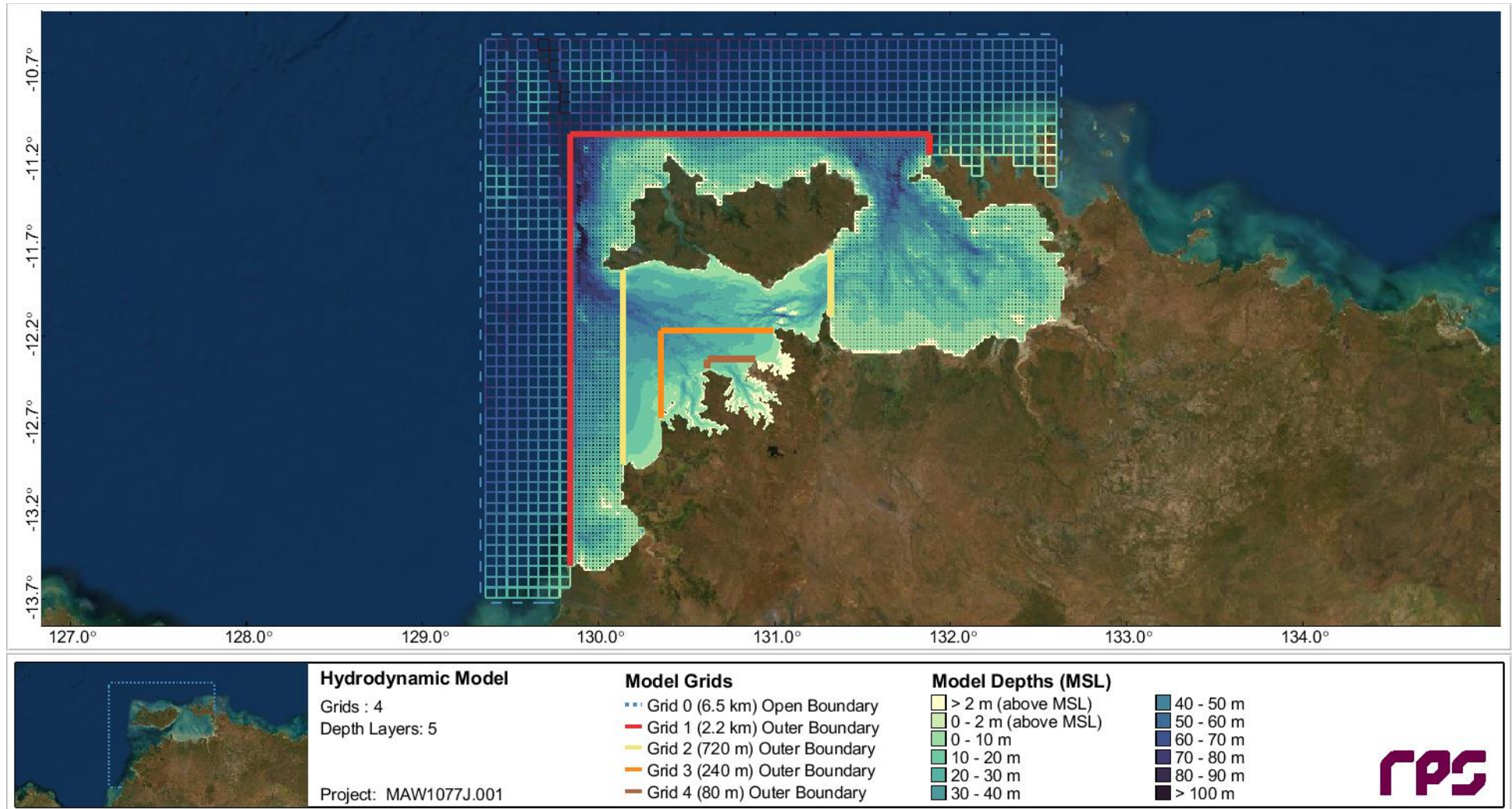
Figure 4.1   Hydrodynamic grid setup showing the domain decomposition scheme applied and the model bathymetry.
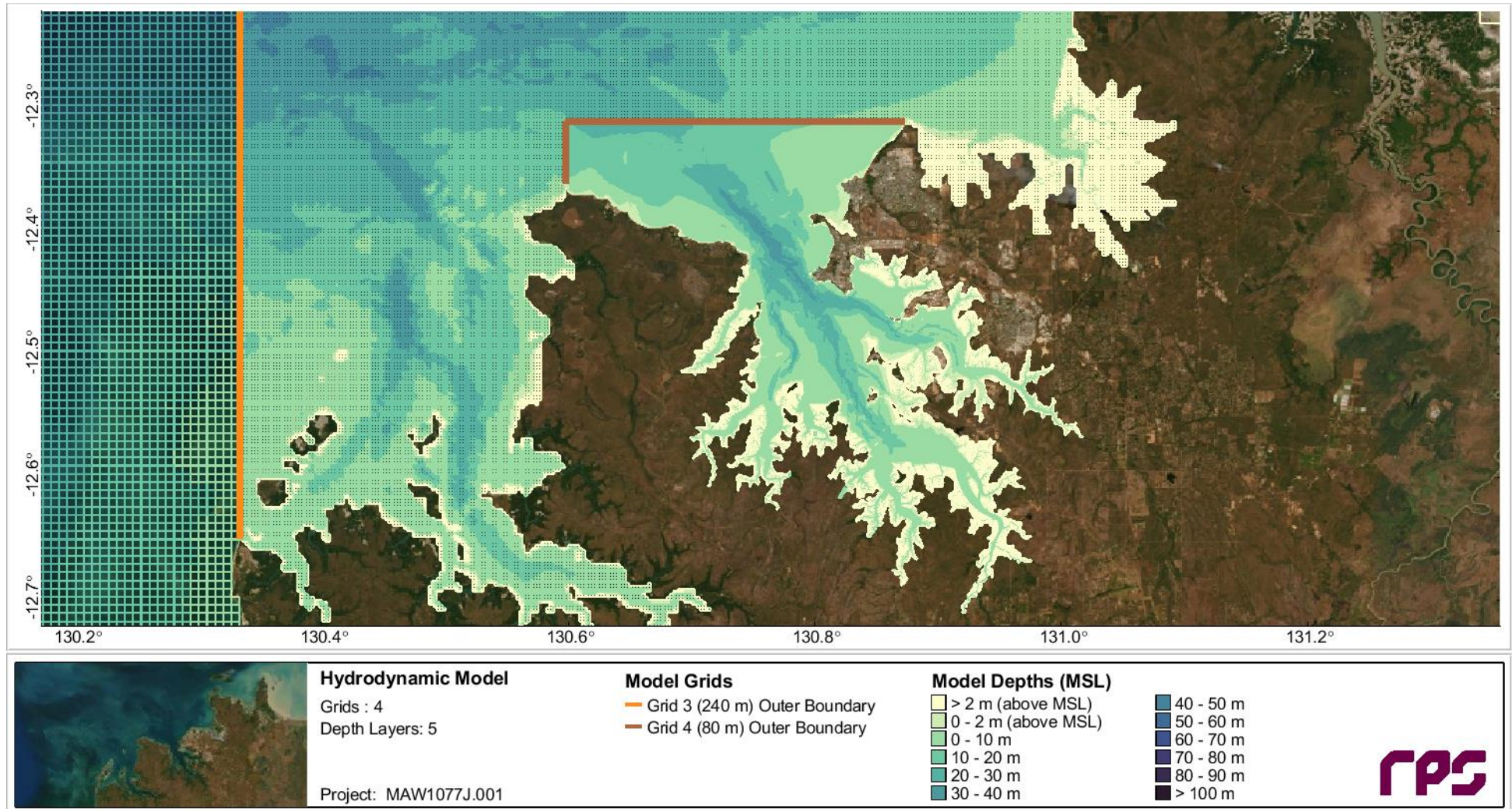
Figure 4.2 Hydrodynamic grid setup showing the domain decomposition scheme applied and the model bathymetry, focusing on the innermost grids.

4.1.3　Boundary and Initial Conditions

4.1.3.1　Overview

As the hydrodynamics in the study area are controlled primarily by tidal flows and wind forcing, these processes were explicitly included in the developed model.

The model was forced on the open boundaries of the outer sub-domain with time series of water elevation obtained for the chosen simulation period. Spatially-varying wind speed and wind direction data was used to force the model across the entire domain.

4.1.3.2　Water Elevation

Water elevations at hourly intervals were obtained from the TPXO8.0 database (Egbert & Erofeeva, 2002), which is a recent iteration of a global model of ocean tides derived from measurements of sea-surface topography by the TOPEX/Poseidon satellite-borne radar altimeters. Tides are provided as complex amplitudes of earth-relative sea-surface elevation for eight primary (M_2, S_2, N_2, K_2, K_1, O_1, P_1, Q_1), two long-period (M_f, M_m) and three non-linear (M_4, MS_4, MN_4) harmonic constituents at a spatial resolution of 0.25°.

The tidal sea level data was augmented with non-tidal sea level elevation data from the global Hybrid Coordinate Ocean Model (HYCOM; Bleck, 2002; Chassignet *et al.*, 2003; Halliwell, 2004), created by the USA's National Ocean Partnership Program (NOPP) as part of the Global Ocean Data Assimilation Experiment (GODAE). The HYCOM model is a three-dimensional model that assimilates observations of sea surface temperature, sea surface salinity and surface height, obtained by satellite instrumentation, along with atmospheric forcing conditions from atmospheric models to predict drift currents generated by such forces as wind shear, density, sea height variations and the rotation of the Earth.

The HYCOM model is configured to combine the three vertical coordinate types currently in use in ocean models: depth (z-levels), density (isopycnal layers), and terrain-following (σ-levels). HYCOM uses isopycnal layers in the open, stratified ocean, but uses the layered continuity equation to make a dynamically smooth transition to a terrain-following coordinate in shallow coastal regions, and to z-level coordinates in the mixed layer and/or unstratified seas. Thus, this hybrid coordinate system allows for the extension of the geographic range of applicability to shallow coastal seas and unstratified parts of the world ocean. It maintains the significant advantages of an isopycnal model in stratified regions while allowing more vertical resolution near the surface and in shallow coastal areas, hence providing a better representation of the upper ocean physics than non-hybrid models. The model has global coverage with a horizontal resolution of 1/12th of a degree (~7 km at mid-latitudes) and a temporal resolution of 24 hours.

4.1.3.3　Wind Forcing

Spatially-variable wind data was sourced from the Global Data Assimilation System (GDAS), which is used by the National Centers for Environmental Prediction (NCEP) Global Forecast System (GFS) model to place observations into a gridded model space for the purpose of starting, or initializing, weather forecasts with observed data. The GFS Forecasts model variant used has a horizontal resolution of 1/12th of a degree and a temporal resolution of 6 hours (NCEP, 2016).

Measured wind data sourced from Australia's IMOS national reference station Darwin (NSRDAR) was analysed and compared with the closest CFSR model hindcast data point to provide confirmation of the accuracy of CFSR winds in the project area. Time series comparisons of the measured and modelled wind data at the NRSDAR location are shown in Figure 4.3 for the validation period (1 January to 1 March 2019). Given the measured data had significant gaps during the validation period, an additional comparison is provided in Figure 4.4 for the winter/dry season sediment dispersion model scenario period (1 April 2019 to 10 July 2019). The visual comparisons of the measured and modelled wind parameters show the overall patterns and ranges of the wind parameters are well matched at the NRSDAR location.

A statistical summary of CFSR model skill at the NRSDAR location for the period 1 January 2019 to 1 June 2022 is presented in Table 4.1. The statistical summary confirms that the CFSR model performance is strong for all parameters at the NRSDAR location. The good agreement between CFSR-modelled and NRSDAR-measured winds provides confidence in the use of CFSR wind data as a forcing input to both the hydrodynamic and wave models.
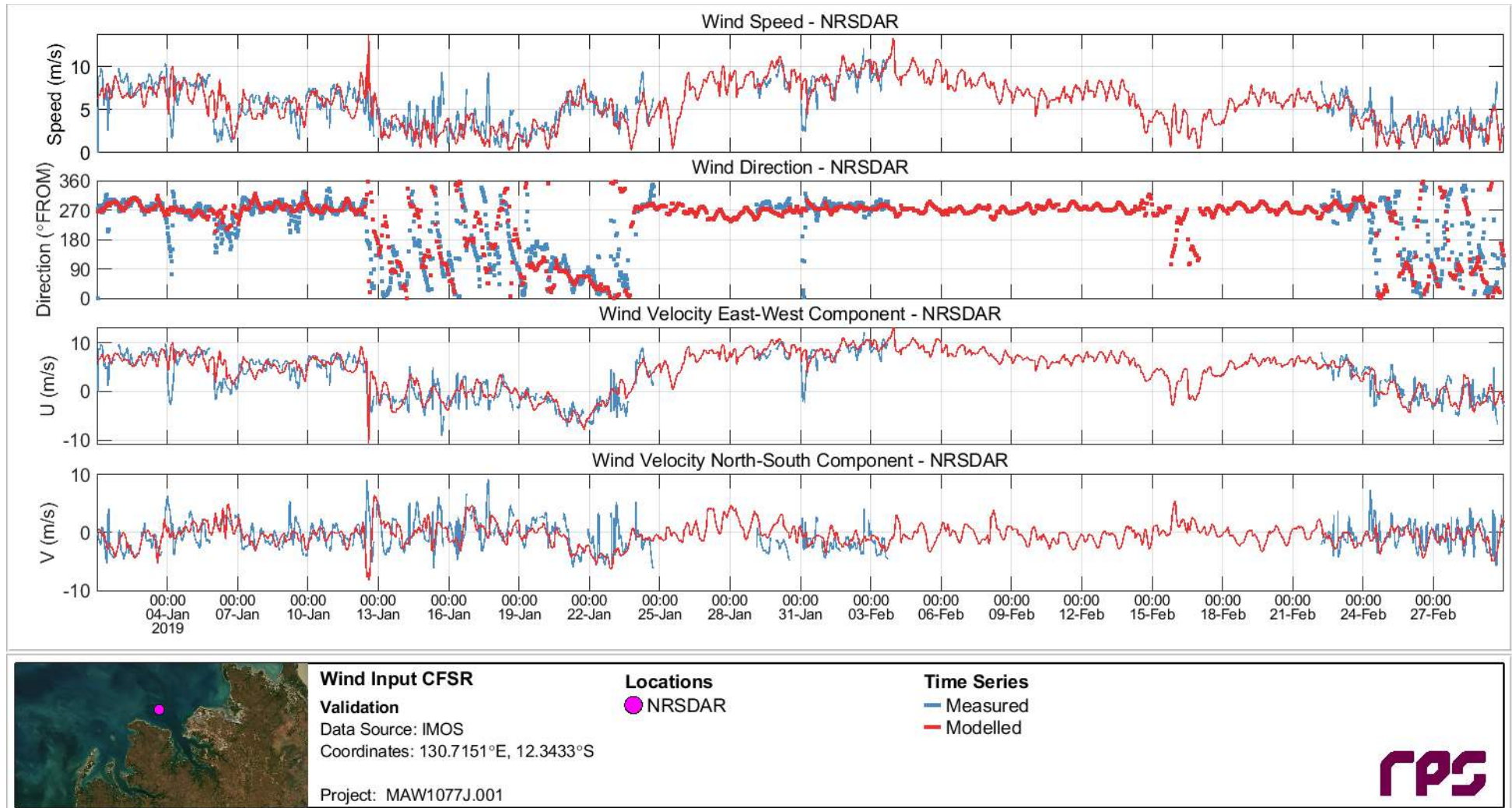
Figure 4.3 Time series comparisons of wind speed, direction, U and V components as measured at the NRSDAR station and as extracted at the closest grid point in the CFSR model over the wave and hydrodynamic model validation period (1 January 2019 to 1 March 2019).
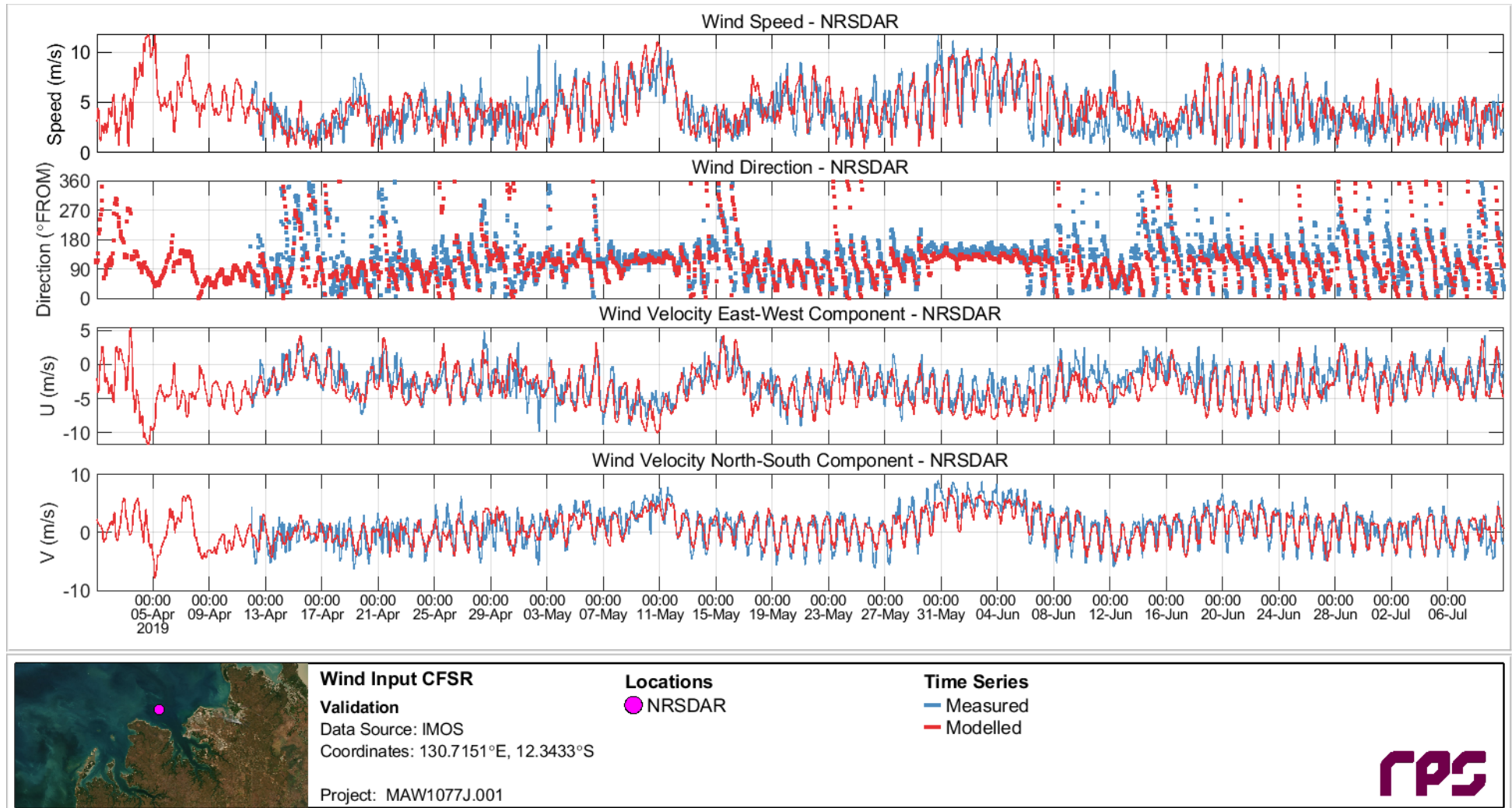
Figure 4.4 Time series comparisons of wind speed, direction, U and V components as measured at the NRSDAR station and as extracted at the closest grid point in the CFSR model over the winter/dry season sediment dispersion model scenario period (1 April 2019 to 10 July 2019).

Table 4.1 **Statistical summary of quality of agreement between measured and modelled wind velocity components at the NRSDAR station over the period 1 January 2019 to 1 June 2022.**

Wind Component	Skill Measure		
	IOA *	MAE †	RMSE †
U (east-west) (m/s)	0.90	1.82	2.39
V (north-south) (m/s)	0.77	1.67	2.17

* IOA values closer to 1 indicate higher model skill.

† MAE/RMSE values closer to 0 indicate higher model skill.

Spatial wind fields were prepared and used as forcing inputs across the model domains for both the Delft3D hydrodynamic and wave model. Winds covering the relevant periods were extracted from the Climate Forecast System Reanalysis (CFSR) hindcast data set. The CFSRv2 Reanalysis (Saha *et al.*, 2014) data product features output at spatial resolution of 0.2° at hourly intervals, contains 64 vertical levels in the atmosphere, and is coupled with ocean circulation and sea ice models.

4.1.4 Model Validation

4.1.4.1 Measured Data Source

Validation data was sourced from Australia's Integrated Marine Observing System (IMOS), enabled by the National Collaborative Research Infrastructure Strategy (NCRIS). It is operated by a consortium of institutions as an unincorporated joint venture, with the University of Tasmania as Lead Agent.

4.1.4.2 Comparison of Modelled and Measured Currents

The first months of 2019 were selected as the candidate validation period for the hydrodynamic model. Results presented here for a one-month validation period demonstrate the model performance under spring and neap tides, and given the dominant influence of tidal forcing this period captures most of the expected range for current speeds.

The time series comparison of measured and modelled data (Figure 4.5) shows excellent agreement between modelled and measured currents and water levels. A statistical summary of the hydrodynamic model skill at the NRSDAR location for the period 1 to 31 January 2019 is presented in Table 4.2. The statistical summary confirms that the hydrodynamic model performance is excellent for all parameters at the NRSDAR location.

Table 4.2 **Statistical summary of quality of agreement between measured and modelled water level and current velocity components at the NRSDAR station over the period 1 to 31 January 2019.**

Hydrodynamic Parameter	Skill Measure		
	IOA *	MAE †	RMSE †
Water level	0.99	0.17	0.23
U (east-west) (m/s)	0.98	0.08	0.11
V (north-south) (m/s)	0.98	0.05	0.08

* IOA values closer to 1 indicate higher model skill.

† MAE/RMSE values closer to 0 indicate higher model skill.
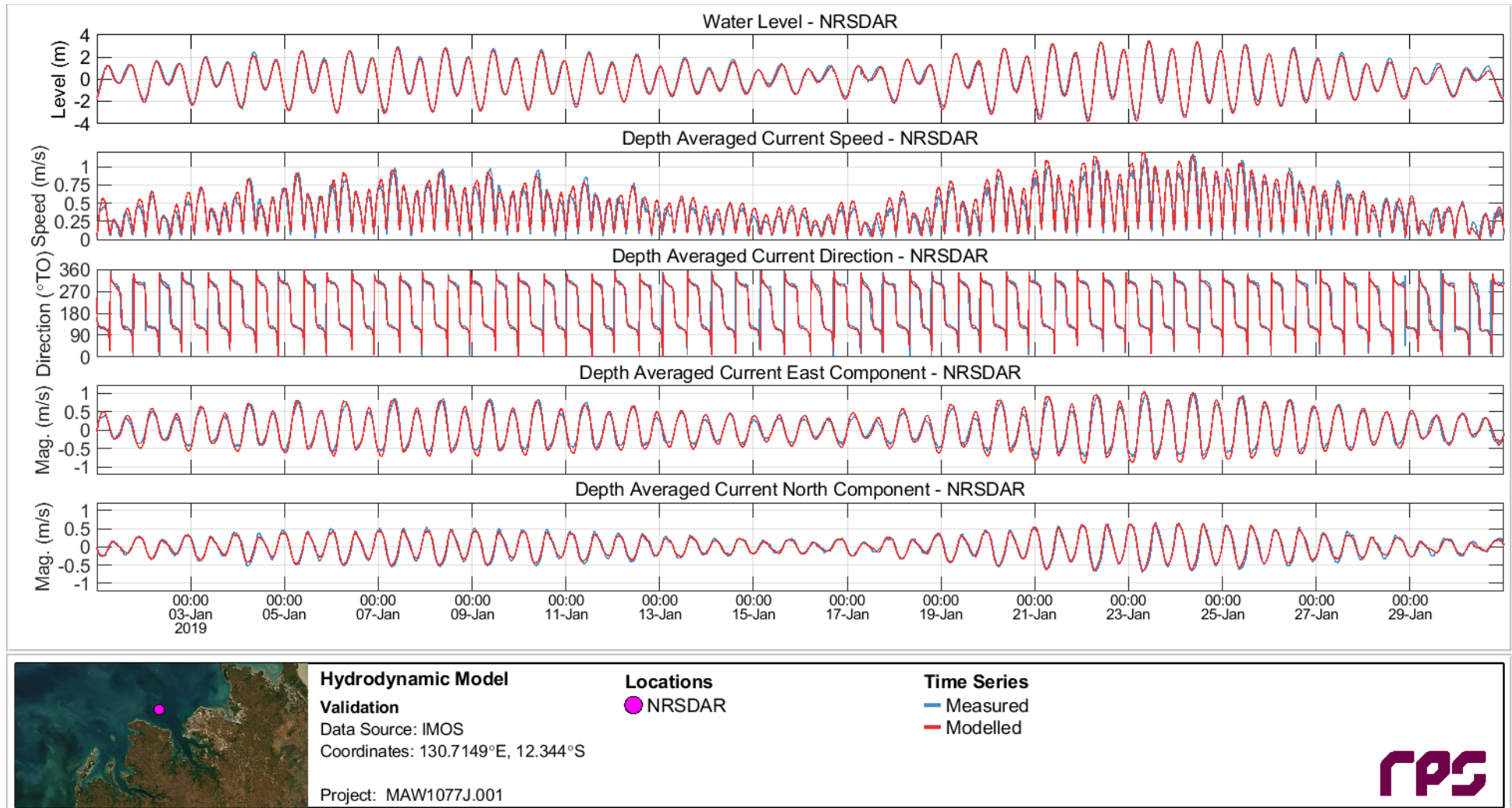
Figure 4.5 Time series comparisons of water level, current speed, direction, U and V components as measured at the NRSDAR station and as extracted at the closest grid point in the hydrodynamic model over the period 1 to 31 January 2019.

4.2 Wave Model (D-WAVE)

4.2.1 Model Description

Reliable forecasting for the fate of fine sediments in the study location required the input of wave spectra information to calculate the shear stress and orbital velocities imposed by waves which will affect the settlement and resuspension of fine material that is initially suspended by trenching and related operations. D-WAVE is a variant of the well-known SWAN wave model that has been customised for compatibility with the Delft3D software suite.

The D-WAVE model is a spectral phase-averaging wave model originally developed by the Delft University of Technology. D-WAVE, a third-generation model based on the energy balance equation, is a numerical model for simulating realistic estimates of wave parameters in coastal areas for given wind, bottom and current conditions.

D-WAVE includes algorithms for the following wave propagation processes: propagation through geographic space; refraction and shoaling due to bottom and current variations; blocking and reflections by opposing currents; and transmission through or blockage by obstacles. The model also accounts for dissipation effects due to white-capping, bottom friction and wave breaking as well as non-linear wave-wave interactions. D-WAVE is fully spectral (in all directions and frequencies) and computes the evolution of wind waves in coastal regions with shallow water depths and ambient currents.

4.2.2 Model Implementation

The D-WAVE model was developed to cover the same grid regions defined by the hydrodynamic model (Figure 4.1 and Figure 4.2). The bathymetry and wind data input to the wave model was the same as used for the hydrodynamic model. Time-varying water level information for each grid node in the wave model was provided by the output of the hydrodynamic model.

CAWCR (Centre for Australian Weather and Climate Research) Wave Hindcast data (Durrant *et al.*, 2020) was used to create boundary conditions as forcing input to the wave model. Wave parameters covering the relevant periods were extracted from the CAWCR model at 20 km intervals and used to generate parametric spectral inputs along each of the wave model open boundaries.

The global resolution of the CAWCR Wave Hindcast is 0.4°, with a resolution of 4 arc-minutes (up to 7 km) in the Australasian and central and south-west Pacific region. The increased coastal resolution near land masses in this region provides better representation of geometry, an important consideration for sheltering effects around islands. High spatial resolution also enables improved representation of bathymetry near coastlines, which in turn results in a more accurate computation of the influence of bottom friction, depth-induced wave breaking and improved modelled intensity of storm systems that can be significantly underestimated in terms of wave height at coarser resolutions (Cavaleri, 2009).

The numerical model underpinning the CAWCR Wave Hindcast is WAVEWATCH III (WW3; Tolman, 1991). WW3 is a third-generation wave model and is widely used in forecasting centres.

The D-WAVE model was configured as three one-way nested cartesian grids, with resolutions of 7 km, 800 m and 250 m, respectively. The outer boundaries of these nested grids correspond with those of Grid 0, Grid 2 and Grid 4 in the hydrodynamic model (Figure 4.1).

The wave model was run in a coupled mode with the hydrodynamic model for the years of 2019 and 2020. The model results were independently validated by comparison to IMOS measured wave data for the Darwin Harbour region. Given the purpose of the wave model is to provide bottom shear stresses and orbital velocities for settlement and resuspension calculations across a large domain in the sediment dispersion model, rather than a more site-specific application such as the design of a structure, it is believed this is an acceptable level of validation.

4.2.3 Model Validation

The first two months of 2019 were selected as the candidate validation period for the wave model because this period included relatively large wave events in comparison to the remainder of 2019. During the validation period, significant wave heights reached up to 2 m for a sustained period towards the end of January,

supported by consistent westerly wind forcing. Outside of the validation period the wave heights at the measurement location tended to be less than 0.75 m.

The wave heights and directions were well reproduced by the wave model, as shown in the time series comparisons (Figure 4.6) and as reinforced by the statistical comparisons (Table 4.3) which have high IOAs of 0.95 and 0.89, respectively. The time series comparison for peak period shows a model underprediction throughout the validation period. This is reflected in the statistical comparison where there is a moderate IOA value of 0.67, however the MAE is less than 1 s. A literature review revealed that other modelling studies using the D-WAVE (SWAN) model had encountered similar underestimation of wave period values – most notably Rogers *et al.* (2003) who investigated methods for improving predictions and found, as did we, that only a limited level of improvement could be achieved.

Given the primary role of the wave model data is to predict seabed shear velocities for sediment transport, this level of error in the wave period is considered acceptable. At the ranges of the significant wave heights (relatively small) and wave periods seen in the project area, the impact on the near-bed orbital velocities is small – in the order of several cm/s. Changes in the order of cm/s are not significant when compared against the magnitudes of the tidal current velocities which range to greater than 1 m/s (Figure 4.5).

Table 4.3 **Statistical summary of quality of agreement between measured and modelled significant wave height, peak period and peak direction at the NRSDAR station over the period 1 January 2019 to 1 March 2019.**

Wave Parameter	Skill Measure		
	IOA *	MAE †	RMSE †
Significant height (m)	0.95	0.15	0.19
Peak period (s)	0.67	0.94	1.11
Peak direction (° from)	0.89	20.8	36.7

* IOA values closer to 1 indicate higher model skill.

† MAE/RMSE values closer to 0 indicate higher model skill.
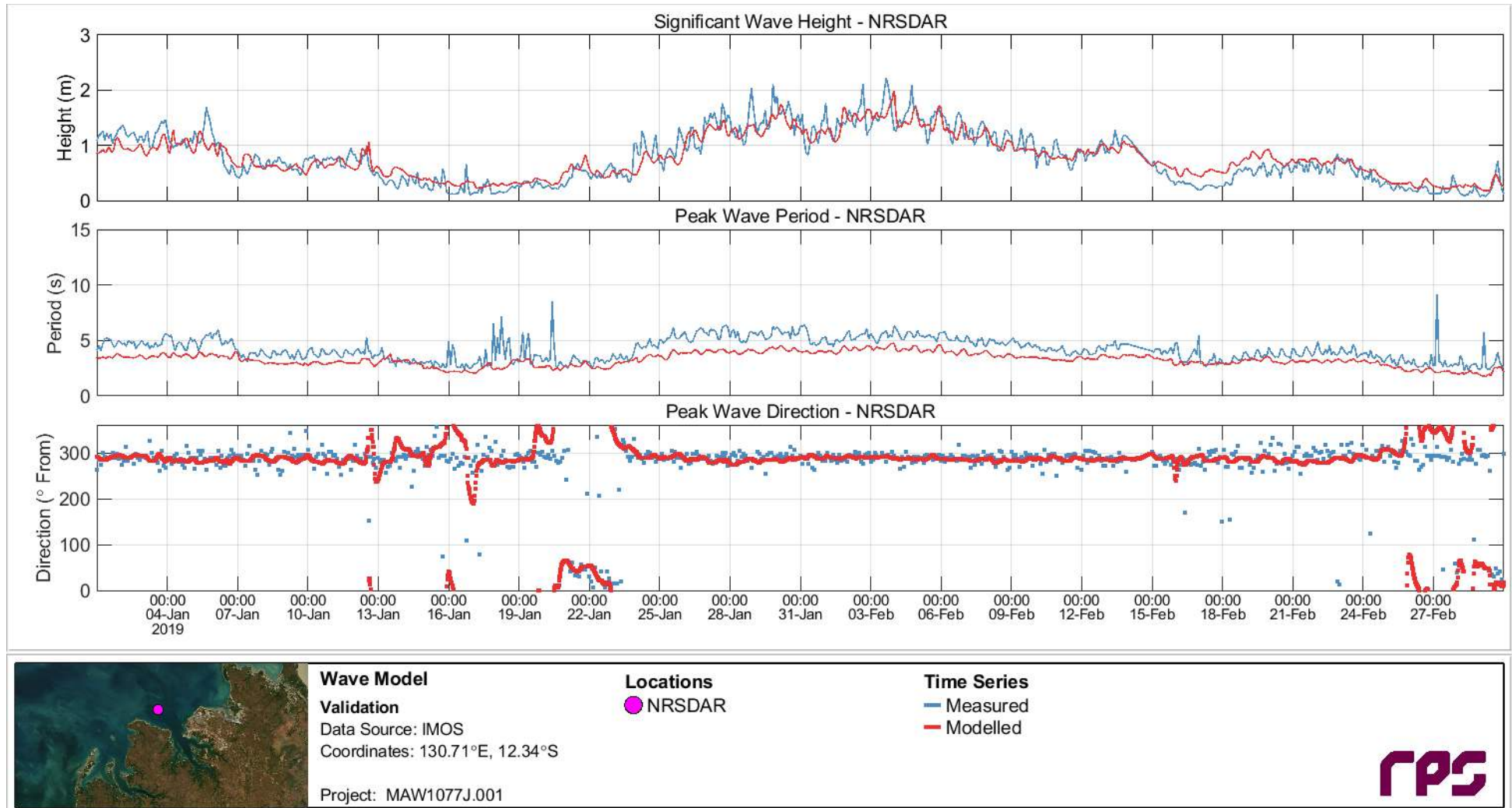
Figure 4.6 **Time series comparisons of significant wave height, peak period and peak direction as measured at the NRSDAR station and as extracted at the closest grid point in the wave model over the period 1 January 2019 to 1 March 2019.**

5 APPROACH TO SEDIMENT FATE MODELLING

Estimates for the three-dimensional distribution of sediments suspended by trenching and disposal operations have been derived for the full duration of the pipeline trenching and disposal program using numerical modelling. The approach of modelling operations in full and in three dimensions is in line with best practice for sediment dispersion modelling as outlined by WAMSI Dredging Science Node guidance (Sun *et al.*, 2016).

This modelling relied upon specification of sediment discharges over time for each of the expected sources of sediment suspension and predicted the evolution of the combined sediment plumes via current transport, dispersion, sinking and sedimentation. The model allowed for the subsequent resuspension of settling sediments due to the erosive effects of currents and waves. Thus, the fate of sediments was assessed beyond their initial settling.

Forcing was provided using predictions of three-dimensional current fields and two-dimensional wave fields for the study area, which are described in Section 2.

5.1 Model Description

Modelling of the dispersion of suspended sediment resulting from the various trenching and disposal operations was undertaken using an advanced sediment fate model, Suspended Sediment FATE (SSFATE), operating within the RPS DREDGEMAP model framework. This model computes the advection, dispersion, differential sinking, settlement and resuspension of sediment particles. The model can be used to represent inputs from a wide range of suspension sources, producing predictions of sediment fate both over the short-term (minutes to days following a discharge source) and longer term (days to years following a discharge source).

SSFATE allows the three-dimensional predictions of SSC and seabed sedimentation to be assessed against allowable exposure thresholds. Sedimentation thresholds often relate to burial depths or rates, while SSC thresholds are usually more complicated, involving tiered exposure duration and intensities. As a result, assessing the project-generated sediment distributions against these thresholds in both three-dimensional space and time is a computationally intensive task. A variety of SSC threshold formulations have recently been applied in Australian coastal waters and at present there are no general guidelines.

SSFATE is a computer model originally developed jointly by the US Army Corps of Engineers (USACE) Engineer Research and Development Center (ERDC) and RPS to estimate SSC generated in the water column and deposition patterns generated due to dredging operations in a current-dominated environment, such as a river (Johnson *et al.*, 2000; Swanson *et al.*, 2000, 2004). RPS has significantly enhanced the capability of SSFATE to allow the prediction of sediment fate in marine and coastal environments where wave forcing becomes important for reworking the distribution of sediments (Swanson *et al.*, 2007).

SSFATE is formulated to simulate far-field effects (~25 m or larger scale) in which the mean transport and turbulence associated with ambient currents are dominant over the initial turbulence generated at the discharge point. A five-class particle-based model predicts the transport and dispersion of the suspended material. The classes include the 0-130 μm range of sediment grain sizes that typically result in plumes. Heavier sediments tend to settle very rapidly, remain more stable over time and are not relevant over the longer durations (>1 hour) and larger spatial scales (>25 m) of interest here. Table 5.1 shows the standard material classes used in SSFATE for suspended sediment.

Table 5.1 Material size classes used in SSFATE.

Material Class Description	Particle Size Range (μm)
Clay	<7
Fine Silt	7-34
Coarse Silt	35-74
Fine Sand	75-130
Coarse Sand	>130

Particle advection is calculated using three-dimensional current fields, obtained from hydrodynamic modelling, thus the model can account for vertical changes in the currents within the water column. For example, as particles sink towards the seabed they will tend to be moved at slower speeds due to the slowing of currents by friction at the seabed. Particle diffusion is assumed to follow a random walk process using a Lagrangian approach of calculating transport, which uses a grid-less space to remove limitations of grid resolution, artefacts due to grid boundaries, and also maintain a high degree of mass conservation.

Following release into the model space, the sediment cloud evolves according to the following processes:

- Advection due to the three-dimensional current field.

- Diffusion by a random walk model with the mass diffusion rate specified, ideally, from measurements at the site. As particles represent an ensemble of real particles, each particle in the model has an associated Gaussian distribution governed by particle age and the mass diffusion properties of the surrounding water.

- Settlement or sinking of the sediment due to buoyancy forces. Settlement rates are determined from the particle class sizes and include allowance for flocculation and other concentration-dependent behaviour, following the model of Teeter (2000). The SSFATE model calculates the settling velocity for four of the five classes, with a settling velocity of 0.1 m/s assumed for coarse sand (Teeter, 2000; Swanson, 2007). The settling velocities are calculated from typical values of coefficients within SSFATE. The formulas used to calculate settling velocities, and the typical values of coefficients from the formulas, are presented below.

$$If\ \bar{C}_{ll} \leq\ C\ \leq\ \bar{C}_{ul}\ then$$

$$Ws_i = a\left(\frac{C}{\bar{\bar{C}}_{ul}}\right)^{n_i}$$

$$If\ C\ \geq\ \bar{C}_{ul}\ then$$

$$Ws_i\ = a$$

$$If\ C\ \leq\ \bar{C}_{ll}$$

$$Ws_i = a\left(\frac{\bar{C}_{ll}}{\bar{\bar{C}}_{ul}}\right)^{n_i}$$

Where:

$$a = \frac{1}{C}\sum_i a_i C_i \qquad \bar{C}_{ul} = \frac{1}{C}\sum_i C_{ul_i} C_i \qquad \bar{C}_{ll} = \frac{1}{C}\sum_i C_{ll_i} C_i$$

- C_{uli} and C_{lli} are the nominal upper and lower concentration limits, respectively, for enhanced settling of grain class i, and C is the total concentration for all grain size classes (except coarse sand).

- a_i is a grain-size class average maximum floc settling velocity.

- n_i is a grain-size dependent exponent.

Table 5.2   Typical values of coefficients for calculating settling velocities in SSFATE.

Sediment Grain Size Class	Size Range (µm)	C_{lli} (mg/L)	C_{uli} (mg/L)	a_i (m/s)	n_i
Clay	<7	50	1,000	0.0008	1.33
Fine Silt	7-34	150	3,000	0.0023	1.10
Coarse Silt	35-74	250	5,000	0.0038	0.90
Fine Sand	75-130	400	8,000	0.0106	0.80

- Potential deposition to the seabed determined using a model that couples the deposition across particle classes (Teeter, 2000). The likelihood and rate of deposition depends on the shear stress at the seabed. High shear inhibits deposition, and in some cases excludes it altogether with sediment remaining in suspension. The model allows for partial deposition of individual particles according to a practical deposition rate, thereby allowing the bulk sediment mass to be represented by fewer particles.

- Potential resuspension from the seabed, if previously deposited, at a rate governed by exceedance of a shear stress threshold at the seabed due to the combined action of waves and currents. Different thresholds are applied for resuspension depending upon the size of the particle and the duration of sedimentation, based on empirical studies that have demonstrated that newly-settled sediments will have higher water content and are more easily resuspended by lower shear stresses (Swanson *et al.*, 2007). The resuspension flux calculation also accounts for armouring of fine particles within the interstitial spaces of larger particles. Thus, the model can indicate whether deposits will stabilise or continue to erode over time given the shear forces that occur at the site. Resuspended material is released back into the water column to be affected by the processes defined above.

SSFATE formulations and proof of performance have been documented in a series of USACE Dredging Operations and Environmental Research (DOER) Program technical notes (Johnson *et al.*, 2000; Swanson *et al.*, 2000), and published in the peer-reviewed literature (Andersen *et al.*, 2001; Swanson *et al.*, 2004; Swanson *et al.*, 2007). SSFATE has been applied and validated by RPS against observations of sedimentation and suspended sediments at multiple locations in Australia, notably Cockburn Sound for Fremantle Ports and Mermaid Sound for the LNG Foundation Project dredging program.

5.2   Model Limitations

There are inherent limitations to the accuracy of numerical models. The possible sources of uncertainty within the modelling conducted for the sediment fate assessment of the DPD project include:

- *The equations and algorithms applied in the model*. The formulations included in the model, as discussed in Section 5.1, were selected to achieve the best possible representation of the relevant processes and have been proven to be valid over a range of projects.

- *The accuracy of the physical (current and wave) inputs to the model*. Current and wave forcing inputs were provided from validated hydrodynamic and wave models created and customised for the study area. The accuracy of these models is suitable, as good correlations with field measurements have been achieved, with the uncertainties minimised and quantifiable. The hydrodynamic and wave models are described in Section 2. It should be noted that the model inputs are a hindcast of past metocean conditions; the overall trends reflected in this data will be broadly reflected in future conditions, but conditions on any given day during the actual trenching operations may be quite different.

- *The accuracy of trenching methodology inputs to the model*. Specification of the proposed trenching and disposal methodologies was provided by Santos after consultation with the trenching contractors tendering to perform the work. Any assumptions made to achieve a realistic representation of the trenching and disposal activities are outlined in Section 5.6 and were based on extensive past project experience.

- *The accuracy of the material properties input to the model*. Geotechnical information obtained by RPS during the benthic/environmental survey investigations for the DPD project (RPS, 2022) and during previous site investigations for the Bayu-Undan Pipeline Project (Santos, 2022e, 2022f) was provided by Santos and is discussed in Section 5.5. From this data, the properties of the *in situ* material to be trenched are reasonably well-known. However, it is not possible to determine how the material properties will be changed by the action of the dredges, particularly the CSD cutting rock and the mixing of the material with seawater in the process of pumping it to the hopper/SHB. Therefore, assumptions were made in the model with regard to the material that is released into the water column from trenching and the material properties of the sediments that are to be placed at the proposed spoil ground.

- *The accuracy of the trenching and disposal sediment source terms input to the model*. The source definition in the model is flexible and can be applied to any sediment source by specifying the time-varying flux rate, particle size distribution (PSD) and vertical profile in the water column. This information will be specific to the equipment used and the material encountered at the site, and therefore can only be determined with confidence from a pilot study at the site or field measurements during trenching. In the absence of such data, conservative assumptions were made with regard to these parameters. The

assumptions are outlined in Section 5.6 and were based on literature review, including the recent WAMSI Dredging Science Node reports, and extensive past project experience.

The major sources of uncertainty for the sediment fate modelling are the modelled trenching methodology and sediment source inputs to the model. The assumptions made were based on literature review and experience and aimed to give a good representation of the sources of suspended sediment that will result from the proposed trenching and disposal activities. However, as there were uncertainties in the inputs to the model, the results should be considered as indicative of the expected ranges in magnitude and distribution of suspended sediments and sedimentation, rather than an exact prediction.

5.3   Model Domain and Bathymetry

The DREDGEMAP model domain established for the Barossa DPD project trenching works extended approximately 100 km north-south by 100 km east-west (Figure 5.1). The model grid covers the section of the Northern Territory coastline from Dundee Beach in the west to Cape Hotham in the east and offshore to the Tiwi Islands. The offshore boundaries of the domain were imposed at a reasonable distance from the proposed trenching areas, to allow potential sediment drift patterns in offshore directions to be adequately captured.

This region lies within the model domain of the Delft3D hydrodynamic and wave models that provide the current and wave inputs to DREDGEMAP (see Section 2). A grid resolution of 100 m by 100 m was selected to ensure that existing features in the domain, including the many bays, islands, channels and passages of Darwin Harbour and Beagle Gulf, were adequately defined.
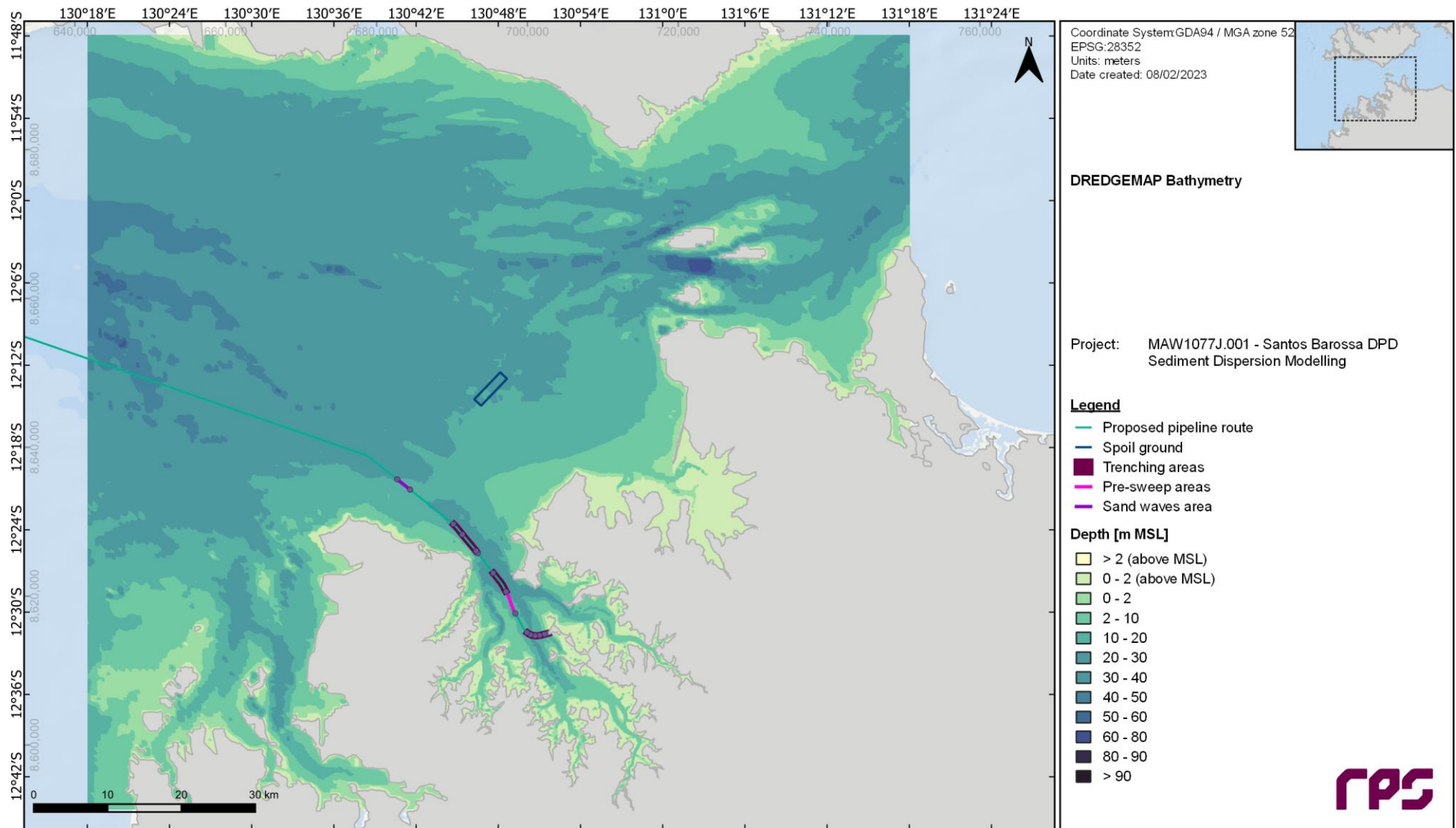
Figure 5.1   DREDGEMAP model domain and bathymetry (m MSL). Note the trenching area widths shown on this and other Figures in this report are exaggerated to aid visual clarity.

5.4 Trenching Project Description and Model Operational Assumptions

5.4.1 Overview

Information outlining the proposed trenching and disposal operations for the Barossa DPD project has been drawn from input data provided by Santos and its potential trenching contractors, and subsequent meetings and email discussions (Santos, 2022a-f; RPS, 2022), including feedback from AIMS (Physical Oceanographer Dr Hemerson Tonin). At the time of commencement of modelling, the collated information represented the best available data with regard to geotechnical properties of the project areas, the trenching and construction methodologies expected to be used within these areas, and the characteristics of vessels planned to be engaged for the work.

The operations requiring modelling have been broken into two main activities:

- Trenching of sediment and rock along the pipeline route.

- Disposal of trenched sediment and rock at the nominated spoil ground.

It should be noted that the proposed backfill and stabilisation of the pipeline will use quarry rock material, and this activity has not been modelled because the methods as currently understood will not represent a significant source of suspended sediment.

The pipeline route trenching areas and spoil ground are all within NT waters (Figure 1.1).

The following sections outline the details of the operations for each of these activities and highlight any assumptions that were made.

5.4.2 Methods and Equipment

5.4.2.1 Pipeline Route Trenching

The material to be trenched from the pipeline route will consist mainly of marine sediments (approximately 209,000 m^3) and rock material (approximately 97,000 m^3).

The trenching operations for the pipeline route have been divided into eleven sections as outlined in Table 5.3, with the three pre-sweep areas and the sand wave area only requiring sediments to be removed and the other seven trenching sections requiring removal of both sediment and rock material.

The breakdown of the proposed trenching activities, including the locations of the pipeline KPs and spoil grounds, are shown in Figure 1.1. The trenching in each of the seven trenching sections was assumed to be completed with either: a backhoe dredge (BHD; Trench Zones 1 and 2); or a trailing suction hopper dredge (TSHD) conducting a pre-sweep to remove surface sediments, followed by a cutter suction dredge (CSD) crushing harder material, and a post-sweep with the TSHD to remove the CSD-crushed material. Trenching of the pre-sweep and sand wave sections is assumed to only require the TSHD.

Typically, a TSHD will remove the sediments or material that has been previously crushed by a CSD while a BHD or CSD will remove rock, and the quantities of each material type assumed in this case are detailed in Section 5.4.3. The assumed BHD has a bucket size up to 16 m^3 and total installed power of 2416 kW, while the TSHD hopper size was assumed to be 15,000 m^3 and the CSD was assumed to have a total installed power of 28,200 kW. It has been specified that overflow of fines from the TSHD hopper will be permitted, with a 'green valve' incorporated into the overflow system, and that dewatering of the split hopper barges (SHBs) that accompany the BHD will also occur.

The estimated cycle times for trenching within each pipeline section where the BHD will operate are presented in Table 5.4, and those for each pipeline section where the TSHD will operate are presented in Table 5.5.

The potential for sediment mobilisation by TSHD propeller-wash effects has been considered along all relevant pipeline sections. This has been done using supplied data on vessel characteristics, and local depth and seabed composition. For the purposes of the modelling assessment, the relevant vessel specifications are as outlined in Table 5.6.

Table 5.3   Provisional outline of proposed pipeline trenching and disposal activities.

Pipeline Zone	Pipeline Location Start KP	Pipeline Location End KP	Vessel	Task Description	Disposal Location
Trench Zone 1	122.2	121.88	BHD & 2 SHBs	-	Spoil ground
Trench Zone 2	121.88	121.2	BHD & 2 SHBs	-	Spoil ground
Pre-Sweep Area 1	121.2	120.574	TSHD	-	Spoil ground
Trench Zone 3	120.574	119.98	TSHD (pre/post-sweep) & CSD	TSHD pre-sweep - CSD crush - TSHD post-sweep	Spoil ground
Trench Zone 4	119.9	119.44	TSHD (pre/post-sweep) & CSD	TSHD pre-sweep - CSD crush - TSHD post-sweep	Spoil ground
Pre-Sweep Area 2	116.431	113.235	TSHD	-	Spoil ground
Trench Zone 5	113.235	110.2	TSHD (pre/post-sweep) & CSD	TSHD pre-sweep - CSD crush - TSHD post-sweep	Spoil ground
Pre-Sweep Area 3	106.831	106.471	TSHD	-	Spoil ground
Trench Zone 6	106.471	103.6	TSHD (pre/post-sweep) & CSD	TSHD pre-sweep - CSD crush - TSHD post-sweep	Spoil ground
Trench Zone 7	103.6	101.766	TSHD (pre/post-sweep) & CSD	TSHD pre-sweep - CSD crush - TSHD post-sweep	Spoil ground
Sand Waves Area	94.4	92.2	TSHD	-	Spoil ground

Table 5.4   Estimated cycle times for each pipeline section where the BHD will be operating.

Pipeline Zone	Non-Dewatering Time (min)	Dewatering Time (min)	Disposal Time (min)	Sailing Time (min)	Total Cycle Time (min)
Trench Zone 1	108	217	15	250	590
Trench Zone 2	108	217	15	250	590

Table 5.5   Estimated cycle times for each pipeline section where the TSHD will be operating.

Pipeline Zone	Non-Overflow Time (min)	Overflow Time (min)	Disposal Time (min)	Sailing Time (min)	Total Cycle Time (min)
Pre-Sweep Area 1	20	160	15	140	335
Trench Zones 3-4	20	160	15	132	327
Pre-Sweep Area 2	20	160	15	132	327
Trench Zone 5	20	160	15	96	291
Pre-Sweep Area 3	20	160	15	80	275
Trench Zones 6-7	20	160	15	72	267
Sand Waves Area	20	160	15	64	259

Table 5.6   Relevant vessel specifications for propeller wash assessment.

Item	TSHD	SHB
Vessel draft (loaded/empty)	10 m / 3 m	5 m / 2 m
Number of propellers, type	Two, ducted	Two, ducted
Diameter of propellers	4 m	1.5 m
Thrust power (kW per propeller)	8,000 kW	1,150 kW

5.4.2.2 Spoil Ground Disposal

As outlined in Table 5.3, it was assumed that all material removed by the BHD will be placed into one of two waiting SHBs and transported to the offshore disposal area (shown in Figure 1.1). All material removed by the TSHD will be transported directly to the offshore disposal area.

It was assumed that the BHD will be accompanied by two SHBs, each assumed to be approximately 2,700 m^3 in capacity, to be used for disposal of trenched material. Material discharges from the SHBs were assumed to occur between depths of 5 m and 2 m below mean sea level.

The TSHD hopper doors, from which discharge will occur, were assumed to be opened at a depth of 10 m below sea level. The modelled vessel draft was reduced as spoil is discharged to a minimum depth of 5 m below sea level when empty.

The SHBs will be self-propelled and the potential for sediment mobilisation by propeller-wash effects has been considered along all relevant pipeline sections. This has been done using supplied data on vessel characteristics, and local depth and seabed composition. For the purposes of the modelling assessment, the relevant specifications were as outlined in Table 5.6.

It was assumed that the broad aim of the spoil disposal patterns will be to evenly distribute the total volume of allocated material across the entire spoil ground area by the conclusion of all activities, so the spacing of individual disposal operations (which are restricted to a comparatively small area within the spoil ground) was designed to achieve this. The surface area of the proposed spoil grounds is approximately 6,290,000 m^2; given the volume of material to be placed in the spoil ground, a theoretical thickness of 5-10 cm is expected if the spoil is evenly distributed.

5.4.3 Quantities and Production Rates

For trenching of each section along the pipeline route, the proposed trench depths and quantities for each material type were specified for input to the modelling (Table 5.7). The stated quantities include allowances for contingency; hence, they are conservative volume estimates. The table has two material categories, defined as "sediments" (sand/silt/clay/gravel) assumed to be able to be removed by a TSHD and "rock" (siltstone/claystone/sandstone/phyllite) assumed to require a CSD to remove. Some of the weaker rock may be able to be removed by the TSHD; however, to err on the side of conservatism it was assumed that all the rock material would require cutting by CSD.

It is understood that:

- The estimated material quantities were based on the latest surveyed bathymetry and a geotechnical model based on seismic refraction survey data.

- The estimated production rates were averages based on trench contractor estimated durations for each equipment type and the material volume for each zone.

- The estimated production rates were average values inclusive of expected downtime estimates.

Table 5.7   Modelled trench depths, quantities of material type, and production rates by material type for trenching of each pipeline section.

Pipeline Zone	Trench Depth Nominal below seabed (m)	Trenched Quantities (m³)			Production Rates (m³/week)	
		Sediment	Rock	Total	Sediment	Rock
Trench Zone 1	3.2	11,963	4,703	16,665	12,000	9,800
Trench Zone 2	1.5	3,988	1,568	5,555	12,000	9,800
Pre-Sweep Area 1	-	6,130	-	6,130	86,000	-
Trench Zone 3	2.3	7,764	14,419	22,183	86,000	27,200
Trench Zone 4	1	6,349	1,120	7,469	86,000	27,200
Pre-Sweep Area 2	-	34,840	-	34,840	86,000	-
Trench Zone 5	1	29,567	19,712	49,279	86,000	27,200
Pre-Sweep Area 3	-	2,955	-	2,955	86,000	-
Trench Zone 6	2.5	64,097	52,443	116,541	86,000	27,200
Trench Zone 7	1	26,801	2,978	29,779	86,000	27,200
Sand Waves Area	-	14,817	-	14,817	86,000	-
Totals		**209,270**	**96,942**	**306,212**	**-**	**-**

5.4.4   Schedules

For trenching of each section along the pipeline route, the proposed duration and sequencing of operations has been specified for input to the modelling (Table 5.8 and Table 5.9). Table 5.8 has two material categories, as described in Section 5.4.3.

The modelled sequence of trenching has been specified to represent a worst-case scenario where the TSHD, CSD and BHD operate concurrently, as outlined in Table 5.9. The TSHD modelled sequence is assumed to start in Pre-Sweep Area 1, moving offshore along the pipeline route to Trench Zone 3, and then proceeding consecutively to each zone from Trench Zone 4 out to the Sand Waves Area. Once the TSHD has completed its first pass over each of the trenching sections it will begin removing the material that has been crushed by the CSD, starting at Trench Zone 3, moving offshore along the pipeline route out to Trench Zone 7.

The BHD modelled sequence starts in Trench Zone 1 then moves to Trench Zone 2, with the BHD assumed to commence work at the same time as the TSHD on day one of the dredging program.

The CSD cannot start until the TSHD has pre-swept some of the zones, and the schedule minimises the amount of time that two pieces of equipment are in the same zone at the same time. To meet this condition the CSD will start in week two of the program in Trench Zone 3 then move sequentially offshore to Trench Zone 7.

The CSD is scheduled to finish after 28 days (on day 35 of the program because it starts in week two), the BHD is scheduled to finish after 30 days, and the TSHD will finish after 40 days.

Modelling of each section involves a series of trenching and related disposal activities.

Table 5.8   Modelled durations of trenching and disposal operations by material type for each pipeline section.

Pipeline Zone	Duration of Operations (weeks)			Total Duration (Weeks)		
	Sediments (BHD/TSHD)	Rock (BHD/CSD)	Crushed Material (TSHD)	BHD	TSHD	CSD
Trench Zone 1	2.17	1.05	-			
Trench Zone 2	0.72	0.35	-			
Pre-Sweep Area 1	0.14	-	-			
Trench Zone 3	0.18	0.64	0.33			
Trench Zone 4	0.15	0.05	0.03			
Pre-Sweep Area 2	0.80	-	-		-	
Trench Zone 5	0.61	0.87	0.40			
Pre-Sweep Area 3	0.06	-	-			
Trench Zone 6	1.21	2.31	0.99			
Trench Zone 7	0.50	0.13	0.06			
Sand Waves Area	0.27	-	-			
Totals	**6.81**	**5.39**	**1.81**	**4.29**	**5.72**	**4.00**

Table 5.9   Modelled sequencing of trenching and disposal operations assuming concurrent TSHD, CSD and BHD operation (worst case).

Week	TSHD		CSD		BHD		Comments
	Pipeline Zone	Duration (weeks)	Pipeline Zone	Duration (weeks)	Pipeline Zone	Duration (weeks)	
1	Pre-Sweep Area 1	0.14	-	-	Trench Zone 1	3.22	TSHD and BHD begin together on Day 1 of program
	Trench Zone 3	0.18					
	Trench Zone 4	0.15					
	Pre-Sweep Area 2	0.80					
2	Trench Zone 5	0.61	Trench Zone 3	0.64	Trench Zone 1	3.22	CSD starts in Week 2 once TSHD has pre-swept Trench Zones 3/4 and commenced Pre-Sweep Area 2
	Pre-Sweep Area 3	0.06	Trench Zone 4	0.05			
			Trench Zone 5	0.87			
3	Trench Zone 6	1.21	Trench Zone 6	2.31			-
4	Trench Zone 7	0.50			Trench Zone 2	1.07	-
	Sand Waves Area	0.27					
5	Trench Zone 3	0.33					TSHD begins post-sweep of CSD-crushed material
	Trench Zone 4	0.03					
	Trench Zone 5	0.40					
	Trench Zone 6	0.99	Trench Zone 7	0.13			
6	Trench Zone 7	0.06	-	-	-	-	-
Totals	**-**	**5.72**	**-**	**4.00**	**-**	**4.29**	**-**

5.4.5   Scenario Summary

At the time of modelling commencement the high-level schedule for the trenching works indicated an April/May 2023 start for trenching of the pipeline route. Analysis of wind data in the region from 2012-2021 has shown that the period of 2019-2020 is likely to be representative of typical conditions. Thus, the sediment dispersion modelling simulations were conducted using hydrodynamic and wave data drawn from this period, with nominal start dates for model simulation purposes being chosen as 1 April 2019 (winter/dry) and 1 October 2019 (summer/wet). While trenching for the DPD project is now expected to commence in late 2023 or early 2024, the modelling scenarios are still considered representative of potential environmental conditions.

A summary of the scenarios that were modelled is as follows:

- Scenario 1: trenching works simulated to commence on 1 April 2019 (winter/dry start):

    1. TSHD trenching and disposal operations were simulated to occur between 1 April 2019 and 10 May 2019.

    2. CSD trenching and disposal operations were simulated to occur between 8 April 2019 and 5 May 2019.

    3. BHD trenching and disposal operations were simulated to occur between 1 April 2019 and 30 April 2019.

    4. A simulation run-on period was assumed to occur between 10 May 2019 and 10 July 2019. Sediments suspended in the water column during previous operations were subject to settlement and progressively-reducing levels of resuspension during this time.

- Scenario 2: trenching works simulated to commence on 1 October 2019 (summer/wet start):

    1. TSHD trenching and disposal operations were simulated to occur between 1 October 2019 and 9 November 2019.

    2. CSD trenching and disposal operations were simulated to occur between 8 October 2019 and 4 November 2019.

    3. BHD trenching and disposal operations were simulated to occur between 1 October 2019 and 30 October 2019.

    4. A simulation run-on period was assumed to occur between 9 November 2019 and 9 January 2020. Sediments suspended in the water column during previous operations were subject to settlement and progressively-reducing levels of resuspension during this time.

The outcomes of the summer/wet season-start and winter/dry season-start scenarios have been analysed and presented separately, for comparison.

5.5   Geotechnical Information

The trenched material from the pipeline route will consist mainly of marine sediments (approximately 209,000 m^3) and rock material (approximately 97,000 m^3). The critical geotechnical information required as input to the modelling is: (i) PSD data for the sediments to be trenched along the pipeline route; and (ii) *in situ* dry bulk density for the materials to be trenched along the pipeline route.

The PSD data used in the modelling was based on field data collected for the DPD project by RPS as part of the Environmental Survey during October 2021 and January 2022 along the proposed pipeline corridor and at the proposed offshore spoil ground (RPS, 2022). The specified PSD for each zone was determined based on an average of the PSD results of all samples taken within each zone during site investigations.

The geotechnical sampling points from which PSDs were acquired within each zone are summarised in Table 5.10, including the total number of PSD samples used to determine the averages. The locations of the geotechnical sampling points from the RPS October 2021 and January 2022 site investigations are shown in Figure 5.2. The resultant PSDs for each pipeline section have been redistributed to match the material size classes used in the DREDGEMAP model, as shown in Table 5.11.

Dry bulk density values were not available from current or past field investigations, but wet bulk density and voids ratio information for the project area was available from geotechnical studies conducted for the project and for the Bayu-Undan Pipeline Project (Santos, 2022e, 2022f). The wet bulk density and void ratio values

were used to estimate dry bulk density for modelling purposes. The dry bulk density values applied to each zone are outlined in Table 5.12.

Table 5.10   Summary of geotechnical data used in the derivation of model PSDs for each pipeline section.

Pipeline Zone	Pipeline Location Start KP	Pipeline Location End KP	No. of PSD Samples
Trench Zone 1	122.2	121.88	2
Trench Zone 2	121.88	121.2	
Pre-Sweep Area 1	121.2	120.574	4
Trench Zone 3	120.574	119.98	4
Trench Zone 4	119.9	119.44	5
Pre-Sweep Area 2	116.431	113.235	12
Trench Zone 5	113.235	110.2	7
Pre-Sweep Area 3	106.831	106.471	3
Trench Zone 6	106.471	103.6	4
Trench Zone 7	103.6	101.766	6
Sand Waves Area	94.4	92.2	23
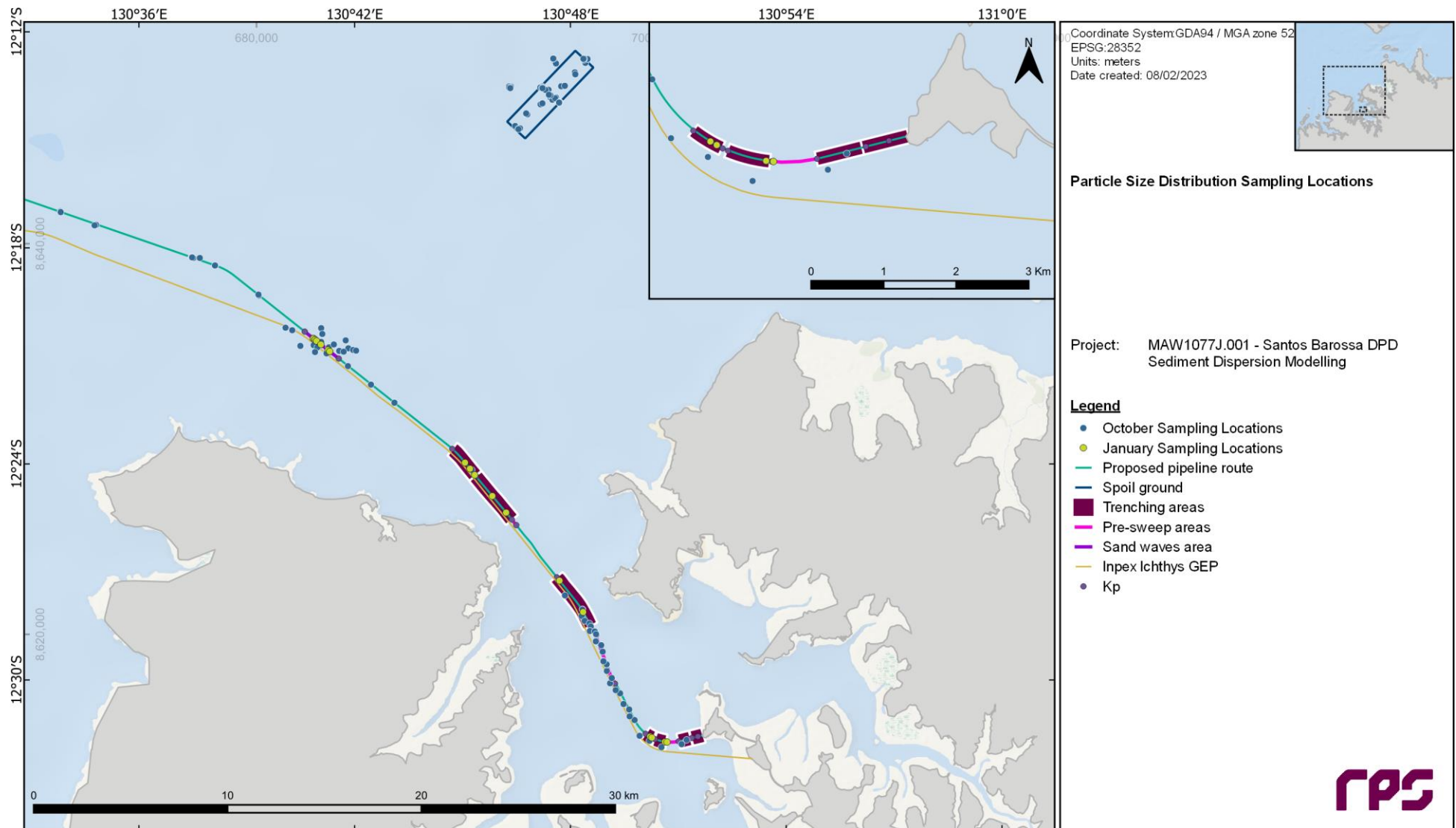
Figure 5.2 **PSD sediment sample locations, with blue dots representing the 2021 survey and green dots representing the January 2022 survey. Note the trenching area widths shown on this and other Figures in this report are exaggerated to aid visual clarity.**

Table 5.11 *In situ* PSDs broken down into DREDGEMAP material classes for each pipeline section to be dredged, derived from available geotechnical information.

Sediment Grain Size Class	Size Range (µm)	Trench Zone 1 (%)	Trench Zone 2 (%)	Pre-Sweep Area 1 (%)	Trench Zone 3 (%)	Trench Zone 4 (%)	Pre-Sweep Area 2 (%)	Trench Zone 5 (%)	Pre-Sweep Area 3 (%)	Trench Zone 6 (%)	Trench Zone 7 (%)	Sand Waves Area (%)
Clay	<7	5.43	5.43	7.33	7.02	8.86	4.44	2.94	6.23	7.75	8.72	1.24
Fine Silt	7-34	8.61	8.61	8.89	8.32	11.66	6.45	4.36	9.23	9.52	9.00	1.90
Coarse Silt	35-74	7.75	7.75	5.52	4.62	7.76	5.09	3.82	9.49	8.89	6.08	2.78
Fine Sand	75-130	8.64	8.64	4.69	3.29	4.69	3.93	3.06	6.36	5.96	3.74	2.49
Coarse Sand	>130	69.58	69.58	73.57	76.76	67.04	80.09	85.82	68.69	67.88	72.47	91.60

Table 5.12 *In situ* wet bulk densities and estimated dry bulk densities, based on the available wet bulk density and voids ratio data.

Pipeline Zone	Wet Bulk Density (Sediment)	Wet Bulk Density (Rock)	Estimated Dry Bulk Density (Sediment)	Estimated Dry Bulk Density (Rock)
Trench Zone 1	1.83	2.35	1.21	2.16
Trench Zone 2	1.83	2.35	1.21	2.16
Pre-Sweep Area 1	1.83	-	1.21	-
Trench Zone 3	1.83	2.35	1.21	2.16
Trench Zone 4	1.83	2.35	1.21	2.16
Pre-Sweep Area 2	1.83	-	1.21	-
Trench Zone 5	1.83	2.35	1.21	2.16
Pre-Sweep Area 3	1.83	-	1.21	-
Trench Zone 6	1.83	2.35	1.21	2.16
Trench Zone 7	1.83	2.35	1.21	2.16
Sand Waves Area	1.89	-	1.32	-

5.6 Model Sediment Sources

5.6.1 Overview

To accurately represent the pipeline trenching and disposal operations in DREDGEMAP, a range of information was defined for the proposed operations, including trenching and disposal methodology, production rates, and sediment/rock types and quantities (see Section 5.4). It is evident that there will be six different sources of suspended sediment plumes during trenching and disposal operations, which can be broadly defined as:

1. Direct suspension of material from the BHD bucket, from grabbing and lifting sediments and rock through the water column, accounting for periods of no-dewatering and dewatering from the SHBs.

2. Disposal of sediment and rock excavated by the BHD from the SHBs to the spoil ground.

3. Direct suspension of material by the TSHD during trenching of sediments, and CSD-crushed material, accounting for no-overflow and overflow periods.

4. Disposal of sediment and CSD-crushed material removed by the TSHD to the spoil ground.

5. Direct suspension of material by the CSD during trenching of rock and casting material behind the dredge at low velocity, just above the seabed.

6. Indirect suspension of material due to the propeller-wash of the SHB and TSHD while trenching.

Each of these sources of suspended sediment plumes will vary in strength and persistence depending on the nature of the operations. In the DREDGEMAP model, each source is defined by specifying the time-varying flux rate, PSD and vertical profile in the water column. The following sections outline how the information provided has been used to represent the trenching operations in the model and explain any assumptions that have been made to supplement the available information.

5.6.2 Representation of BHD Trenching

A BHD will be used to excavate all sediment and rock from Trench Zone 1 and Trench Zone 2. The BHD will use a large excavator arm fitted with an open bucket of (nominally) 16 m^3 capacity. The excavator will lift material in the bucket and deliver it to one of two waiting SHBs – assumed for the purposes of modelling to be 2,700 m^3 in capacity – for transport to the proposed offshore spoil ground for disposal.

Sources of sediment suspension from this type of operation include:

- Disturbance of the seabed sediments by the excavator bucket.

- Dewatering of the SHB, resulting in the discharge of water and entrained sediments.

Past observations have shown that material is suspended due to the initial grab at the seabed. Further suspension is generated as sediment spills from the bucket as it is lifted through the water column. Spillage of water and sediment also occurs as the bucket breaks free of the water surface and drains freely. Only sediments <130 µm in diameter are considered "lost" (i.e. suspended into the water column), because the coarser material spilled from the bucket while being lifted to the surface will fall immediately to the bottom where it will be re-excavated during subsequent grabs. As such, the distribution of material suspended by the bucket spillage is assumed to be distributed across the four smaller sediment size classes in the model.

For the trenching of sediments during periods with no dewatering from the SHB, the PSD used in the model is based on PSDs from nearby boreholes (see Section 5.5), with the proportion >130 µm removed and the remaining distribution normalised to 100% by scaling up the proportions in the four remaining size classes (Table 5.13). The same PSD is used for the rock component, assuming that due to the excavation action of the BHD the rock will break down into similar proportions of fines. Because the trenching action of the excavator involves no cutting or hydraulic pumping, this is a conservative assumption.

During dewatering periods, an increase in the rate of release of fine sediments, and hence initial turbidity, is observed (Anchor Environmental, 2003). The water released during dewatering of the SHB contains a high proportion of fines because the coarse material settles rapidly in the hopper while the fine material remains in suspension. After the barge begins dewatering, a PSD heavily weighted towards finer particles has been assumed based on previous field measurements of SHB dewatering at Geraldton Port (OPR, 2010), with the

proportion >75 µm removed and the remaining distribution normalised to 100% by scaling up the proportions in the three remaining size classes (Table 5.14).

Table 5.15 shows the assumed vertical distribution of the suspended material during the BHD operations while the barge is not dewatering. The distribution is higher at the seabed and water surface, to represent the larger loss rate of material during the initial grab and as the bucket breaks free of the water column. After the barge begins dewatering, a uniform distribution of sediments throughout the water column, between the hull depth and the seabed, has been assumed to represent a continuous stream of material being discharged from the barge (Table 5.16).

Loss rates from similar operations are known to vary based on such factors as the size and type of bucket (i.e. open or closed), nature of the seabed material, presence of debris, current speed and depth of water, as well as the care of the operator (Hayes & Wu, 2001; Anchor Environmental, 2003). Reported rates compared by Anchor Environmental (2003) varied from 0.1% to 10%, with a mean of 2.1%. In the absence of measurements for the specific situation and equipment, the mean of 2.1% of production rate is assumed for BHD operations during periods with no dewatering, and a rate of 2.4% of production rate is assumed for all BHD operations during dewatering periods. The latter value is in line with the average overflow rate calculated for the TSHD hopper overflow (see Section 5.6.4).

Table 5.13 **Assumed PSDs of sediments initially suspended into the water column during BHD trenching operations along the pipeline route while the SHB is not dewatering.**

Sediment Grain Size Class	Size Range (µm)	PSD (%) for Sediment and Rock Removal – Trench Zone 1	PSD (%) for Sediment and Rock Removal – Trench Zone 2
Clay	<7	17.84	17.84
Fine Silt	7-34	28.29	28.29
Coarse Silt	35-74	25.47	25.47
Fine Sand	75-130	28.39	28.39
Coarse Sand	>130	0.00	0.00

Table 5.14 **Assumed PSDs of sediments initially suspended into the water column during BHD trenching operations along the pipeline route while the SHB is dewatering.**

Sediment Grain Size Class	Size Range (µm)	PSD (%) for Sediment and Rock Removal – Trench Zone 1	PSD (%) for Sediment and Rock Removal – Trench Zone 2
Clay	<7	48.45	48.45
Fine Silt	7-34	29.73	29.73
Coarse Silt	35-74	21.83	21.83
Fine Sand	75-130	0.00	0.00
Coarse Sand	>130	0.00	0.00

Table 5.15 **Assumed vertical distribution of sediments initially suspended into the water column during BHD trenching operations along the pipeline route while the SHB is not dewatering.**

Elevation	Example Elevation (m ASB) – 10 m Water Depth	Vertical Distribution (%) of Sediments
Surface/water depth	10	23
0.8 x water depth	8	16
0.5 x water depth	5	14
0.3 x water depth	3	19
0.1 x water depth	1	28

Table 5.16   Assumed vertical distribution of sediments initially suspended into the water column during BHD trenching operations along the pipeline route while the SHB is dewatering.

Elevation	Example Elevation (m ASB) – 10 m Water Depth and 5 m Hull Depth	Vertical Distribution (%) of Sediments
Surface/water depth	10	8
Hopper hull elevation	5	23
0.66 x hull elevation	3.3	23
0.33 x hull elevation	1.7	23
0.50 m (ASB)	0.5	23

5.6.3   Representation of Disposal of BHD-Trenched Material

All material trenched by the BHD will be placed into one of two waiting 2,700 m³ SHBs and transported to the proposed offshore spoil ground for disposal (Figure 1.1). This material will include all sediment and rock material from Trench Zone 1 and Trench Zone 2.

For the disposal of sediment trenched by BHD, the PSD used in the model is based on PSDs from nearby boreholes (see Section 5.5). The same PSD is used for the rock component, assuming that due to the excavation action of the BHD the rock will break down into similar proportions of fines. Because the trenching action of the excavator involves no cutting or hydraulic pumping, this is a conservative assumption. This PSD is adjusted by removal of the component treated as suspended during trenching (see Section 5.6.2), but as this represents only 2.1-2.4% of the mass for the minor components, the modified PSD is not significantly different to the *in situ* PSD (Table 5.17).

Once at the offshore spoil ground, the SHB will open to release the sediments from the bottom of the hull at a depth of approximately 5 m below sea level. Previous observations of sediment dumping from hopper vessels (e.g., CSMW, 2005) have shown that there is an initial rapid descent of solids, with the heavy particles tending to entrain lighter particles, followed by a billowing of lighter components back into the water column after contact with the seabed (Figure 5.3). A proportion of the lighter components will also remain suspended and may be trapped by density layers, if present.

Because simulations in this study focused on the far-field fate of sediment particles due to transport and sinking after the initial dump phase, simulations were run with the initial vertical distribution specified to represent the post-collision phase for a case where a high proportion of the sediments are resuspended after collision with the seabed. To represent this, an assumed vertical distribution for the sediments (Table 5.18) has been specified following published information from previous hopper disposal operations (CSMW, 2005; NEPA, 2001). This vertical distribution, with the majority of the material input near the seabed and only 7% of the material released in the upper half of the water column, is in line with values quoted in the recent literature review by Mills & Kemps (2016), which found that sediment resuspension from individual dredged material disposal events was generally less than 10% of the disposed material load.

It is estimated that 95-99% of the bulk load deposits directly onto the seabed in a typical case, with the remainder released into the water column (CSMW, 2005, NEPA, 2001). It is difficult to find other definitive source values in the literature, but a value of 5% of each load agrees well with past experience and appears to be a conservative estimate based on the values quoted above. Accordingly, 5% of each hopper load was placed in suspension in the water column in the sediment fate model.

In addition to the proportion of material immediately suspended in the water column, disposal from the barge will result in the stockpiling of sediment as a mound on the seabed that will be subject to resuspension by tidal and wave forces. Because fine sediments in the deposited mass may be subject to ongoing resuspension and dispersion over time, it was necessary to specify the deposits as a further source of sediment potentially subject to resuspension.

The proportion of the newly deposited trenched material available for resuspension is characterised by a finite limit regulated by PSDs and the occurrence of natural sediment capping. As a result of the selective resuspension of the smaller-sized particles (silts and clays), the deposited mound surface layer gradually contains a greater proportion of larger particle sizes. These larger particles act as armouring against bottom shear stress, protecting and retaining the remaining fine particles in the mound. Therefore, in the model it was assumed that 5% of the deposited mass – representing the volume of the upper surface layer – would be

subject to resuspension. It should be noted that the model maintains a mass balance estimate of the remaining sediment of each size class within each grid cell to derive an estimate of the median particle size in the surface-layer sediments. In turn, the potential for ongoing resuspension of fines is calculated. In this way, the model represents the increased armouring of sediments as the average particle size increases.

The disposal time for the SHB within each trenching cycle was assumed to be 15 minutes (Table 5.4). The disposal location within the spoil ground was varied for each trenching cycle in a randomised manner, with the aim of ensuring an even distribution of trenched material within the spoil ground by the conclusion of activities.

Table 5.17   Assumed PSDs of sediments initially suspended into the water column during SHB disposal operations at the offshore spoil ground.

Sediment Grain Size Class	Size Range (µm)	PSD (%) for Sediment and Rock Disposal – Trench Zone 1	PSD (%) for Sediment and Rock Disposal – Trench Zone 2
Clay	<7	4.53	4.53
Fine Silt	7-34	7.94	7.94
Coarse Silt	35-74	7.22	7.22
Fine Sand	75-130	8.44	8.44
Coarse Sand	>130	71.88	71.88

Table 5.18   Assumed vertical distribution of sediments initially suspended into the water column during SHB disposal operations at the offshore spoil ground.

Elevation	Example Elevation (m ASB) – 30 m Water Depth	Vertical Distribution (%) of Sediments
Surface/water depth	30	2
0.6 x water depth	18	5
0.4 x water depth	12	15
0.15 x water depth	4.5	35
0.1 x water depth	3	43
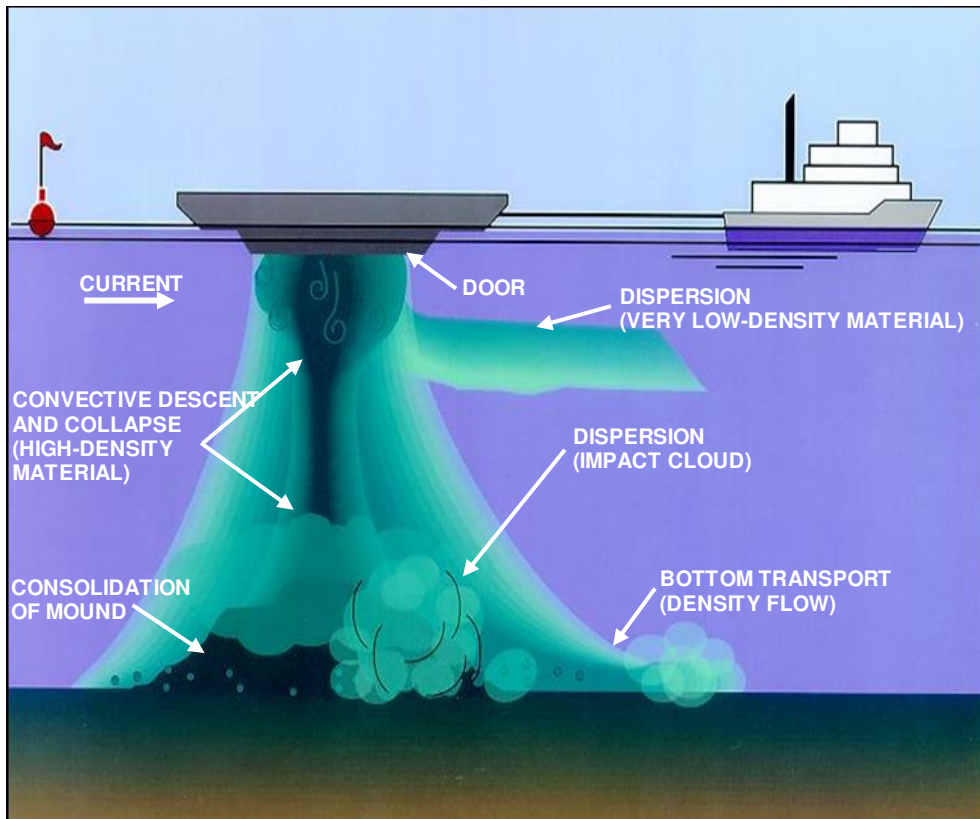
Figure 5.3   Conceptual diagram showing the general behaviour of sediments dumped from a barge/SHB in open water and the vertical distribution of material set up by entrainment and billowing (Source: Moritz & Randall, 1992).

5.6.4   Representation of TSHD Trenching

A TSHD will be used to excavate all sediments from Pre-Sweep Areas 1, 2 and 3, Trench Zones 3, 4, 5, 6 and 7, the Sand Waves Area, and all rock material crushed by CSD in Trench Zones 3, 4, 5, 6 and 7, with disposal at the proposed offshore spoil ground (Figure 1.1). For the purposes of modelling, the capacity of the TSHD to be used for trenching of the pipeline route and borrow grounds was assumed to be 15,000 m^3.

TSHD vessels remove sediments by dragging a large draghead over the seabed and drawing up the disturbed sediment by hydraulic suction. Sources of sediment suspension from this type of operation include:

- Hydraulic disturbance of the seabed sediments by the trailing arm.

- Propeller-wash generated as the vessel manoeuvres.

- Overflow of the on-board hoppers, resulting in the discharge of water and entrained sediments.

The characteristics of each of these sources vary greatly due to a wide range of factors (USACE, 2008) making the generalisation of source terms difficult. It appears however, that the overflow source term is dominant, being typically an order of magnitude greater than the draghead and propeller-wash terms.

For the pre-sweep trenching of the sediment during periods with no overflow, the PSDs used in the model are based on PSDs from nearby boreholes (see Section 5.5). The PSDs applied during periods with no overflow to pre-sweep trenching along the pipeline route are shown in Table 5.19. For the post-sweep trenching of the material that has been crushed by the CSD during periods with no overflow, the PSDs are based on the assumed PSD for the crushed material as outlined in Section 5.6.6, with an adjustment made to account for the loss of fine material during CSD operations (Table 5.21).

During overflow periods, an increase in the rate of release of fine sediments, and hence initial turbidity, is observed (Anchor Environmental, 2003). The overflow water contains a high proportion of fines because the coarse material settles rapidly in the hopper while the fine material remains in suspension. After the hopper begins overflowing, PSDs heavily weighted towards finer particles have been assumed based on previous field

measurements of hopper barge dewatering at Geraldton Port (OPR, 2010), with the proportion >75 µm removed and the remaining distribution normalised to 100% by scaling up the proportions in the three remaining size classes. The PSDs applied during overflow periods to pre-sweep trenching along the pipeline route are shown in Table 5.20 and post-sweep trenching of CSD-crushed material are shown in Table 5.22.

Table 5.23 shows the assumed vertical distribution of the suspended material during the TSHD operations while the hopper is not overflowing. The distribution is concentrated near the seabed and decreases in intensity towards the surface, to represent the disturbance of seabed material by the draghead and propeller-wash effects (HR Wallingford, 2003). After the hopper begins overflowing, a uniform distribution of sediments throughout the water column, between the hull depth and the seabed, has been assumed to represent a continuous stream of material being discharged from the hopper through an overflow system incorporating a 'green valve' (Table 5.24). This is consistent with measured ADCP profiles presented by Hitchcock & Bell (2004), which show a reasonably even distribution of sediment through the water column during hopper overflow.

It should be noted that the installation of a green valve within an overflow system is designed to reduce the proportion of air entrained into the overflow mixture, which in turn will result in a reduced proportion of discharged material mixing and billowing upwards to the water surface. To account for this process in the modelling, the vertical distribution applied during hopper overflow (Table 5.24) is not uniform throughout the entire water column, but only from the hull depth to the seabed.

Table 5.19 Assumed PSDs of sediments initially suspended into the water column during TSHD trenching operations along the pipeline route for pre-sweep of sediment while the hopper **is not** overflowing.

Sediment Grain Size Class	Size Range (µm)	PSD (%) for Sediment Removal – Pre-Sweep Area 1	PSD (%) for Sediment Removal – Trench Zone 3	PSD (%) for Sediment Removal – Trench Zone 4	PSD (%) for Sediment Removal – Pre-Sweep Area 2	PSD (%) for Sediment Removal – Trench Zone 5	PSD (%) for Sediment Removal – Pre-Sweep Area 3	PSD (%) for Sediment Removal – Trench Zone 6	PSD (%) for Sediment Removal – Trench Zone 7	PSD (%) for Sediment Removal – Sand Waves Area
Clay	<7	7.33	7.02	8.86	4.44	2.94	6.23	7.75	8.72	1.24
Fine Silt	7-34	8.89	8.32	11.66	6.45	4.36	9.23	9.52	9.00	1.90
Coarse Silt	35-74	5.52	4.62	7.76	5.09	3.82	9.49	8.89	6.08	2.78
Fine Sand	75-130	4.69	3.29	4.69	3.93	3.06	6.36	5.96	3.74	2.49
Coarse Sand	>130	73.57	76.76	67.04	80.09	85.82	68.69	67.88	72.47	91.60

Table 5.20 Assumed PSDs of sediments initially suspended into the water column during TSHD trenching operations along the pipeline route for pre-sweep of sediment while the hopper **is** overflowing.

Sediment Grain Size Class	Size Range (µm)	PSD (%) for Sediment Removal – Pre-Sweep Area 1	PSD (%) for Sediment Removal – Trench Zone 3	PSD (%) for Sediment Removal – Trench Zone 4	PSD (%) for Sediment Removal – Pre-Sweep Area 2	PSD (%) for Sediment Removal – Trench Zone 5	PSD (%) for Sediment Removal – Pre-Sweep Area 3	PSD (%) for Sediment Removal – Trench Zone 6	PSD (%) for Sediment Removal – Trench Zone 7	PSD (%) for Sediment Removal – Sand Waves Area
Clay	<7	50.37	51.05	48.31	50.65	51.82	47.51	48.36	50.64	52.99
Fine Silt	7-34	30.02	29.93	31.03	29.14	28.36	29.49	29.46	29.58	27.30
Coarse Silt	35-74	19.61	19.03	20.67	20.21	19.82	23.00	22.18	19.80	19.72
Fine Sand	75-130	0.00	0.00	0.00	0.00	0.00	0.00	0.00	0.00	0.00
Coarse Sand	>130	0.00	0.00	0.00	0.00	0.00	0.00	0.00	0.00	0.00

Table 5.21   **Assumed PSDs of sediments initially suspended into the water column during TSHD trenching operations along the pipeline route for post-sweep of material that has been crushed by CSD while the hopper is not overflowing.**

Sediment Grain Size Class	Size Range (µm)	PSD (%) for Sediment Removal – Trench Zone 3	PSD (%) for Sediment Removal – Trench Zone 4	PSD (%) for Sediment Removal – Trench Zone 5	PSD (%) for Sediment Removal – Trench Zone 6	PSD (%) for Sediment Removal – Trench Zone 7
Clay	<7	4.37	3.89	1.80	3.50	4.59
Fine Silt	7-34	5.19	5.13	2.67	4.30	4.74
Coarse Silt	35-74	2.88	3.41	2.34	4.01	3.20
Fine Sand	75-130	2.05	2.06	1.87	2.69	1.97
Coarse Sand	>130	85.50	85.50	91.32	85.50	85.50

Table 5.22   **Assumed PSDs of sediments initially suspended into the water column during TSHD trenching operations along the pipeline route for post-sweep of material that has been crushed by CSD while the hopper is overflowing.**

Sediment Grain Size Class	Size Range (µm)	PSD (%) for Sediment Removal – Trench Zone 3	PSD (%) for Sediment Removal – Trench Zone 4	PSD (%) for Sediment Removal – Trench Zone 5	PSD (%) for Sediment Removal – Trench Zone 6	PSD (%) for Sediment Removal – Trench Zone 7
Clay	<7	52.53	52.05	53.06	52.00	52.69
Fine Silt	7-34	28.83	28.77	27.83	28.11	28.36
Coarse Silt	35-74	18.64	19.18	19.11	19.89	18.95
Fine Sand	75-130	0.00	0.00	0.00	0.00	0.00
Coarse Sand	>130	0.00	0.00	0.00	0.00	0.00

Table 5.23   **Assumed vertical distribution of sediments initially suspended into the water column during TSHD trenching operations along the pipeline route while the hopper is not overflowing.**

Elevation	Example Elevation (m ASB) – 30 m Water Depth	Vertical Distribution (%) of Sediments
10.0 m (ASB)	10	5
7.0 m (ASB)	7	15
3.0 m (ASB)	3	20
2.0 m (ASB)	2	40
1.0 m (ASB)	1	20

Table 5.24   **Assumed vertical distribution of sediments initially suspended into the water column during TSHD trenching operations along the pipeline route while the hopper is overflowing**

Elevation	Example Elevation (m ASB) – 30 m Water Depth and 10m Hull Depth	Vertical Distribution (%) of Sediments
Hopper hull elevation	20	20
0.75 x hull elevation	15	20
0.50 x hull elevation	10	20
0.25 x hull elevation	5	20
0.50 m (ASB)	0.5	20

The resuspension of sediment when the TSHD hopper is not overflowing was estimated by combining the draghead and propeller-wash terms. The propeller-wash component typically dominates the draghead component, but both sources were assessed. Propeller-wash generation was estimated by applying a model of the bed-induced shear stress from the TSHD vessel over the range of under-keel clearances expected during the dredging operations.

Field measurements of draghead-induced sediment suspension were reported by Coastline Surveys Ltd (CSL, 1999). The inferred production rate was less than 1 kg/s and it was concluded that, generally, draghead production is small in comparison to the quantity of sediment released via overflow. Given the above, a loss rate of 0.6% of the gross production rate, representing a combined sediment flux due to losses from the draghead and propeller-wash, was assumed when the TSHD is not overflowing. This rate is within the range of values (less than 1%) summarised in a review of contemporary practice conducted as part of the WAMSI Dredging Science Node by Kemps & Masini (2017).

The resuspension of sediment from hopper overflow is the most complex source term associated with a TSHD. The discharged water-sediment mixture forms a negatively-buoyant jet (dynamic plume) that descends towards the seabed. Due to mixing and entrainment as the plume descends, not all of the sediment in the dynamic plume directly descends to the seabed, forming a passive plume in the water column below the TSHD. Based on evidence from numerous field measurements, Spearman *et al.* (2011) state that the dynamic plume retains the bulk of the overflow sediment, with a small proportion (in the range of 5-15%) contained in the passive plume. The proportion of sediment contained in the passive plume is a function of the air content in the overflow mixture, with the use of a green valve shown to significantly reduce the proportion of the overflow sediment that forms the passive plume (Spearman *et al.*, 2011).

The overflow source term was calculated for each discrete trench zone and material type based on a method outlined in Becker *et al.* (2015) and recommended in Kemps & Masini (2017). This method was applied as it allows the proportion of fines in the material being trenched in each zone to be considered in determination of the source terms. This is important given the significant variations in the fines proportion between trench zones and material types. Additionally, this method allows for the use of a green valve in the overflow system to be accounted for in the source term estimates.

The Becker *et al.* (2015) method considers the following parameters:

- The total flux of fines entering the hopper during trenching.
- The proportion of the trenched fines flux that settles (and is trapped) in the hopper.
- The proportion of the trenched fines flux that exits the hopper in the overflow water.
- The relative proportions of the overflow fines flux that contribute to the dynamic and passive plumes.

In calculating these parameters, the method takes into account:

- The PSDs and dry bulk densities of the material to be trenched.
- The production/pumping rates of the TSHD.
- The rate at which material settles/traps in the hopper.
- The overflow-to-loading ratio based on the trench cycle times.

Becker *et al.* (2015) state that a reasonable estimate of the proportion of overflow fines that becomes the passive plume will fall in the range of 0-20%. This broadly agrees with the range of 5-15% found in Spearman *et al.* (2011). Values of this order of magnitude are confirmed by field measurements taken during operation of a sand dredger (8,225 m^3 capacity) in Hong Kong, which suggested 15% of the overflow fines flux contributed to the passive plume (Whiteside *et al.*, 1995).

It should be noted that in the Hong Kong study a green valve was not employed to moderate the overflow. There is limited experimental data available on the degree to which a green valve will reduce the proportion of the overflow fines flux that becomes a passive plume. DHI (2010) state that an appropriate estimate for the proportion of fines remaining in the passive plume when a green valve is in use is around 7% of the total overflow fines flux, with this assessment informed by monitoring activities undertaken in the vicinity of marine construction vessels in Singapore.

The proposed use of a green valve during the DPD project is accounted for in this modelling study by assuming that 10% of the overflow fines flux will become a passive plume. This represents a moderate value in the context of the ranges stated above. Calculation of the overflow source rates using a proportional value of 10%

are presented in Table 5.25, for each trench zone and material type, expressed as a proportion of the trenching production rate.

Table 5.25   Calculated source rates of sediments initially suspended into the water column during TSHD hopper overflow for pre-sweep sediment and post-sweep CSD-crushed material, using the methodology outlined in Becker *et al.* (2015).

Zone	Source Rate (% Production Rate)	
	Pre-Sweep Material	**Post-Sweep Material**
Pre-Sweep Area 1	2.20	-
Trench Zone 3	2.02	1.26
Trench Zone 4	2.87	1.26
Pre-Sweep Area 2	1.62	-
Trench Zone 5	1.13	0.69
Pre-Sweep Area 3	2.53	-
Trench Zone 6	2.65	1.20
Trench Zone 7	2.41	1.27
Sand Waves Area	0.60	-

The overflow source rate values calculated using the Becker *et al.* (2015) method range from 0.60% to 2.87% of the gross production rate, which compares well with the range of published measurements from TSHD operations (0.1-5.0%; Hayes & Wu, 2001) and is within the range of values used in modelling studies (0.3-9.8%) outlined in a review of contemporary practice by Kemps & Masini (2017). The lower overflow source rate values (<1.5% of total production) were calculated for the trench areas containing material that had lower fines content, such as the Sand Waves Area, Trench Zone 5 and material that has been crushed by CSD (see Sections 5.5 and 5.6.6). Overflow source rate values quoted in literature for areas with low fines content range from 0.3 to 2.1% of total production, giving confidence in the calculated values. For the trenching areas where the fines content is higher (Pre-Sweep Areas 1 and 3 and Trench Zones 3, 4, 6 and 7; Section 5.5), the calculated overflow source rate values are in the mid-range of the literature values.

To further contextualise the overflow source rate values calculated using the Becker *et al.* (2015) method, the corresponding suspended sediment concentrations (SSC) in the hopper overflow have been calculated and compared to values found in literature. Passive plume concentrations calculated without accounting for a green valve are in the range 2,600-6,300 mg/L for the areas with lower fines content (Sand Waves Area, Trench Zone 5, Pre-Sweep Area 2 and material that has been crushed by CSD), and in the range 5,600-8,000 mg/L for the remaining trenching areas. When a green valve is considered, the calculated concentrations are reduced to 2,100-5,100 mg/L for the areas with lower fines content and 4,600-6,500 mg/L for the remaining areas.

Field measurements taken of SSC within overflowing waters adjacent to the hopper are typically in the 5,000-6,000 mg/L range and are generally less than 10,000 mg/L (Hitchcock & Bell, 2004). These values correlate well with data drawn from other Western Australian projects that cannot be cited here for reasons of confidentiality. From comparisons, the calculated values above fall into a range that past experience suggests is realistic.

5.6.5   Representation of Disposal of TSHD-Trenched Material

All material trenched by the TSHD along the pipeline route will be transported to the proposed offshore spoil ground for disposal (Figure 1.1). This material will include all sediment and CSD-crushed rock from Pre-Sweep Areas 1, 2 and 3, Trench Zones 3, 4, 5, 6, and 7, and the Sand Waves Area.

For the disposal of the sediment trenched by TSHD in the pre-sweep of each area, the PSDs used in the model are based on PSDs from nearby boreholes (see Section 5.5). For the disposal of the CSD-crushed material removed by TSHD in the post-sweep trenching, the PSDs are based on the assumed PSD for the trenching of the CSD-crushed material as outlined in Section 5.6.4. Both sets of PSDs have been adjusted by removal of the component treated as suspended during trenching along the pipeline route (see Section 5.6.4), but as

this represents only between 1.1% and 3.2% (averaged value depending on the relative contributions of overflow and non-overflow periods to the overall mass flux) of the mass for the minor components, the modified PSDs are not significantly different to the trenched PSDs (Table 5.26 and Table 5.27).

Once at the proposed spoil ground, the hopper will open to release the sediments from the bottom of the hull at a depth of approximately 10 m below sea level. Previous observations of sediment dumping from hopper vessels (e.g. CSMW, 2005) have shown that there is an initial rapid descent of solids, with the heavy particles tending to entrain lighter particles, followed by a billowing of lighter components back into the water column after contact with the seabed (Figure 5.3). A proportion of the lighter components will also remain suspended and may be trapped by density layers, if present.

Because simulations in this study focused on the far-field fate of sediment particles due to transport and sinking after the initial dump phase, simulations were run with the initial vertical distribution specified to represent the post-collision phase for a case where a high proportion of the sediments are resuspended after collision with the seabed. To represent this, an assumed vertical distribution for the sediments (Table 5.28) has been specified following published information from previous hopper disposal operations (CSMW, 2005; NEPA, 2001). This vertical distribution, with the majority of the material input near the seabed and only 15% of the material released at hull depth or above, is in line with values quoted in the recent literature review by Mills & Kemps (2016), which found that sediment resuspension from individual dredged material disposal events was generally less than 10% of the disposed material load.

It is estimated that 95-99% of the bulk load deposits directly onto the seabed in a typical case, with the remainder released into the water column (CSMW, 2005, NEPA, 2001). It is difficult to find other definitive source values in the literature, but a value of 5% of each load agrees well with past experience and appears to be a conservative estimate based on the values quoted above. Accordingly, 5% of each hopper load was placed in suspension in the water column in the sediment fate model.

In addition to the proportion of material immediately suspended in the water column, disposal from the hopper will result in the stockpiling of sediment as a mound on the seabed that will be subject to resuspension by tidal and wave forces. Because fine sediments in the deposited mass may be subject to ongoing resuspension and dispersion over time, it was necessary to specify the deposits as a further source of sediment potentially subject to resuspension.

The proportion of the newly deposited trenched material available for resuspension is characterised by a finite limit regulated by PSDs and the occurrence of natural sediment capping. As a result of the selective resuspension of the smaller-sized particles (silts and clays), the deposited mound surface layer gradually contains a greater proportion of larger particle sizes. These larger particles act as armouring against bottom shear stress, protecting and retaining the remaining fine particles in the mound. Therefore, in the model it was assumed that 5% of the deposited mass – representing the volume of the upper surface layer – would be subject to resuspension. It should be noted that the model maintains a mass balance estimate of the remaining sediment of each size class within each grid cell to derive an estimate of the median particle size in the surface-layer sediments. In turn, the potential for ongoing resuspension of fines is calculated. In this way, the model represents the increased armouring of sediments as the average particle size increases.

The disposal time for the hopper material within each trench cycle was assumed to be 15 minutes (Table 5.5). The disposal location within the spoil ground was varied for each trench cycle in a randomised manner, with the ultimate aim of ensuring an even distribution of trenched material within each spoil ground by the conclusion of all activities.

Table 5.26   Assumed PSDs of sediments initially suspended into the water column during TSHD hopper disposal operations at spoil ground for the pre-sweep material.

Sediment Grain Size Class	Size Range (μm)	PSD (%) for Sediment Removal – Pre-Sweep Area 1	PSD (%) for Sediment Disposal – Trench Zone 3	PSD (%) for Sediment Disposal – Trench Zone 4	PSD (%) for Sediment Disposal– Pre-Sweep Area 2	PSD (%) for Sediment Disposal – Trench Zone 5	PSD (%) for Sediment Disposal – Pre-Sweep Area 3	PSD (%) for Sediment Disposal – Trench Zone 6	PSD (%) for Sediment Disposal – Trench Zone 7	PSD (%) for Sediment Disposal – Sand Waves Area
Clay	<7	5.92	5.68	7.79	3.57	1.32	4.69	6.29	8.11	1.24
Fine Silt	7-34	8.05	7.53	10.97	5.95	3.47	8.27	8.63	8.65	1.90
Coarse Silt	35-74	4.97	4.12	7.30	4.74	3.20	8.74	8.22	5.84	2.78
Fine Sand	75-130	4.69	3.29	4.69	3.93	3.06	6.36	5.96	3.74	2.49
Coarse Sand	>130	76.37	79.38	69.26	81.82	88.95	71.94	70.89	73.67	91.60

Table 5.27   Assumed PSDs of sediments initially suspended into the water column during TSHD hopper disposal operations at spoil ground for the post-sweep of CSD-crushed material.

Sediment Grain Size Class	Size Range (μm)	PSD (%) for Sediment Disposal – Trench Zone 3	PSD (%) for Sediment Disposal – Trench Zone 4	PSD (%) for Sediment Disposal – Trench Zone 5	PSD (%) for Sediment Disposal – Trench Zone 6	PSD (%) for Sediment Disposal – Trench Zone 7
Clay	<7	3.40	2.92	1.12	2.56	3.60
Fine Silt	7-34	4.65	4.60	2.31	3.79	4.21
Coarse Silt	35-74	2.54	3.06	2.09	3.66	2.85
Fine Sand	75-130	2.05	2.06	1.87	2.69	1.97
Coarse Sand	>130	87.36	87.36	92.61	87.30	87.37

Table 5.28 Assumed vertical distribution of sediments initially suspended into the water column during TSHD hopper disposal operations at the offshore spoil ground.

Elevation	Example Elevation (m ASB) – 20 m Water Depth and 10 m Hull Depth	Vertical Distribution (%) of Sediments
Surface/water depth	20	5
Hopper hull elevation	10	10
0.75 x hull elevation	7.5	20
0.50 x hull elevation	5	30
0.25 x hull elevation	2.5	35

5.6.6 Representation of CSD Trenching

For this project it is proposed that a large CSD will be used to cut/crush all rock from Trench Zones 3, 4, 5, 6 and 7. The CSD proposed for the project will be trenching rock with a strength of up to approximately 40 MPa, therefore a large CSD is required. For the purposes of modelling a CSD with a total installed power of 28,200 kW was specified. The proposed methodology that has been modelled is for all material cut/crushed by CSD to be cast behind the dredge at low velocity, just above the seabed. The crushed material will be subsequently removed by TSHD and taken to the proposed offshore spoil ground. There are several proposed methodologies for the CSD trenching component of the program; however, this methodology was anticipated to represent a "worst case" in terms of the generation of suspended sediment due to the additional pass with the TSHD that is required (see Section 5.6.4). A similar methodology was used in the Ichthys project for CSD operations (INPEX, 2010, 2011). Sources of sediment suspension from this type of operation include:

- Centrifugal dispersion of seabed sediments by the rotating cutterhead.

- Suspension of sediments due to casting/pumping behind the dredge and billowing of lighter components back into the water column after contact with the seabed.

Past studies have found that CSDs cutting rock produce material of mixed size-fractions, ranging from fine silts to small rock fragments (Fitzpatrick *et al.*, 2009). Based on past dredging operations in Darwin Harbour, approximately 80% of the material generated by the CSD was assumed to be in the form of rocks and gravel (RPS, 2009). PSDs were estimated for each zone by adjusting the measured PSDs to have 80% in the coarse sand size class and calculating a weighted reduction of the proportion of each of the smaller size classes. The PSDs applied to CSD crushing and casting back material while trenching along the pipeline route are shown in Table 5.29.

The plume that results from the action of the CSD cutterhead is typically concentrated near the seabed, with only small concentrations reaching the surface (CSMW, 2005). The majority of the source is located near the seabed, mostly within 3 m of the bottom. The casting of material behind the CSD via a pipeline just above the seabed will result in a similar plume vertical profile. Sediment release from the pipe will occur as a stream of slurry that will have an initial rapid descent of solids followed by a billowing of lighter components back into the water column after contact with the seabed (Swanson *et al.*, 2004). The plume that results from disposal of a stream of slurry from a pipe is typically concentrated near the seabed, with most of the material within 3 m of the bottom, and lower concentrations extending up towards the surface (Swanson *et al.*, 2004). Table 5.30 shows the assumed vertical distribution of the suspended material for the CSD cutterhead and casting source.

There is a reasonable amount of literature pertaining to the generation rate of suspended sediments at the cutterhead during CSD operations. Results from field measurement and empirical models have been presented by Hayes & Wu (2001) and Anchor Environmental (2003). A broad range of source rates have been found, generally being less than 0.5% of the gross production rate (USACE, 2008). Hayes & Wu (2001) quote a maximum source rate of 0.51% from approximately 400 observations, with most rates less than 0.3%. Anchor Environmental (2003) quote additional data, citing a median source rate of 0.3% of gross production based on the collected data set. A validation model study undertaken for a project in Cockburn Sound, Western Australia, dredging sedimentary rock, found that 0.3% was a suitable input for a large CSD (Fitzpatrick *et al.*, 2009). Investigation of the data sets from the studies presented showed that the largest observed rates resulted from the dredging of very fine sediment with high water content, typical of riverine or sedimentary estuarine conditions, rather than open coastal environments. Given the location of the trenching within the vicinity of

Darwin Harbour, for this study a source rate of 0.5% of the gross production rate (more typical of estuarine trenching) has been adopted for the CSD cutterhead source.

For the casting back of material via a pipeline it is estimated that 95-99% of the bulk load will deposit directly onto the seabed in a typical case, with the remainder released into the water column (CSMW, 2005, NEPA, 2001). It is difficult to find other definitive source values in the literature, and no site-specific sampling has been conducted for pipe placement operations, but a value of 5% of production rate agrees well with past experience and appears to be a conservative estimate based on the values quoted above. Accordingly, a source of 5% of the gross production rate was placed in suspension in the water column in the sediment fate model.

Table 5.29   Assumed PSDs of sediments initially suspended into the water column during CSD trenching operations along the pipeline route for crushing and casting of material.

Sediment Grain Size Class	Size Range (µm)	PSD (%) for Sediment Removal – Trench Zone 3	PSD (%) for Sediment Removal – Trench Zone 4	PSD (%) for Sediment Removal – Trench Zone 5	PSD (%) for Sediment Removal – Trench Zone 6	PSD (%) for Sediment Removal – Trench Zone 7
Clay	<7	6.03	5.37	2.94	4.83	6.33
Fine Silt	7-34	7.16	7.08	4.36	5.93	6.54
Coarse Silt	35-74	3.98	4.71	3.82	5.54	4.42
Fine Sand	75-130	2.83	2.85	3.06	3.71	2.72
Coarse Sand	>130	80.00	80.00	85.82*	80.00	80.00

* The coarse sand fraction of the Trench Zone 5 PSD was initially more than 80%, so no further adjustment was applied.

Table 5.30   Assumed vertical distribution of sediments initially suspended into the water column during CSD trenching operations along the pipeline route for crushing and casting of material.

Elevation	Example Elevation (m ASB) – 30 m Water Depth	Vertical Distribution (%) of Sediments
3.0 m (ASB)	3	16
2.5 m (ASB)	2.5	16
2.0 m (ASB)	2	16
1.0 m (ASB)	1	22
0.5 m (ASB)	0.5	30

5.6.7   Representation of SHB/TSHD Propeller-Wash

Modelling of sediments suspended by propeller-induced motion at the seabed was conducted to estimate likely sediment concentrations generated by the TSHD and SHB propellers while manoeuvring during trenching operations. A specialised numerical model developed by RPS, named PROPMAP, was used to estimate a time- and space-varying rate of sediment flux from the seabed due to the thrust imposed by each vessel's propellers at the seabed level behind the moving vessel. The model uses characteristics of the vessel of interest to estimate the three-dimensional thrust-field generated by the propellers. This thrust-field is then combined with the grain size and degree of cohesion of the seabed sediments, and the varying under-keel clearance along the typical vessel paths, to calculate variations in the suspended sediment flux from the seabed in time and space.

The following details were used as input to PROPMAP to calculate variable rates of sediment flux from the seabed due to propeller-wash effects:

- Vessel tracks and speeds.

- Vessel draft, engine power and propeller size.

- Bathymetry along the vessel tracks.

- Grain size distributions of the sediment, defining the proportions of clay and silt along the vessel tracks.

The calculation steps applied by PROPMAP at discrete intervals along each vessel path were as follows:

- Based on the vessel's engine power and propeller size, determine the propeller-induced velocity profile.

- Based on the vessel's draft and the local bathymetry, determine the intersection of the thrust-field with the seabed and find the thrust imposed on it.

- Based on the velocity of water flow at the seabed, calculate the shear stress acting on it.

- Based on the calculated shear stress, and the sediment grain size and cohesiveness, calculate a theoretical erosion flux (mass per unit time) for seabed sediment.

Propeller-induced velocity profiles were calculated using empirical expressions from Blaauw & van de Kaa (1978). Thrust at the seabed will depend upon the level of the bed, which will intersect as a plane (Figure 5.4). For an under-keel clearance of 1 m, a velocity field exceeding 5 m/s would intersect the bed in this example, while at a clearance of 4 m the bed velocity would be reduced to <2 m/s. The influence of this thrust will vary with the sediment grain size. Consequently, outcomes will be sensitive to the magnitude of the thrust, the under-keel clearance and the PSD of the bed.

Sediment erosion flux was estimated from the derived velocity field using the empirical formulations of van Rijn (1989). The sediment flux component attributable to propeller-wash was found to be depth-limited for areas where the under-keel clearance was less than 3 m, assuming a fully-loaded vessel (maximum draft). Simulations over deeper areas, including the areas where vessels would transit to the spoil grounds, indicated that flux would be minimal (compared to other sources) and representative of short-lived suspension of the surface-layer sediments followed by rapid settlement. This settlement time was estimated to be shorter than the simulation output time step. Propeller-wash was found to be more significant in the shallow areas and would be greater over sediments previously suspended by dredging.

These findings were used to inform the definition of the sediment flux rates during TSHD dredging operations (see Section 5.6.4).

In summary, propeller-wash effects were considered: (i) along each pipeline section during trenching; (ii) between each pipeline section and the spoil grounds during disposal.

In the absence of definitive information relating to the seabed composition of the areas traversed by the SHB or TSHD between the pipeline, and spoil ground for simplicity the seabed composition was assumed to be described by the PSD of the area from which the vessel began its journey.
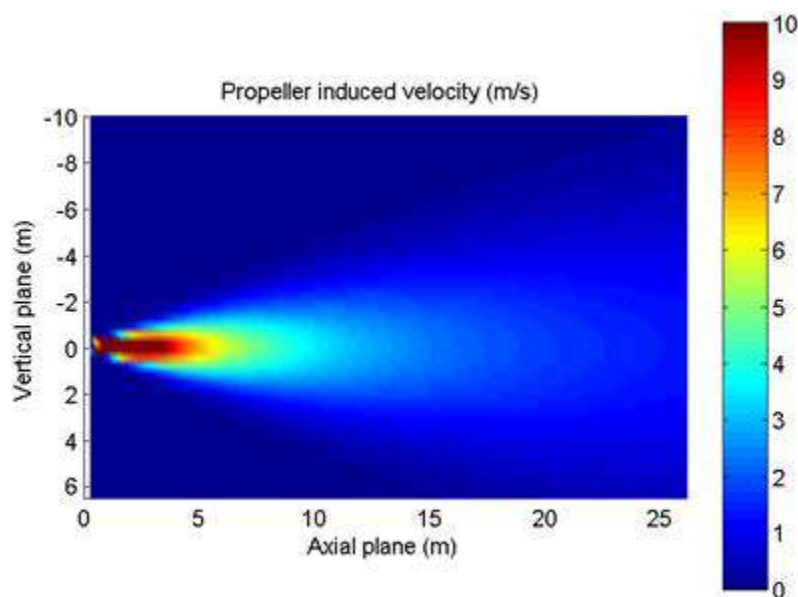
Figure 5.4   Two-dimensional view of a propeller-induced velocity profile.

5.6.8 Summary of Source Rates

For each source of suspended sediment plumes during trenching and disposal operations, as described in the preceding sections, Table 5.31 and Table 5.32 summarise the associated loss rates and approximate volumes of suspended sediment expected. The volumes assigned to the respective non-overflow and overflow periods for TSHD trenching, and non-dewatering period for BHD trenching, are based on the modelled cycle times detailed in Table 5.4 and Table 5.5.

A total of approximately 23,489 m^3 of sediment is expected to be initially suspended in the water column over the course of the modelled program. This volume represents approximately 7.7% of the *in situ* trenched volume (306,212 m^3, see Table 5.7). If all deposited material assumed to be available for potential resuspension following spoil ground disposal operations is actually resuspended, a total of 41,245 m^3 of sediment will be suspended in the water column over the program duration; this will represent approximately 13.5% of the *in situ* trenched volume.

Table 5.31   Summary of sediment sources applied in the model.

Operation	Source Rate (% Production Rate)	Trenched Volume (m^3)	Suspended Volume (m^3)
BHD excavator bucket	2.10	22,220	511
BHD excavator bucket + dewatering from SHB	2.40		
Disposal from SHB	5 (water column)		1,085
	5 (seabed; potential)		*1,085*
TSHD draghead + propeller-wash	0.60	281,725*	6,004
TSHD draghead + propeller-wash + overflow	Specified per zone (see table below)		
Disposal from TSHD	5 (water column)		13,786
	5 (seabed; potential)		*13,786*
CSD draghead + casting behind	0.5 (cutterhead)	90,672	*453*
	5 (casting behind)		*4,534*
Totals		**394,617***	**23,489** *41,245*

* Note these volumes include the proportion of material that has been crushed by CSD and subsequently picked up by TSHD, therefore this material is included twice. The total *in situ* trenched volume is 306,212 m^3 (Table 5.7).

Table 5.32   Sediment source rates applied in the model for the TSHD while overflowing.

Pipeline Zone	Source Rate (% Production Rate)	
	Pre-Sweep Material	**Post-Sweep Material**
Pre-Sweep Area 1	2.80	-
Trench Zone 3	2.62	1.86
Trench Zone 4	3.47	1.86
Pre-Sweep Area 2	2.22	-
Trench Zone 5	1.73	1.29
Pre-Sweep Area 3	3.13	-
Trench Zone 6	3.25	1.80
Trench Zone 7	3.01	1.87
Sand Waves Area	1.20	-

6 ENVIRONMENTAL THRESHOLD ANALYSIS

Predictions of SSC and sedimentation for each scenario were assessed against a series of water quality and sedimentation thresholds to categorise the modelled outcomes into management zones of influence and impact, defined with regard to environmental sensitivities in the study region. The thresholds and the approach to be applied to the DPD project are based on the extensive environmental monitoring and threshold work that INPEX completed for the Ichthys project environmental impact statements, and its capital and maintenance dredge management plans in Darwin Harbour (INPEX, 2010, 2011, 2013, 2018).

6.1 Thresholds

To calculate areas of potential impact from trenching-induced excess SSC and sedimentation, INPEX established seasonal tolerance limits/thresholds for sensitive receptors including mangrove, seagrass and hard coral habitats (Table 6.1). The INPEX tolerance limits for SSC were derived from its comprehensive site-specific water quality monitoring data (covering multiple years and locations), and the tolerance limits for sedimentation were derived from habitat-specific dose-response experiments and field observations reported in the scientific literature (INPEX, 2018). The defined tolerance limits also varied across four trenching impact reporting zones, which were defined based on available water quality monitoring data (INPEX, 2018). The trenching impact reporting zones are named as follows, with the spatial extents agreed for this study shown in Figure 6.1:

- East Arm.
- Middle Arm.
- Middle Harbour.
- Offshore.

Table 6.1   Tolerance limits for excess SSC and sedimentation (INPEX, 2018).

Habitat	Trenching Impact Reporting Zone	Season	SSC (mg/L)	Sedimentation (mm)
Mangrove	Anywhere	All	N/A	50
Coral	East Arm	Dry	11.9	15
		Wet	23.8	
	Middle Arm	Dry	12.4	15
		Wet	27.0	
	Mid Harbour	Dry	10.7	15
		Wet	28.4	
	Offshore	Dry	17.9	15
		Wet	64.2	
Seagrass	Anywhere	Dry	13.3	40
		Wet	60.6	
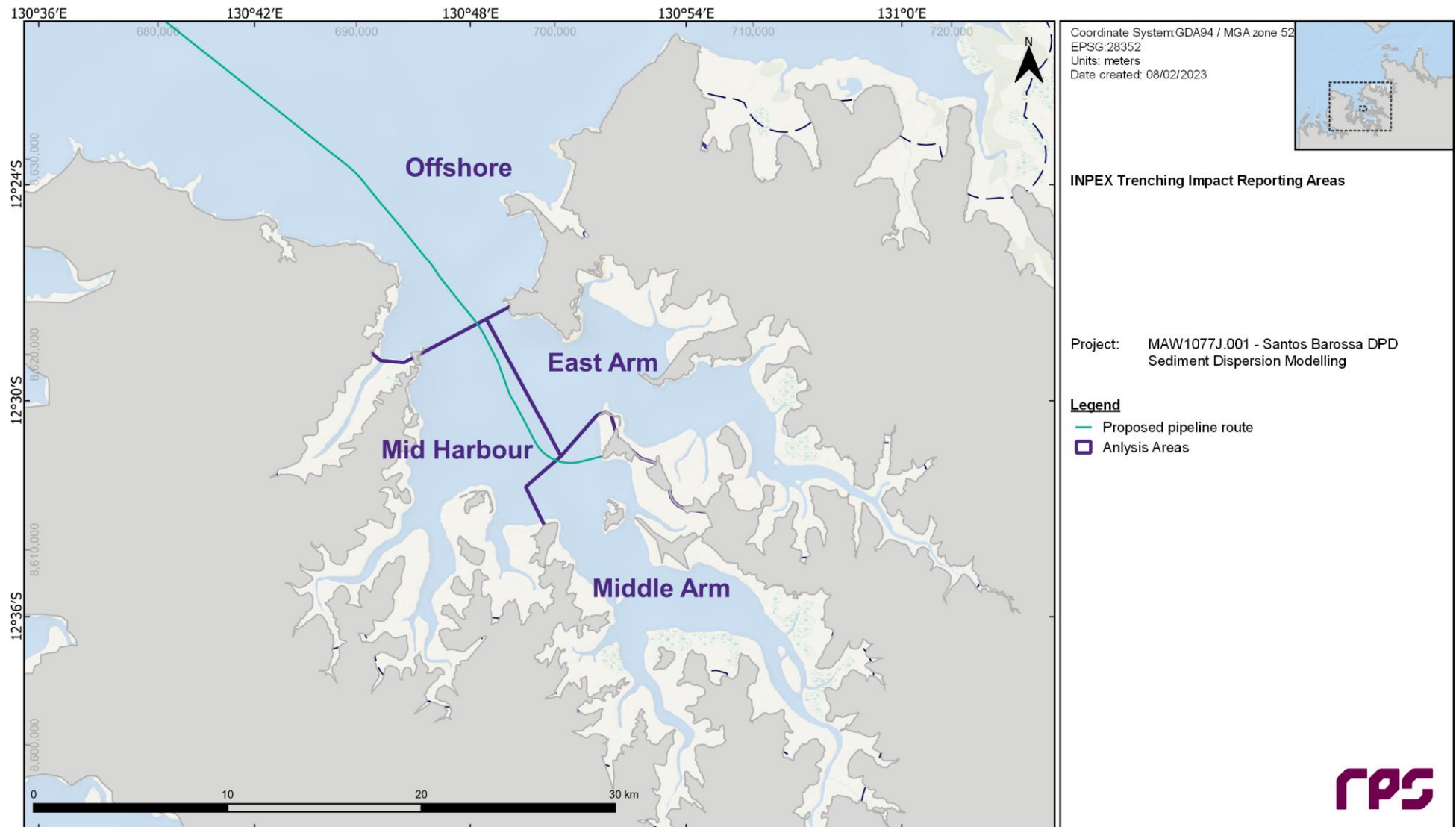
Figure 6.1 Delineation of the proposed trenching impact reporting zones (East Arm, Middle Arm, Mid Harbour and Offshore) based on INPEX, 2010. Thresholds used to define the management zones will vary in magnitude between the trenching impact reporting zones.

6.2   Management Zones

Three management zones were defined in the approach applied by INPEX (2010, 2011, 2013, 2018), based on varying levels of impact on sensitive receptor communities: a Zone of High Impact (ZoHI), a Zone of Moderate Impact (ZoMI), and a Zone of Influence (ZoI). The definition of each of these management zones, and how the thresholds have been applied to the sediment dispersion modelling results to determine the predicted management zones for the proposed trenching and disposal program, is presented in the following sections.

6.2.1   Zone of High Impact

The Zone of High Impact (ZoHI) is defined as the area where direct impact from trenching and disposal will occur, such as removal of substrate or smothering of substrate (INPEX, 2018). Predicted impacts within this zone are expected to be severe and often irreversible. This zone includes the top width of the trench footprint and disposal area with a 20 m buffer extending outwards from these areas. The results from the sediment dispersion modelling will have no effect on the outline of the ZoHI as it is defined here, and as such this zone is not presented in this report.

6.2.2   Zone of Moderate Impact

The Zone of Moderate Impact (ZoMI) is defined as the area where sensitive receptor communities are predicted to be indirectly impacted by elevated SSC and sedimentation due to trenching and disposal activities (INPEX, 2018). Damage/mortality of sensitive receptor communities may occur, but the disturbed areas are considered to have good potential for recovery.

Sensitive receptors are within the ZoMI if their respective ecological tolerance limits for SSC are exceeded for 10% of the time or where the simulated sedimentation thickness exceeds their respective sedimentation tolerance limits at the end of the simulation (INPEX, 2018). For this project the maximum sedimentation thickness predicted at any time throughout the trenching operations was used for comparison against the sedimentation tolerance limits. Due to the variable nature of the sedimentation with tidal cycles and the strong currents in Darwin Harbour, larger amounts of sedimentation may occur earlier in the trenching program.

The predicted ZoMI based on exceedances of the thresholds for SSC was evaluated over the duration of each trenching scenario by:

- Creating a three-dimensional time series (hourly) of trenching-excess SSC values in each model grid cell for the entire trenching program.
- Calculating the 90th percentile SSC value of each cell (i.e. the value that is exceeded 10% of the time).
- Assessing the 90th percentile data against the seasonal threshold SSC values for each sensitive receptor habitat type and trenching impact reporting zone.

The predicted ZoMI based on exceedances of the thresholds for sedimentation was evaluated over the duration of each trenching scenario by:

- Calculating the maximum trenching-excess sedimentation thickness values in each model grid cell for the entire trenching program. A density of 700 kg/m^3 was assumed for newly deposited sediments in the modelling based on field observations of the *in situ* density of surface material present over the mangrove areas of Darwin Harbour (INPEX, 2009).
- Assessing the maximum trenching-excess sedimentation thickness data against the seasonal threshold sedimentation thickness values for each sensitive receptor habitat type and trenching impact reporting zone.

The overall predicted ZoMI for each scenario was then calculated by combining both of the predicted ZoMIs from exceedance of thresholds for SSC and sedimentation thickness.

6.2.3   Zone of Influence

The Zone of Influence (ZoI) is defined as the area where sensitive receptor communities are predicted to be indirectly influenced by elevated SSC and sedimentation (INPEX, 2018). Sensitive receptor communities may,

at some time experience detectable elevations in SSC and sedimentation (beyond expected background levels). However, no sublethal stress or mortality of benthic communities is expected to occur (INPEX, 2018).

Sensitive receptor communities are predicted to be indirectly influenced where their respective ecological tolerance limits for SSC are exceeded for 5% of the time or where the simulated sedimentation thickness exceeds 3 mm at the end of the simulation (INPEX, 2018). For this project the maximum sedimentation thickness predicted at any time throughout the trenching operations was used for comparison against the 3 mm sedimentation tolerance limit. Due to the variable nature of the sedimentation with tidal cycles and the strong currents in Darwin Harbour, larger amounts of sedimentation may occur earlier in the trenching program.

The predicted ZoI based on exceedances of the thresholds for SSC was evaluated over the duration of each trenching scenario by:

- Creating a three-dimensional time series (hourly) of trenching-excess SSC values in each model grid cell for the entire trenching program.
- Calculating the 95th percentile SSC value of each cell (i.e. the value that is exceeded 5% of the time).
- Assessing the 95th percentile data against the seasonal threshold SSC values for each sensitive receptor habitat type and trenching impact reporting zone.

The predicted ZoI based on exceedances of the thresholds for sedimentation was evaluated over the duration of each trenching scenario by:

- Calculating the maximum trenching-excess sedimentation thickness values in each model grid cell for the entire trenching program. A density of 700 kg/m^3 was assumed for newly deposited sediments in the modelling based on field observations of the *in situ* density of surface material present over the mangrove areas of Darwin Harbour (INPEX, 2009).
- Assessing the maximum dredge excess sedimentation thickness data against the 3 mm tolerance limit.

The overall predicted ZoI for each scenario was then calculated by combining both of the predicted ZoIs from exceedance of thresholds for SSC and sedimentation thickness.

7 RESULTS OF SEDIMENT FATE MODELLING

7.1 General Plume Movement

7.1.1 Summary

Simulations indicated that there may be significant spatial patchiness in the distribution of SSC and sedimentation at any point in time during the trenching and disposal operations because of variability in the number of sediment suspension sources, variability in the flux from each of these sources, and the varying dynamics of the transport, settlement and resuspension processes affecting the sediments.

The SSC results presented in the following section are depth-averaged. It should be noted, however, that there is significant variability in the vertical distributions of SSC in the water column, with a distinct increase in concentration towards the seabed. Most material will initially be suspended low in the water column, and material suspended higher in the water column will sink as it moves away from the source. Frequent resuspension of material will also mostly affect the lower reaches. Thus, the spatial area affected above a given concentration is typically greater in the near-seabed layer than in the near-surface layer. Nonetheless, there are instances throughout the simulations where elevated concentrations will occur in the near-surface layers – during SHB/TSHD disposal operations, or during strong resuspension events affecting sediments that have migrated to shallow areas – but these will typically not be sustained for extended periods of time.

The localised movement and dispersion of the trenching-generated suspended sediment is governed over short time scales by the tide, with very strong tidal flows in the areas where trenching is planned to occur and at the offshore disposal ground. Most of the activities related to trenching of the pipeline route will take place within Darwin Harbour, which is dominated by tidal currents year-round and is relatively sheltered from the variations in large-scale circulation observed offshore. Beyond the harbour entrance, superimposed on the tidal motion is the gradual migration of sediment due to the wind-driven residual component of the current, which drives some seasonal differences in the overall drift patterns of the suspended sediments. However, given the strength of the tidal currents even in the area offshore of the harbour the seasonal differences are small. The sediment plume extends slightly more southwards during the winter/dry season scenario and slightly more northwards during summer/wet season scenario.

7.1.2 Plume Movement over the Spring and Neap Tide

Given the dominance of the tidal flows in the Darwin area the typical sediment plume movements are predicted to reflect the oscillations of the ebbing and flooding tide. Figure 7.1 and Figure 7.2 show example two-hourly snapshot sequences of modelled sediment plume movement during a spring tide cycle and a neap tide cycle, respectively, in the winter/dry season scenario. On the ebbing tide sediment plumes from trenching at zones within the harbour are predicted to move towards the harbour entrance, or in a north-westerly direction parallel to the coast for the trenching zones outside the harbour entrance. On the flooding tide the sediment plumes from trenching zones outside and near the harbour entrance are predicted to move into the harbour, typically staying close to the western side (Woods Inlet and West Arm), and at trenching zones inside the harbour the sediment plumes move deeper into the harbour, extending south into Middle Arm. At the proposed offshore disposal site sediment plumes from disposal operations move south-west towards Darwin Harbour on the ebbing tide and north-east towards Clarence Strait on the flooding tide. As is expected, the predicted plume drift trajectories during the spring tide periods are much longer than during neap tide periods, with the suspended material being more widely dispersed and SSC becoming patchy.

Figure 7.3 and Figure 7.4 show example two-hourly snapshot sequences of modelled sediment plume movement during a spring tide cycle and a neap tide cycle, respectively, in the summer/wet season scenario. The figures reveal the patterns of plume movement are very similar to those of the winter/dry season scenario, which is expected given the dominance of the tide on the hydrodynamics of Darwin Harbour and Beagle Gulf.

Project commencement in dry season
All operations - Trenching and Spoil Disposal
Suspended Sediment Concentration [mg/L]
Spring tide - 21st April 2019

Project: MAW1077J.001 - Santos Barossa DPD Sediment Dispersion Modelling

Coordinate System: GDA94 / MGA zone 52
EPSG:28352
Units: meters
Date created: 09/02/2023

Legend

— Proposed pipeline route
— Spoil ground
■ Trenching areas
— Pre-sweep areas
— Sand waves area

SSC [mg/L]

□ 1 - 2.5
□ 2.5 - 5
□ 5 - 10
□ > 10

Figure 7.1 **Example two-hourly snapshots of modelled sediment plume movement during a nominal spring tide cycle in the winter/dry season scenario (based on 21 April 2019 6am to 2pm, flooding to ebbing tide). At this point in the simulation the TSHD is working near the northern end of Trench Zone 6, the CSD is working near the southern end of Trench Zone 6, and the BHD is working in Trench Zone 1. Note the trenching area widths shown on this and other Figures in this report are exaggerated to aid visual clarity.**

Figure 7.2 **Example two-hourly snapshots of modelled sediment plume movement during a nominal neap tide cycle in the winter/dry season scenario (based on 15-16 April 2019 8pm to 6am, ebbing to flooding tide). At this point in the simulation the TSHD is working in Trench Zone 6, the CSD is working in Trench Zone 5, and the BHD is working in Trench Zone 1. Note the trenching area widths shown on this and other Figures in this report are exaggerated to aid visual clarity.**
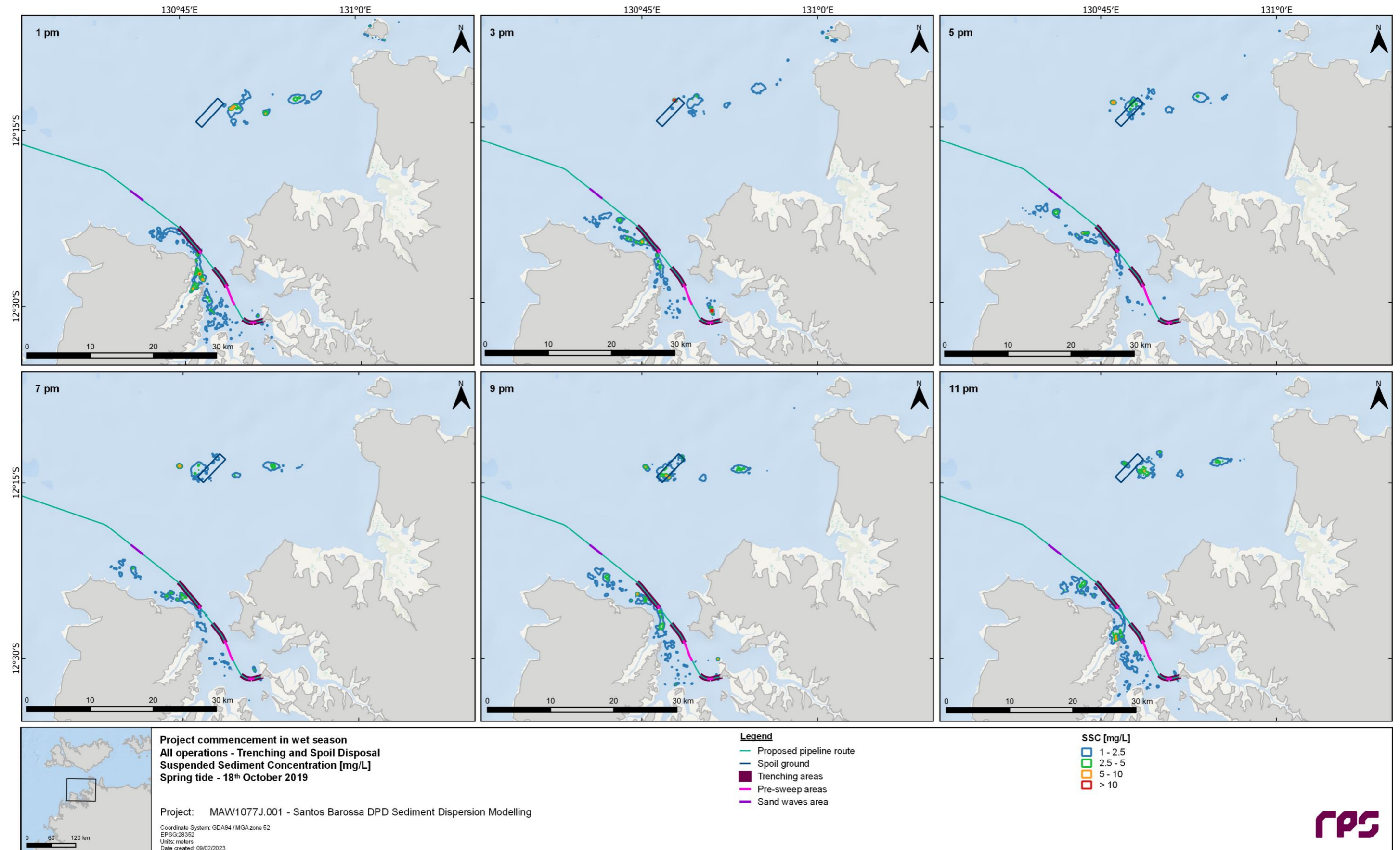
Figure 7.3 **Example two-hourly snapshots of modelled sediment plume movement during a nominal spring tide cycle in the summer/wet season scenario (based on 18 October 2019 1pm to 11pm, from high tide ebb to slack tide to high tide flood). At this point in the simulation the TSHD is working in Trench Zone 6, the CSD is working in Trench Zone 5, and the BHD is working in Trench Zone 1. Note the trenching area widths shown on this and other Figures in this report are exaggerated to aid visual clarity.**
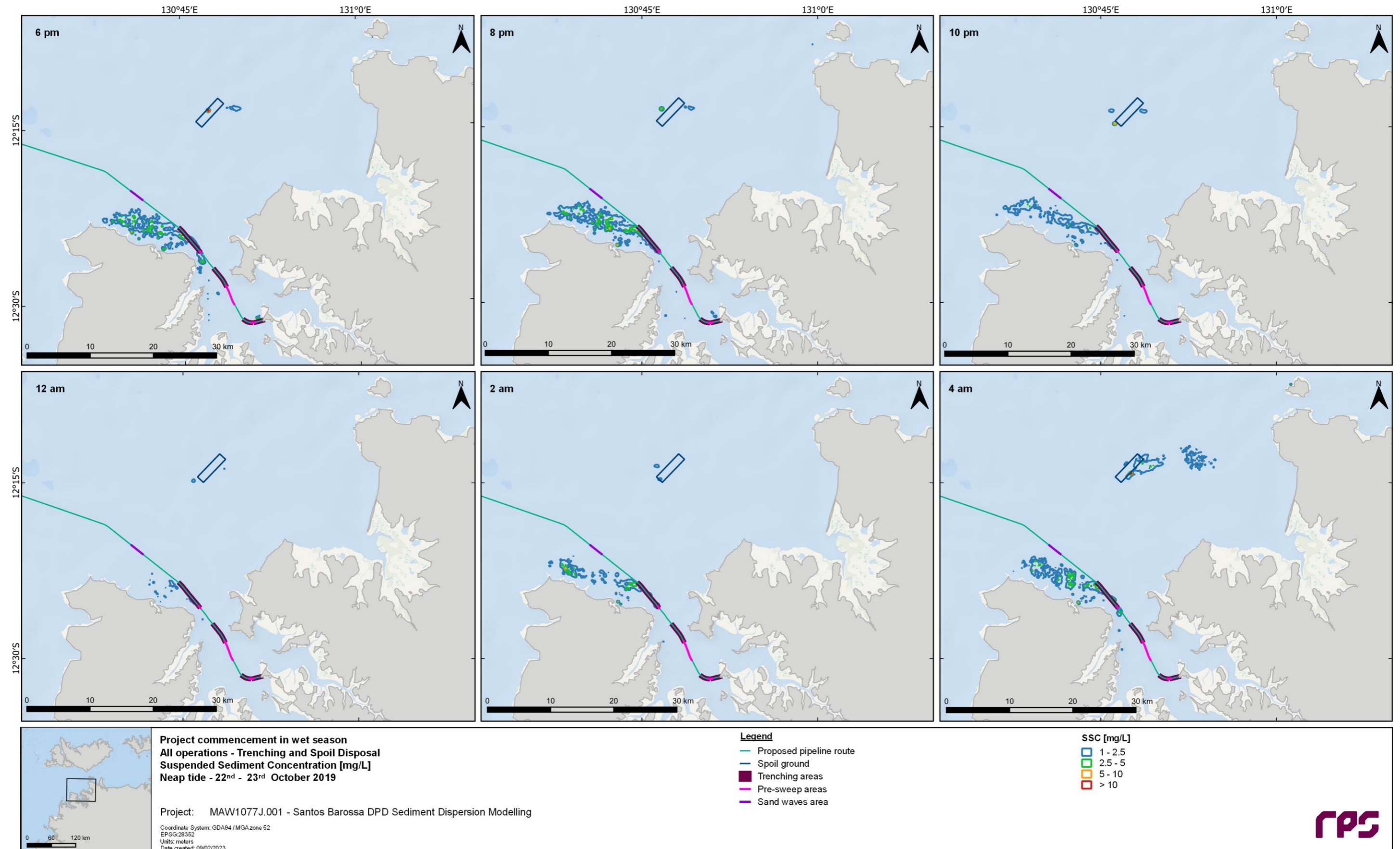
Figure 7.4 Example two-hourly snapshots of modelled sediment plume movement during a nominal neap tide cycle in the summer/wet season scenario (based on 22-23 October 2019 6pm to 4am, ebbing to slack tide to flooding). At this point in the simulation the TSHD is working in Trench Zone 7, the CSD is working in Trench Zone 6, and the BHD is working in Trench Zone 1. Note the trenching area widths shown on this and other Figures in this report are exaggerated to aid visual clarity.

7.1.3   Plume Movement at the Disposal Ground

The localised movement and dispersion of the suspended sediment generated by disposal/dumping at the offshore disposal area is also dominated over short time scales by the tide, with very strong tidal flows at the offshore disposal ground. As such, the movement of the predicted suspended sediment plumes reflect the ebbing and flooding tidal oscillations with longer trajectories during spring tides and shorter trajectories during neap tides. Additional variability occurs at the disposal area due to the sporadic nature of the disposal sources, which are variable in time and space.

To show more clearly the predicted variability and persistence of suspended sediment plumes generated by dumping at the offshore disposal area, and the potential for interaction of plumes from consecutive disposals, a more detailed snapshot sequence (hourly and zoomed to the disposal area) of depth-averaged SSC for a typical spring and neap tide sequence in the winter/dry season scenario has been presented. Figure 7.5 and Figure 7.6 present hourly depth-averaged SSC snapshots for a 12-hour period during a typical spring tide, while Figure 7.7 and Figure 7.8 present hourly snapshots for a 12-hour period during a typical neap tide. Disposal times from the TSHD and BHD are outlined in each caption and individual disposal plumes are identified with dashed circles overlaid on the panels.

The snapshot sequences show that during spring tide periods the interaction between suspended sediment plumes from consecutive disposals is minimal, due to the rapid movement and dispersion of the plumes. The exception to this is when the timings and locations of disposals from the TSHD and BHD are close together (see dashed circles 1 and 2 in Figure 7.5 and Figure 7.6). It should be noted that the SSC generated from BHD disposals is predicted to be significantly lower than for TSHD disposals, due to the lower volume of material in each load. During neap tide periods, when plume movement is slower and trajectories are shorter, there is more potential for interaction between consecutive disposals; however, the predicted depth-averaged SSC of the interacting plumes remains relatively low.
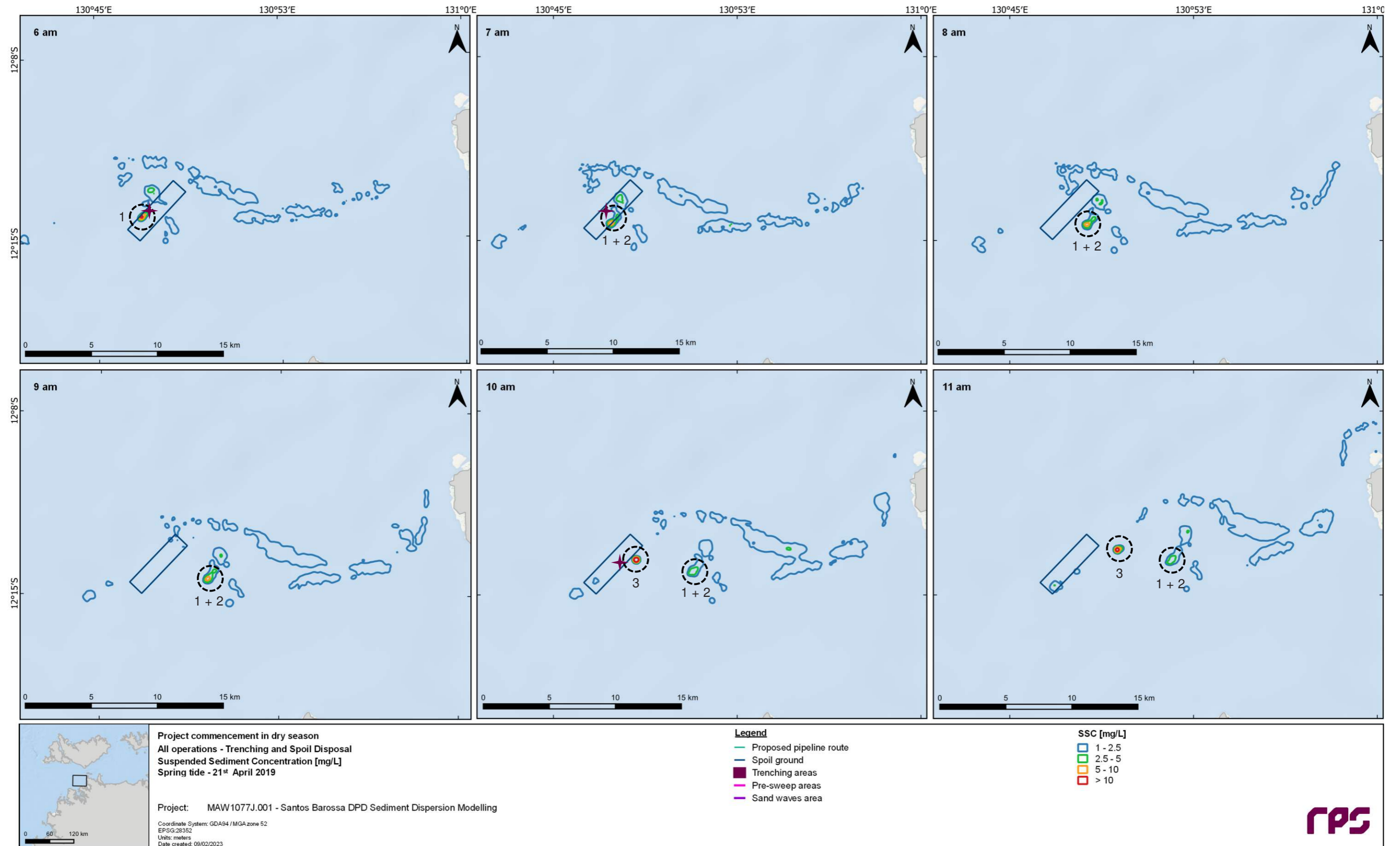
Figure 7.5 Example hourly snapshots of modelled sediment plume movement at the spoil ground during a nominal spring tide cycle in the winter/dry season scenario (based on 21 April 2019 6am to 11am, flooding to start of ebbing tide). At this point in the simulation, disposals from the TSHD occur at 5:10am, first seen in the 6am snapshot (dashed circle 1) and at 9:40am, first seen in the 10am snapshot (dashed circle 3), and a disposal from the BHD occurs at 6:10am, first seen in the 7am snapshot (dashed circle 2). The purple crosses show the location of disposals that have occurred prior to the snapshot in which the associated plumes first appear.
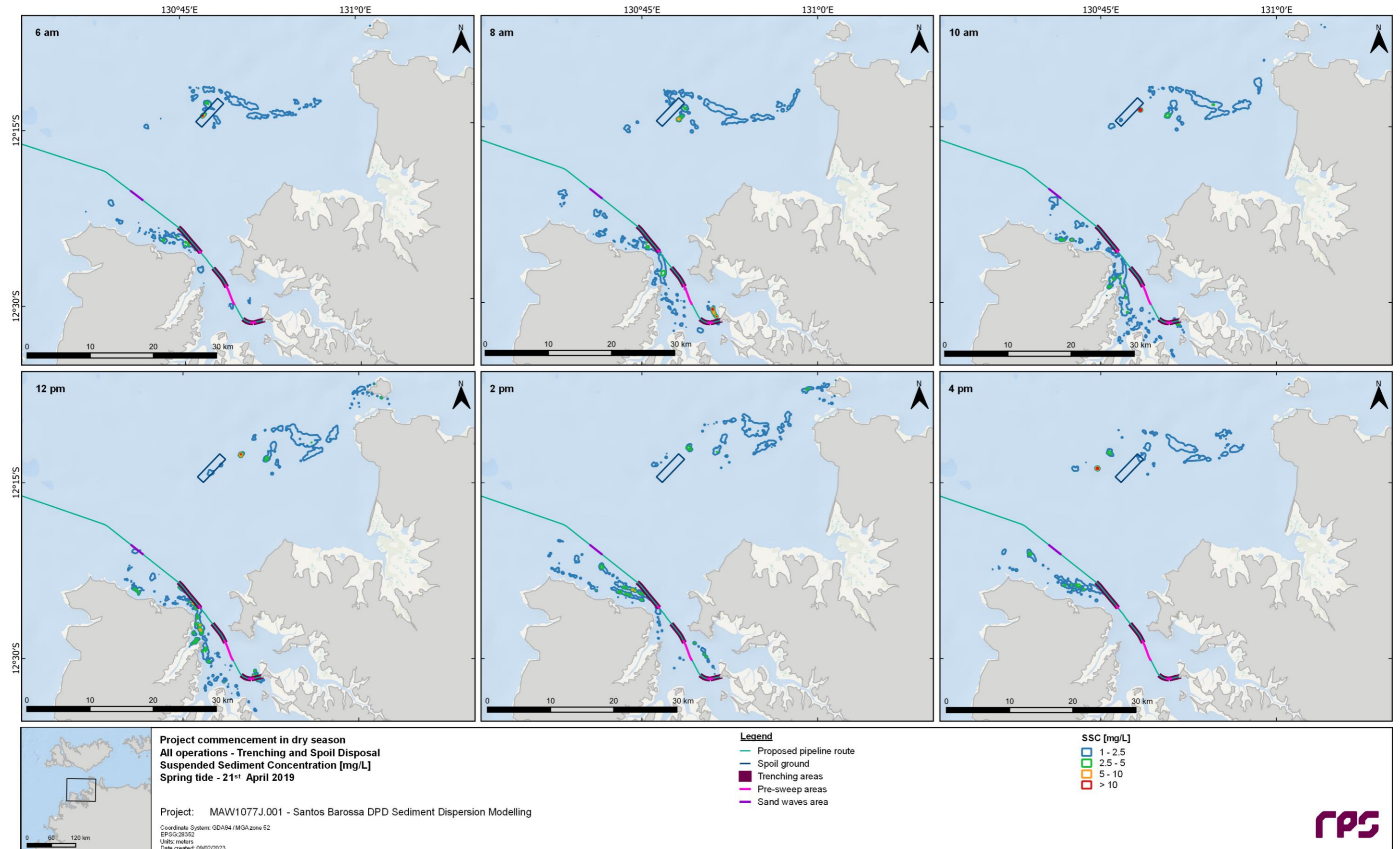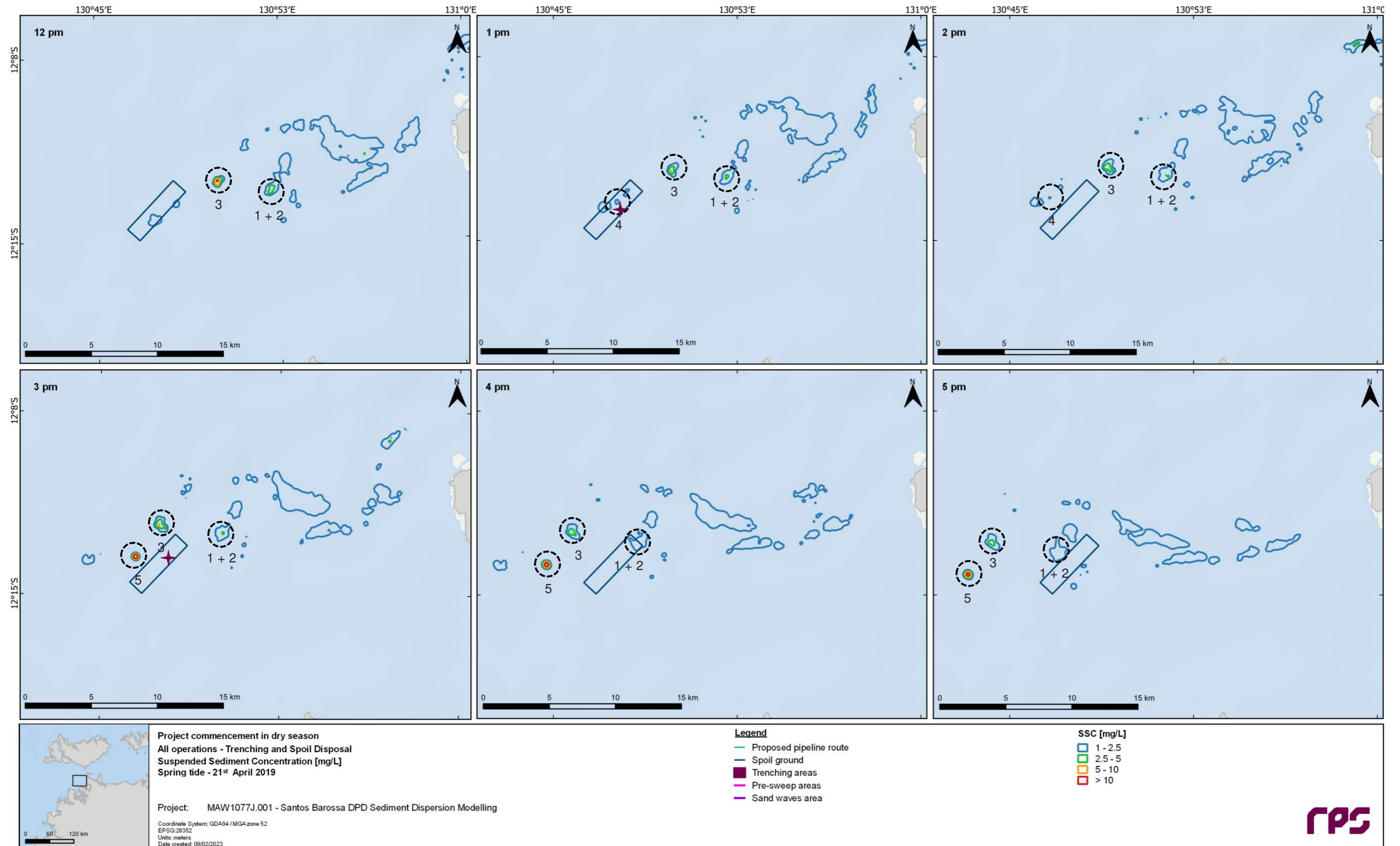
Figure 7.6 Example hourly snapshots of modelled sediment plume movement at the spoil ground during a nominal spring tide cycle in the winter/dry season scenario (based on 21 April 2019 12pm to 5pm, ebbing tide). At this point in the simulation, a disposal from the TSHD occurs at 2:05pm, first seen in the 3pm snapshot (dashed circle 5), and a disposal from the BHD occurs at 12:30pm, first seen in the 1pm snapshot (dashed circle 4). The purple crosses show the location of disposals that have occurred prior to the snapshot in which the associated plumes first appear.
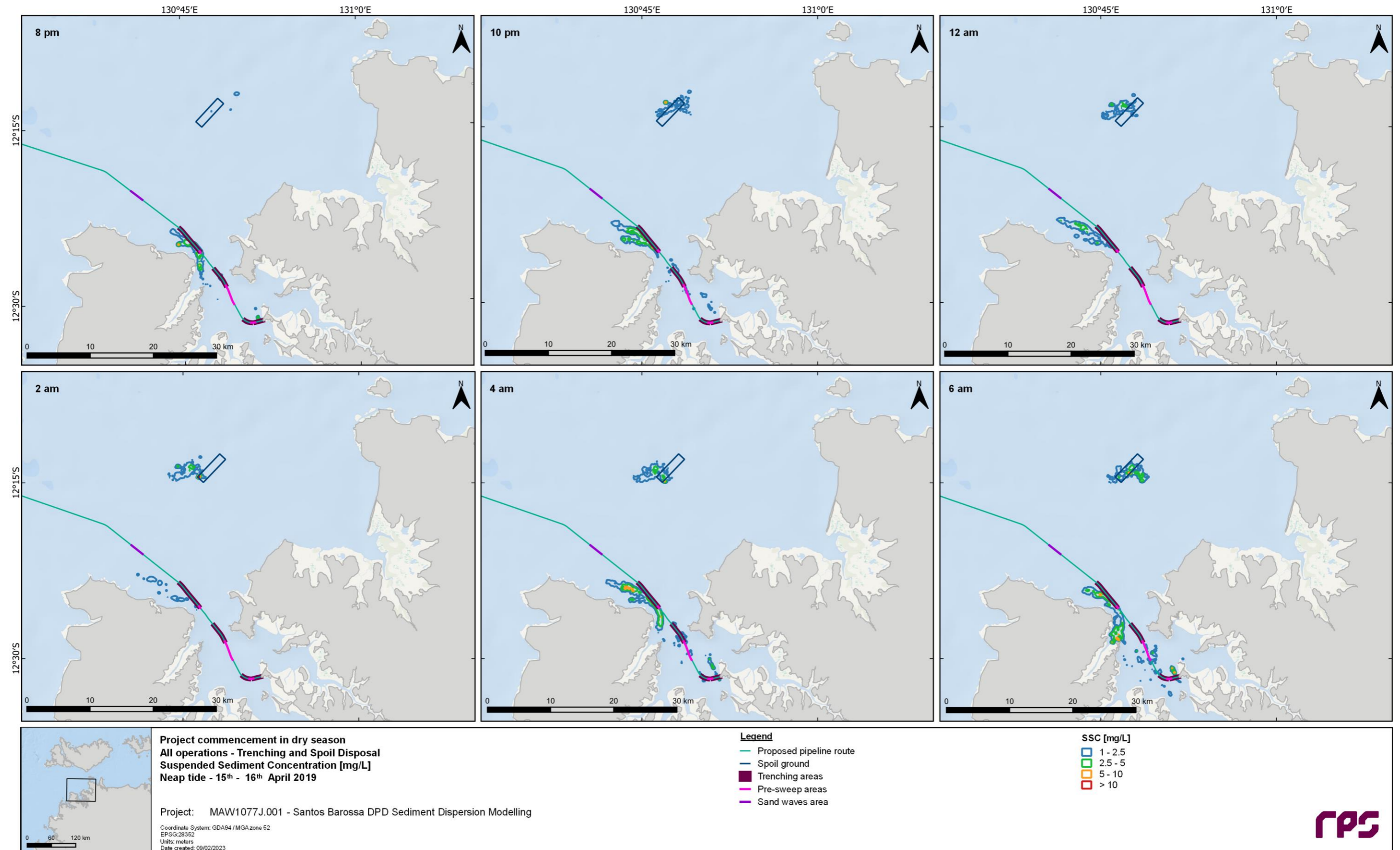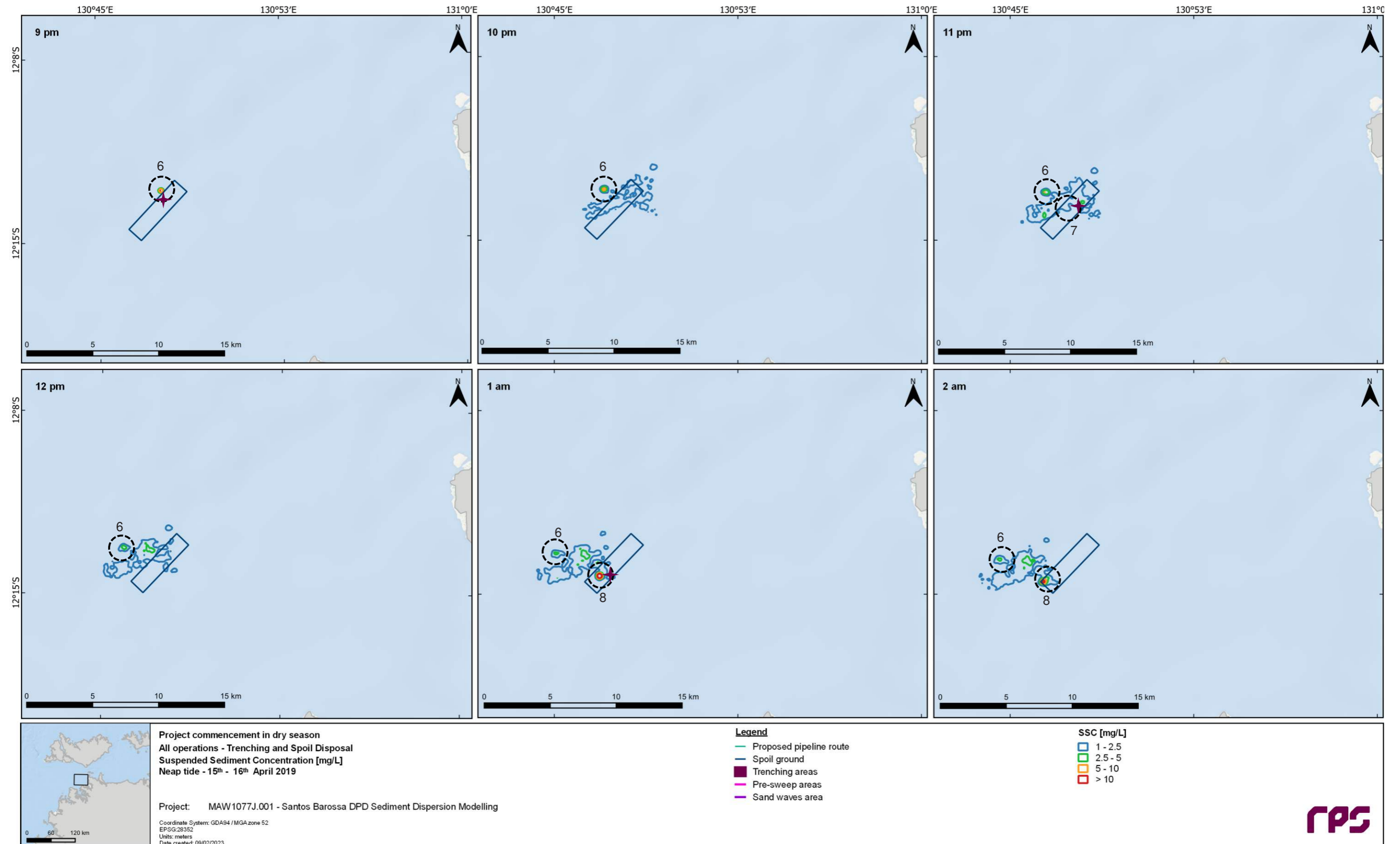
Figure 7.7 Example hourly snapshots of modelled sediment plume movement at the spoil ground during a nominal neap tide cycle in the winter/dry season scenario (based on 15-16 April 2019 9pm to 2am, ebbing tide). At this point in the simulation, disposals from the TSHD occur at 8:10pm, first seen on the 9pm snapshot (dashed circle 6) and at 12:36am, first seen on the 1am snapshot (dashed circle 8), and a disposal from the BHD occurs at 10:10pm, first seen on 11pm snapshot (dashed circle 7). The purple crosses show the location of disposals that have occurred prior to the snapshot in which the associated plumes first appear.
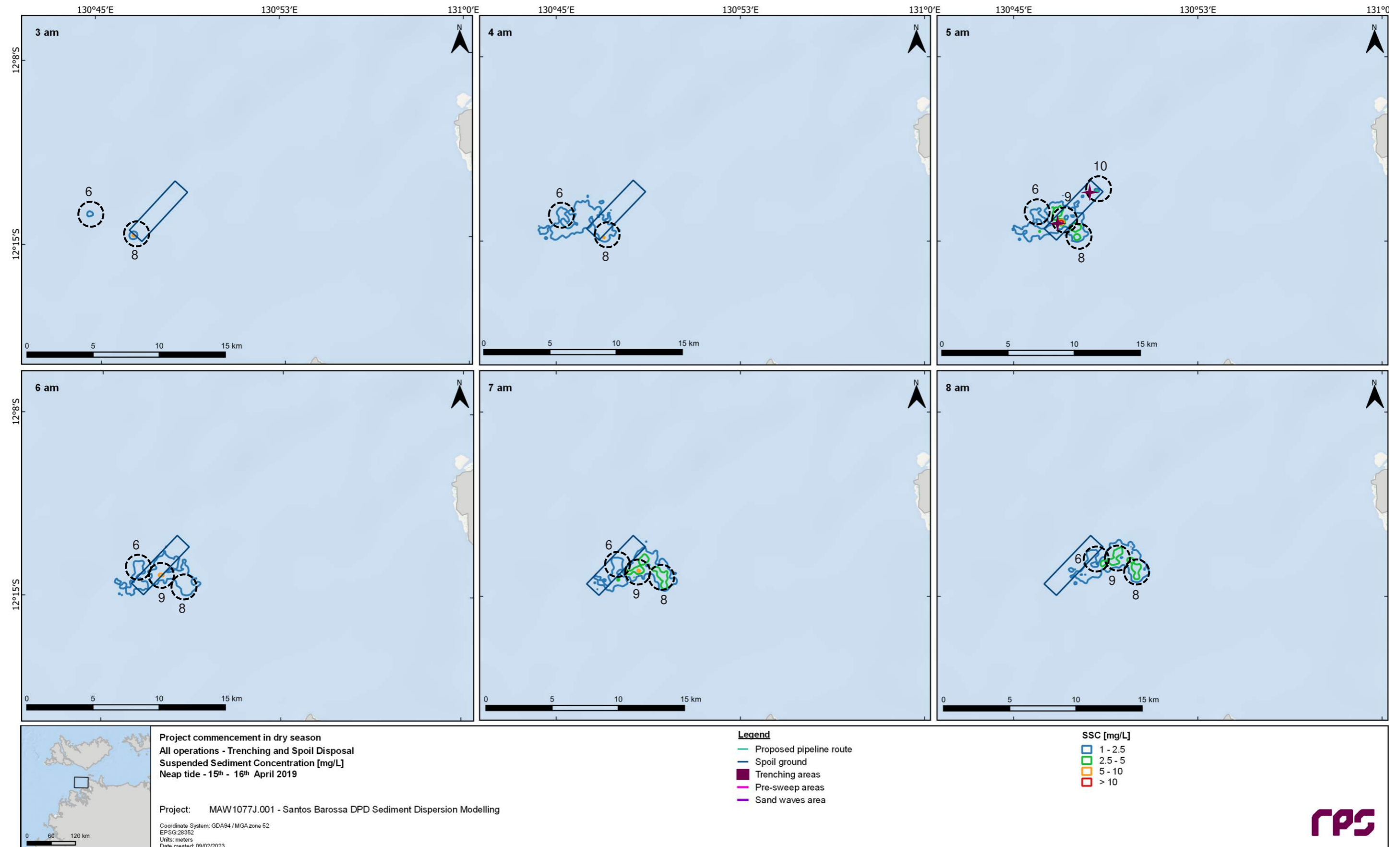
Figure 7.8 Example hourly snapshots of modelled sediment plume movement at the spoil ground during a nominal neap tide cycle in the winter/dry season scenario (based on 16 April 2019 3am to 8am, flooding tide). At this point in the simulation, disposals from the TSHD occur at 4:55am, first seen on the 5am snapshot (dashed circle 9) and BHD occur at 4:35 am, first seen on the 5am snapshot (dashed circle 10). The purple crosses show the location of disposals that have occurred prior to the snapshot in which the associated plumes first appear.

7.2   Spatial and Temporal Characteristics of SSC

7.2.1   Spatial Distribution of SSC

The results observed on any given day will not always be representative of the typical transport patterns, and plume concentrations and distributions are forecast to vary markedly. To explore this variability, statistical distributions for each scenario are examined. Percentile distributions will summarise the outcomes over the duration of the trenching and disposal operations (not including the run-on period) and do not represent an instantaneous plume footprint at any point in time.

Forecasts of median depth-averaged SSC values (values exceeded 50% of the time) do not exceed 1 mg/L in both seasonal scenarios, while at the 80th percentile values 1 mg/L or greater are forecast to be found in small, isolated patches just offshore of West Point (in line with Trench Zone 6) and at Wickham Point near the shore crossing area.

At the 90th percentile, the winter/dry season scenario forecasts show depth-averaged SSC values 1 mg/L or greater are found in a continuous band stretching north-westwards parallel with the coast to just offshore Charles Point, and southwards into Darwin Harbour extending a short way into Woods Inlet and to the eastern side of Talc Head. Smaller patches above 1 mg/L are predicted at other locations: around Wickham Point, in the middle Harbour area, in the vicinity of the proposed offshore disposal site, and in the shallows at South West Vernon Island (Figure 7.9). The corresponding summer/wet season scenario forecast shows a similar spatial area affected by SSC levels above 1 mg/L with some slight seasonal differences evident (Figure 7.11). In the summer/wet season scenario, the predicted 90th percentile SSC forecast shows the largest band above 1 mg/L has a shorter extent to the south and does not extend into Woods Inlet, a slightly larger area in the middle Harbour, and an extension of 1 mg/L concentrations to the north-east at the offshore disposal site.

At the 95th percentile, the winter/dry season scenario forecasts show depth-averaged SSC values 1 mg/L or greater are found in a continuous band stretching north-westwards parallel with the coast past Charles Point, and southwards into Darwin Harbour extending a short way into Woods Inlet and West Arm, with smaller patches above 1 mg/L extending from Wickham Point into the middle Harbour and a short way into Middle Arm. Depth-averaged SSC values 1 mg/L or greater are also found in the vicinity of the proposed offshore disposal site extending outwards to the east and west, with a larger extent to the east (Figure 7.10). Some very small patches above 1 mg/L are predicted in the shallows at South West Vernon Island. As found in the 90th percentile SSC distributions, the corresponding summer/wet season forecast shows a similar spatial area above 1 mg/L with some slight seasonal differences (Figure 7.12). Again, during the summer/wet season the largest band above 1 mg/L has a shorter extent to the south and there is an extension of 1 mg/L concentrations to the north-east at the offshore disposal site.

In both scenarios the 95th percentile depth-averaged SSC values are predicted to exceed 2.5 mg/L (but remain below 5 mg/L) in isolated patches in the vicinity of Trench Zone 6, extending ~8 km north-west and also south into Woods Inlet in the winter/dry season scenario, and extending ~13 km north-west with only minimal extent to the south in the summer/wet season scenario. Additionally, in both seasons the 95th percentile depth-averaged SSC values are predicted to exceed 2.5 mg/L in a relatively small patch extending north from Wickham Point and a very small patch in the shallows at South West Vernon Island.

To put the depth-averaged results into context of the variability within the water column, maps of the predicted 90th and 95th percentile maximum-in-water-column trenching-excess SSC throughout the entire trenching program have been included in Figure 7.13 and Figure 7.14 for the winter/dry season scenario and Figure 7.15 and Figure 7.16 for the summer/wet season scenario. The regions predicted to have elevated levels of SSC are similar to the depth-averaged results, however the spatial area above a given concentration is greater for the maximum-in-water-column SSC. The plots reveal that there is significant variability in the vertical distributions of SSC in the water column and the results show there is a distinct increase in concentration towards the seabed. Thus, the spatial area affected above a given concentration is greater in the near-seabed layer than in the near-surface layer. The 90th percentile results for both seasonal scenarios do not exceed 10 mg/L, with the 95th percentile values only exceeding 10 mg/L (but remaining below 16 mg/L) in the vicinity of the offshore disposal area for both seasonal scenarios, and in the vicinity of Trench Zone 6 extending ~15 km north-west in the summer/wet season scenario.

Figure 7.9 Predicted 90th percentile depth-averaged trenching-excess SSC throughout the entire trenching program (not including run-on period) for the winter/dry season scenario (based on 1 April to 10 May 2019). Note the trenching area widths shown on this and other Figures in this report are exaggerated to aid visual clarity.
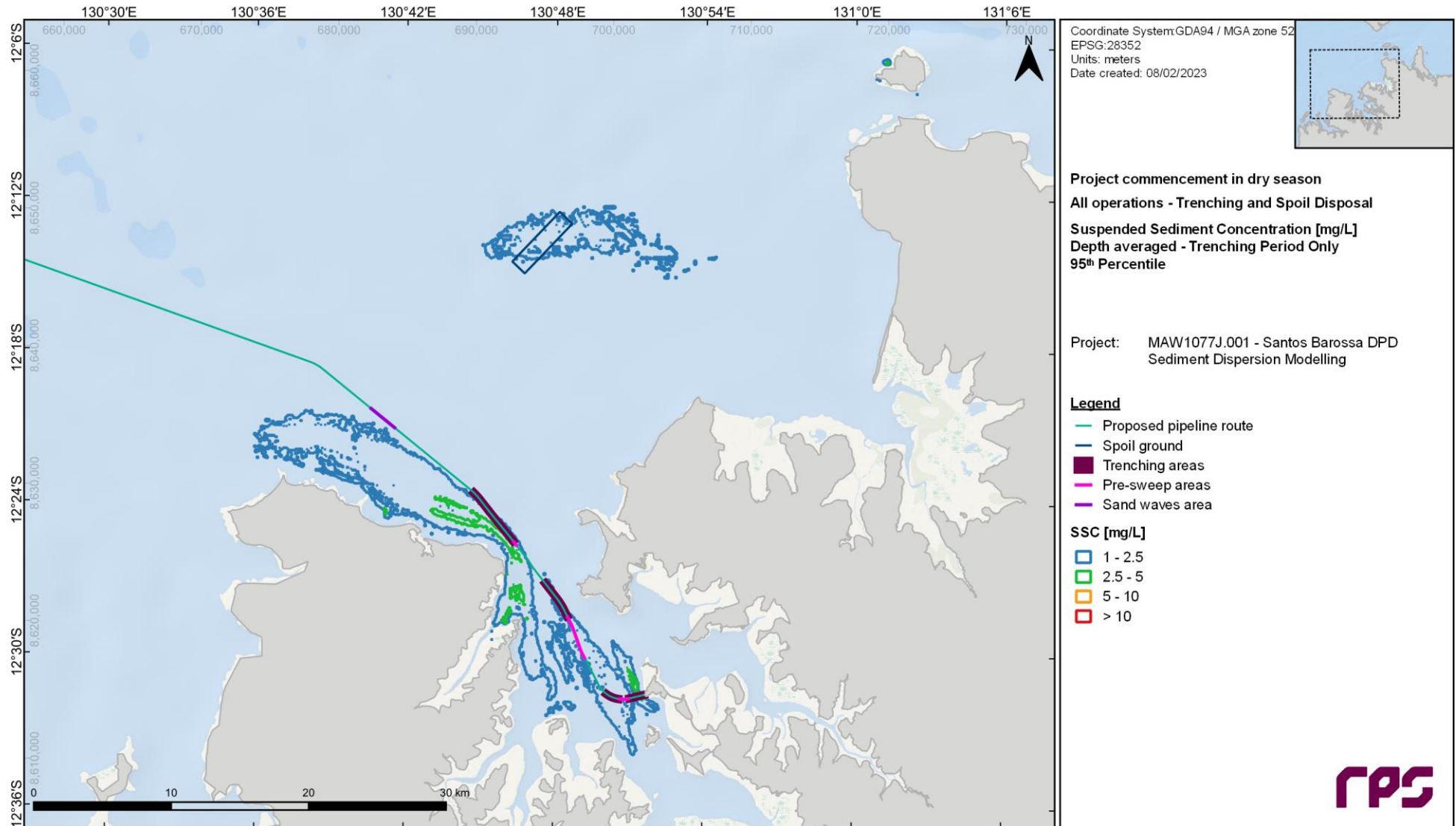
**Figure 7.10   Predicted 95th percentile depth-averaged trenching-excess SSC throughout the entire trenching program (not including run-on period) for the winter/dry season scenario (based on 1 April to 10 May 2019). Note the trenching area widths shown on this and other Figures in this report are exaggerated to aid visual clarity.**
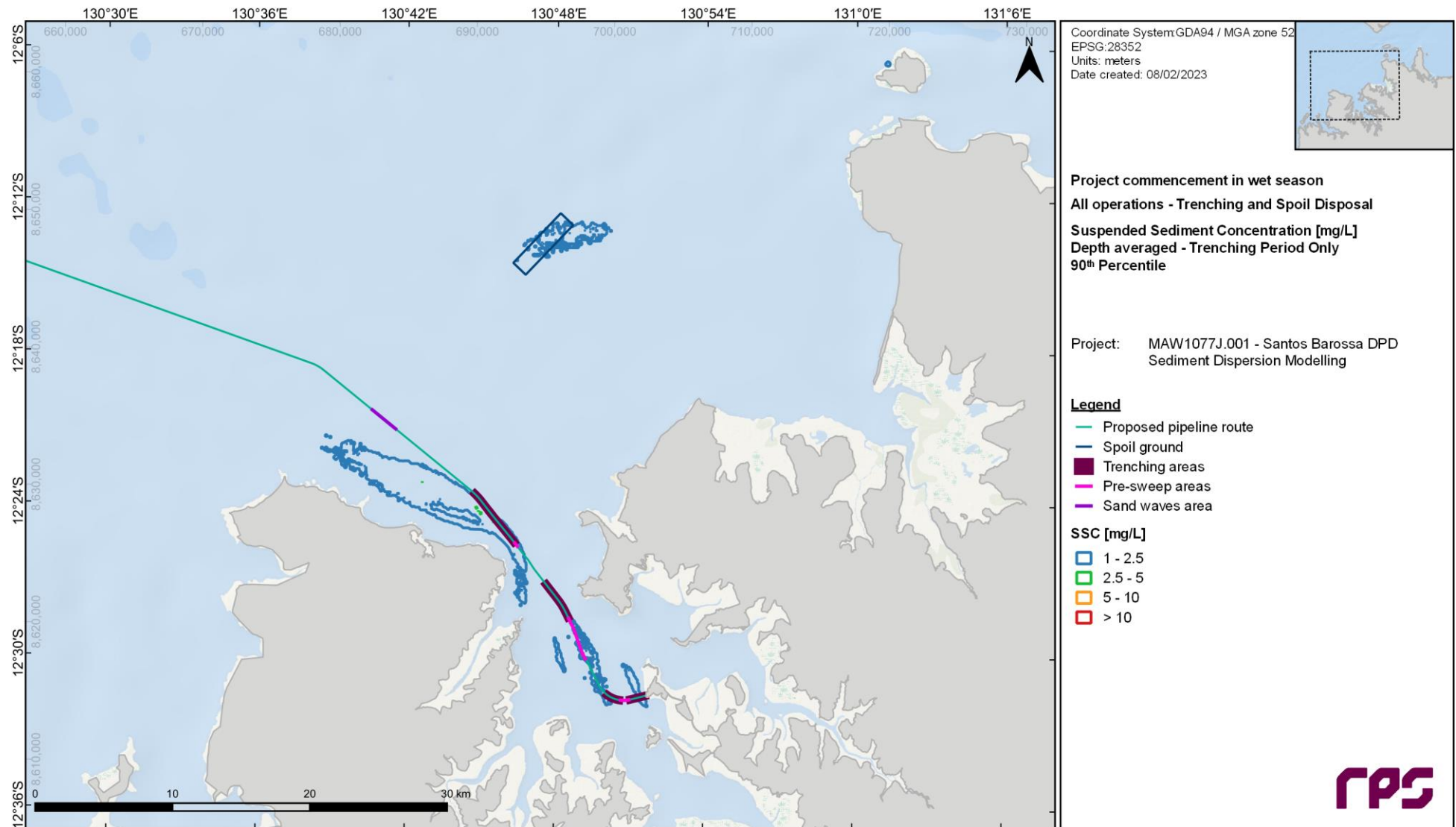
Figure 7.11   Predicted 90th percentile depth-averaged trenching-excess SSC throughout the entire trenching program (not including run-on period) for the summer/wet season scenario (based on 1 October to 9 November 2019). Note the trenching area widths shown on this and other Figures in this report are exaggerated to aid visual clarity.
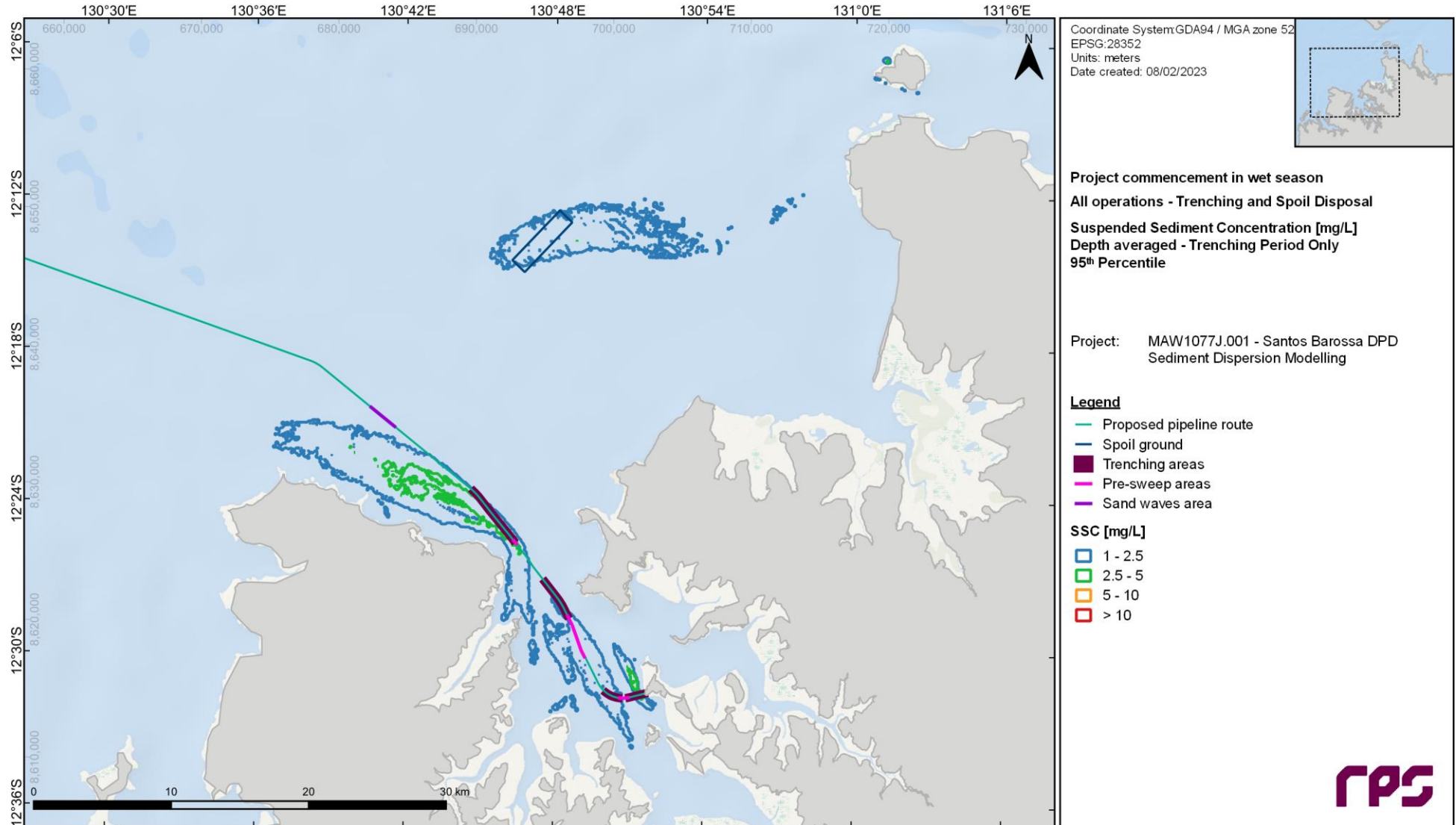
Figure 7.12 Predicted 95th percentile depth-averaged trenching-excess SSC throughout the entire trenching program (not including run-on period) for the summer/wet season scenario (based on 1 October to 9 November 2019). Note the trenching area widths shown on this and other Figures in this report are exaggerated to aid visual clarity.
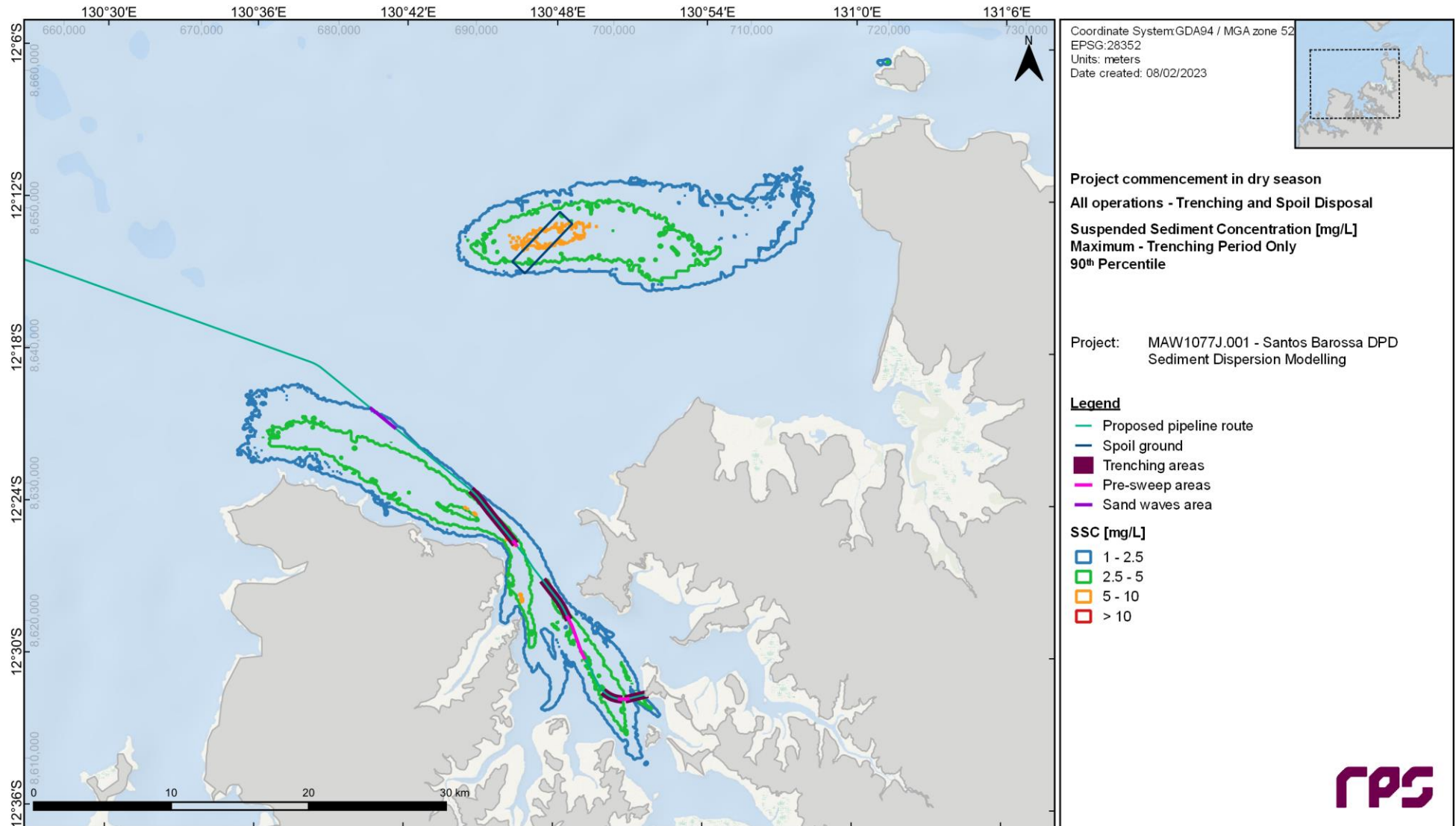
Figure 7.13 Predicted 90th percentile maximum-in-water-column trenching-excess SSC throughout the entire trenching program (not including run-on period) for the winter/dry season scenario (based on 1 April to 10 May 2019). Note the trenching area widths shown on this and other Figures in this report are exaggerated to aid visual clarity.
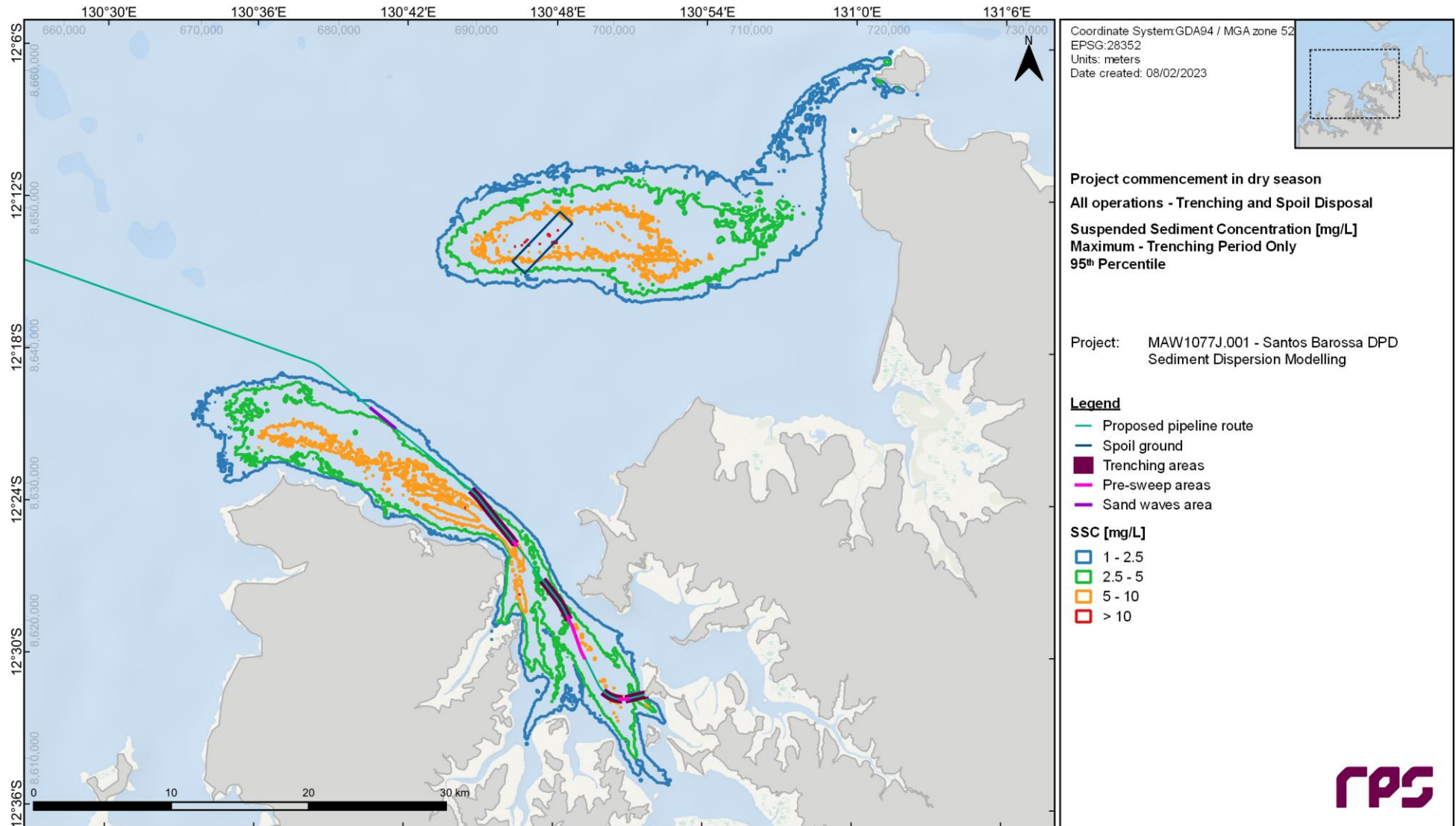
Figure 7.14 Predicted 95th percentile maximum-in-water-column trenching-excess SSC throughout the entire trenching program (not including run-on period) for the winter/dry season scenario (based on 1 April to 10 May 2019). Note the trenching area widths shown on this and other Figures in this report are exaggerated to aid visual clarity.
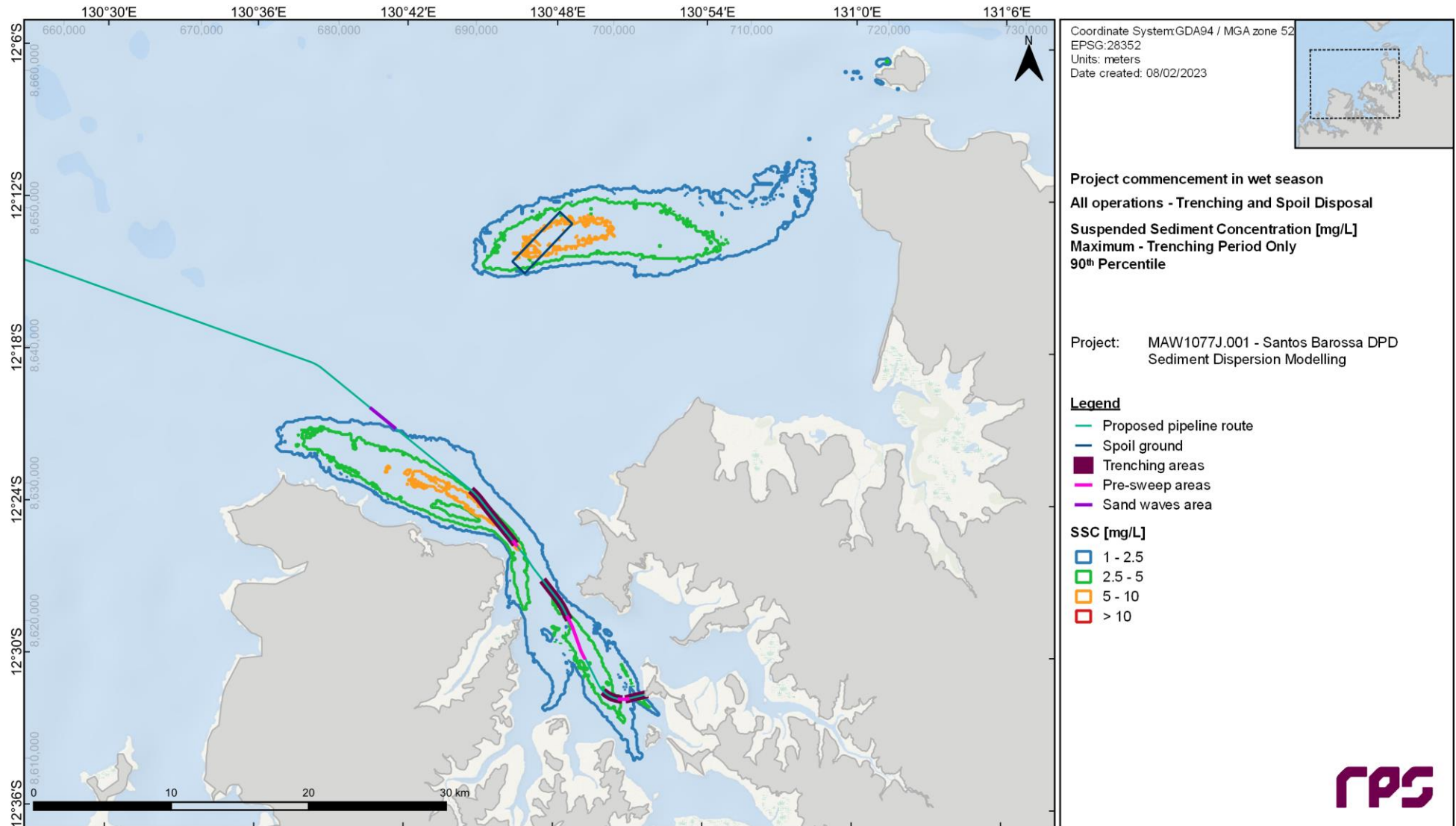
Figure 7.15 Predicted 90th percentile maximum-in-water-column trenching-excess SSC throughout the entire trenching program (not including run-on period) for the summer/wet season scenario (based on 1 October to 9 November 2019). Note the trenching area widths shown on this and other Figures in this report are exaggerated to aid visual clarity.
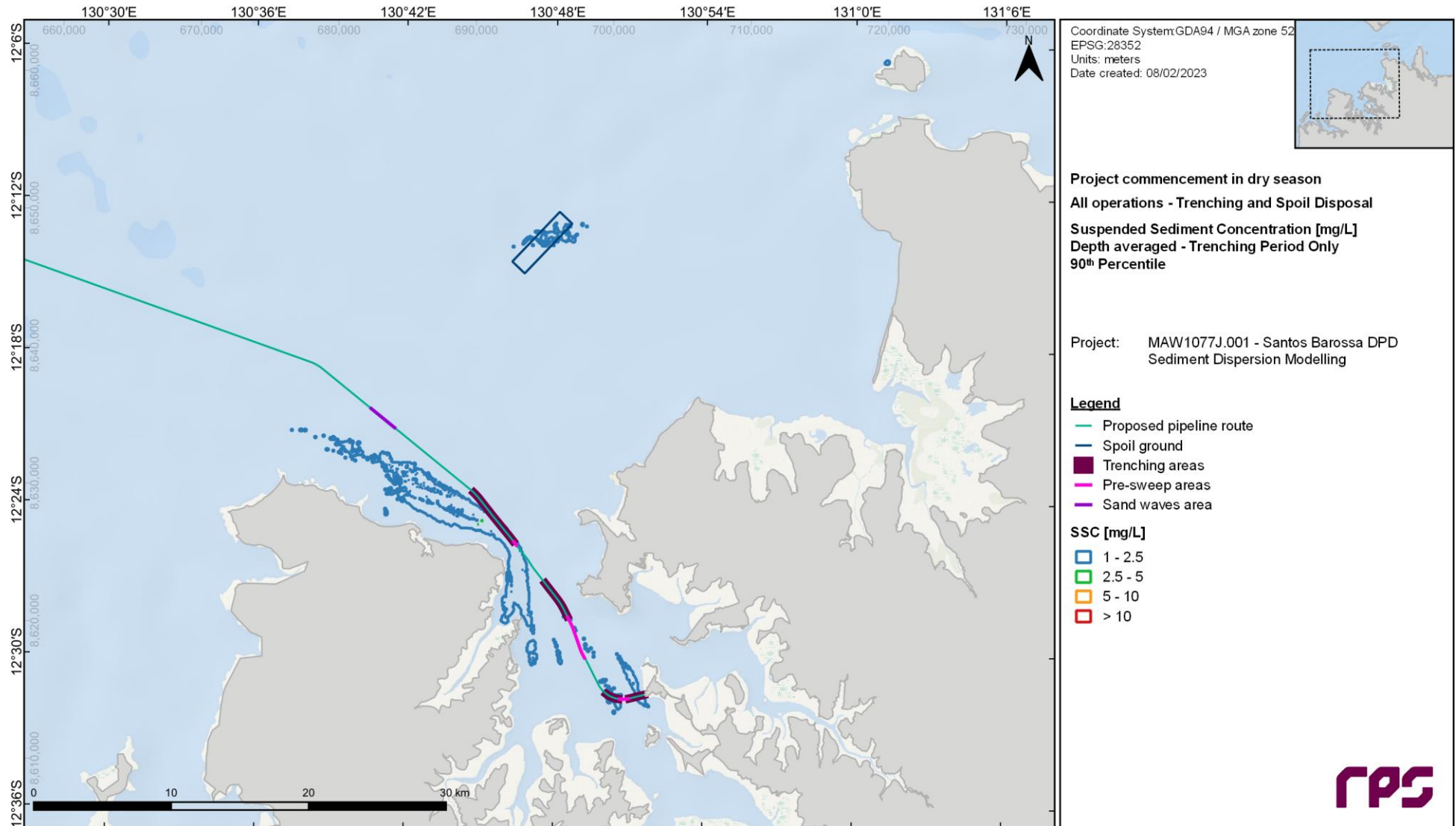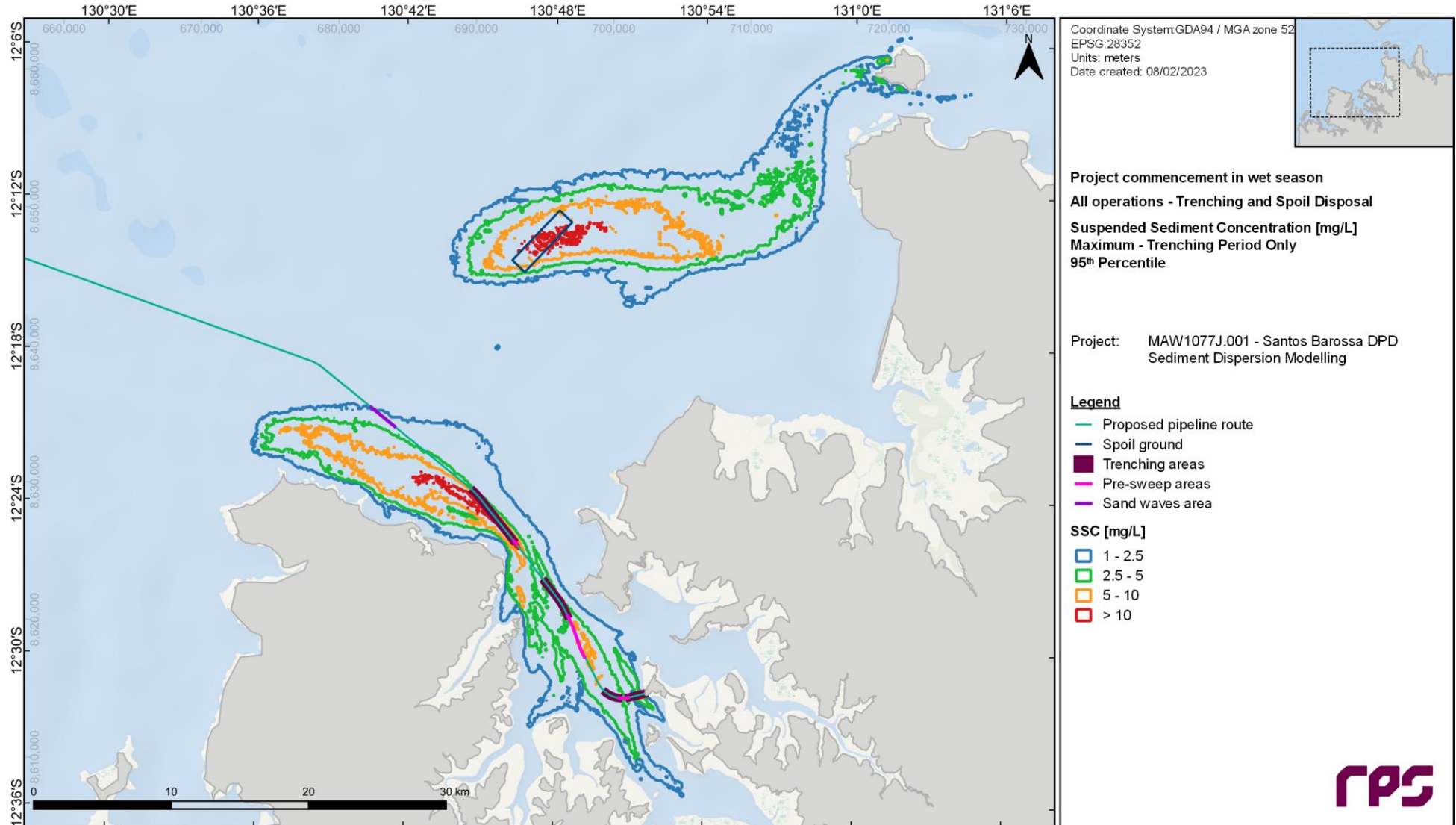
Figure 7.16 Predicted 95th percentile maximum-in-water-column trenching-excess SSC throughout the entire trenching program (not including run-on period) for the summer/wet season scenario (based on 1 October to 9 November 2019). Note the trenching area widths shown on this and other Figures in this report are exaggerated to aid visual clarity.

7.2.2   Temporal Variability of SSC

The simulations indicated that there will be significant temporal variability in the distribution of SSC during the trenching and disposal operations. The vulnerability of sensitive receptors to elevated levels of SSC is a function of exposure intensity and duration (Sun *et al.*, 2020), and it will also depend on whether the exposure duration comprises multiple isolated (in time) events or a consecutive period of events.

To explore the temporal exposure of sensitive receptor sites, a time series analysis at a set of sensitive locations has been conducted to supplement the spatial maps. The set of analysis locations was selected from among the existing sensitive receptor monitoring sites that the model predicted would be reached by elevated SSC levels. In addition to the sensitive receptor monitoring sites, a set of locations was defined at the proposed offshore disposal area, and also at the Vernon Islands where elevated SSC levels were predicted by the model. Figure 7.17 and Table 7.1 present the locations of the points selected for the time series analysis. For presentation purposes the points have been split into groups as follows:

1.   *WI_S*, *CHI* and *WED1* are the monitoring sites inside Darwin Harbour.

2.   *CPW_1*, *MAN* and *CHP* are the monitoring sites outside Darwin Harbour.

3.   *VI_S* and *VI_E* are the Vernon Island sites.

4.   *OD1* to *OD5* are the offshore disposal ground long cross-section sites (aligned south-west to north-east).

5.   *OD6* to *OD9* are the offshore disposal ground short cross-section sites (aligned north-west to south-east).

Table 7.1   Time series analysis point locations (reference datum: GDA94).

Point Name	Point Abbreviation	Longitude (°)	Latitude (°)
Woods Inlet South	WI_S	130.7683	-12.47390
Channel Island	CHI	130.8735	-12.55080
Weed Reef 1	WED1	130.7999	-12.48760
Charles Point West 1	CPW_1	130.6467	-12.38680
Mandorah	MAN	130.7700	-12.43530
Charles Point	CHP	130.6839	-12.40950
Vernon Islands – South West	VI_S	131.0184	-12.10627
Vernon Islands – East	VI_E	131.0700	-12.07746
Offshore Disposal Area Point 1	OD1	130.7553	-12.26529
Offshore Disposal Area Point 2	OD2	130.7814	-12.23756
Offshore Disposal Area Point 3	OD3	130.7904	-12.22830
Offshore Disposal Area Point 4	OD4	130.8001	-12.21846
Offshore Disposal Area Point 5	OD5	130.8253	-12.19286
Offshore Disposal Area Point 6	OD6	130.7773	-12.21576
Offshore Disposal Area Point 7	OD7	130.7869	-12.22465
Offshore Disposal Area Point 8	OD8	130.7952	-12.23249
Offshore Disposal Area Point 9	OD9	130.8036	-12.23999

Time series plots showing predicted depth-averaged and maximum-in-water-column trenching-excess SSC for each of the selected locations are presented for both the winter/dry and summer/wet season scenarios in Figure 7.18 through Figure 7.27 (note the scale on the y-axes changes between Figures). Supplementary to the plots, Table 7.2 presents the predicted 95th percentile, 98th percentile and maximum trenching-excess SSC for each of the selected locations in each seasonal scenario. The percentile values are presented because in some of the plots, to maintain a scale that clearly shows the general patterns of temporal variation at all sites, the y-axis limit has purposefully been selected to cut off the peaks. Lower percentiles have not been presented as at all sites analysed, for both the depth-averaged and maximum-in-water-column trenching-excess SSC, the median and 80th percentiles values are less than 1 mg/L.
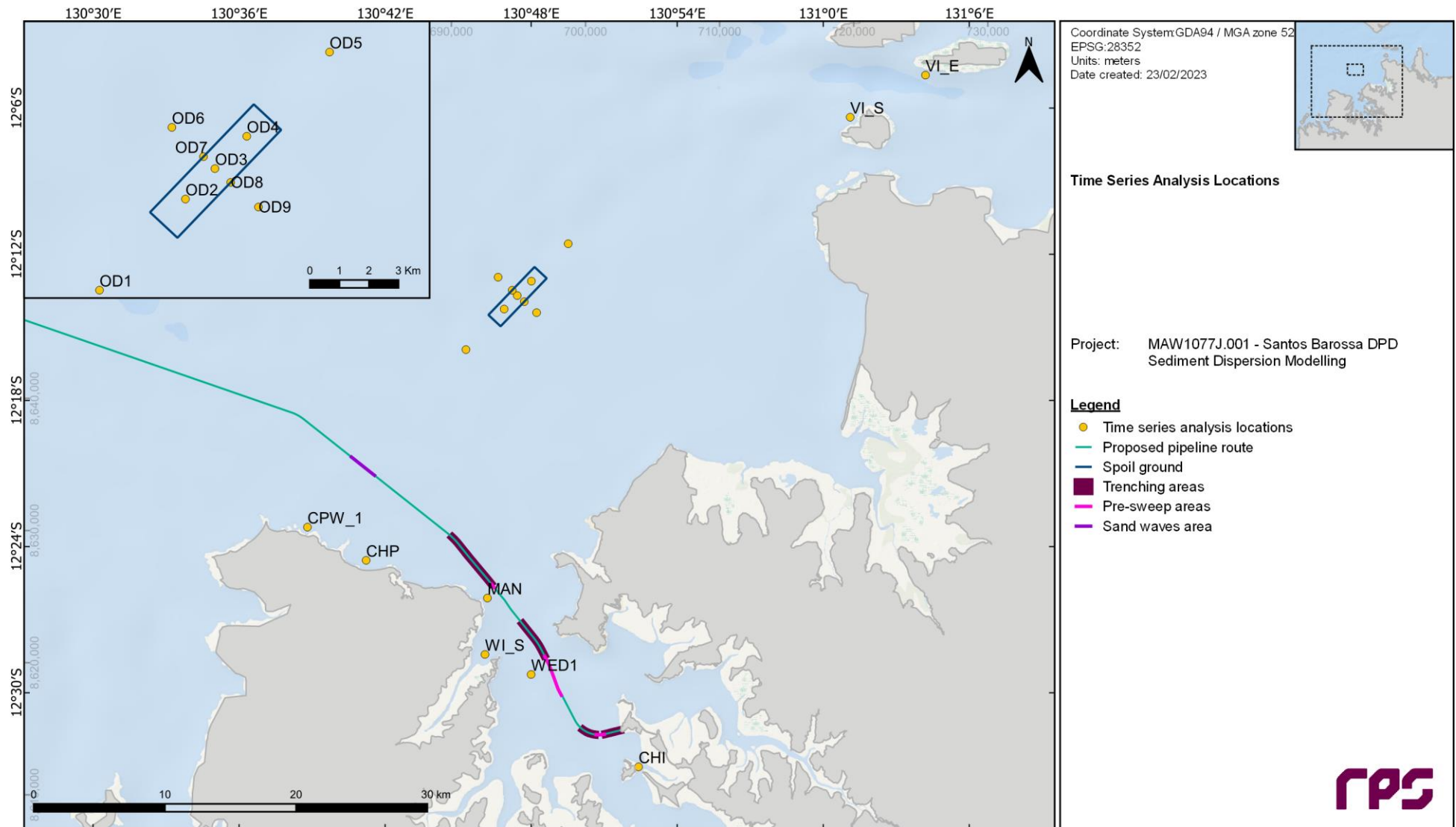
Figure 7.17 Time series analysis point locations. Note the trenching area widths shown on this and other Figures in this report are exaggerated to aid visualisation.

The temporal variation in trenching-excess SSC at all analysis sites reflects the spatial patchiness of the plumes and the oscillations of the dominant tidal flows in the area, with rapidly changing (over hourly scales) sharp peaks and troughs.

At the sites inside Darwin Harbour (Figure 7.18 and Figure 7.19) the intensity of SSC depends on the proximity to the trenching areas, with the plume rarely reaching *CHI* and only at low concentrations typically less than 4 mg/L. At *WI_S* the exposures show a clear tidal signal, with plumes predicted to reach the site during spring tidal periods and with minimal SSC exposure during neap tides. This site also shows seasonal differences, with higher peaks during the winter/dry season, reflecting the more southerly drift pattern during the dry season as found in the spatial plots. *WED1* sees similar levels of SSC to *WI_S*, however because it is in the mid-harbour close to the dredging areas there are minimal seasonal differences.

The sites outside Darwin Harbour along the coast from West Point to Charles Point (Figure 7.20 and Figure 7.21) show a similar pattern of exposure to the sites inside the harbour, with higher predicted SSC levels during spring tide periods, particularly towards the end of the trenching period when the dredging takes place closer to these sites. At *CPW1* and *MAN* the predicted trenching-excess SSC is relatively low, being less than 1 mg/L 98% of the time (Table 7.2). *CHP* is predicted to have higher SSC intensities than the other two sites, particularly during the summer/wet season when drift patterns tend towards the north-west along this section of the coast. However, as was found for all sites, the duration of the peaks in predicted SSC at *CHP* are short, and this is reflected in the 98th percentile SSC values which are less than 7 mg/L in both seasonal scenarios.

The time series of trenching-excess SSC at the Vernon Islands sites (Figure 7.22 and Figure 7.23) show that SSC intensities are predicted to be relatively low, particularly at *VI_E*. Peak SSC concentration are predicted to be typically higher in the summer/wet season scenario, showing the effect of increased drift trajectories towards the Clarence Strait during this season.

At the offshore disposal area sites, the temporal variability in predicted SSC also reflects the tidal oscillations with periods of spring and neap tides evident. However, superimposed on this signal is additional variability due to the sporadic nature of the disposal sources, which are variable in time and space (Figure 7.24 to Figure 7.27). The locations within the disposal ground (*OD2*, *OD3*, *OD4*, *OD7* and *OD8*) show similar overall patterns with periods of higher and lower SSC; however, the timings and intensities of the individual peaks vary due to the relative proximity of each site to individual disposal events. Although the peaks in SSC vary significantly between the sites, at the 95th and 98th percentile levels the values at the sites within the disposal area are very similar (less than 10 mg/L). These sites reveal that elevated SSC levels (in the order of 100-200 mg/L) occur immediately after disposal events but are rapidly dispersed and do not persist for long periods of time (scales of hours). The sites along the two cross-sectional alignments lying outside the disposal ground (*OD1*, *OD5*, *OD6* and *OD9*) show that the intensity of the modelled SSC values is predicted to reduce significantly within 1-3 km of the disposal ground boundaries.

Table 7.2 Percentiles (95th and 98th) and maximum predicted trenching-excess SSC (depth-averaged and maximum-in-water-column) for each of the time series analysis points, throughout the entire trenching program and run-on period for the winter/dry and summer/wet season scenarios.

Points	95th Percentile				98th Percentile				Maximum			
	Depth-Averaged		Maximum in Water Column		Depth-Averaged		Maximum in Water Column		Depth-Averaged		Maximum in Water Column	
	Dry	Wet	Dry	Wet	Dry	Wet	Dry	Wet	Dry	Wet	Dry	Wet
WI_S	1	1	1	1	2	1	3	1	15	6	16	6
CHI	0*	0*	0*	0*	0*	0*	0*	0*	4	2	6	5
WED1	1	1	2	2	1	1	4	4	4	4	17	15
CPW_1	0*	0*	0*	0*	0*	1	0*	1	3	10	5	17
MAN	1	0*	1	1	1	1	1	1	6	3	7	4
CHP	1	1	1	2	3	6	3	7	51	55	65	71
VI_S	0*	0*	1	1	0*	1	1	2	2	3	5	8
VI_E	0*	0*	0*	0*	0*	0*	0*	0*	0*	0*	2	3
OD1	0*	0*	1	1	0*	0*	1	1	1	3	6	19
OD2	1	1	4	4	1	1	8	9	33	9	163	42
OD3	1	1	5	5	1	2	9	10	10	14	52	88
OD4	1	1	4	5	1	1	7	7	6	11	27	50
OD5	0*	0*	1	1	0*	0*	2	2	2	2	17	16
OD6	0*	0*	2	2	1	1	5	5	9	3	47	21
OD7	1	1	5	6	1	2	9	10	18	5	102	36
OD8	1	1	4	5	1	2	8	10	13	12	68	86
OD9	0*	0*	2	2	1	1	5	5	6	3	36	19

* These values are greater than 0.0 but less than 0.5 mg/L.

Figure 7.18   Time series of predicted trenching-excess SSC at the *WI_S*, *WED1* and *CHI* sites throughout the entire trenching program and run-on period in the winter/dry season scenario.
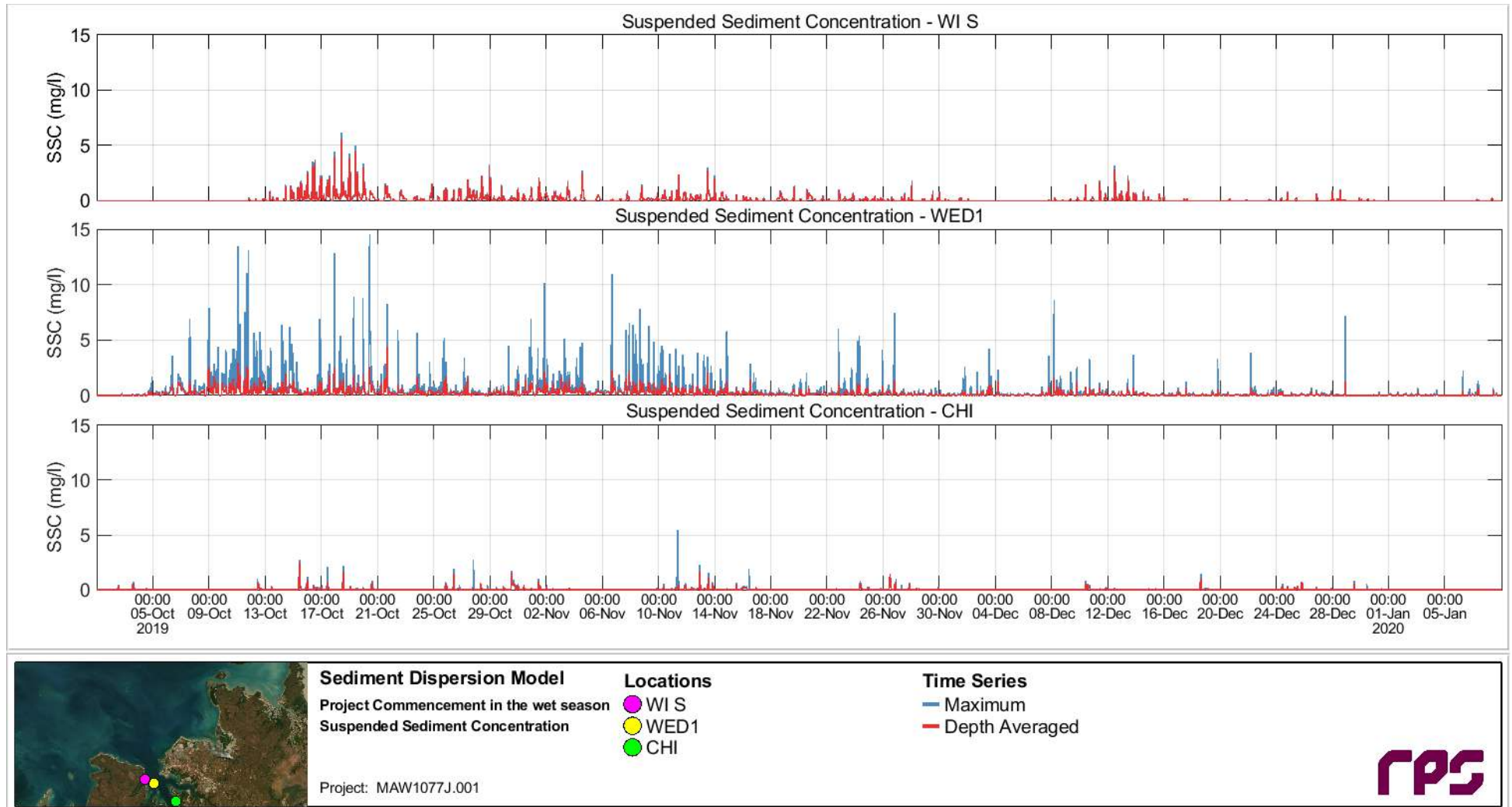
Figure 7.19 Time series of predicted trenching-excess SSC at the *WI_S*, *WED1* and *CHI* sites throughout the entire trenching program and run-on period in the summer/wet season scenario.
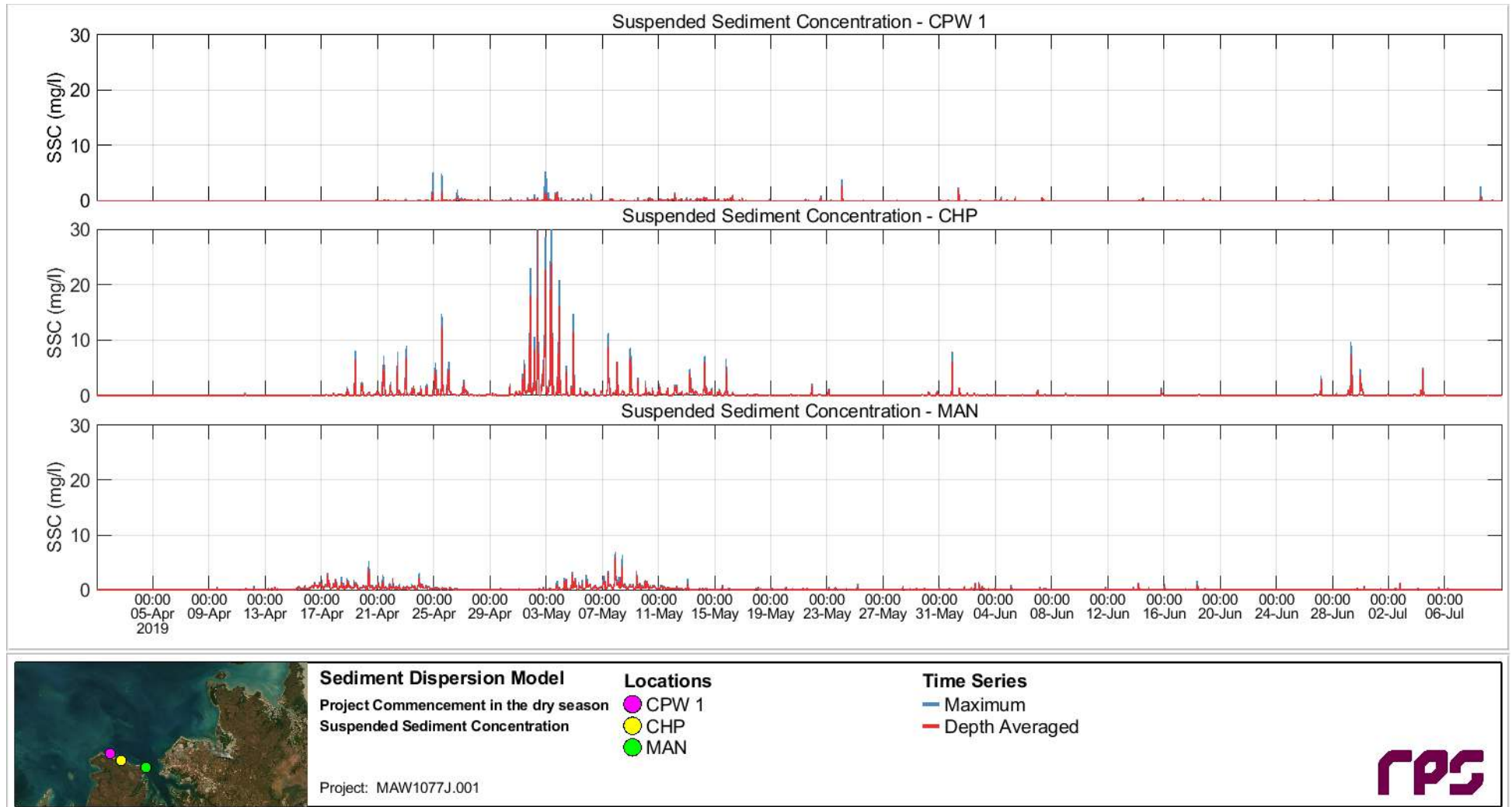
Figure 7.20   Time series of predicted trenching-excess SSC at the *CPW1*, *MAN* and *CHP* sites throughout the entire trenching program and run-on period in the winter/dry season scenario.
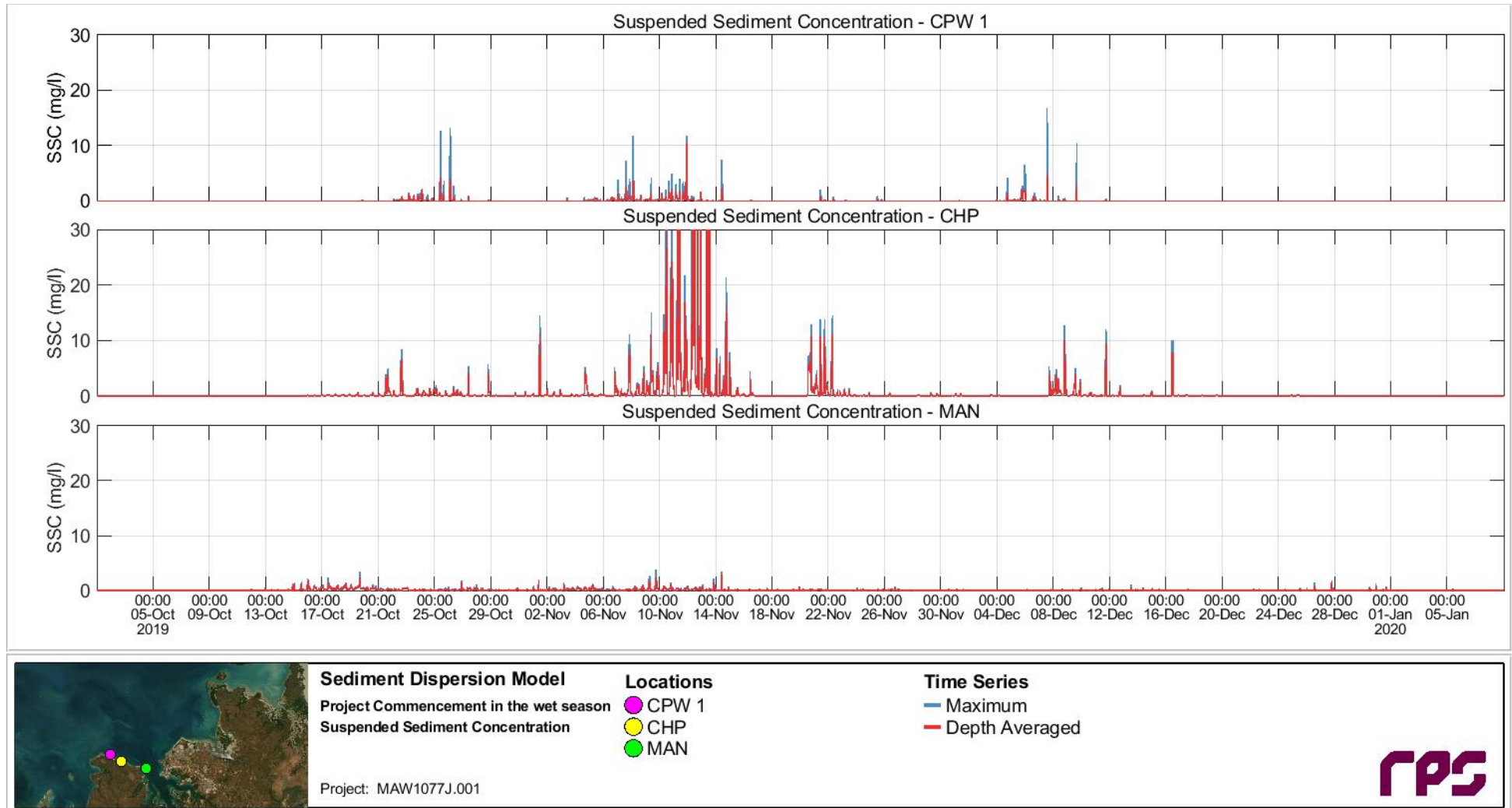
Figure 7.21 Time series of predicted trenching-excess SSC at the *CPW1*, *MAN* and *CHP* sites throughout the entire trenching program and run-on period in the summer/wet season scenario.
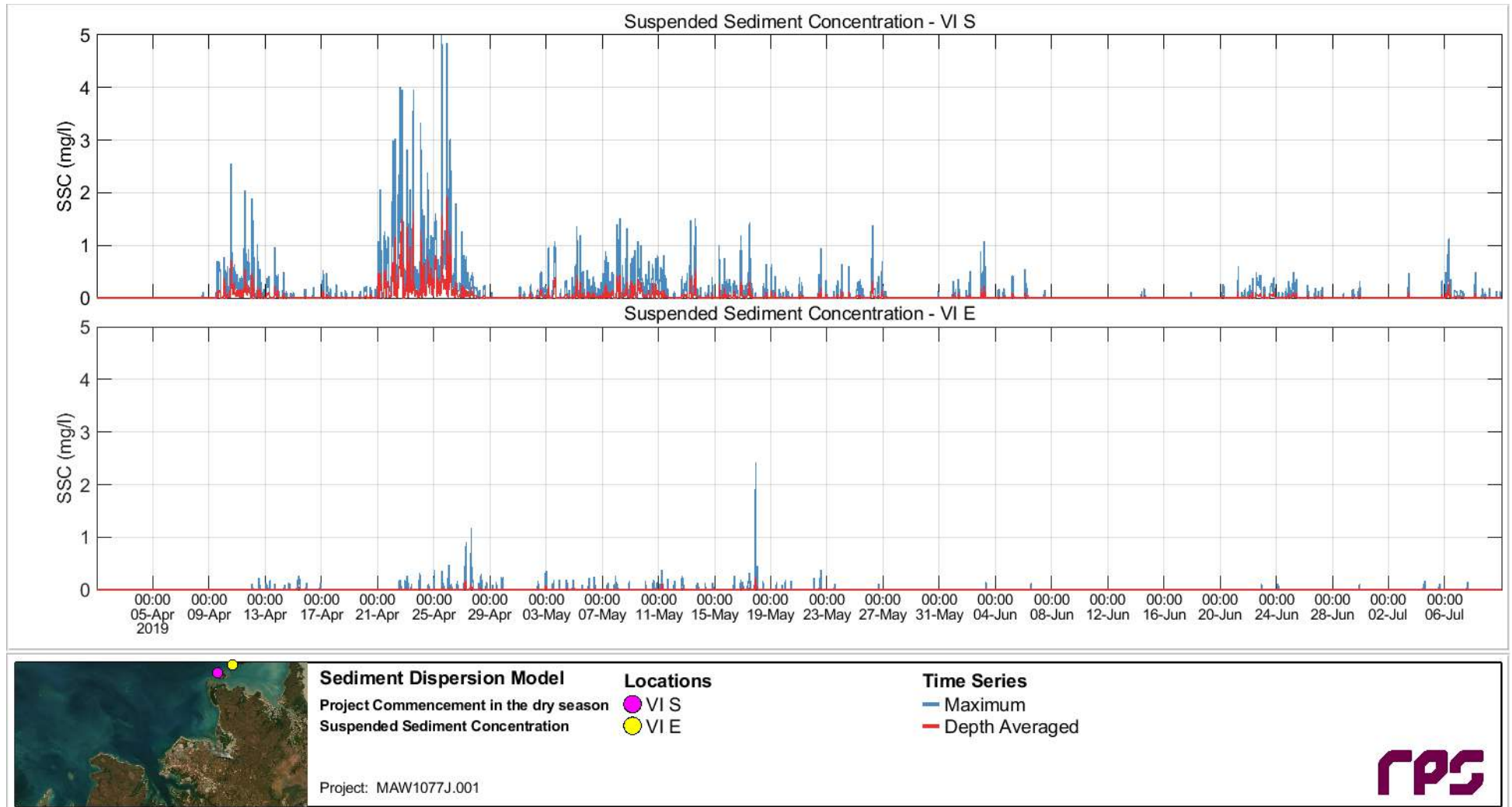
Figure 7.22 **Time series of predicted trenching-excess SSC at the *VI_S* and *VI_E* sites throughout the entire trenching program and run-on period in the winter/dry season scenario.**
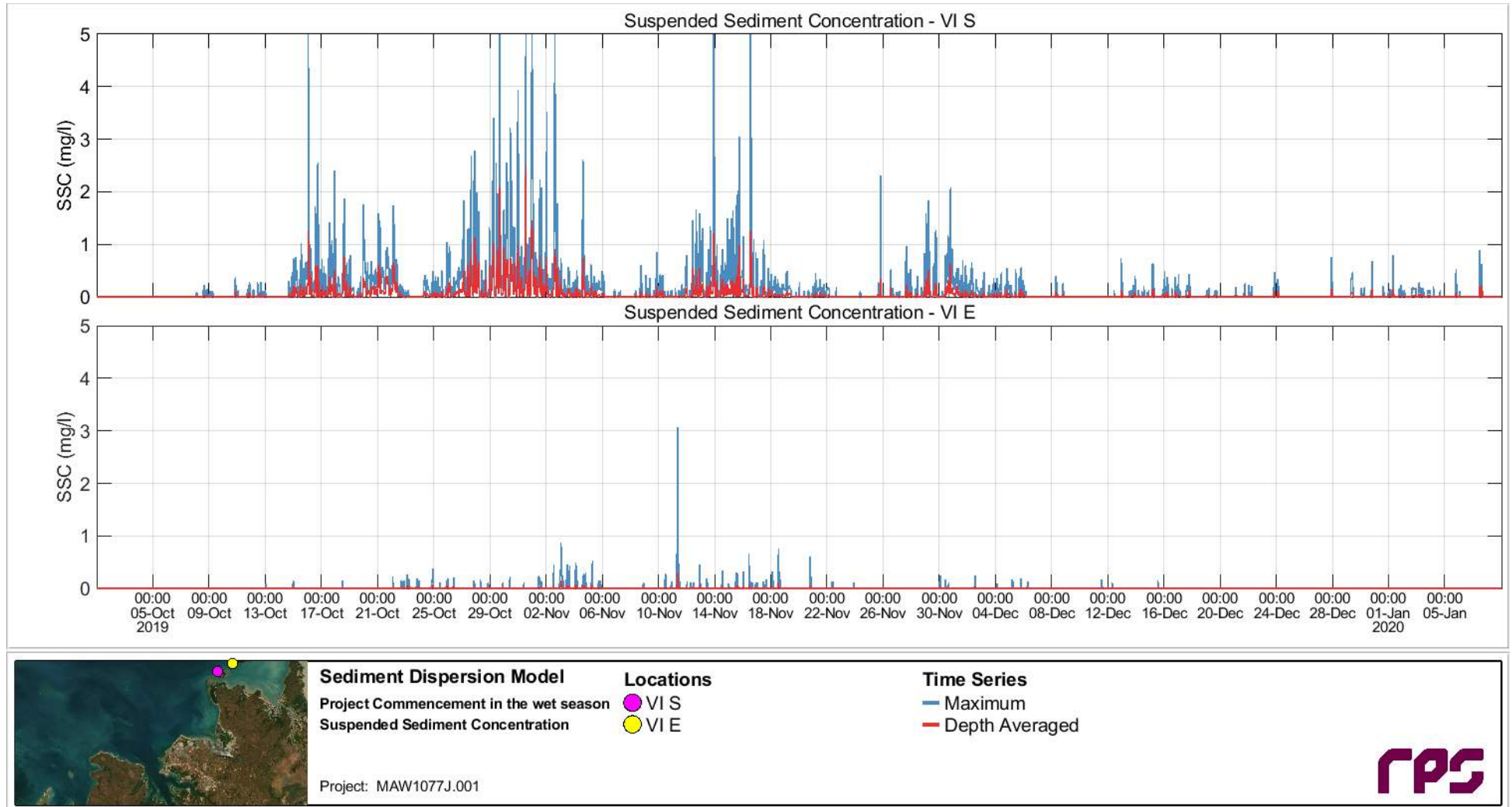
Figure 7.23 **Time series of predicted trenching-excess SSC at the *VI_S* and *VI_E* sites throughout the entire trenching program and run-on period in the summer/wet season scenario.**
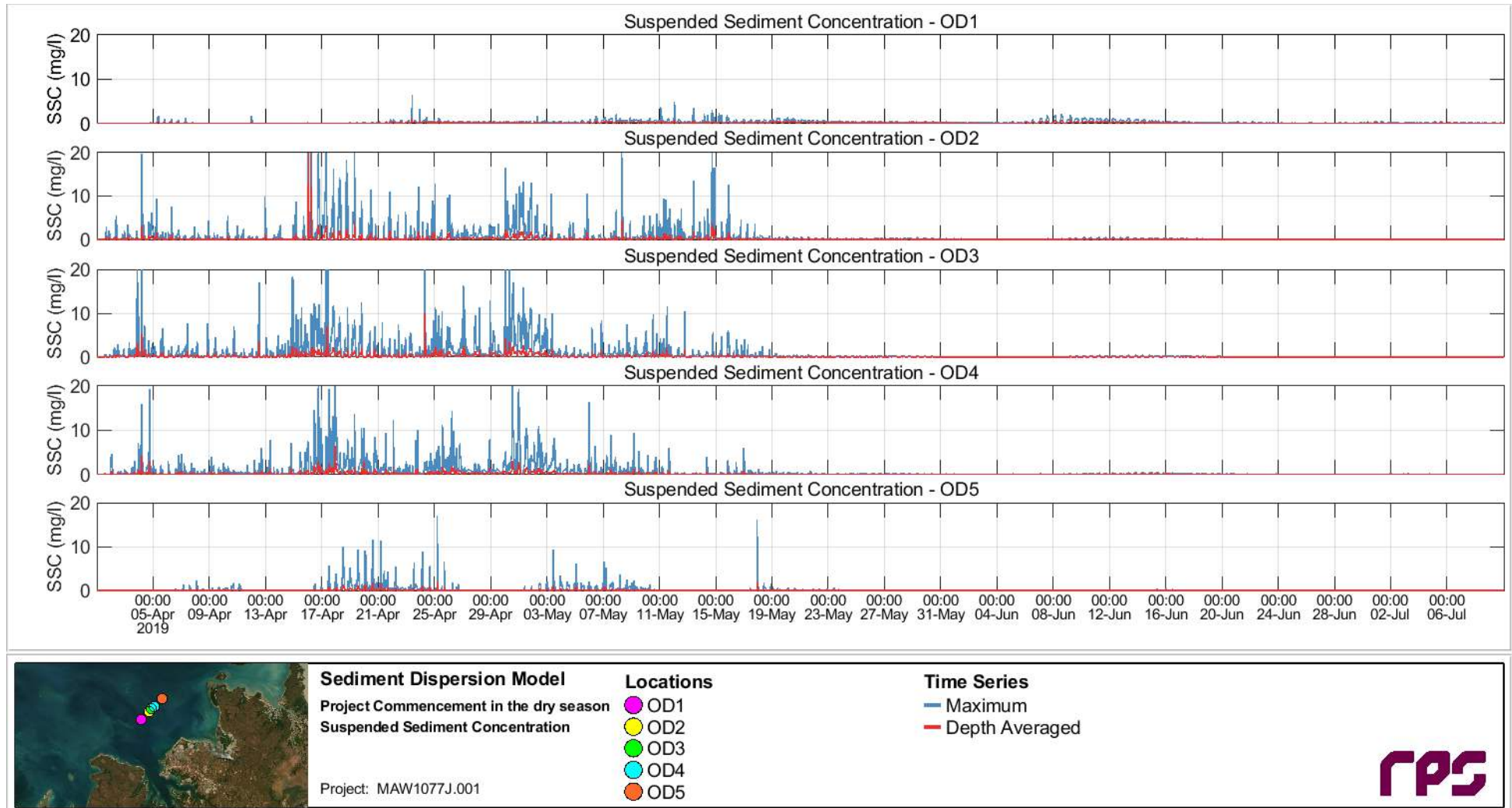
Figure 7.24 **Time series of predicted trenching-excess SSC at the *OD1* to *OD5* sites throughout the entire trenching program and run-on period in the winter/dry season scenario.**

Figure 7.25 **Time series of predicted trenching-excess SSC at the *OD6* to *OD9* (via *OD3*) sites throughout the entire trenching program and run-on period in the winter/dry season scenario.**

Figure 7.26 **Time series of predicted trenching-excess SSC at the *OD1* to *OD5* sites throughout the entire trenching program and run-on period in the summer/wet season scenario.**
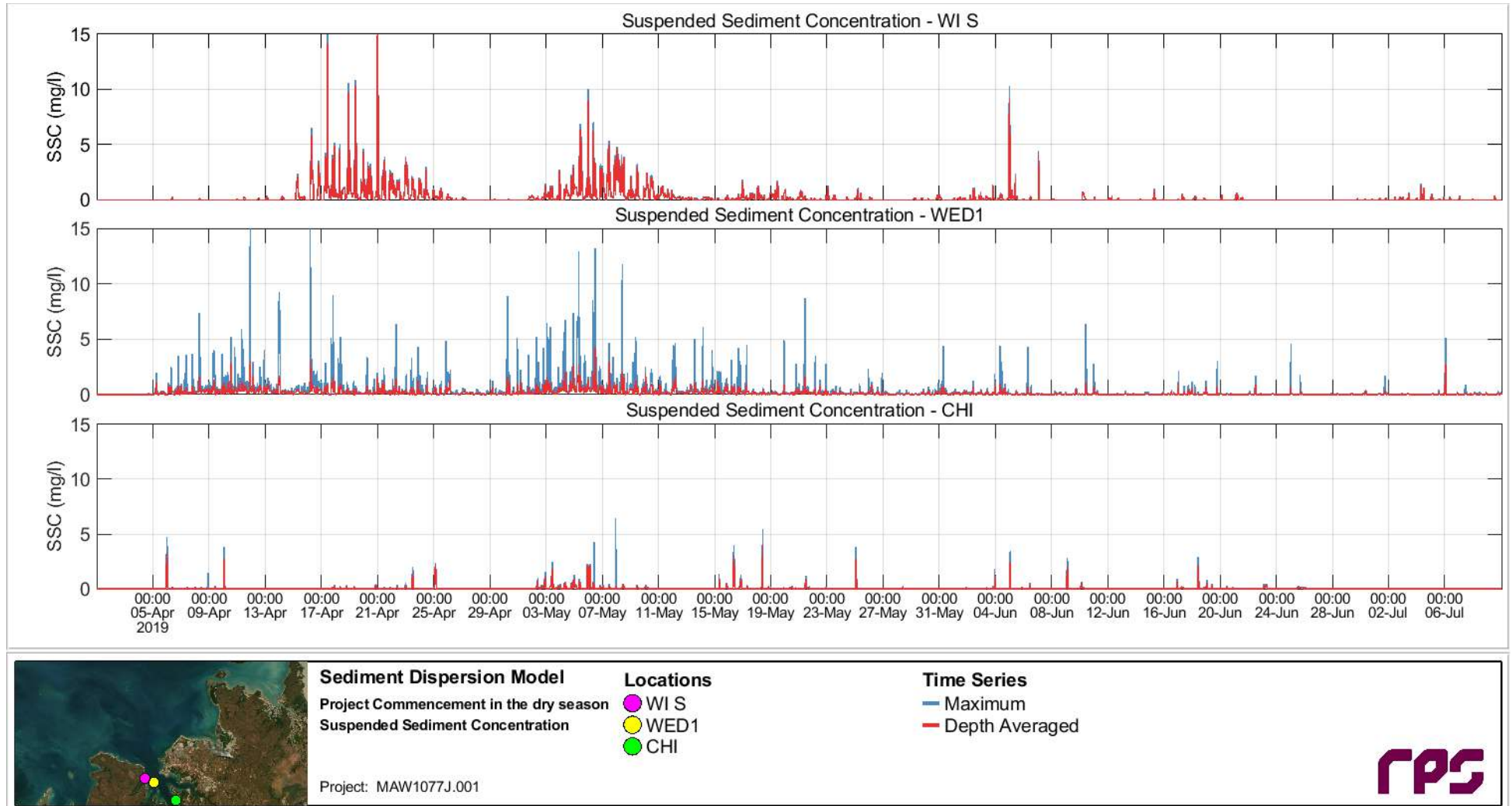
Figure 7.27   Time series of predicted trenching-excess SSC at the *OD6* to *OD9* (via *OD3*) sites throughout the entire trenching program and run-on period in the summer/wet season scenario.

7.3 Spatial and Temporal Characteristics of Sedimentation

7.3.1 Spatial Distribution of Sedimentation

Given the strong tidal flows in the Darwin area, settlement of the finer trenching-generated sediment is minimal with fine material (clay and silts) being continuously resuspended on each tide, particularly during spring tide periods where even fine sand size material is predicted to be resuspended. Coarse material (sand size) is predicted to settle rapidly near the trenching zones and at the proposed offshore disposal area, but the fine material will remain suspended, or will deposit at slack tide only to be resuspended on the following tide. This results in suspended sediment plumes having long drift trajectories, with sediments dispersed widely but at low concentrations, and with sediments deposited in thin layers.

Figure 7.28 presents the predicted maximum trenching-excess sediment thickness over the entire trenching and spoil disposal program, and Figure 7.29 and Figure 7.30 present the trenching-excess sediment thickness at the end of the trenching program (not including run-on period) and at the end of the run-on period respectively, for the winter/dry season scenario. A comparison of the spatial distributions in these three figures shows that sedimentation of greater than 1 mm thickness is typically limited to the vicinity of the trenching and disposal operations, with deposited sediments at greater distances being of very low concentration/thickness and most likely consisting of finer material that is resuspended and further dispersed by the end of the trenching program and run-on period.

The spatial distributions of sedimentation for the summer/wet season scenario (Figure 7.31, Figure 7.32 and Figure 7.33) show a similar pattern of deposition, with sedimentation of greater than 1 mm thickness typically limited to the vicinity of the trenching and disposal operations, and sediments deposited at greater distances being of very low concentration/thickness and further dispersed by the end of the trenching program and end of the run-on period. A small additional patch of sedimentation with a thickness greater than 1 mm is predicted in the shallows at South West Vernon Island for the summer/wet season scenario.

It should be noted that the disposal area sediment thickness values do not represent all material that will be placed at the disposal ground, but only the proportions of the material assumed to be initially suspended during placement or deposited in the surface layer available for potential resuspension (see Sections 5.6.3 and 5.6.5 for source rates). As such, actual sediment thicknesses within the disposal area may be greater than the values presented in the figures here.
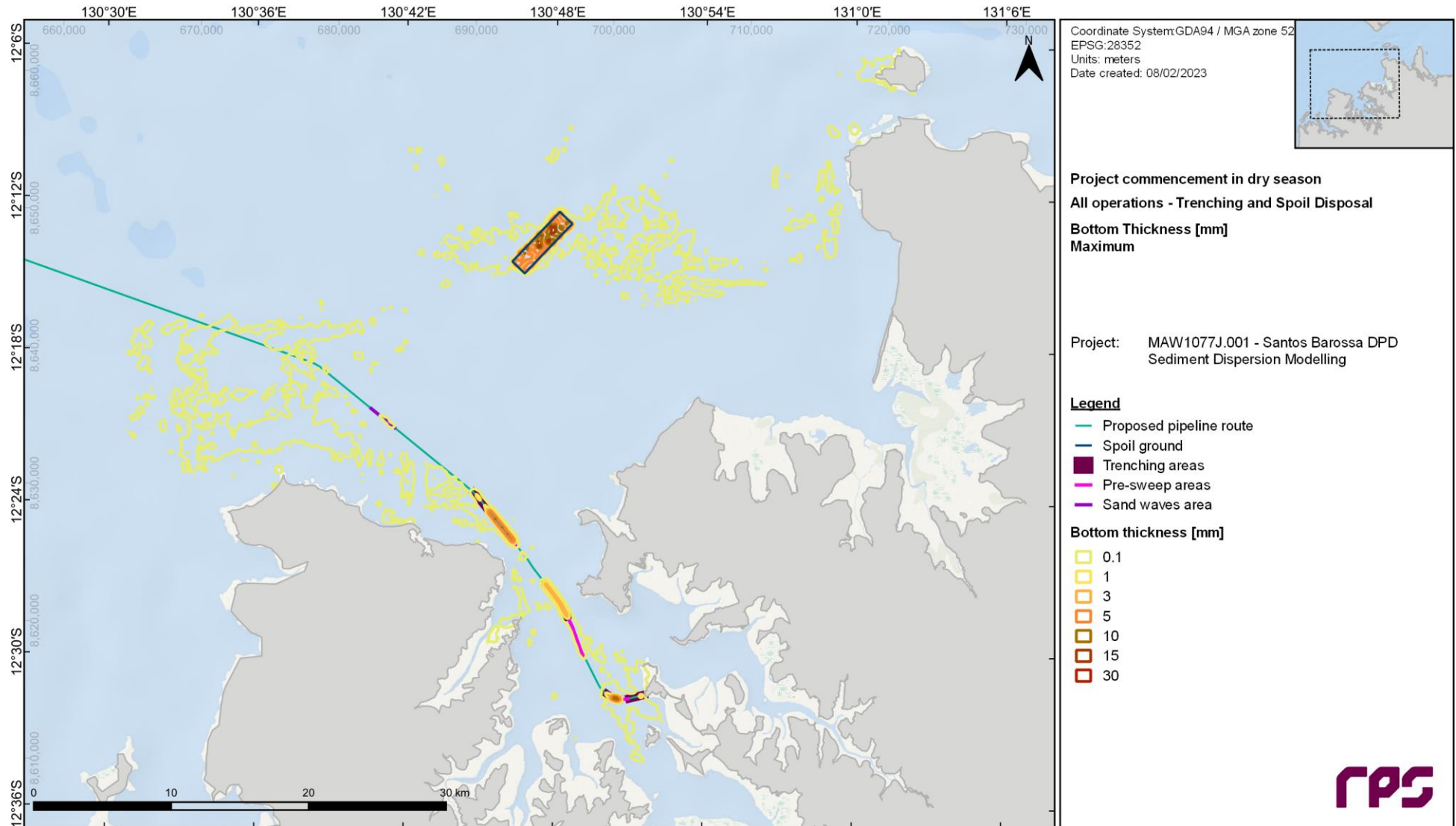
Figure 7.28   Predicted maximum trenching-excess bottom thickness (mm) throughout the entire trenching program for the winter/dry season scenario (based on 1 April to 10 May 2019). Note the trenching area widths shown on this and other Figures in this report are exaggerated to aid visual clarity.
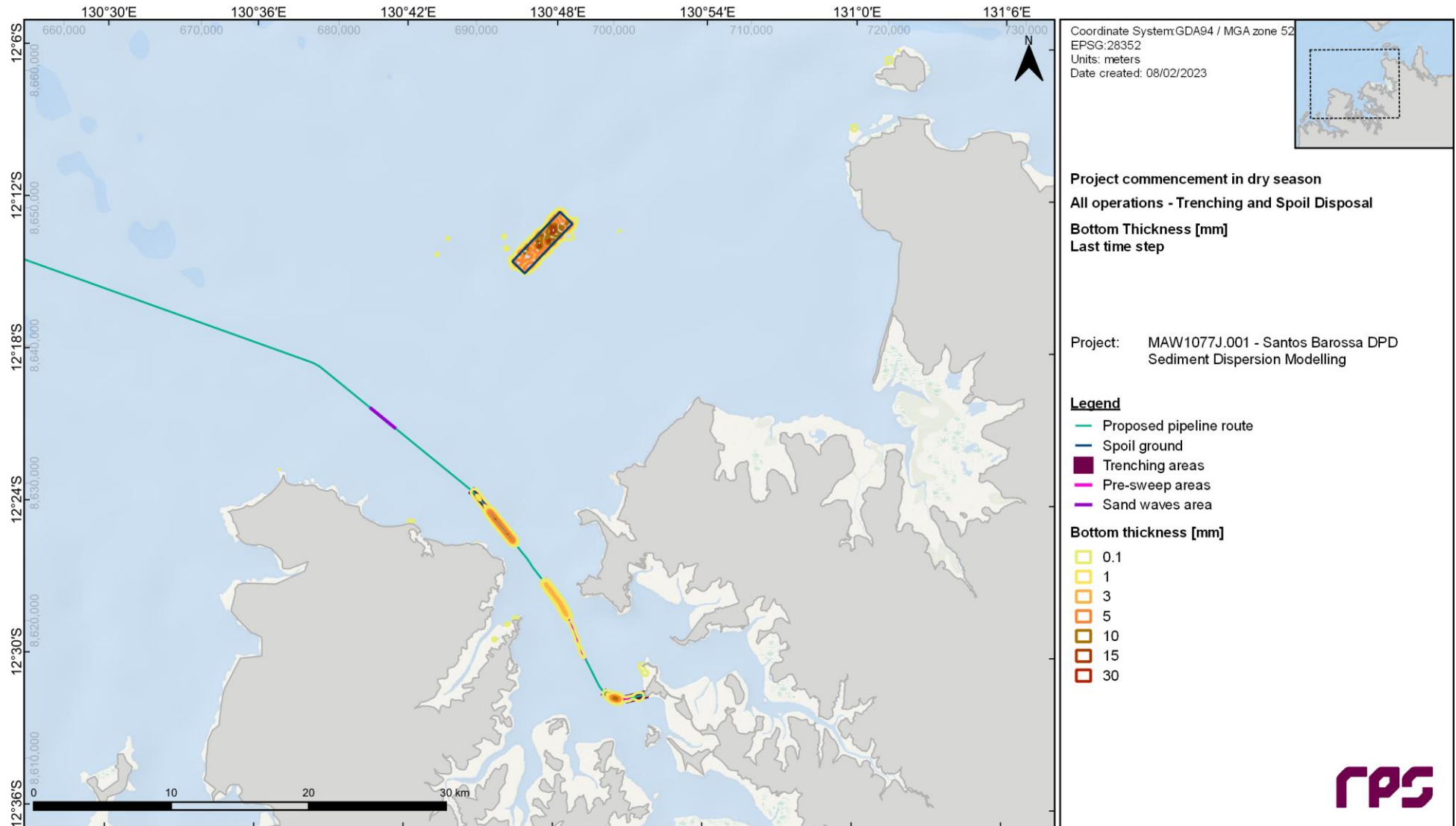
Figure 7.29 **Predicted trenching-excess bottom thickness (mm) at the last time step of the trenching program (not including run-on period) for the winter/dry season scenario (based on 10 May 2019). Note the trenching area widths shown on this and other Figures in this report are exaggerated to aid visual clarity.**
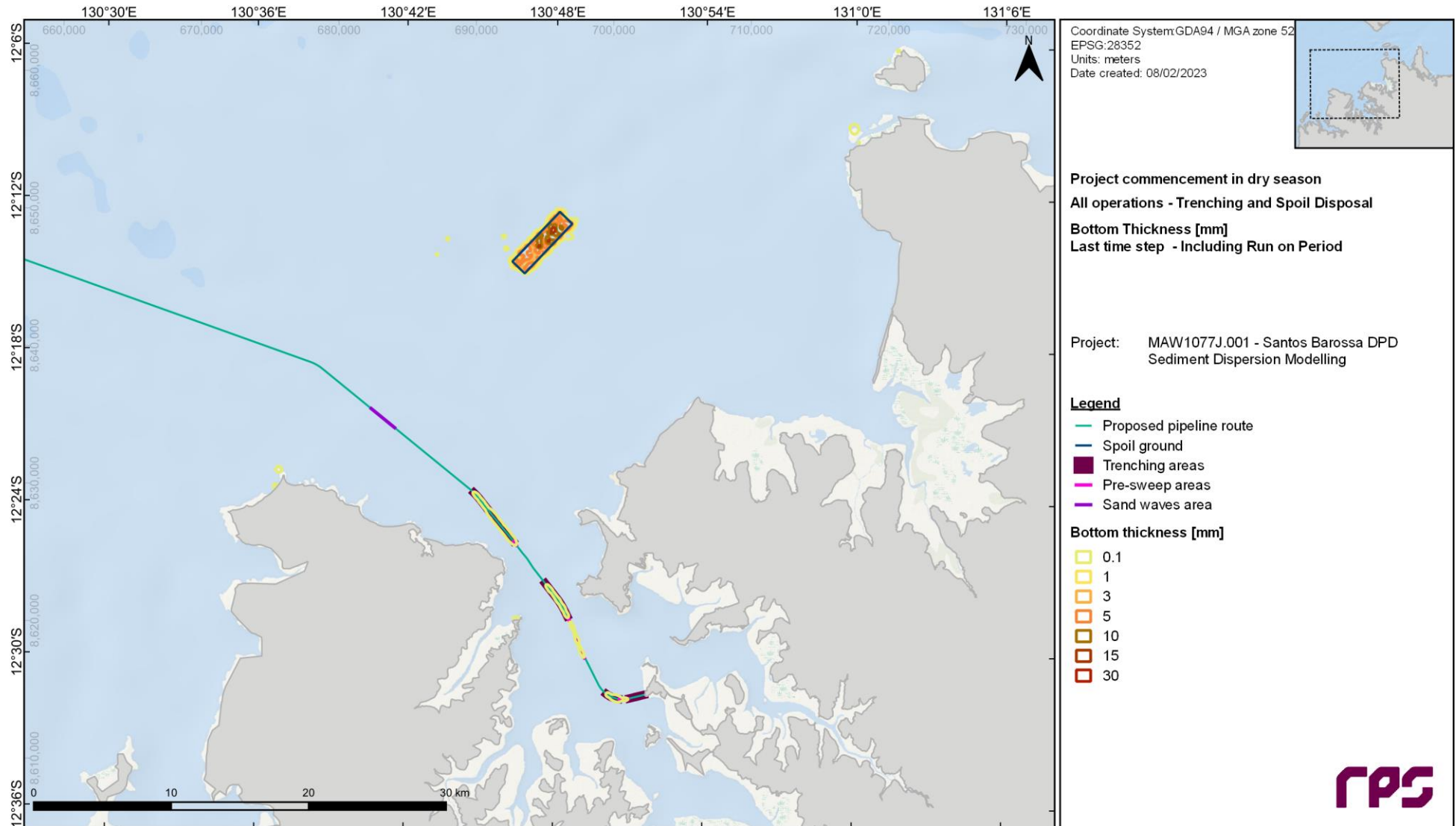
Figure 7.30 Predicted trenching-excess bottom thickness (mm) at the last time step of the simulation (end of run-on period) for the winter/dry season scenario (based on 10 July 2019). Note the trenching area widths shown on this and other Figures in this report are exaggerated to aid visual clarity.
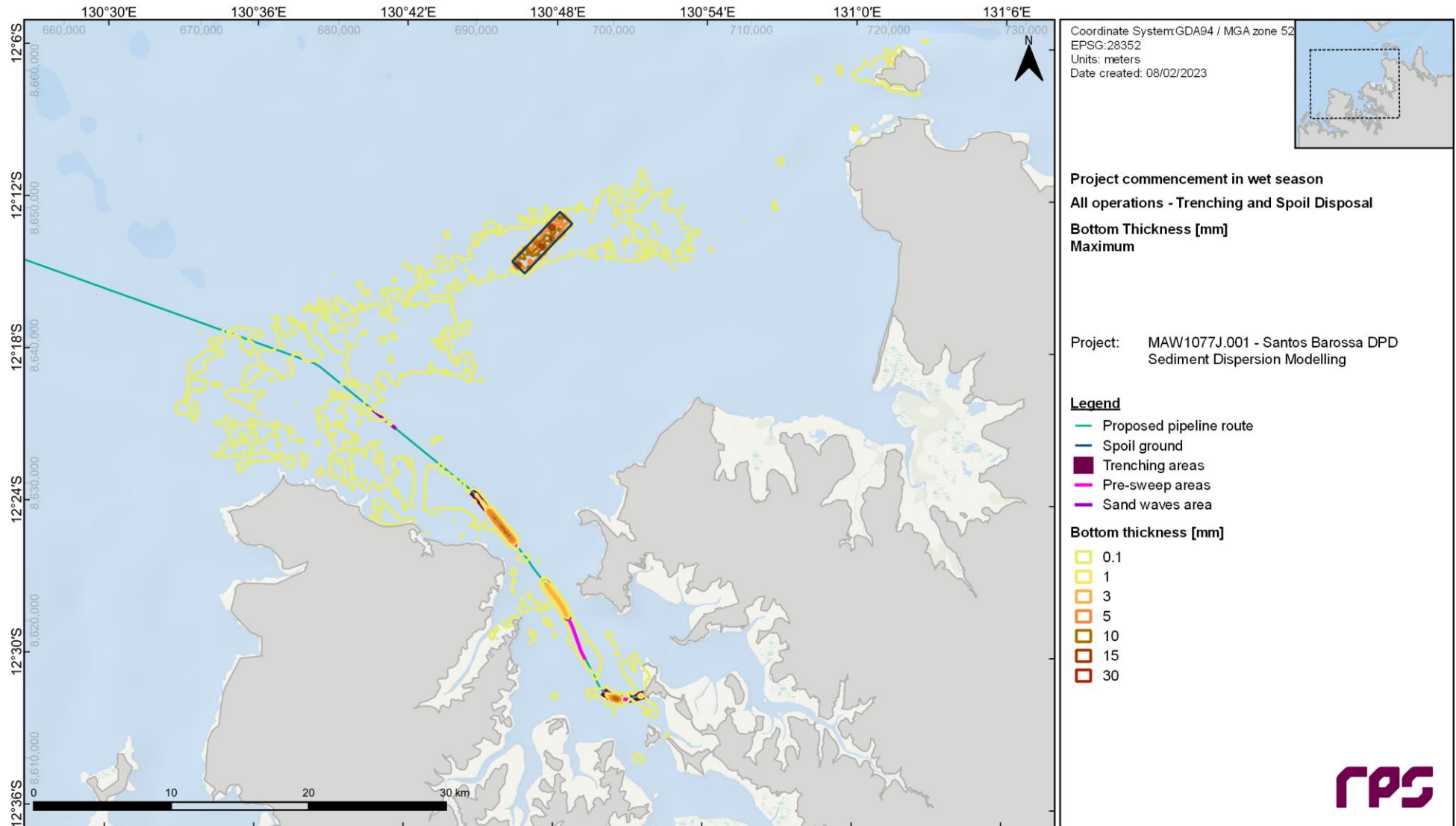
Figure 7.31 **Predicted maximum trenching-excess bottom thickness (mm) throughout the entire trenching program for the summer/wet season scenario (based on 1 October to 9 November 2019). Note the trenching area widths shown on this and other Figures in this report are exaggerated to aid visual clarity.**
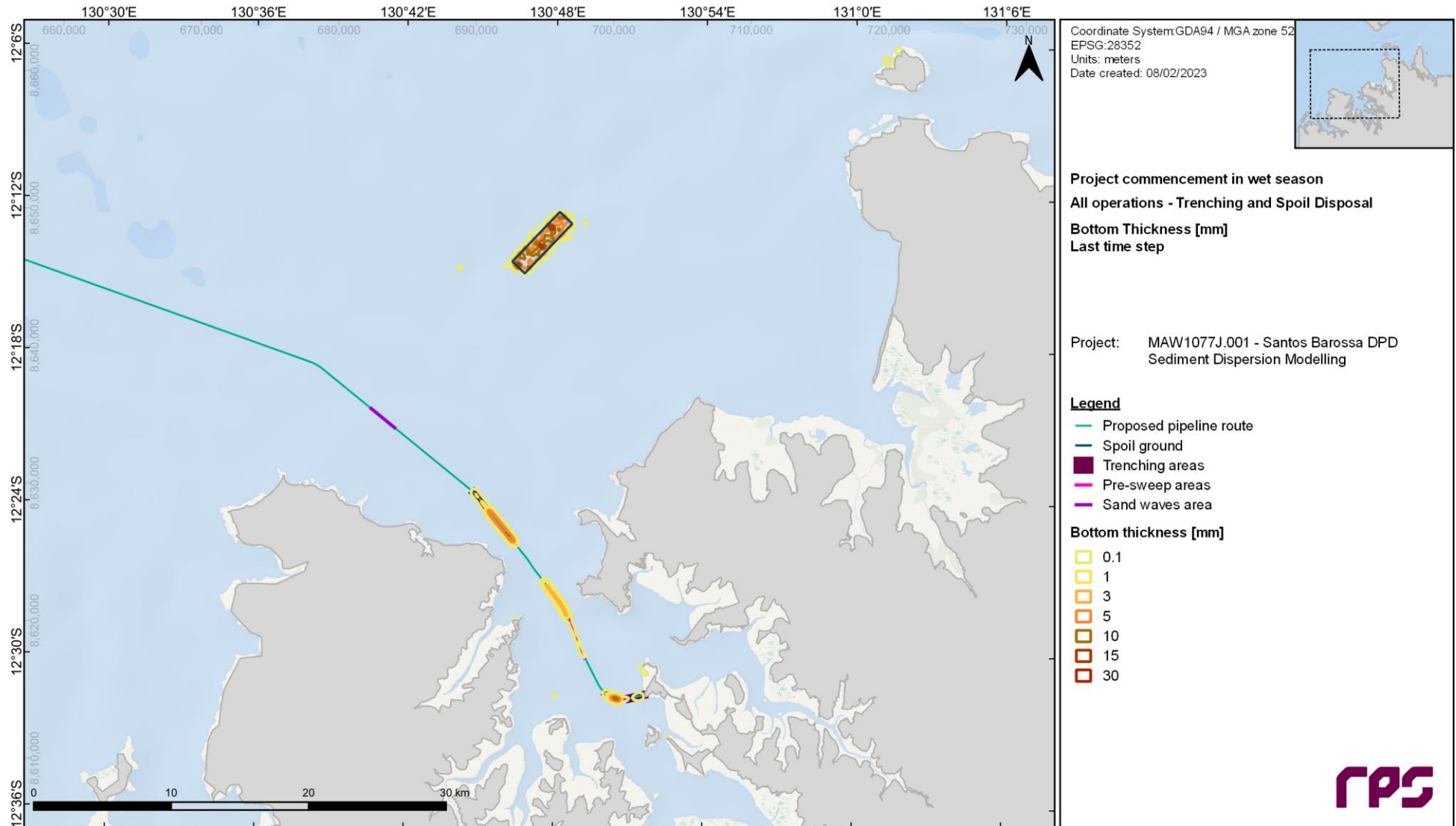
Figure 7.32 **Predicted trenching-excess bottom thickness (mm) at the last time step of the trenching program (not including run-on period) for the summer/wet season scenario (based on 9 November 2019). Note the trenching area widths shown on this and other Figures in this report are exaggerated to aid visual clarity.**
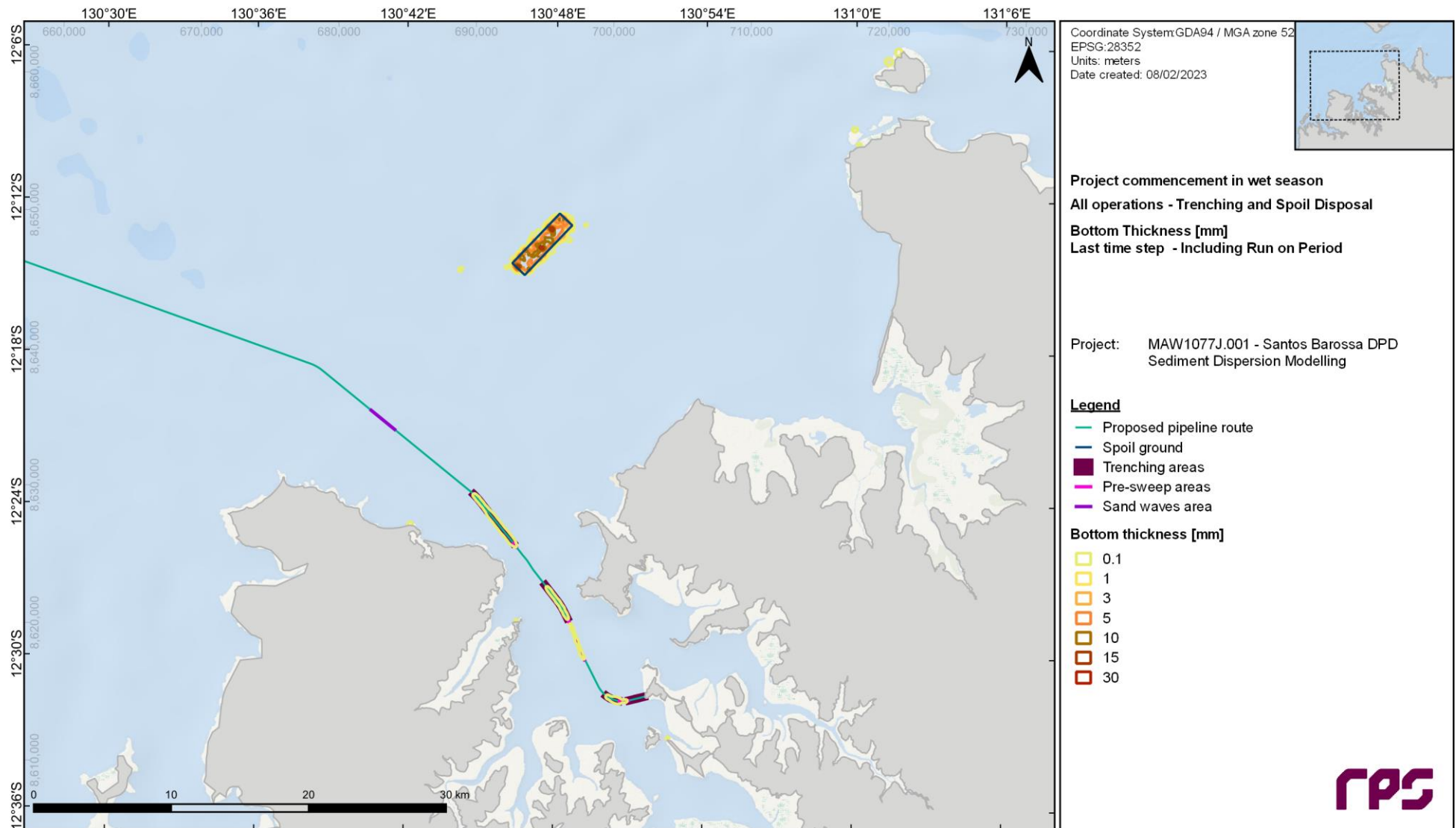
Figure 7.33   Predicted trenching-excess bottom thickness (mm) at the last time step of the simulation (end of run-on period) for the summer/wet season scenario (based on 9 January 2020). Note the trenching area widths shown on this and other Figures in this report are exaggerated to aid visual clarity.

7.3.2   Temporal Variability of Sedimentation

To explore the temporal exposure of sensitive receptor sites to sedimentation generated by the trenching and disposal operations, a time series analysis at a set of sensitive locations has been conducted to supplement the spatial maps. The set of analysis locations is the same as was used for the time series analysis of SSC (Figure 7.17 and Table 7.1).

As indicated by the spatial maps, the time series analysis shows that the deposition rates at distance from the trenching and disposal areas are low, forming only very thin layers of material. At all sites other than those around the disposal area, the predicted thicknesses remain less than 0.2 mm and those plots have not been included here. The low rates of deposition are due to the magnitude of the tidal currents in the area: material that is suspended is dispersed rapidly and widely, with material deposited at slack tide being typically resuspended on the next tide – or the following spring tide period.

Time series plots showing predicted trenching-excess bottom thickness for each of the offshore disposal area sites are presented for both the winter/dry and summer/wet season scenarios in Figure 7.34 through Figure 7.37. The plots reinforce the finding that deposition beyond the immediate vicinity of the disposal area is very low, with predicted bottom thickness values at *OD1*, *OD5*, *OD6* and *OD9* being less than 0.2 mm at all times, and with corresponding values at *OD7* and *OD8* (on the edge of the disposal area) never exceeding 0.5 mm. At the sites within the disposal area (*OD2*, *OD3* and *OD4*) there are variation in thickness based on their relative proximity to where disposals have occurred in the modelling. Some slight reduction of the predicted bottom thickness can be seen during the run-on periods, but as the deposited material is typically the coarser sediments the sedimentation levels are relatively stable during ambient conditions.
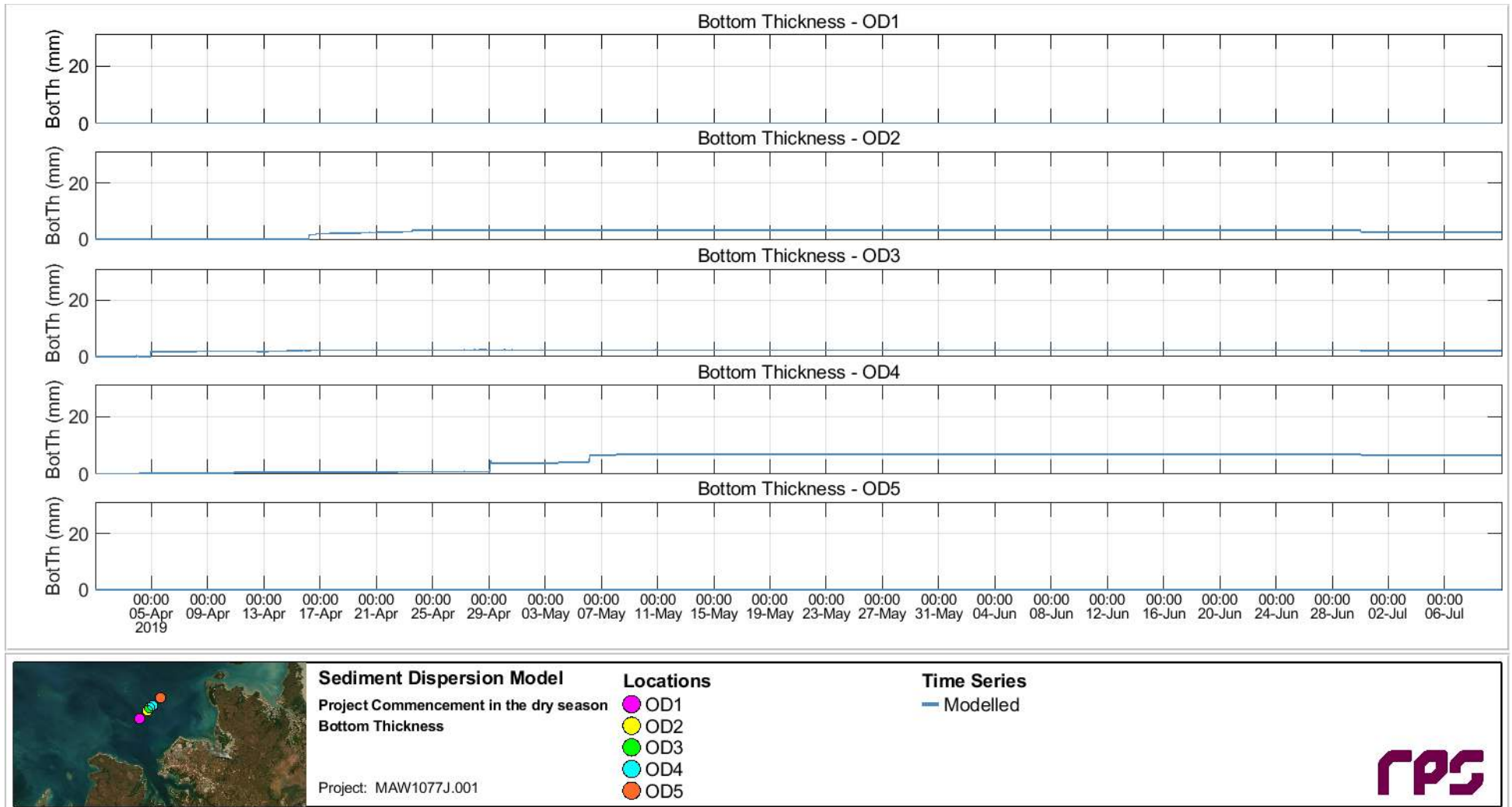
Figure 7.34 Time series of predicted trenching-excess bottom thickness at the *OD1* to *OD5* sites throughout the entire trenching program and run-on period in the winter/dry season scenario.
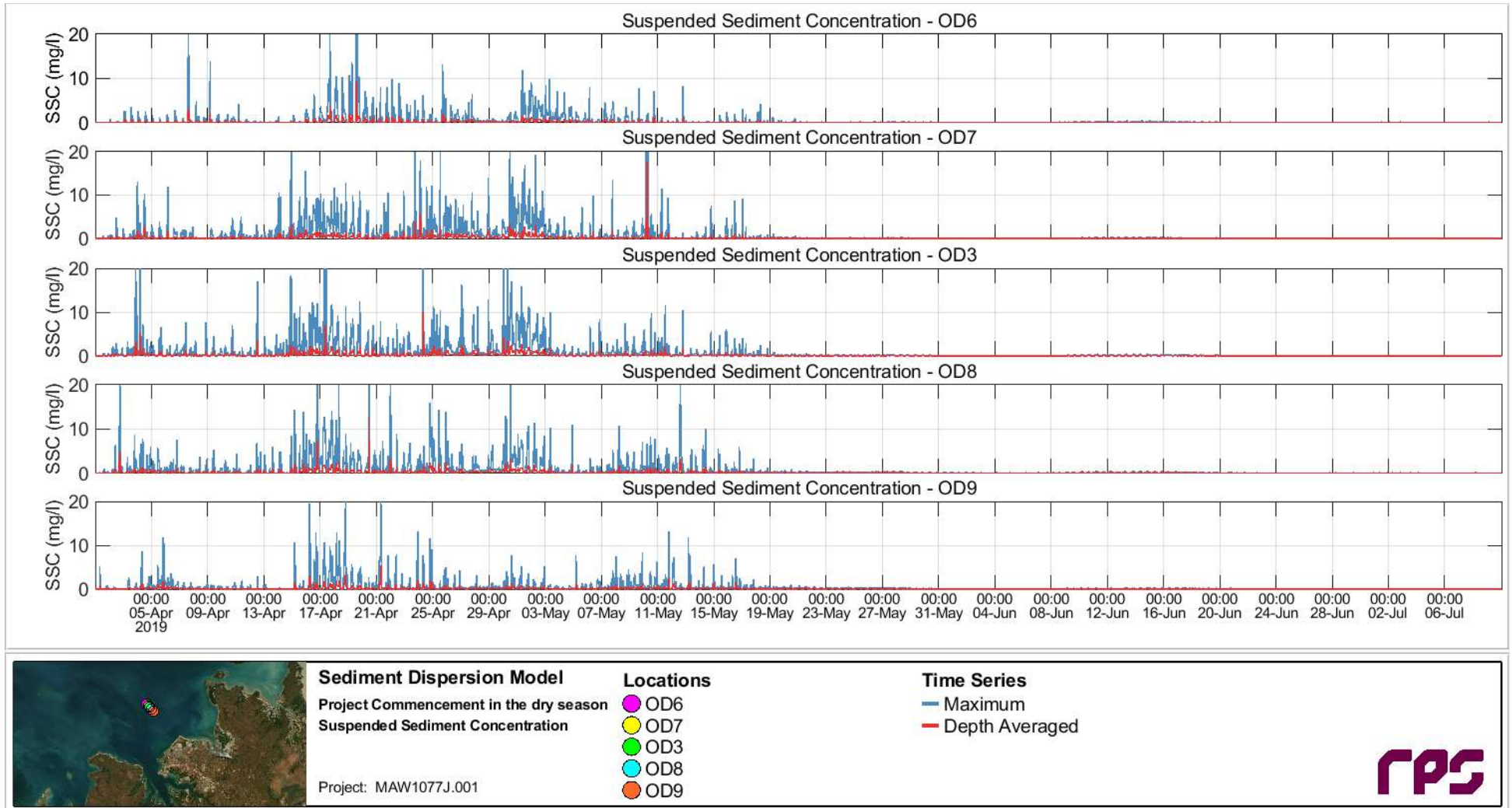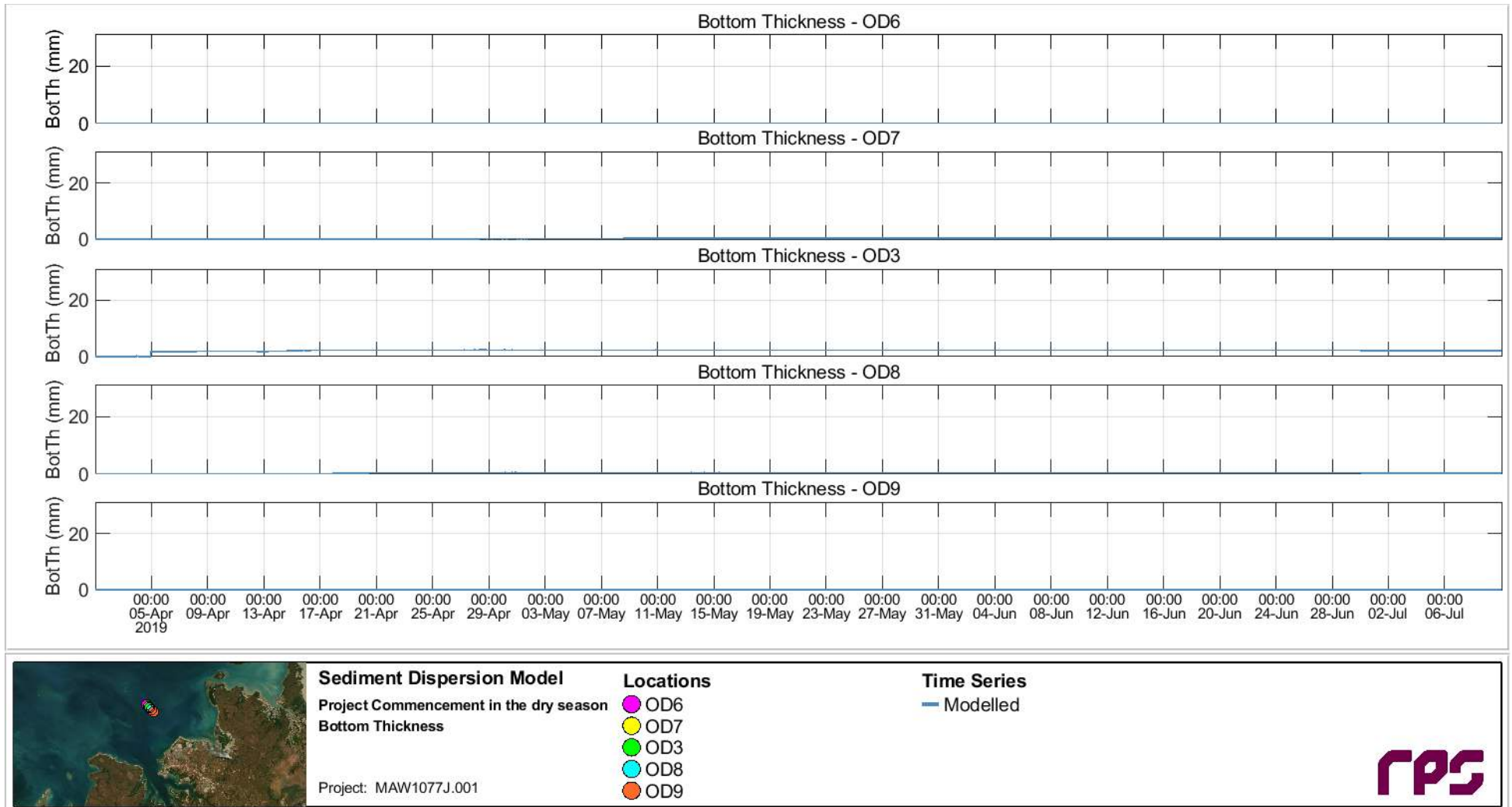
Figure 7.35   Time series of predicted trenching-excess bottom thickness at the *OD6* to *OD9* (via *OD3*) sites throughout the entire trenching program and run-on period in the winter/dry season scenario.
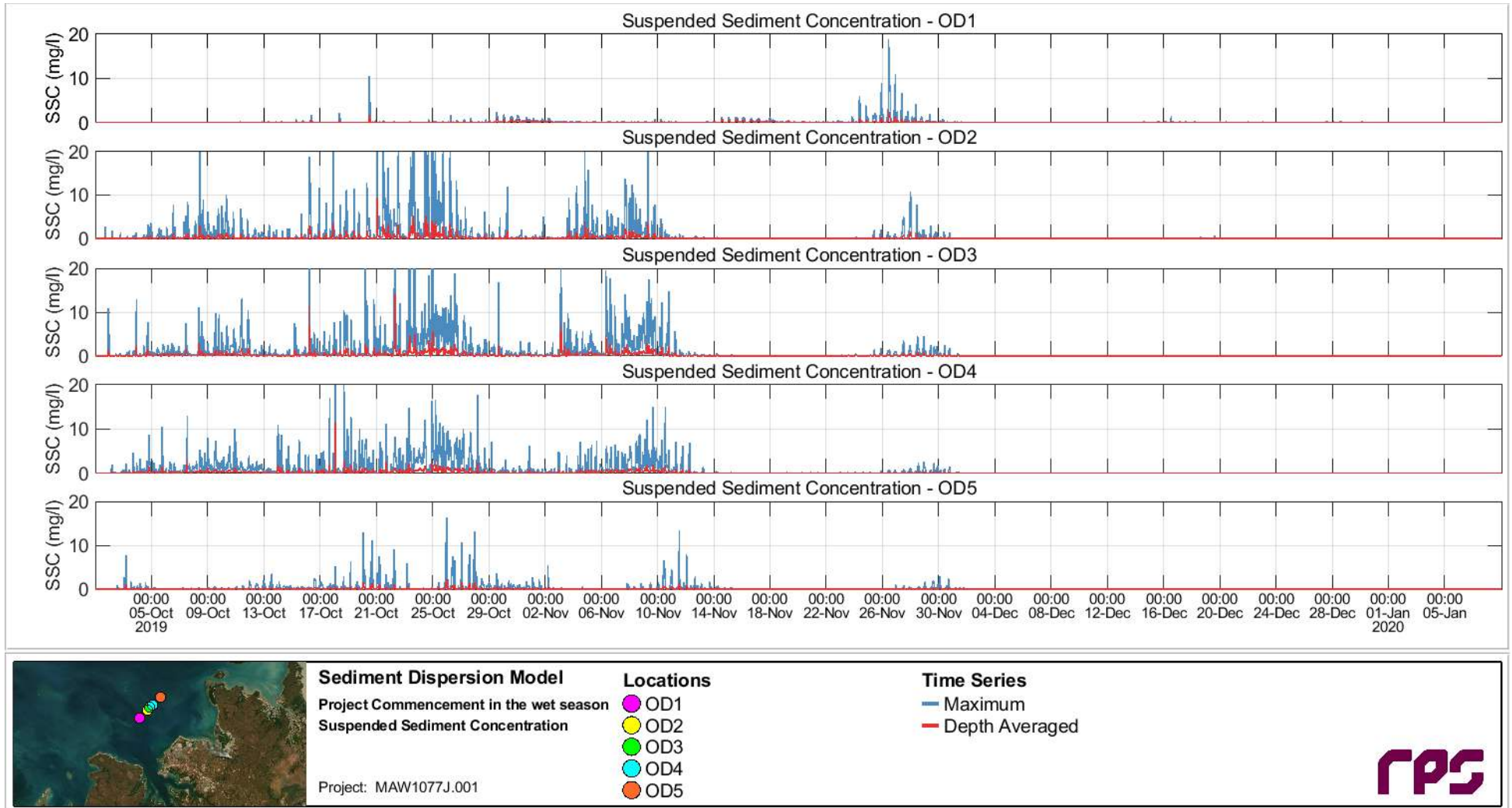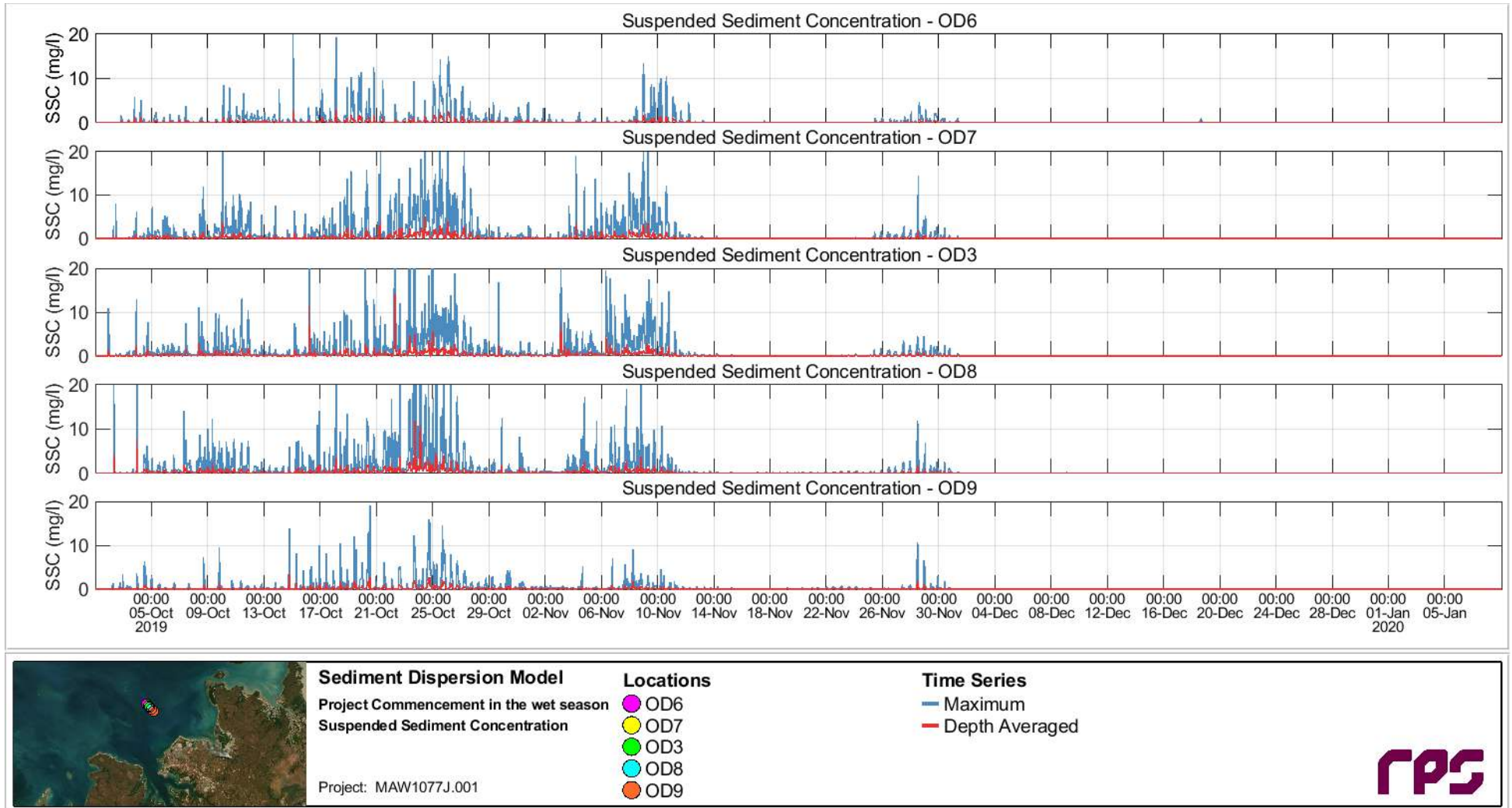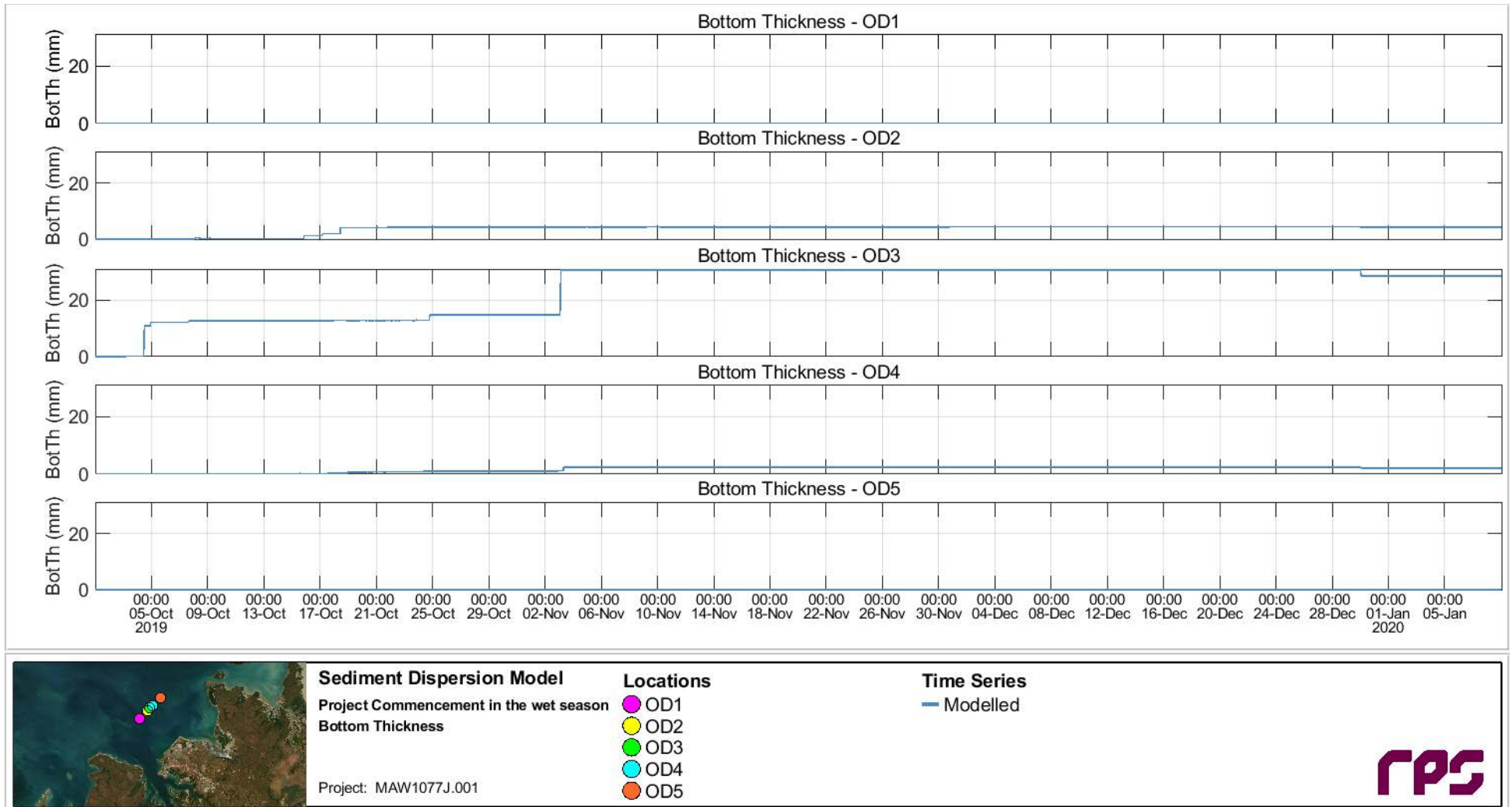
Figure 7.36 Time series of predicted trenching-excess bottom thickness at the *OD1* to *OD5* sites throughout the entire trenching program and run-on period in the summer/wet season scenario.
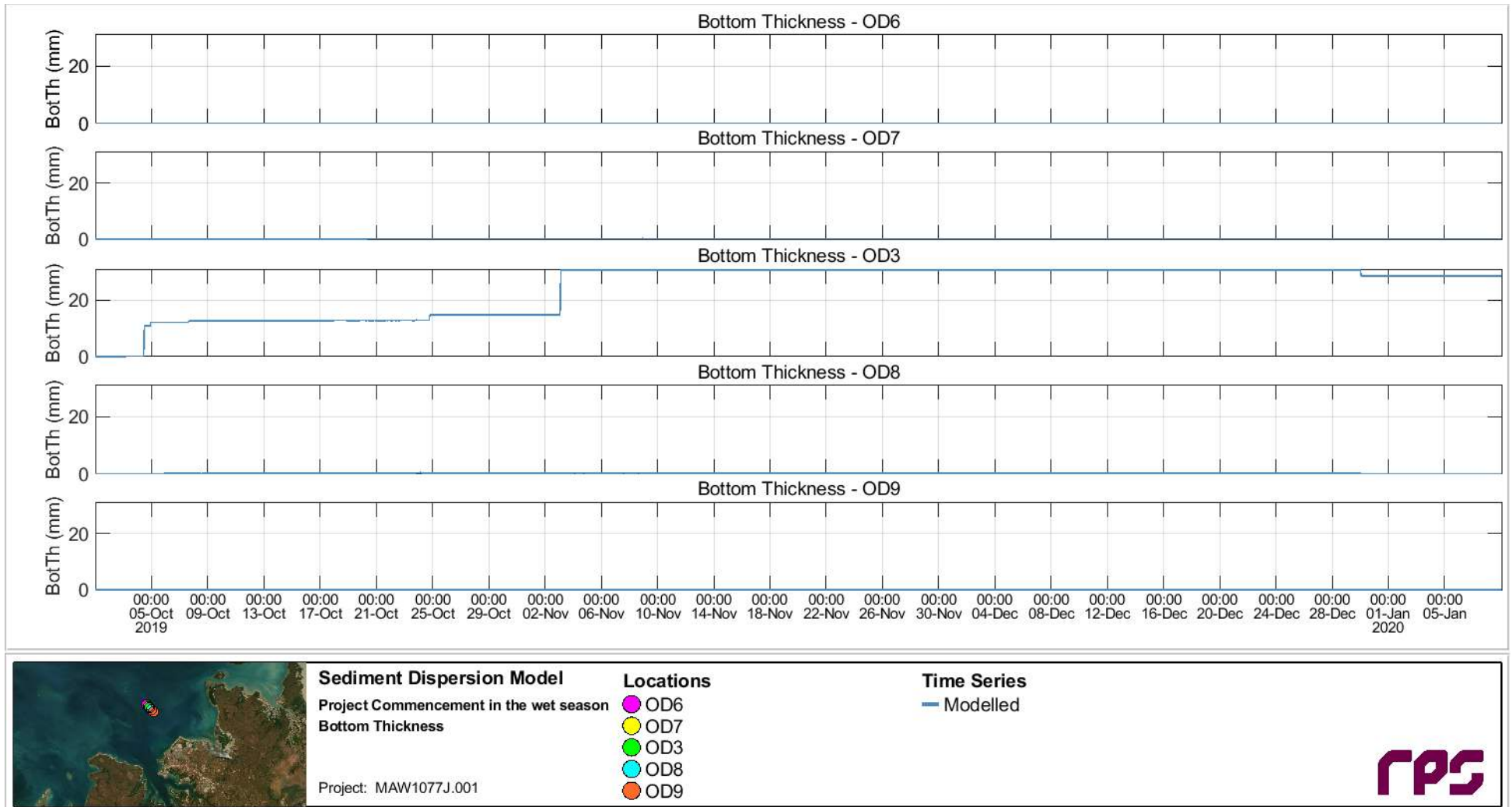
Figure 7.37   Time series of predicted trenching-excess bottom thickness at the *OD6* to *OD9* (via *OD3*) sites throughout the entire trenching program and run-on period in the summer/wet season scenario.

7.4   Prediction of Management Zone Extents

The calculated extents of the defined management zones – ZoI and ZoMI – over the entire program of trenching and disposal operations for the winter/dry season scenario are presented in Figure 7.38 and Figure 7.39, and for the summer/wet season scenario the extents are presented in Figure 7.40 and Figure 7.41. From the figures it is evident that the predicted ZoMI for the trenching and disposal operations for both seasonal scenarios is restricted to the trenching and spoil disposal footprints, which are also within the ZoHI as defined in Section 6.2.1.

The predicted ZoI for the trenching and disposal operations for both seasonal scenarios is also generally restricted to within or close to the trenching and spoil disposal footprints, with the exception of a very small patch in the shallows at South West Vernon Island in the summer/wet season scenario. This isolated patch may be attributable to the combined effects of model bathymetry and hydrodynamics, representing sediments that are transported into the shallowest possible grid cells and then trapped upon reversal of the tide. While it is clear that there is a potential for sediments released at the offshore disposal ground to be found in the indicated area, the persistence of material remaining at the water-land boundary in this location may be overstated.

It should be noted that the management zones shown are the result of exceedance of the sedimentation thresholds only; no exceedance of the SSC thresholds occurred at the predicted 90th and 95th percentile depth-averaged SSC levels for both modelled seasonal scenarios (see Figure 7.9 to Figure 7.12).
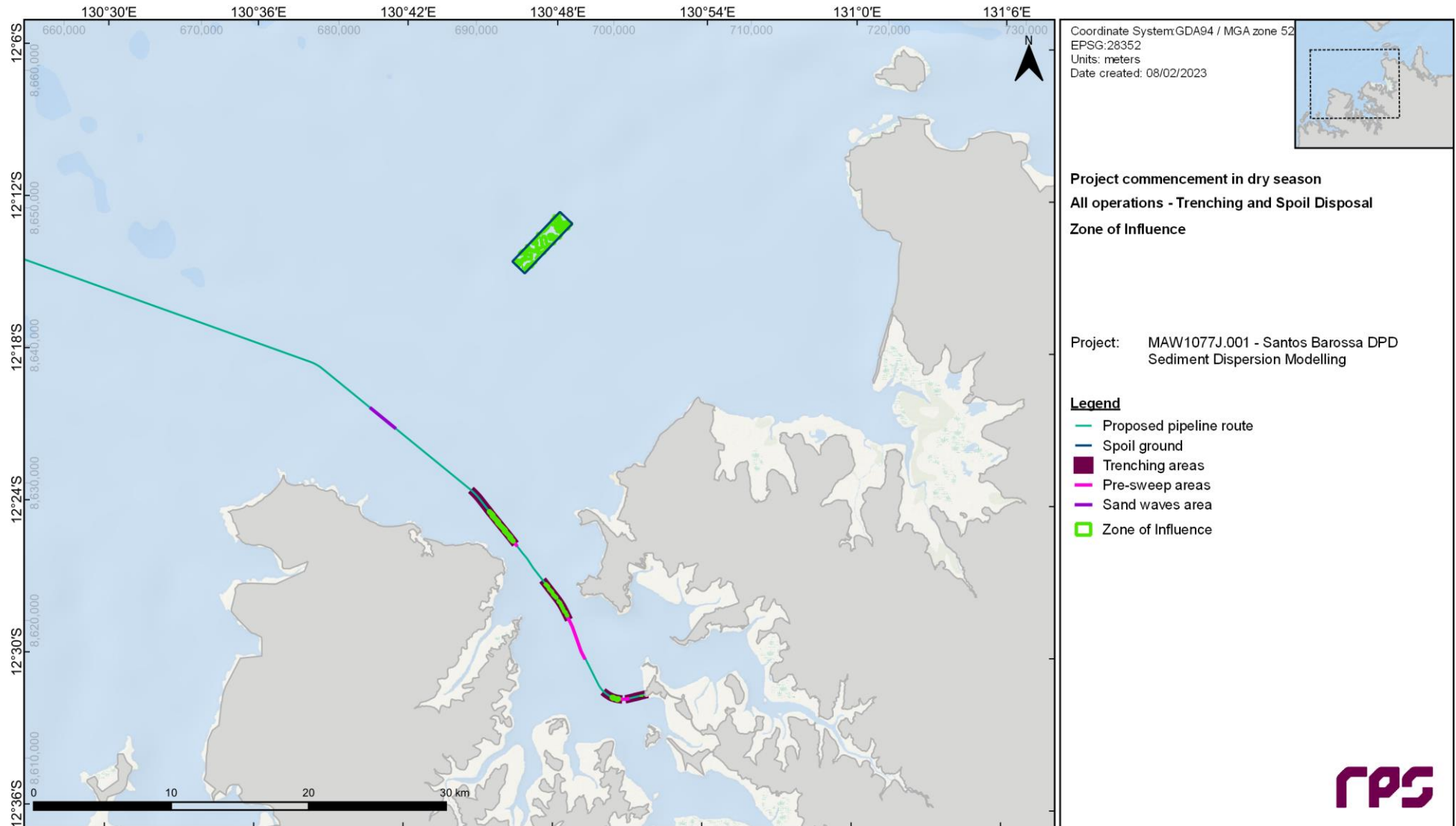
Figure 7.38 **Predicted Zone of Influence following application of the appropriate spatial thresholds in Table 6.1 to the 95th percentile SSC and maximum sedimentation throughout the entire trenching program for the winter/dry season scenario (based on 1 April to 10 May 2019). Note the trenching area widths shown on this and other Figures in this report are exaggerated to aid visual clarity.**
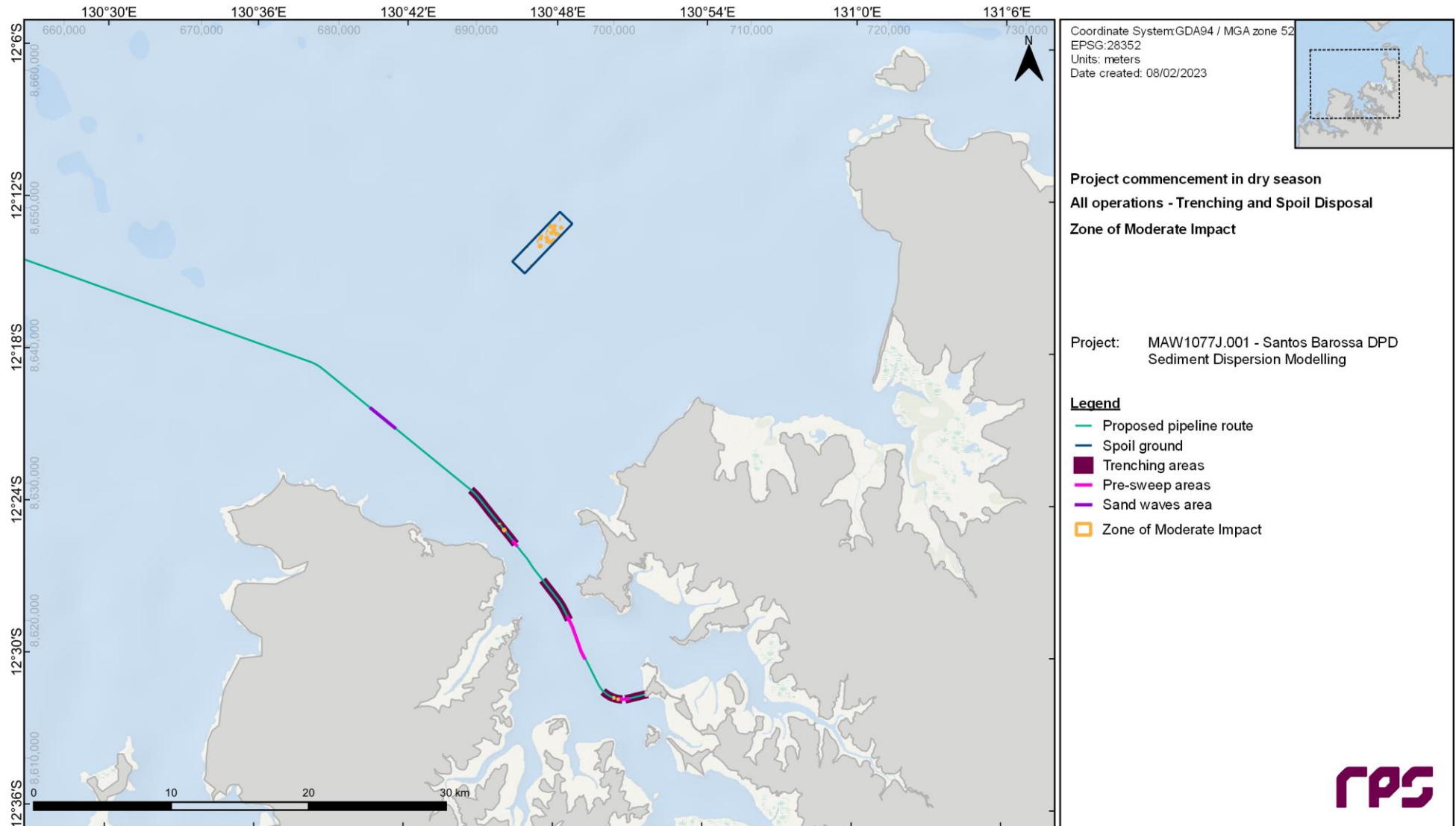
Figure 7.39 **Predicted Zone of Moderate Impact following application of the appropriate spatial thresholds in Table 6.1 to the 90th percentile SSC and maximum sedimentation throughout the entire trenching program for the winter/dry season scenario (based on 1 April to 10 May 2019). Note the trenching area widths shown on this and other Figures in this report are exaggerated to aid visual clarity.**
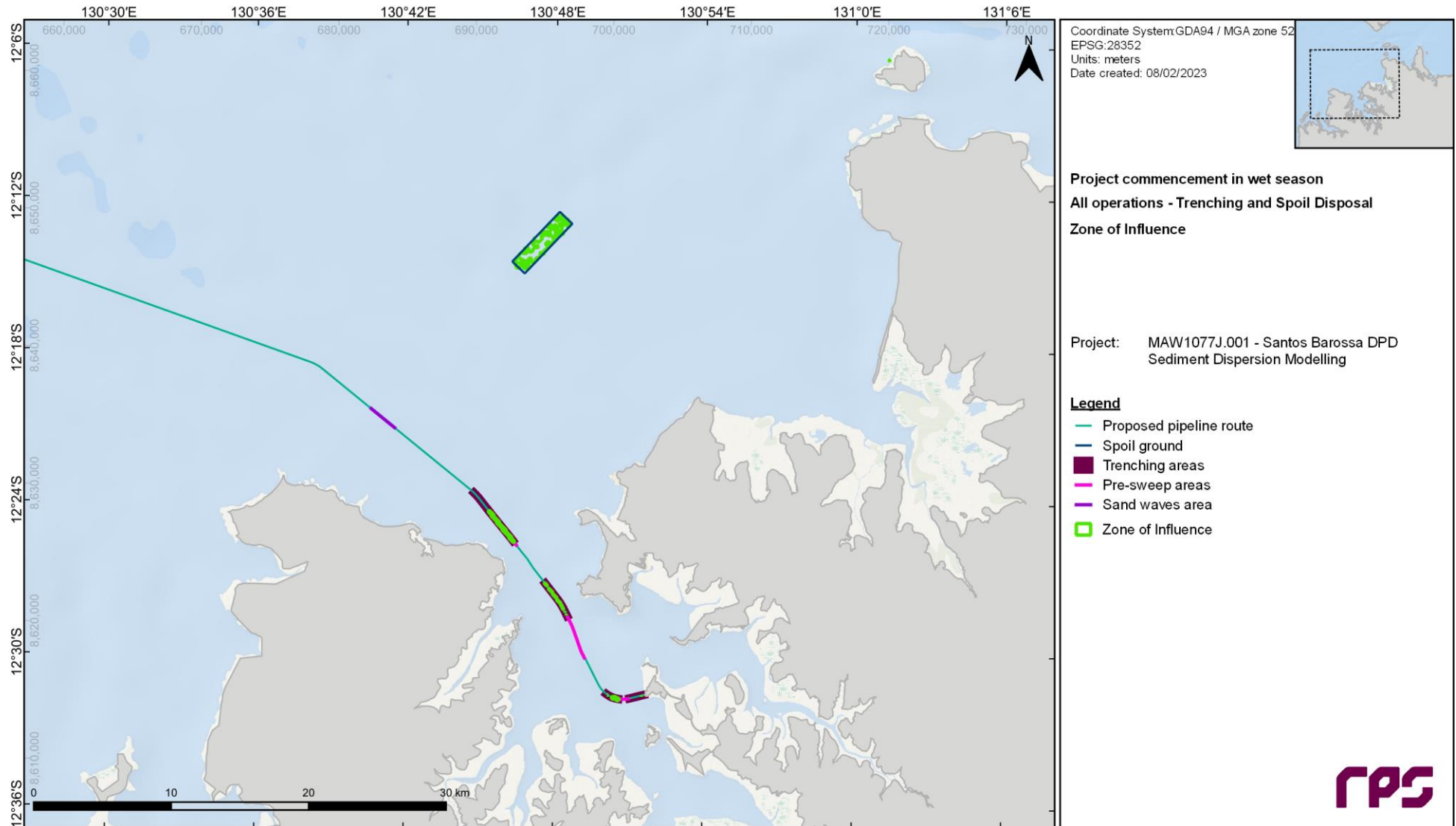
Figure 7.40 **Predicted Zone of Influence following application of the appropriate spatial thresholds in Table 6.1 to the 95th percentile SSC and maximum sedimentation throughout the entire trenching program for the summer/wet season scenario (based on 1 October to 9 November 2019). Note the trenching area widths shown on this and other Figures in this report are exaggerated to aid visual clarity.**
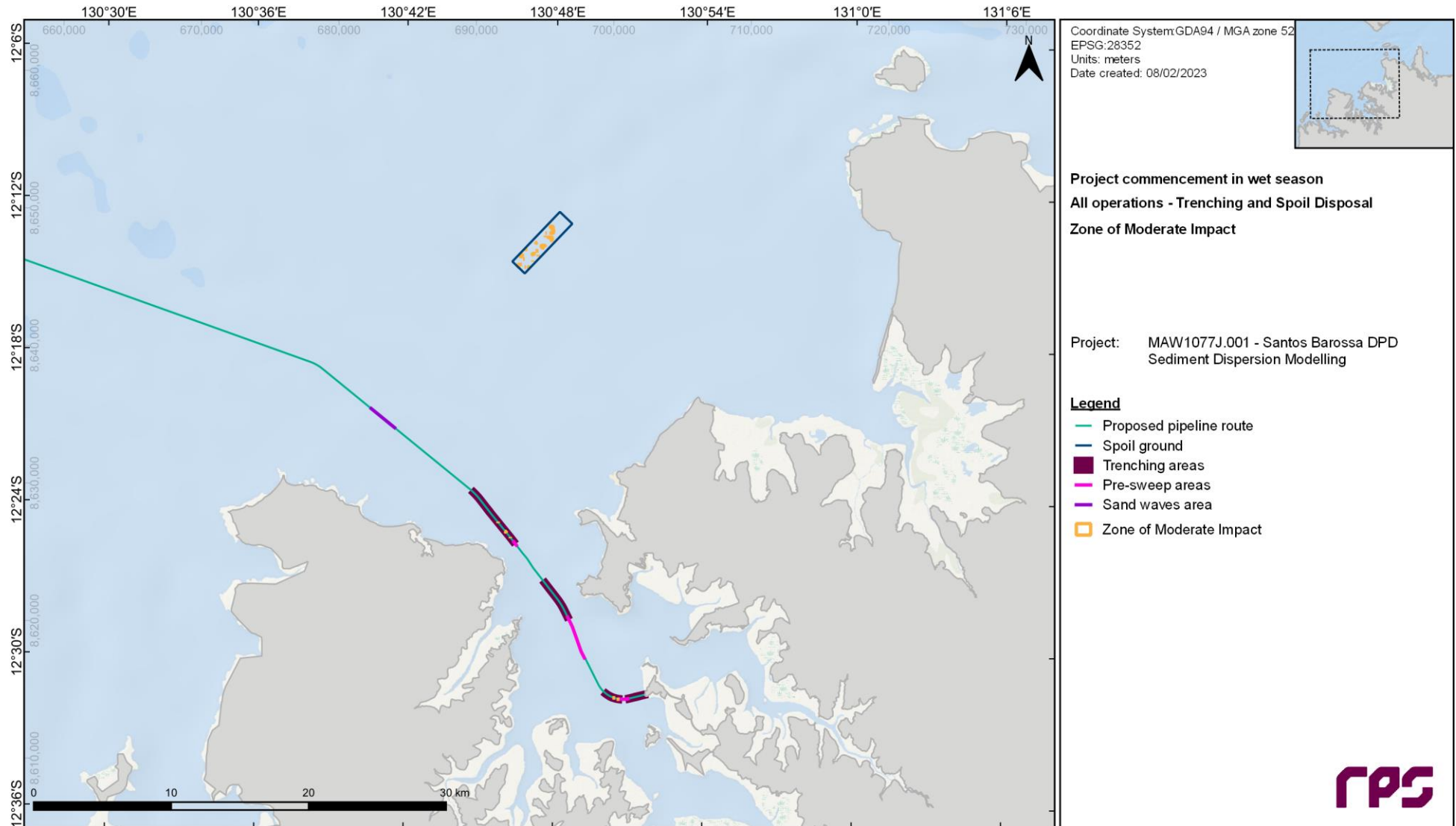
Figure 7.41   Predicted Zone of Moderate Impact following application of the appropriate spatial thresholds in Table 6.1 to the 90th percentile SSC and maximum sedimentation throughout the entire trenching program for the summer/wet season scenario (based on 1 October to 9 November 2019). Note the trenching area widths shown on this and other Figures in this report are exaggerated to aid visual clarity.

8   CONCLUSIONS

The main conclusion from the sediment dispersion modelling conducted for the proposed trenching and disposal operations, associated with the Barossa DPD project are outlined in the following sections.

8.1   General Plume Movement

- The localised movement of the trenching-generated suspended sediment is dominated by the ebbing and flooding tidal oscillations, due to the very strong tidal flows in the project area.

- Some slight seasonal differences in the overall drift patterns are evident due to the wind-driven residual currents, with plumes predicted to extend slightly more southwards in the winter/dry season and slightly more northwards during the summer/wet season.

- At the spoil ground the interaction between suspended sediment plumes from consecutive disposals is minimal during spring tide periods, with more potential for interaction between consecutive disposals during neap tide periods, when plume movement is slower, and trajectories are shorter. However, the predicted depth-averaged SSC of the interacting plumes remains relatively low.

8.2   Spatial and Temporal Distributions of SSC

- Forecasts of median depth-averaged SSC values do not exceed 1 mg/L in both seasonal scenarios, while at the 80th percentile values greater than 1 mg/L are forecast in small, isolated patches.

- At the 90th and 95th percentile levels, predicted depth-averaged SSC values do not exceed 5 mg/L in both seasonal scenarios.

- The temporal variation in predicted SSC, reflects the spatial patchiness of the plumes and the oscillations of tidal flows, with rapidly changing (over hourly scales) sharp peaks and troughs in SSC.

- At the sensitive receptor monitoring sites, the duration of the peaks in SSC are predicted to be short (in the order of hours), the 98th percentile SSC is predicted to be less than 7 mg/L at all sites in both seasons.

- At the spoil ground elevated SSC levels (in the order of 100-200 mg/L) occur immediately after disposal events but are rapidly dispersed and do not persist for long periods (scales of hours). The intensity of the modelled SSC values are predicted to reduce significantly within 1-3 km of the spoil ground boundaries.

8.3   Spatial and Temporal Distributions of Sedimentation

- Settlement of coarse material (sand size) is predicted to be rapid and near the trenching and offshore disposal areas, but the fine material is predicted to remain suspended, or will deposit at slack tide only to be resuspended on the following tide, particularly during spring tide periods.

- Suspended sediment plumes are predicted to have long drift trajectories, with sediments dispersed widely but at low concentrations, and with sediments deposited in thin layers.

- Sedimentation of greater than 1 mm thickness is predicted to be limited to the trenching and disposal areas, with a small patch predicted at South West Vernon Island for the summer/wet season scenario.

- Deposition within the spoil ground varies in thickness based on the locations of disposals in the modelling.

- Some slight reduction of the predicted bottom thickness occurs in the run-on periods, but as the deposited material is typically the coarser sediments the thickness is relatively stable during ambient conditions.

8.4   Management Zone Extents

- The predicted management zones are the result of exceedance of the sedimentation thresholds only; no exceedance of the SSC thresholds occurred for both modelled seasonal scenarios.

- The predicted ZoMI for the trenching and disposal operations for both seasonal scenarios is restricted to the trenching and spoil disposal footprints, which are also within the ZoHI as defined in Section 6.2.1.

- The predicted ZoI for the trenching and disposal operations for both seasonal scenarios is also generally restricted to within or close to the trenching and spoil disposal footprints, with the exception of a very small patch in the shallows at South West Vernon Island in the summer/wet season scenario. However, it should be noted that this patch may accentuated due to model limitations.

9   REFERENCES

Anchor Environmental 2003, *Literature review of effects of resuspended sediments due to dredging operations*, prepared for Los Angeles Contaminated Sediments Task Force. Los Angeles, CA, USA by Anchor Environmental CA LP, Irvine, CA, USA.

Andersen, E, Johnson, B, Isaji, T & Howlett, E 2001, 'SSFATE (Suspended Sediment FATE), a model of sediment movement from dredging operations', presented at WODCON XVI, World Dredging Congress and Exposition, Kuala Lumpur, Malaysia.

Australian Institute of Marine Science (AIMS) 2022, *Expert review of dredge plume modelling assessment report*, prepared by AIMS for Santos Ltd, July 2022.

Becker, J, van Eekelen, E, van Wiechen, J, de Lange, W, Damsma, T, Smolders, T & van Koningsveld, M 2015, 'Estimating source terms for far field dredge plume modelling', *Journal of Environmental Management*, vol. 149, pp. 282-293.

Blaauw, HG & van de Kaa, EJ 1978, 'Erosion of bottom and sloping banks caused by the screw race of manoeuvring ships', publication 202, Waterloopkundig Laboratorium Delft (Hydraulics Laboratory), Delft, Netherlands, 12 pp.

Bleck, R 2002, 'An oceanic general circulation model framed in hybrid isopycnic-Cartesian coordinates', *Ocean Modelling*, vol. 4, no. 1, pp. 55-88.

Bureau of Meteorology (BoM) 2021, *Climate statistics for Australian locations, Darwin Airport: Site number 014015* (http://www.bom.gov.au/climate/averages/tables/cw_014015.shtml).

Cavaleri, L 2009, 'Wave modeling – missing the peaks', *Journal of Physical Oceanography*, vol. 39, no. 11, pp. 2757-2778.

CDM Smith 2022, *Darwin Pipeline Duplication (DPD) project NT EPA referral*, Document No. BAA-201 0003, prepared by CDM Smith for Santos Ltd, Perth, WA, Australia.

Chassignet, EP, Smith, LT, Halliwell, GR & Bleck, R 2003, 'North Atlantic simulations with the Hybrid Coordinate Ocean Model (HYCOM): impact of the vertical coordinate choice, reference pressure, and thermobaricity', *Journal of Physical Oceanography*, vol. 33, pp. 2504-2526.

Coastline Surveys Limited (CSL) 1999, *Marine aggregate mining benthic & surface plume study final report*, report prepared for United States Department of the Interior Minerals Management Service, Washington, DC, USA by Coastline Surveys Ltd, Falmouth, UK.

Coastal Sediment Management Workgroup (CSMW) 2005, *Results from CSMW task 2 (natural and anthropogenic turbidity)*, prepared by the Coastal Sediment Management Workgroup, Government of California, CA, USA.

ConocoPhillips 2019, *Bayu-Undan gas export pipeline environment plan*, prepared by ConocoPhillips, Perth, WA, Australia.

DHI 2010, *Wheatstone Project: Dredge spoil modelling, Appendix B – LWI and DHI spill rate assessments*, prepared for Chevron Australia Pty Ltd, Perth, WA, Australia by DHI, Kota Kinabalu, Malaysia.

Durrant, T, Hemer, M, Smith, G, Trenham, C & Greenslade, D 2020, *CAWCR wave hindcast – Aggregated collection*, Commonwealth Scientific and Industrial Research Organisation (CSIRO), Melbourne, VIC, Australia.

Egbert, GD & Erofeeva, SY 2002, 'Efficient inverse modeling of barotropic ocean tides', *Journal of Atmospheric and Oceanic Technology*, vol. 19, no. 2, pp. 183-204.

Flater, D 1998, *XTide: harmonic tide clock and tide predictor* (www.flaterco.com/xtide/).

General Bathymetric Chart of the Oceans (GEBCO) 2021, *GEBCO 2021 Grid*, GEBCO Compilation Group (doi:10.5285/c6612cbe-50b3-0cff-e053-6c86abc09f8f).

Halliwell, GR 2004, 'Evaluation of vertical coordinate and vertical mixing algorithms in the HYbrid-Coordinate Ocean Model (HYCOM)', *Ocean Modelling*, vol. 7, no. 3-4, pp. 285-322.

Harper, BA 2010, 'Modelling the Tracy storm surge – implications for storm structure and intensity estimation', *Australian Meteorological and Oceanographic Journal*, vol. 60, pp. 187-197.

Hayes, D & Wu, PY 2001, 'Simple approach to TSS source strength estimates', in *Proceedings of the WEDA XXI Conference*, Western Dredging Association, Houston, TX, USA.

Hitchcock, DR & Bell, S 2004, 'Physical impacts of marine aggregate dredging on seabed resources in coastal deposits, *Journal of Coastal Research*, vol. 20, no. 1, pp. 101-114.

HR Wallingford 2003, *Protocol for the field measurement of sediment release from dredgers: a practical guide to measuring sediment release from dredging plant for calibration and verification of numerical models*, produced for VBKO TASS Project by HR Wallingford Ltd & Dredging Research Ltd, Wallingford, UK.

INPEX: see *INPEX Browse Ltd* or *INPEX Operations Australia Pty Ltd*.

INPEX Browse Ltd 2010, *Ichthys gas field development project: Draft environmental impact statement*, prepared by INPEX Browse Ltd, Perth, WA for review by the general public and by the Commonwealth Government, Canberra, ACT and the Northern Territory Government, Darwin, NT.

INPEX Browse Ltd 2011, *Ichthys gas field development project: Supplement to the draft environmental impact statement*, prepared by INPEX Browse Ltd, Perth, WA for the Commonwealth Government, Canberra, ACT and the Northern Territory Government, Darwin, NT.

INPEX Operations Australia Pty Ltd 2013, *Dredging and spoil disposal management plan – East Arm*, prepared by INPEX Operations Pty Ltd, Perth, WA, Australia.

INPEX Operations Australia Pty Ltd 2018, *Ichthys project – Maintenance dredging and spoil disposal management plan* [L060-AH_PLN_60010], prepared by INPEX Operations Pty Ltd, Perth, WA, Australia.

Johnson, BH, Andersen, E, Isaji, T, Teeter, AM & Clarke, DG 2000, 'Description of the SSFATE numerical modeling system', *DOER Technical Notes Collection* (ERDC TN-DOER-E10), US Army Engineer Research and Development Center, Vicksburg, MS, USA.

Kemps, H & Masini, R 2017, *Estimating dredge source terms – a review of contemporary practice in the context of Environmental Impact Assessment in Western Australia*, report of Theme 2 – Project 2.2 prepared for the Dredging Science Node, Western Australian Marine Science Institution, Perth, WA, Australia, 29 pp.

Makarynska, D 2019a, *Developing an integrated long-term monitoring program for Darwin Harbour – Water quality pilot project WP1: Neap tide trial*, Report No. 10/2019S, Department of Environment and Natural Resources, Darwin, NT, Australia.

Makarynska, D 2019b, *Developing an integrated long-term monitoring program for Darwin Harbour – Water quality pilot project WP2: Intra-annual water quality variability*, Report No. 22/2019D, Department of Environment and Natural Resources, Darwin, NT, Australia.

Mills, D & Kemps, H 2016, *Generation and release of sediments by hydraulic dredging: a review*, report of Theme 2 – Project 2.1 prepared for the Dredging Science Node, Western Australian Marine Science Institution, Perth, WA, Australia, 97 pp.

Moritz, HR & Randall, RE 1992, *Users guide for the open water disposal area management simulation*, Contract Report DACW39-90-K-0015, Texas A&M University, College Station, TX, USA.

National Centers for Environmental Prediction (NCEP) 2016, *The Global Forecast System (GFS) - Global Spectral Model (GSM)* (www.emc.ncep.noaa.gov/GFS/doc.php), National Centers for Environmental Prediction, College Park, MD, USA.

National Environment & Planning Agency (NEPA) 2001, *Port Bustamante Container Terminal: Environmental Impact Assessment*, National Environment & Planning Agency, Kingston, Jamaica.

National Oceanic and Atmospheric Administration (NOAA) 2018, *WAVEWATCH III,* National Oceanic and Atmospheric Administration, College Park, MD, USA (polar.ncep.noaa.gov/waves/index.shtml).

Nicholas, WA, Smit, N, Siwabessy, PJW, Nanson, R, Radke, L, Li, J, Brinkman, R, Atkinson, R, Dando, N, Falster, G, Harries, S, Howard, FJF, Huang, Z, Picard, K, Tran, M & Williams, D 2019, *Characterising marine abiotic patterns in the Darwin-Bynoe Harbour region: Summary report, physical environments, Darwin Harbour mapping project*, Department of Environment and Natural Resources, Darwin, NT, Australia (http://pid.geoscience.gov.au/dataset/ga/127386).

Northern Territory (NT) Government 2011, *East Arm wharf expansion project: Draft environmental impact statement, executive summary* (https://ntepa.nt.gov.au/__data/assets/pdf_file/0012/286788/EAW-Exec-Summary.pdf).

Oakajee Port and Rail (OPR) 2010, *Oakajee Deepwater Port: Dredging, Breakwater Construction and Land Reclamation Management Plan* [301012-01054-1000-EN-PLN-0003 rev. 0], prepared for Oakajee Port and Rail Pty Ltd, Perth, WA, Australia by Oceanica Consulting Pty Ltd, Nedlands, WA, Australia.

Rogers, WE, Hwang, PA & Wang, DW 2003, 'Investigation of wave growth and decay in the SWAN model: Three regional-scale applications', *Journal of Physical Oceanography*, vol. 33, pp. 366-389.

RPS 2009, *Ichthys gas field development project: Dredge and disposal modelling*, prepared by RPS, Perth, WA, Australia for INPEX Browse Ltd (INPEX document no. C036-AH-REP-0007), Perth, WA, Australia.

RPS 2022, *Santos Barossa DPD: Pipeline benthic survey report* [EN20291.007 Rev. D], prepared by RPS, Perth, WA, Australia for Santos Ltd, Perth, WA, Australia.

Saha, S, Moorthi, S, Wu, X, Wang, J, Nadiga, S, Tripp, P, Behringer, D, Hou, Y-T, Chuang, H-Y, Iredell, M, Ek, M, Meng, J, Yang, R, Mendez, MP, van den Dool, H, Zhang, Q, Wang, W, Chen, M & Becker, E 2014, 'The NCEP climate forecast system version 2', *Journal of Climate*, vol. 27, no. 6, pp. 2186-2208.

Santos 2022a, *Dredge Plume Overview*, PDF drawing provided to RPS by Santos Ltd, Perth, WA, Australia.

Santos 2022b, *Darwin Pipeline Project - Section I - Project Schedule_rev2_For Tender Submission*, PDF schedule provided to Santos Ltd, Perth, WA, Australia by DEME Offshore, Antwerp, Belgium and Van Oord, Rotterdam, Netherlands.

Santos 2022c, *Barossa project – Nearshore pipeline trench and backfill alignment details* [BAS-200 0523 001 to BAS-200 0523 012], PDF drawings provided to RPS by Santos Ltd, Perth, WA, Australia.

Santos 2022d, *Nearshore pipeline rock supply specification* [BAS-200 0550 D], report provided to Santos Ltd, Perth, WA, Australia by Atteris Pty Ltd, Perth, WA, Australia.

Santos 2022e, personal communication (email), selected extract from Fugro document *Nearshore GEP PSI Report BAS-200 0561_0* provided to Nuala Page, RPS by Xander van Beusekom, Santos Ltd on 2nd March 2022.

Santos 2022f, personal communication (email), selected extract from Fugro document *Bayu-Undan to Darwin Pipeline Project Detailed Engineering, Appendix E – Geotechnical Data, Vol 3 of* 6 provided to Nuala Page, RPS by Xander van Beusekom, Santos Ltd on 11th March 2022.

Smit, N, Billyard, R & Ferns, L 2000, *Beagle Gulf benthic survey: Characterisation of soft substrates*, Technical Report No. 66, Parks and Wildlife Commission of the Northern Territory, Darwin, NT, Australia.

Spearman, JR, de Heer, AFM, Aarninkhof, SGJ & van Koningsveld, M 2011, 'Validation of the TASS system for predicting the environmental effects of trailing suction hopper dredgers', *Terra et Aqua*, no. 125, pp. 14-22.

Sun, C, Shimizu, K & Symonds, G 2016, *Numerical modelling of dredge plumes: a review*, report of Theme 3 – Project 3.1.3 prepared for the Dredging Science Node, Western Australian Marine Science Institution, Perth, WA, Australia, 55 pp.

Sun, C, Branson, P & Mills D 2020, *Guideline on dredge plume modelling for environmental impact assessment*, report of Theme 2/3, prepared for the Dredging Science Node, Western Australian Marine Science Institution, Perth, WA, Australia.

Swanson, JC, Isaji, T, Ward, M, Johnson, BH, Teeter, A & Clarke, DG 2000, 'Demonstration of the SSFATE numerical modelling system', *DOER Technical Notes Collection* (ERDC TN-DOER-E12), US Army Engineer Research and Development Center, Vicksburg, MS, USA.

Swanson, JC, Isaji, T, Clarke, D & Dickerson, C 2004, 'Simulations of dredging and dredged material disposal operations in Chesapeake Bay, Maryland and Saint Andrew Bay, Florida', in *Proceedings of the WEDA XXIV Conference/36th TAMU Dredging Seminar*, Western Dredging Association, Orlando, FL, USA.

Swanson, JC, Isaji, T & Galagan, C 2007, 'Modeling the ultimate transport and fate of dredge-induced suspended sediment transport and deposition', presented at WODCON XVIII, World Dredging Congress and Exposition, Orlando, FL, USA.

Teeter, AM 2000, 'Clay-silt sediment modeling using multiple grain classes: Part I: settling and deposition', in WH McAnally & AJ Mehta (Eds.), *Proceedings in Marine Science: Coastal and Estuarine Fine Sediment Processes*, pp. 157-171, Elsevier BV, Amsterdam, Netherlands.

Tolman, HL 1991, 'A third-generation model for wind waves on slowly varying, unsteady, and inhomogeneous depths and currents', *Journal of Physical Oceanography*, vol. 21, no. 6, pp. 782-797.

US Army Corps of Engineers (USACE) 2008, *The four Rs of environmental dredging: Resuspension, release, residual, and risk* (ERDC/EL TR-08-4), Dredging Operations and Environmental Research Program, US Army Corps of Engineers, Washington, DC, USA.

van Rijn, LC 1989, *Sediment transport by currents and waves*, report H461, Delft Hydraulics Laboratory, Delft, Netherlands.

Whiteside, PGD, Ooms, K & Postma, G 1995, 'Generation and decay of sediment plumes from sand dredging overflow', presented at WODCON XIV, World Dredging Congress and Exposition, Amsterdam, Netherlands.

Williams, D, Wolanski, EJ & Spagnol, SB 2006, *Hydrodynamics of Darwin Harbour*, in: *The environment in Asia Pacific harbours*, Wolanski, EJ (ed.), pp. 461-476.

Willmott, CJ 1981, 'On the validation of models', *Physical Geography*, vol. 2, pp. 184-194.

Willmott, CJ 1982, 'Some comments on the evaluation of model performance', *Bulletin of the American Meteorological Society*, vol. 63, no. 11, pp. 1309-1313.

Willmott, CJ, Ackleson, SG, Davis, RE, Feddema, JJ, Klink, KM, Legates, DR, O'Donnell, J & Rowe, CM 1985, 'Statistics for the evaluation and comparison of models', *Journal of Geophysical Research: Oceans*, vol. 90, no. C5, pp. 8995-9005.

Willmott, CJ & Matsuura, K 2005, 'Advantages of the mean absolute error (MAE) over the root mean square error (RMSE) in assessing average model performance', *Journal of Climate Research*, vol. 30, pp. 79-82.

Appendix A – Expert Review of Sediment Dispersion Modelling Assessment Report

Australian Government | AUSTRALIAN INSTITUTE OF MARINE SCIENCE

Expert Review of Dredge Plume Modelling Assessment Report
Document: MAW1077J.001 - Santos Barossa DPD Sediment Dispersion Modelling Rev0.pdf

prepared for Santos Limited
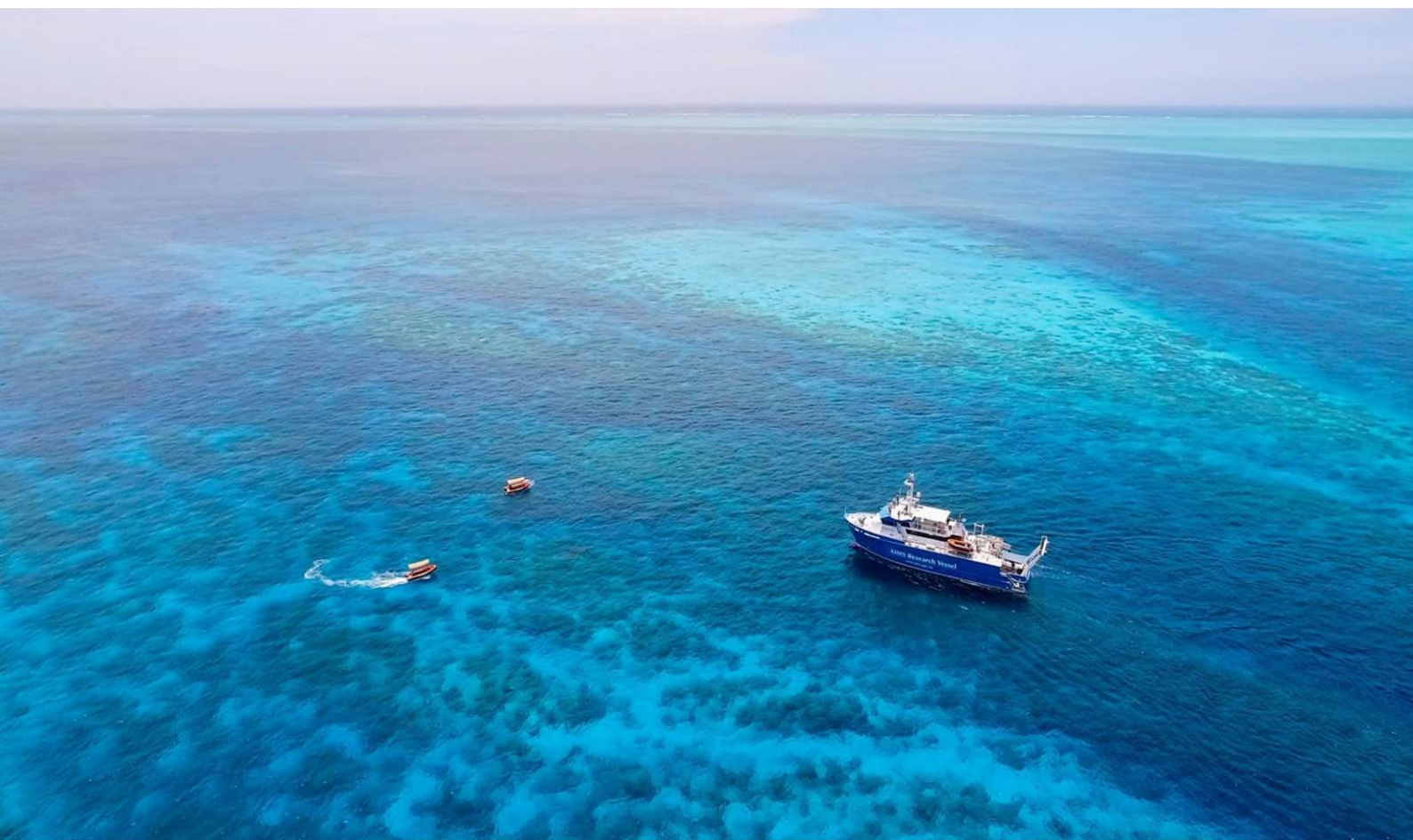
Dr Hemerson Tonin (h.tonin@aims.gov.au) July 2022

Australian Institute of Marine Science

PMB No 3	PO Box 41775	Indian Ocean Marine Research Centre
Townsville MC Qld 4810	Casuarina NT 0811	University of Western Australia, M096
		Crawley WA 6009

> "The Australian Institute of Marine Science (AIMS) acknowledges the Traditional Owners as the ongoing custodians of country throughout Australia, and in particular across northern Australia where AIMS operates in partnership with Aboriginal and Torres Strait Islander peoples. AIMS acknowledges and celebrates their continued connection to country, including sea country, and pays respects to all elders past, present and future."

Project Leader shall ensure that documents have been fully checked and approved prior to submittal to client				
Revision History:		Name	Date	Comments
1	Prepared by:	Hemerson Tonin	28/07/2022	
	Reviewed by:	Claire Streten	29/07/2022	
	Approved by:	Claire Streten	29/07/2022	

Cover photo:

Current picture 'RV Solander in Western Australia. Image: N. Thake

Darwin Pipeline Duplication (DPD) - Expert Review of Dredge Plume Modelling Assessment Report

Background

In March 2022, the Australian Institute of Marine Science (AIMS) was invited by SANTOS to assist in the Darwin Pipeline Duplication (DPD) plan as an external advisory prior to submission to the Northern Territory – Environmental Protect Agency (NT-EPA). The contribution of AIMS would involve review and provision of advice on source terms to be used for modelling in a workshop organised by Santos and for the numerical modelling provider (RPS) prior to modelling and then further technical review of modelling deliverables, including modelling report, and ad-hoc advice as required. As part of this engagement, the current document is related to a qualitative and quantitative assessment of the component related to the numerical modelling report of the dredging plume (technical review). This assessment by AIMS' team follows the best practices currently employed in Australia and will address the following key points:

- Baseline information on site/environmental conditions: if meteo-oceanographic conditions, as well as if geographic and temporal extension of the numerical modelling were adequate.
- Modelling approach: if the implemented modelling approach was adequate to represent and predict the dredging operation and the discharge of the sediment at specific site. This adequacy should contemplate the dredging plume, sediment suspended concentration, sediment deposition and others significant processes.
- Dredging operation: if the dredging and disposal of sediments were adequately represented numerically in the same context proposal to be carried out *in situ*.
- Model calibration and validation: if the level of accuracy demonstrated through calibration and validation procedures was adequate and reliable to predict sediment transport from the dredging and disposal activity, and,
- If reported results and conclusions could be based on the information contained in the report to be submitted to NT-EPA.

Overall Assessment

The report is prepared with a logical development in order to present the assumptions, modelling and results in a clear manner. However, there are deficiencies and areas for improvement in the report. There is an omission found in the numerical modelling (both hydrodynamics and waves) section that have the potential to impact the quality of the study. For example, the results of the numerical model can, and should, be assessed qualitatively and quantitatively (Williams & Esteves, 2017). There is no statistical analysis of model performance, including biases and errors – as is common in most model validation exercises – and emphasized in the modelling guidelines on dredge plume modelling studies, both by the Northern Territory (NT-EPA, 2013) and others (e.g. GBRMPA, 2012; Sun *et al.*, 2020). Discussion of the performance of the suite of models would benefit from a consistent qualitative approach, beyond a somewhat simplistic discussion as it was sometimes presented in the document.

Another important point that has not received due attention is related to the analysis of residual currents. Such currents are crucial in the transport of fine sediments (Sun *et al*, 2020) even more so when this class of sediment has a high incidence of occurrence in the region to be dredged, and therefore also discharged in the spoil ground. Therefore, the analysis of residual currents and estimation of the respective transport associated with them, in the region of the spoil ground could

be better explored to estimate the potential long term transport and fate, particularly of disposal material.

The absence of presentation of results in the form of time series was also observed. The joint analysis of the results in the form of maps and time series form a valuable tool for the analysis of impacts (space-time and intensity exposure; NT-EPA, 2013; GBRMPA, 2012; Sun et al. 2020).

The report presents a comprehensive modelling effort to understand the potential impact of dredging campaign and fate of dredge material.

However noting the limitations and deficiencies listed above, there is opportunity to improve the report. In relation to specific terms of the review:

- The modelling, in general conforms to the NT-EPA and main Australian modelling guidelines,
- The report does not describe observational data that adequately describes the environmental conditions of the dredging and placement locations.
- The modelling approach applies a hierarchy of hydrodynamic, wave and sediment transport models. The models themselves (e.g. Delft3D, SWAN and SSFATE) are suitable and commonly used in similar studies.
- For model validation and calibration, there is a lack a quantitative assessment of model skill (where appropriate) or a consistent qualitative approach to demonstrate model performance.
- A section at the end of the document summarizing the findings (list of dot points referring to the main text) would help the general understanding of the outcomes achieved by the implemented numerical modelling.

Rationale for making Assessment

It is undeniable that there is great complexity in carrying out hydrodynamic modelling to assess coastal processes, including sedimentation and sediment plume analysis. Although the report under review addresses almost all the points recommended by the main Australian guidelines, the most relevant deficiency that the report presents is the lack of quantitative and temporal evaluation/discussion of the implemented modelling suite. We understand the current study serves its purposes, but by making a few changes it will bring the necessary and desired confidence to decision makers.

Key Point's Assessment

- Assessing if the report meets the key point from the main Australian guidelines for the use of hydrodynamic modelling for dredging projects, such as NT-EPA (2013), GBRMPA (2012) and Sun *et al*. (2020).

The report addressed most of the recommendations contained in the guidelines of hydrodynamic modelling for dredging projects and key points for assessment recommendations were met. A relevant point partially addressed in the report is related to the thresholds. Although the threshold for each species found in the region were documented by previous studies by INPEX, the report presents the results on maps at different percentile levels (and only calculated from the average value in the water column; a similar approach should be performed for the maximum values observed in the water column). So, ecological vulnerability is also a function of exposure (intensity and period subject to, Sun *et al.*, 2020; Fraser *et al.*, 2017; McCook *et al.*, 2015). In this context, the presentation of time series of suspended sediment and of deposition time series in sensitive regions should be presented to estimate the pressure on marine receptors (GBRMPA, 2012).

- Baseline information on site/environmental conditions

The amount of environmental data available for carrying out the study was adequate, both in spatial and temporal coverage, however, the meteo-oceanographic analyses did not define typical and extreme periods. Although the dredging campaign is suspended during extreme events, numerical simulations for these periods are suggested to evaluate the remobilization of discharged material in the spoil ground. The evaluation of wave modelling also lacks a better qualitative and quantitative discussion of the results obtained. For example, unlike the other comparative graphs, the presentation related to the wave direction is not shown through continuous lines, which makes it difficult to evaluate the implemented model against measured data. The wave modelling showed an almost constant bias over time that is not mentioned also.

In relation to the wind field used as forcing in the model, the same data source used to evaluate the implemented model (for currents and waves) also provides wind measurements, with regular intervals of 10min. Therefore, it would be the opportunity to compare the measured wind with the NCEP-GFS for relevant periods to demonstrate its validity, limitations and possible implications in numerical modelling.

- Modelling approach

Although there are numerical models that are capable of solving hydrodynamic-wave-sediment in a single integrated modelling suite, the numerical modelling methodology used to assess the transport, settlement and resuspension of sediments resulting from dredging used a combination of internationally recognized numerical models (Delft3D, SWAN and SSFATE).

3

- Dredging and disposal description

The report presents a reliable spatial distribution of the sediment classes in the region of interest (based on surveys and literature). The dredging and disposal scenarios considered presented the necessary exposure to cover possible meteo-oceanographic conditions (wet and dry seasons). However, there is a lack of resuspension scenario of extreme event. In addition, the numerical modelling presented in the report assumed an initial vertical distribution of sediments that does not occur in time and space every time the disposal operation takes place. The discharge of high volume of fine sediments at different times of the day (therefore under different tidal cycle conditions) would transport the sediments according to the instantaneous condition of the tide with different behaviour in the water column, and as consequence, it would be possible an interaction between subsequent disposals, mainly during the operation of TSHD, where its cycles are shorter over time. The report assumes: "Sediments suspended in the water column during previous operations were subject to settlement and progressively-reducing levels of resuspension during this time". Thus, the presentation of the result of the discharge of sediments (mostly fine) in different tidal cycles would be relevant for evaluation (near slack of water and maximum current), as well as the interaction between two consecutive dumps ("best case" and "worst case" scenarios to evaluate the persistence of suspended sediments between disposals of sediments in sequence; GBRMPA, 2012; Sun *et al.*, 2020).

- Model calibration and validation

This is an essential and crucial topic in the analysis of this document on the numerical modelling of Sediment Dispersion Modelling Report. A numerical modelling study including hydrodynamics, waves and sediments with a prognostic focus to support decision-makers must have a level of accuracy, both temporal and spatial, beyond any doubts or possible to quantify its range of variability. The report presents the constant pursuit of this achievement in the hydrodynamic model, in the wave model and in the sediment transport component. However, the models present relevant and systematic weaknesses in the calibration and validation of numerical modelling. The first point to be highlighted is the total lack of statistical metrics of the results of the numerical model (hydrodynamics and waves) compared to the available data (named in the report as validation, there is no calibration presented in this document). These statistical metrics assist in verifying the extent to which the model has been well implemented and is capable of fulfilling its assumptions in a manner appropriate to what it was designed for. A second point about assessing the model results is related to the residual currents. The report made an "in passing" mention on the impacts of residual currents (page 48), but does not present an assessment per se. The computation of residual currents in the sites where the dredging and discharge operations of sediments take place is a valuable tool to evaluate the time-integrated error in the transport of suspended sediments. As for the waves, the report also showed a total lack of metric (quantitative) evaluation.

On a visual inspection, the results of both models (hydrodynamic and waves) show good results, however, there are several methodologies for the quantitative and qualitative evaluation of numerical models used in engineering, and Williams & Esteves (2017) presents a good summary of them. As for the disposal of sediments, some instantaneous maps of the maximum concentration of sediments in the water column could be presented to assess whether plumes resulting from consecutive discharges

could interact with each other. A sequence of vertical sections during the disposal and later moments would be valued to evaluate the behaviour of the dynamic of the sediments during its displacement in the water column.

- Results and conclusions

Results for sediment dispersion modelling in the report, for both wet and dry seasons, were presented as "throughout entire trenching program", were those results related to end of operations (dredging and disposal) or to the end of numerical simulations? In addition, as mentioned before, the presentation of time series in key sites (mainly in the spoil ground, due to the availability of fine materials) would be of great value to observe the temporal behaviour of the SSC until it reaches safe levels (thresholds), or even infer whether there is interaction between consecutive discharges of sediment. An extra point of observation would be to present the snapshot sequence (as shown in figures 5.1. and 5.2) for the wet season too. As a final comment, the presentation of general remarks/conclusions at the end of the document as a list of dot points (referring to the main text) would facilitate the general understanding of the outcome of the study.

Reviewer's references

Fraser, M.W.; Short, J.; Kendrick, G.A.; McLean, D.; Keesing, J.; Byrne, M.; Caley, M.J.; Clarke, D.; Davis, A.R.; Erftemeijer, P.L.A., Field, S.; Gustin-Craig, S.; Huisman, J.; Keough, M.; Lavery, P.S. Masini, R.; McMahon, K.; Mengersen, K.; Rasheed, M; Statton, J.; Stoddart, J.; Wu, P. (2017). *Effects of dredging on critical ecological processes for marine invertebrates, seagrasses and macroalgae, and the potential for management with environmental windows using Western Australia as a case study*. Ecological Indicators, 78, 229-242

GBRMPA (2012). The use of Hydrodynamic Numerical Modelling for Dredging Projects in the Great Barrier Reef Marine Park, August 2012. https://www.gbrmpa.gov.au/our-work/Managing-multiple-uses/ports/dredging-and-dredge-material-disposal (accessed: 10/07/2022)

McCook, L.J.; Schaffelke, B.; Apte, S.C.; Brinkman, R.; Brodie, J.; Erftemeijer, P.; Eyre, B.; Hoogerwerf, F.; Irvine, I.; Jones, R.; King, B.; Marsh, H.; Masini, R.; Morton, R.; Pitcher, R.; Rasheed, M.; Sheaves, M.; Symonds, A.; Warne, M.St.J. (2015). *Synthesis of current knowledge of the biophysical impacts of dredging and disposal on the Great Barrier Reef: Report of an Independent Panel of Experts,* Great Barrier Reef Marine Park Authority, Townsville.

Northern Territory – Environment Protection Agency (2013). *Guideline for the environmental assessment of marine dredging in the Northern Territory*. April 2013. Version 2.0. 32pp. https://ntepa.nt.gov.au/consultation/environmental-guidelines (accessed: 10/07/2022)

Sun, C; Branson, P.M. & Mills D. (2020). *Guideline on dredge plume modelling for environmental impact assessment*. Prepared for the Dredging Science Node, Western Australian Marine Science Institution (WAMSI), Perth, Western Australia. 73pp.

Williams, J.J. & Esteves, L.S. (2017). *Guidance on Setup, Calibration, and Validation of Hydrodynamic, Wave, and Sediment Models for Shelf Seas and Estuaries*. Advances in Civil Engineering Volume 2017, Article ID 5251902, 25 pages. https://doi.org/10.1155/2017/5251902 (accessed: 10/07/2022)

Appendix B – Expert Review AIMS Comments and RPS Response Table Rev 1

Topic	AIMS Expert Review Comment	RPS Response and Report Update
1	The results of the numerical model can, and should, be assessed qualitatively and quantitatively (Williams & Esteves, 2017). There is no statistical analysis of model performance, including biases and errors – as is common in most model validation exercises – and emphasized in the modelling guidelines on dredge plume modelling studies, both by the Northern Territory (NT-EPA, 2013) and others (e.g., GBRMPA, 2012; Sun et al., 2020).	The quantitative statistics have been calculated and added to the report to support the existing time series plots.
2	Another important point that has not received due attention is related to the analysis of residual currents. Such currents are crucial in the transport of fine sediments (Sun et al, 2020) even more so when this class of sediment has a high incidence of occurrence in the region to be dredged, and therefore also discharged in the spoil ground. Therefore, the analysis of residual currents and estimation of the respective transport associated with them, in the region of the spoil ground could be better explored to estimate the potential long-term transport and fate, particularly of disposal material.	Residual currents are included in the hydrodynamic modelling as described in Section 4.1.3. They are also discussed in the results sections (Section 7) where the seasonal differences in SSC drift patterns are attributed to seasonal differences in the direction of the drift currents. Note the differences are small.
Some additional discussion of residual currents has been included in Section 2. See also the Comment 4 response.
3	The absence of presentation of results in the form of time series was also observed. The joint analysis of the results in the form of maps and time series form a valuable tool for the analysis of impacts (space-time and intensity exposure; NT-EPA, 2013; GBRMPA, 2012; Sun et al. 2020). So, ecological vulnerability is also a function of exposure (intensity and period subject to, Sun et al., 2020; Fraser et al., 2017; McCook et al., 2015). In this context, the presentation of time series of suspended sediment and of deposition time series in sensitive regions should be presented to estimate the pressure on marine receptors (GBRMPA, 2012).	Time series analysis at a set of 17 points has been included in the results sections (Section 7) and the temporal variation in SSC and sedimentation has been discussed at these sites
4	The report does not describe observational data that adequately describes the environmental conditions of the dredging and placement locations.	A regional metocean conditions discussion has been included at the start of the report (Section 2) with typical wind, wave and current (tides and drift) conditions explained.

5	A section at the end of the document summarizing the findings (list of dot points referring to the main text) would help the general understanding of the outcomes achieved by the implemented numerical modelling.	A conclusions section (Section 8) has been added to the report.
Key Point Assessment		
6	Although the threshold for each species found in the region were documented by previous studies by INPEX, the report presents the results on maps at different percentile levels (and only calculated from the average value in the water column; a similar approach should be performed for the maximum values observed in the water column).	The same percentile levels as used by INPEX have been included. The same percentile analysis was completed for the maximum values and these percentile maps have now been included in the report. Between Santos and RPS it was determined that depth-averaged values were the most relevant for informing the impact of SSC on key benthic habitats that are being assessed (e.g. seagrass and hard corals). This approach is consistent with other dredging proponent referrals in Darwin Harbour that have been recently reviewed and which used depth-averaged results for the threshold analysis. The threshold analysis presented in the report uses the depth-averaged results. Note the same analysis was completed using maximum SSC values in parallel; no thresholds were exceeded for the maximum SSC values either.
7	So, ecological vulnerability is also a function of exposure (intensity and period subject to, Sun et al., 2020; Fraser et al., 2017; McCook et al., 2015). In this context, the presentation of time series of suspended sediment and of deposition time series in sensitive regions should be presented to estimate the pressure on marine receptors (GBRMPA, 2012).	Time series analysis at a set of 17 points has been included in the results sections (Section 7) and the temporal variation in SSC and sedimentation has been discussed at these sites
8	The amount of environmental data available for carrying out the study was adequate, both in spatial and temporal coverage, however, the meteo-oceanographic analyses did not define typical and extreme periods. Although the dredging campaign is suspended during extreme events, numerical simulations for these periods are suggested to evaluate the remobilization of discharged material in the spoil ground.	A separate spoil stability assessment has now been completed with a longer term one-year run-on period, which included a number of storm events. The spoil ground stability study has been included as an addendum to the main report.
9	The evaluation of wave modelling also lacks a better qualitative and quantitative discussion of the results obtained. For example, unlike the	RPS typically always use point markers to plot direction comparisons because the use of continuous lines can make it

	other comparative graphs, the presentation related to the wave direction is not shown through continuous lines, which makes it difficult to evaluate the implemented model against measured data. The wave modelling showed an almost constant bias over time that is not mentioned also.	difficult to distinguish the comparison datasets if/when directional changes cross the 0/360 value and obscure the entire panel at that time step. Quantitative statistics have now been included and discussed the bias in Tp in the modelling.
10	In relation to the wind field used as forcing in the model, the same data source used to evaluate the implemented model (for currents and waves) also provides wind measurements, with regular intervals of 10min. Therefore, it would be the opportunity to compare the measured wind with the NCEP-GFS for relevant periods to demonstrate its validity, limitations and possible implications in numerical modelling.	Comparisons of modelled and measured wind speeds at the NRSDAR station has been conducted and included in the report (Section 4.1.3.3). This section has both time series plots and quantitative statistics. The comparison showed good agreement.
11	Although there are numerical models that are capable of solving hydrodynamic-wave-sediment in a single integrated modelling suite, the numerical modelling methodology used to assess the transport, settlement and resuspension of sediments resulting from dredging used a combination of internationally recognized numerical models (Delft3D, SWAN and SSFATE).	The use of a separate model for the sediment dispersion modelling component is based on the objective of modelling the dredge program in the most time efficient way. Having the wave and hydrodynamic models separate from the dredge dispersion model, allowed the wave and hydrodynamic model to be calibrated/ validated and production runs to be finished upfront, while aspects of the dredge program were being confirmed. In addition, the SSFATE model allows each of the individual dredge operation streams to be modelled and processed individually and cumulatively in a relatively short time frame. This is not practical in a fully coupled Delft3D model, as to assess the effect of individual operations you would essentially have to run the waves and currents multiple times also. This method also allows the dredge program or an individual component of the dredge program to be remodelled relatively quickly without having to rerun the hydrodynamic and wave modelling.

12	The dredging and disposal scenarios considered presented the necessary exposure to cover possible meteo-oceanographic conditions (wet and dry seasons). However, there is a lack of resuspension scenario of extreme event.	A separate spoil stability assessment has now been completed with a longer term one-year run-on period, which included a number of storm events. The spoil ground stability study has been included as an addendum to the main report.
13	The numerical modelling presented in the report assumed an initial vertical distribution of sediments that does not occur in time and space every time the disposal operation takes place. The discharge of high volume of fine sediments at different times of the day (therefore under different tidal cycle conditions) would transport the sediments according to the instantaneous condition of the tide with different behaviour in the water column, and as consequence, it would be possible an interaction between subsequent disposals, mainly during the operation of TSHD, where its cycles are shorter over time. The report assumes: "Sediments suspended in the water column during previous operations were subject to settlement and progressively-reducing levels of resuspension during this time". Thus, the presentation of the result of the discharge of sediments (mostly fine) in different tidal cycles would be relevant for evaluation (near slack of water and maximum current), as well as the interaction between two consecutive dumps ("best case" and "worst case" scenarios to evaluate the persistence of suspended sediments between disposals of sediments in sequence; GBRMPA, 2012; Sun et al., 2020).	Varying the vertical distribution of each disposal based on the tide is not a practical option within the modelling approach. It is theoretically possible but would need a significant amount of time to set up, and given the timings of the disposals in reality will be different to those as-modelled this level of detail would not likely add value or accuracy to the model results. Additionally, the correlation of vertical distributions to tidal states would still have to be justified with reference to literature values, which do not provide the level of detail required to configure a model appropriately. Time series points have been added along two perpendicular cross sections through the disposal ground, zoomed-in snapshot sequences over the disposal ground have been provided to show the interactions between two or more consecutive disposals and the persistence of SSC between them.
14	The models present relevant and systematic weaknesses in the calibration and validation of numerical modelling. The first point to be highlighted is the total lack of statistical metrics of the results of the numerical model (hydrodynamics and waves) compared to the available data (named in the report as validation, there is no calibration presented in this document).	Additional statistical measures of model accuracy have been calculated and added to the report to support the time series plots.
15	A second point about assessing the model results is related to the residual currents. The report made an "in passing" mention on the impacts of residual currents (page 48), but does not present an assessment per se. The computation of residual currents in the sites where the dredging and discharge operations of sediments take place is a	A regional metocean conditions discussion has been added at the start of the report (Section 2) with typical wind, wave and current (tides and drift) conditions explained. Residual currents were included in the hydrodynamic modelling.

	valuable tool to evaluate the time-integrated error in the transport of suspended sediments	
16	As for the disposal of sediments, some instantaneous maps of the maximum concentration of sediments in the water column could be presented to assess whether plumes resulting from consecutive discharges could interact with each other. A sequence of vertical sections during the disposal and later moments would be valued to evaluate the behaviour of the dynamic of the sediments during its displacement in the water column.	An additional section (Section 7.1.2) with discussion of additional hourly mapped snapshots of SSC has been included for typical spring and neap tide sequences, with figures zoomed-in on the disposal area to show the interactions of consecutive disposals at different stages of the tide.
17	Results for sediment dispersion modelling in the report, for both wet and dry seasons, were presented as "throughout entire trenching program", were those results related to end of operations (dredging and disposal) or to the end of numerical simulations?	The percentile results are based on the trenching period only (so not including the run-on period of two months), and the sedimentation results show the maximums throughout the trenching and at the last time-step of trenching (so not considering the run-on period). The presented values are both the more conservative option and thought to be appropriate given the duration of the trenching program period was only ~40 days and the run-on period was 60 days. Comments have been added to the report to make this distinction clearer. We have also added an additional sedimentation map for each scenario, which shows the end of the run-on period (Figures 7.30 and 7.33).
18	In addition, as mentioned before, the presentation of time series in key sites (mainly in the spoil ground, due to the availability of fine materials) would be of great value to observe the temporal behaviour of the SSC until it reaches safe levels (thresholds), or even infer whether there is interaction between consecutive discharges of sediment.	A time series analysis at a set of 17 points has been added to the results sections (Section 7) and the temporal variation in SSC and sedimentation has been discussed at these sites.
19	An extra point of observation would be to present the snapshot sequence (as shown in figures 5.1. and 5.2) for the wet season too.	SSC snapshots for a neap and spring sequence in the summer/wet season scenario have been added to the report (Figures 7.3 and 7.4).
20	The presentation of general remarks/conclusions at the end of the document as a list of dot points (referring to the main text) would facilitate the general understanding of the outcome of the study.	A conclusions section (Section 8) has been added to the report.

SANTOS BAROSSA DPD STUDIES
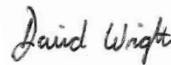
Sediment Dispersion Modelling Addendum 1 - Spoil Stability Assessment

Document status

Version	Purpose of document	Authored by	Reviewed by	Approved by	Review date
Rev A	Issued for internal review	Nuala Page	David Wright	David Wright	04/11/2022
Rev 0	Issued for client review	Nuala Page	David Wright	David Wright	09/11/2022
Rev 1	Issued to client	Nuala Page	Ceri Morgan Peter Ivicevich Xander van Beusekom Andrew Lindsay Lachlan MacArthur	David Wright	23/02/2023

Approval for issue

David Wright   *David Wright*   23 February 2023

This report was prepared by RPS within the terms of RPS' engagement with its client and in direct response to a scope of services. This report is supplied for the sole and specific purpose for use by RPS' client. The report does not account for any changes relating the subject matter of the report, or any legislative or regulatory changes that have occurred since the report was produced and that may affect the report. RPS does not accept any responsibility or liability for loss whatsoever to any third party caused by, related to or arising out of any use or reliance on the report.

Prepared by:

RPS

Nuala Page
Senior Coastal Engineer

Level 2, 27-31 Troode Street
West Perth WA 6005

T   +61 8 9211 1111
E   nuala.page@rpsgroup.com

Prepared for:

Santos Limited

Lachlan MacArthur
Approvals Adviser Barossa Project

First Floor, 53 Ord Street
West Perth WA 6005

T   +61 417 250 717
E   lachlan.macarthur@santos.com

Contents

Tables

Figures

1 INTRODUCTION

1.1 Background

Santos is exploring options for the Darwin pipeline duplication (DPD) project associated with development of the Barossa gas field in northern Australia. The proposed pipeline would run from the offshore point where the Barossa gas export pipeline (GEP) reaches the existing Bayu-Undan pipeline to the Darwin LNG (DLNG) plant at Wickham Point in Darwin Harbour. Sections making up approximately 16 km of the proposed pipeline within the harbour will require trenching using dredge vessels, with the remaining sections – including the section offshore from the harbour – laid on the seabed. Trenched material is proposed to be disposed of at an offshore disposal site adjacent to the existing INPEX spoil ground. Pipeline burial where required is proposed using quarry rock material. Suspended sediment generated during these activities has a potential to cause environmental impacts which must be identified, quantified, mitigated and managed to acceptable levels.

RPS was commissioned by Santos to undertake sediment dispersion modelling of the trenching and disposal operations associated with the Barossa DPD project in support of environmental approvals documentation and the development of the trenching and spoil disposal monitoring and management plan (TSDMMP) for the project. The sediment dispersion modelling has quantified the potential magnitude, intensity and spatial distribution of suspended sediment concentrations (SSC) and sedimentation that would be expected for the trenching and disposal operations proposed for the project. The predicted outcomes are to be used to inform the assessment of the potential for influence or impact upon water quality and benthic habitats in the region.

The sediment fate model inputs, methodologies and assumptions, and the model outcomes following analysis against specified threshold criteria are reported in RPS (2022).

1.2 Additional Modelling Scope

Following the reported outcomes of the sediment dispersion modelling study, Santos and RPS engaged in a peer review process through the Australian Institute of Marine Science (AIMS) and held discussions with the Northern Territory (NT) Department of Environment Parks and Water Security (DEPWS). During this process, queries were raised about the longer-term stability of the trench spoil at the proposed offshore spoil ground – in particular, during storm events. Santos commissioned RPS to conduct an additional spoil stability assessment, which focused on potential remobilisation of the material in the spoil ground after the trenching and disposal operations were complete, over a longer-term (one-year) period, with particular focus on non-cyclonic extreme events that occurred within the modelled period. The spoil stability assessment has quantified the potential magnitude and spatial distribution of sedimentation/deposition that would be expected in the longer term at the spoil ground and surrounding areas for the disposal operations proposed for the project.

This document is presented as an addendum to our previous report (RPS, 2022).

2 CHARACTERISATION OF METOCEAN CONDITIONS AT THE PROPOSED SPOIL GROUND LOCATION

Regional metocean conditions affecting the wider project area have been described in RPS (2022). However, in order to assess the potential for remobilisation of settled material at the spoil ground and identify periods of storm conditions, the winds, waves and currents at the proposed spoil ground area needed a specific analysis. The analysis has been based on data extracted from the validated hydrodynamic and wave model framework at a point in the centre of the proposed spoil ground, and measured wind data at Australia's Integrated Marine Observing System (IMOS) national reference station Darwin (NRSDAR).

2.1 Winds at NRSDAR Station

Measured wind data at the NRSDAR location for the period January 2019 to December 2020 (inclusive) was sourced to provide wind forcing validation for the hydrodynamic and wave model framework (RPS, 2022), and is the closest measured wind data to the offshore disposal ground (~20 km away). A wind rose for the complete two-year dataset is presented in Figure 2.1 and seasonal wind roses are presented in Figure 2.2.

The roses show that winds near the proposed spoil ground have a distinct seasonal pattern, reflecting the dominant south-east trade winds in the region during the dry season, with west to north-westerlies dominant during the wet season. Ambient wind magnitudes vary up to 14 m/s, however these are less than 8 m/s for the majority of the time (>94%). Wind magnitudes are shown to be higher on average in the wet season, which is most likely associated with the formation of mid-to-late afternoon storm cells, and the presence of tropical lows and cyclones in the region during this time of the year.
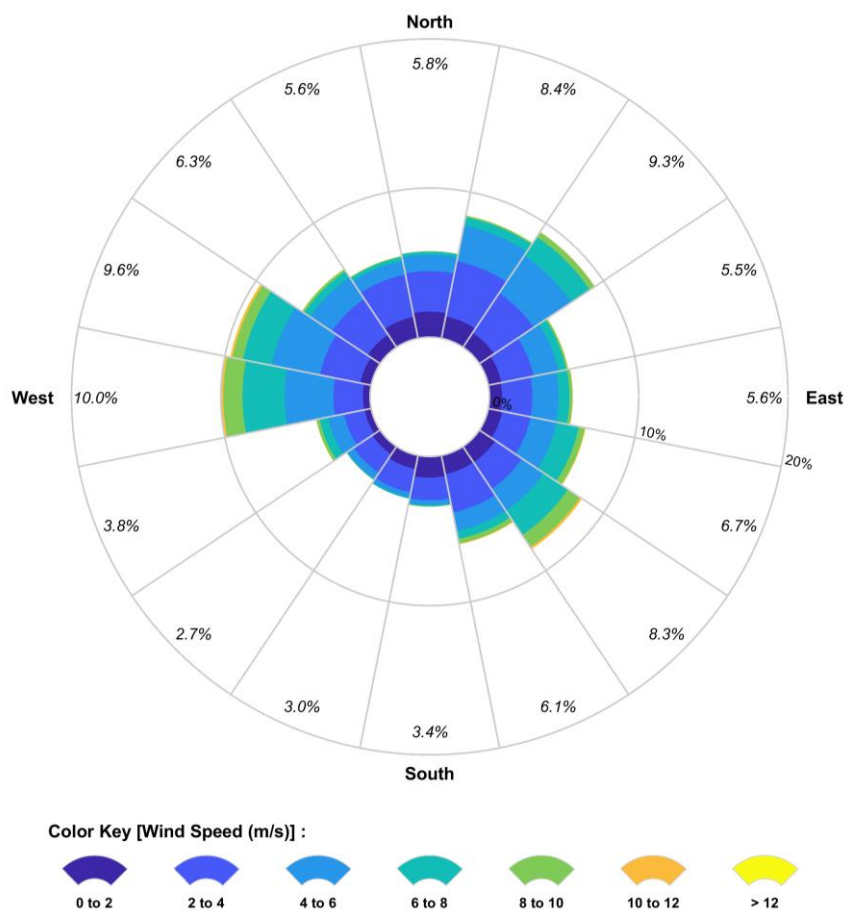
Figure 2.1 **Annualised directional wind speed distribution measured at the NRSDAR station (January 2019 to December 2020). The compass direction shows that from which the wind is blowing.**

Color Key [Wind Speed (m/s)] :

| 0 to 2 | 2 to 4 | 4 to 6 | 6 to 8 | 8 to 10 | 10 to 12 | > 12 |
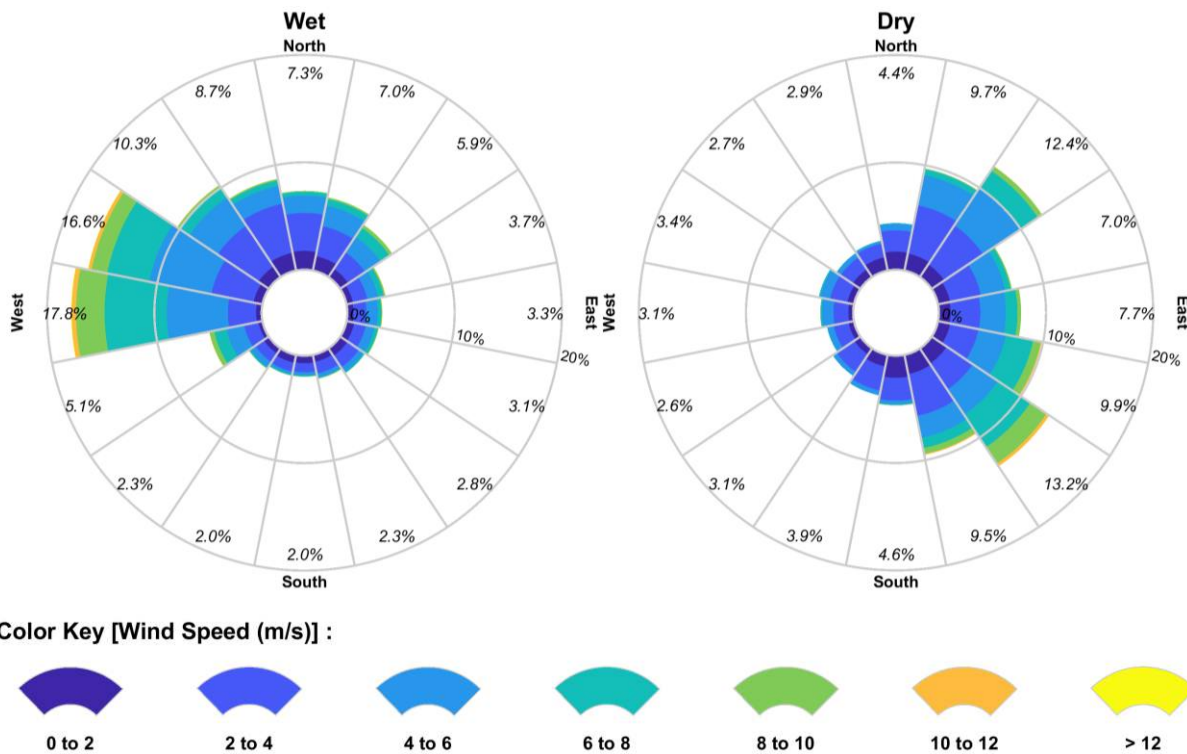
Figure 2.2 **Seasonal directional wind speed distributions measured at the NRSDAR station (January 2019 to December 2020). The compass direction shows that from which the wind is blowing.**

2.2 Waves at Proposed Spoil Ground

Wave conditions were extracted from the validated wave model framework at a point in the centre of the proposed spoil ground for the period 2019-2020 (inclusive). A wave rose of significant wave height (H_s) and mean wave direction (θ_m) for the complete two-year dataset is presented in Figure 2.3 and seasonal wave roses are presented in Figure 2.4. Joint frequency tables of significant wave height and mean wave period (T_m) for the complete dataset (Table 2.1), the wet season (Table 2.2) and the dry season (Table 2.3) are also presented.

The roses and joint frequency tables show that the wave climate at the spoil ground is strongly seasonal, mirroring the seasonality in the wind climate of the region. The seasonal difference is more accentuated in the wave climate due to the uninterrupted fetch for winds from the west-north-westerly direction which are dominant in the wet season, and the relatively short fetch for the south-easterly winds dominant during the dry season.

Therefore, waves at the spoil ground during the dry season are generally low energy sea waves with significant wave heights below 1.0 m almost all (99%) of the time, and mean wave periods between 2-4 s most (~92%) of the time. In the wet season wave heights are generally larger, being less than 1.6 m almost all (99%) of the time and ranging up to 2.2 m during the passage of storm cells and tropical lows within the modelled time period. The mean wave periods are also slightly higher in the wet season, however they remain within the range of sea waves, being between 2-5 s almost all (98%) of the time. The lack of swell wave periods at the spoil ground is expected as Beagle Gulf is sheltered from ocean swell waves by the Tiwi Islands and coastline configuration.

It should be noted that the modelled period included non-cyclonic storms and the passage of tropical lows within the region, but did not include any tropical lows or tropical cyclones whose paths led directly over Beagle Gulf and Darwin Harbour. Therefore, the maximum significant wave heights that may occur at the spoil ground may be larger than was predicted within the modelled period. Wave height measurements from the IMOS NRSDAR station near the entrance to Darwin Harbour (~20 km away) recorded significant wave heights exceeding 3.5 m during the passage of tropical lows in 2012, with peak periods of wave energy also increasing to between about 6-8 seconds (Nicholas *et al.*, 2019).

Figure 2.3 Annualised directional wave height distribution predicted at the centre of the spoil ground (January 2019 to December 2020). The compass direction shows that from which the waves are flowing.
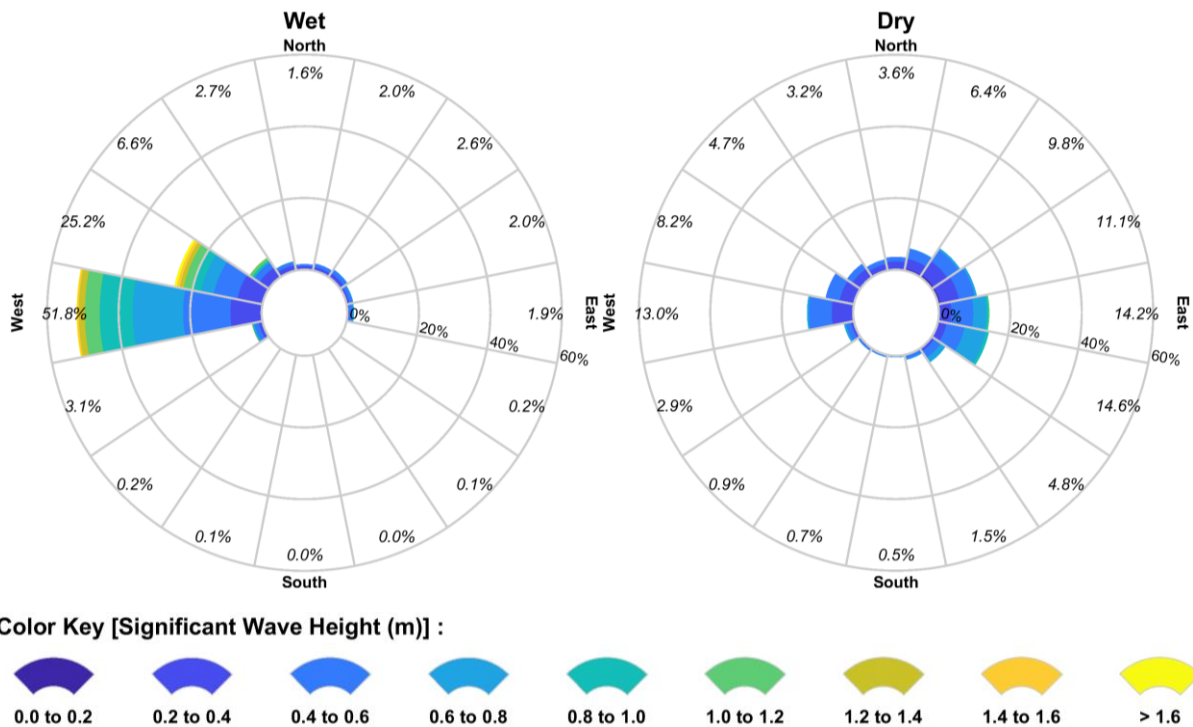
Figure 2.4 Seasonal directional wave height distributions predicted at the centre of the spoil ground (January 2019 to December 2020). The compass direction shows that from which the waves are flowing.

Table 2.1 Annualised joint frequency table of significant wave height and mean wave period predicted at the centre of the spoil ground (January 2019 to December 2020).

H_s (m)	T_m (s)							Sum	Cum.
	1.0 - 2.0	2.0 - 3.0	3.0 - 4.0	4.0 - 5.0	5.0 - 6.0	6.0 - 7.0	>7.0		
0.00 - 0.20	1.0	0.4	0.03	0.01				1.5	1.5
0.20 - 0.40	1.3	16.8	12.6	1.1	0.2	0.1		32.1	33.6
0.40 - 0.60		13.7	21.1	1.2	0.01			36.1	69.7
0.60 - 0.80		3.8	9.2	3.3	0.4			16.8	86.4
0.80 - 1.00		0.2	5.1	1.9	0.05			7.2	93.6
1.00 - 1.20			1.6	2.2	0.05			3.8	97.4
1.20 - 1.40				1.5	0.02			1.5	98.9
1.40 - 1.60				0.7				0.7	99.6
>1.60				0.3	0.2			0.4	100
Sum	2.3	35.0	49.6	12.2	0.9	0.1			
Cum.	2.3	37.2	86.8	99.0	99.9	100	100		

Table 2.2 Wet-season joint frequency table of significant wave height and mean wave period predicted at the centre of the spoil ground (January 2019 to December 2020).

H_s (m)	T_m (s)							Sum	Cum.
	1.0 - 2.0	2.0 - 3.0	3.0 - 4.0	4.0 - 5.0	5.0 - 6.0	6.0 - 7.0	>7.0		
0.00 - 0.20	0.4	0.05						0.5	0.5
0.20 - 0.40	0.5	14.3	10.7	0.6				26.2	26.6
0.40 - 0.60		11.2	16.9	1.0				29.0	55.7
0.60 - 0.80		1.2	10.5	6.7	0.8			19.1	74.7
0.80 - 1.00			8.8	3.8	0.09			12.7	87.4
1.00 - 1.20			2.9	4.4	0.09			7.4	94.8
1.20 - 1.40				3.0	0.05			3.0	97.8
1.40 - 1.60				1.3				1.3	99.1
>1.60				0.6	0.3			0.9	100
Sum	0.9	26.8	49.8	21.2	1.3				
Cum.	0.9	27.7	77.5	98.7	100	100	100		

Table 2.3 Dry-season joint frequency table of significant wave height and mean wave period predicted at the centre of the spoil ground (January 2019 to December 2020).

H_s (m)	T_m (s)							Sum	Cum.
	1.0 - 2.0	2.0 - 3.0	3.0 - 4.0	4.0 - 5.0	5.0 - 6.0	6.0 - 7.0	>7.0		
0.00 - 0.20	1.6	0.8	0.07	0.02				2.5	2.5
0.20 - 0.40	2.0	19.3	14.5	1.6	0.43	0.25		38.1	40.5
0.40 - 0.60		16.3	25.3	1.53	0.02			43.1	83.7
0.60 - 0.80		6.4	8.0	0.02				14.4	98.1
0.80 - 1.00		0.4	1.3					1.7	99.7
1.00 - 1.20			0.3					0.3	100
1.20 - 1.40									100
1.40 - 1.60									100
>1.60									100
Sum	3.6	43.1	49.4	3.2	0.5	0.3			
Cum.	3.6	46.7	96.1	99.3	99.8	100	100		

2.3   Currents at Proposed Spoil Ground

Current conditions were extracted from the validated hydrodynamic model framework at a point in the centre of the proposed spoil ground for the period 2019-2020 (inclusive). The bottom-layer currents are presented as this layer is important for bottom shear stress and sediment resuspension. A current rose for the complete two-year dataset is presented in Figure 2.5 and seasonal current roses are presented in Figure 2.6.

The roses reveal the tide is the dominant influence on currents at the spoil ground, which are oriented along the tidal axis approximately east-west and show minimal seasonal differences. The predicted current speeds in the bottom layer (which are slightly lower than those in the surface layer) are relatively strong, ranging up to 0.95 m/s, and are strongly correlated with the rise and fall of the tide.
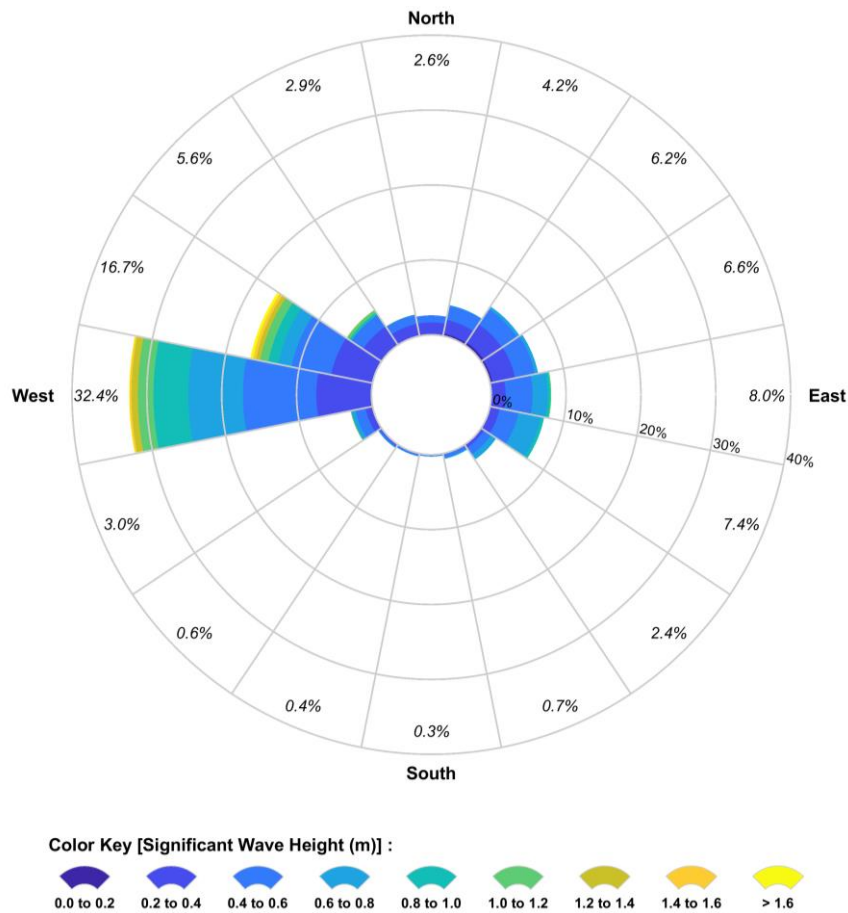

Figure 2.5   Annualised directional current speed distribution predicted at the centre of the spoil ground (January 2019 to December 2020). The compass direction shows that towards which the currents are flowing.

Figure 2.6 Seasonal directional current speed distributions predicted at the centre of the spoil ground (January 2019 to December 2020). The compass direction shows that towards which the currents are flowing.

2.4 Identification of Storm Conditions within the Modelled Period

The wind speed and significant wave height were assessed to identify periods of storm events over the one-year run-on period for the spoil stability assessment. Figure 2.7 and Figure 2.8 present time series of the wind speed measured at the NRSDAR station and the significant wave height predicted at the proposed spoil ground location, for two six-month periods spanning 9 November 2019 to 9 November 2020. From the plots it is evident that the wind speeds and significant wave heights mirror each other, which is to be expected given the dominance of sea waves and minimal swell in the region. Periods with sustained elevation in both the wind and wave magnitudes have been identified and are marked by red boxes on Figure 2.7. Note that no periods of sustained elevated wave magnitudes (H_s >1 m) were identified during the dry season. While the wind magnitudes showed periods of elevation, the limited fetch distance from the dominant south-easterly wind direction means wave magnitudes remained low.

Four storm periods were identified within the modelled scenario:

1. 25 to 29 December 2019.

2. 7 to 13 January 2020. This correlates with dates reported by the Bureau of Meteorology (BoM) for the evolution of Tropical Cyclone Claudia (5 to 16 January 2020).

3. 19 to 25 January 2020.

4. 21 February to 6 March 2020. This correlates with dates reported by the BoM for the evolution of Tropical Cyclone Esther (21 February to 4 March 2020).

Of the four identified storm periods, two were associated with the passage of tropical lows or ex-tropical cyclones within the region, and the other two are likely due to local thunderstorm activity.

Figure 2.7 **Time series of winds measured at the NRSDAR station and significant wave heights predicted at the centre of the spoil ground (9 November 2019 to 9 May 2020). The red boxes indicate periods of storm conditions.**

Figure 2.8   Time series of winds measured at the NRSDAR station and significant wave heights predicted at the centre of the spoil ground (9 May 2020 to 9 November 2020).

3 APPROACH TO SPOIL STABILITY MODELLING

Following (and during) the trenching and disposal program, energy from wave and current action can exceed that required for mobilisation and resuspension of the previously settled material. To investigate the longer-term stability of the proposed spoil ground, simulation of sediment transport of the material within the spoil ground was conducted in SSFATE for a one-year run-on period, following completion of trenching and disposal operations. The assessment used spatially-varying current and wave data, spanning the period of October 2019 to November 2020, taken from the hydrodynamic and wave model framework developed for the project. Only the wet season scenario has been modelled in the spoil stability assessment, as the subsequent run-on period covered an entire year and all seasonal conditions were represented. Additionally, most of the identified storms fell in the wet season and followed on from the end of trenching and disposal operations in this scenario.

The methodology applied for the sediment dispersion modelling of the trenching and disposal operations has been applied to the spoil stability assessment, with some modifications as outlined in this section. For details of the modelling methodology – including the model used, details of the hydrodynamic and wave model framework, model domain and bathymetry, overview of the trenching and disposal operations program, and how the sources of suspended sediment were represented in the model – please refer to our sediment dispersion modelling report (RPS, 2022).

The proposed spoil ground was pre-filled with the material from the TSHD and BHD disposal loads in the same pattern as modelled for the trenching and disposal activities (RPS, 2022). The disposal operations were assumed to have the broad aim of evenly distributing the total volume of allocated material across the entire spoil ground area by the conclusion of all activities. The main difference applied in the spoil stability assessment rests in the volume of disposed material that was assumed to be available for resuspension.

In the modelling of trenching and disposal activities it was assumed that 5% of the deposited mass – representing the volume of the upper surface layer of the spoil mound – would be available for resuspension. This was done to account for the natural sediment capping in the surface layer of the mound that will occur as the smaller-sized particles (silts and clays) are resuspended, leaving the larger particles to act as armouring against bottom shear stress. While the model maintains mass balances of each sediment size class within each grid cell to derive an estimate of the median particle size, and uses this to calculate the potential for ongoing resuspension of fines, it does not precisely represent the process of sediment capping. As such, the assumption that only a proportion of the mound is available for resuspension is necessary so that overestimates of resuspension and in turn SSC do not occur in the modelling.

However, to conduct the spoil stability assessment it was necessary to model the total volume of material that will be placed on the seabed within the spoil ground. It was assumed that 95% of the total disposed volume, rather than 5%, would be placed on the seabed and assumed to be available for resuspension. This assumes that 5% of the material would have been lost to the water column during the disposal operations. It should be noted that this approach may result in overestimation of resuspension and as such the outcomes should be viewed as a guide to the potential for resuspension of the mound, and the stability of the mound, during storm conditions.

The volumes of material placed on the seabed in the spoil ground during disposal operations are outlined in Table 3.1. The surface area of the proposed spoil ground is approximately 6,290,000 m^2; given the volume of material to be placed there, a theoretical thickness of 4-17 cm (depending on depositional density) is expected if the spoil is evenly distributed.

Table 3.1   Summary of sediment sources applied in the model.

Operation	Source Rate (% Disposed Volume)	Trenched Volume (m^3)	Trenching Volume Loss (m^3)	Disposal Volume Loss (m^3)	Spoil Volume (m^3)
Disposal SHB	95 (seabed; potential)	22,220	511	1,085	20,623
Disposal TSHD	95 (seabed; potential)	281,725 *	6,004	13,786	261,935
Totals		303,945 *	6,515	14,871	282,558

* Note these volumes include the proportion of material that has been crushed by CSD and subsequently picked up by TSHD.

The standard particle classes used in SSFATE are set according to the typical size ranges of material that are found within suspended sediment plumes, whereas the grain size of the sediment that remains in disposal areas is typically greater than that which dispersed during the initial trenching and disposal activities. For the assessment of the long-term stability of the spoil material a modified set of grain classes, weighted more towards coarser material, was applied. Table 3.2 shows the modified material classes used in SSFATE for the spoil stability assessment.

Table 3.2   Material size classes used in SSFATE.

Material Class Description	Particle Size Range (µm)
Fines – Clay and Silt	<75
Fine to Medium Sand	75-300
Medium Sand	300-600
Coarse Sand to Pebble	600-10,000
Pebble/Rubble	>10,000

The PSDs that were applied in the sediment dispersion modelling of trenching and disposal activities were based on available geotechnical information for each pipeline section (RPS, 2022). These PSDs have been redistributed to match the modified material size classes used in SSFATE for the spoil stability assessment, as shown in Table 3.3. It is assumed that the material lost during trenching and disposal operations is made up of the finer sediment proportions that are more likely to be suspended into the water column. As such, the PSDs used to represent the material remaining in the spoil ground have been adjusted to remove 5% of the fines and redistribute this proportionally across the four other size classes, as shown in Table 3.4. The modified PSDs applied to the material placed in the spoil ground by TSHD from the post-sweep of CSD-crushed material are outlined in Table 3.5.

Table 3.3 *In situ* PSDs broken down into the modified SSFATE material classes for each pipeline section to be trenched, derived from available geotechnical information.

Sediment Grain Size Class	Size Range (µm)	Trench Zones 1-2 (%)	Pre-Sweep Area 1 (%)	Trench Zone 3 (%)	Trench Zone 4 (%)	Pre-Sweep Area 2 (%)	Trench Zone 5 (%)	Pre-Sweep Area 3 (%)	Trench Zone 6 (%)	Trench Zone 7 (%)	Sand Waves Area (%)
Fines – Clay and Silt	<75	20.7	21.7	20.0	28.3	16.0	11.1	25.0	26.2	23.8	5.9
Fine to Medium Sand	75-300	22.7	11.6	8.7	11.4	10.9	6.6	11.4	11.2	10.0	11.4
Medium Sand	300-600	6.7	4.0	3.4	5.5	6.9	3.3	4.0	4.5	7.6	16.3
Coarse Sand to Pebble	600-10,000	47.1	33.3	31.2	37.9	54.7	59.0	52.8	52.0	49.5	66.1
Pebble/Rubble	>10,000	2.9	29.3	36.8	16.9	11.5	19.9	6.9	6.2	9.1	0.3

Table 3.4 PSDs broken down into the modified SSFATE material classes for each pipeline section to be trenched, adjusted to remove fines lost during trenching and disposal operations.

Sediment Grain Size Class	Size Range (µm)	Trench Zones 1-2 (%)	Pre-Sweep Area 1 (%)	Trench Zone 3 (%)	Trench Zone 4 (%)	Pre-Sweep Area 2 (%)	Trench Zone 5 (%)	Pre-Sweep Area 3 (%)	Trench Zone 6 (%)	Trench Zone 7 (%)	Sand Waves Area (%)
Fines – Clay and Silt	<75	15.7	16.7	15.0	23.3	11.0	6.1	20.0	21.2	18.8	0.9
Fine to Medium Sand	75-300	24.1	12.4	9.2	12.2	11.5	7.0	12.2	12.0	10.6	12.0
Medium Sand	300-600	7.1	4.2	3.6	5.9	7.4	3.5	4.2	4.8	8.1	17.2
Coarse Sand to Pebble	600-10,000	50.0	35.5	33.1	40.5	57.9	62.4	56.4	55.5	52.8	69.6
Pebble/Rubble	>10,000	3.1	31.2	39.1	18.1	12.2	21.0	7.3	6.6	9.7	0.3

Table 3.5 **Modified PSDs of sediments dumped at the spoil ground by TSHD from the post-sweep of CSD-crushed material.**

Sediment Grain Size Class	Size Range (µm)	PSD (%) for Sediment Disposal – Trench Zone 3	PSD (%) for Sediment Disposal – Trench Zone 4	PSD (%) for Sediment Disposal – Trench Zone 5	PSD (%) for Sediment Disposal – Trench Zone 6	PSD (%) for Sediment Disposal – Trench Zone 7
Fines – Clay and Silt	<75	10.6	10.6	5.5	10.0	10.7
Fine to Medium Sand	75-300	10.8	10.8	11.1	11.4	10.7
Medium Sand	300-600	26.2	26.2	27.8	26.2	26.2
Coarse Sand to Pebble	600-10,000	26.2	26.2	27.8	26.2	26.2
Pebble/Rubble	>10,000	26.2	26.2	27.8	26.2	26.2

4   RESULTS OF SPOIL STABILITY MODELLING

Simulation of spoil stability at the proposed spoil ground over the one-year run-on period showed that settlement of the finer spoil material is minimal and there is potential for significant resuspension of the finer proportions. The localised movement and dispersion of the disposal-generated and resuspended sediment is governed by the tide, with very strong tidal flows at the spoil ground.

Coarse material (coarse sand size and above) is predicted to settle rapidly, while available fine material in the spoil is predicted to be continuously resuspended on each tide, particularly during spring tide periods where even fine to medium sand size material is predicted to be resuspended. Deposition is forecast to occur at slack tide, however much of this settled material is resuspended on the following tide. This results in suspended sediment plumes having long drift trajectories, with sediments dispersed widely but at low concentrations, and with sediments deposited in thin layers. Drift trajectories from the spoil ground are predicted to be longest to the north-east towards the Clarence Strait and Van Diemen Gulf.

There is significant variability in the predicted vertical distributions of SSC in the water column at the proposed spoil ground, with a distinct increase in concentration towards the seabed. The higher SSC concentrations near the seabed are due to the resuspended material typically being mixed to the lower reaches (1-3 m) of the water column.

4.1   Spatial Distribution of Mobilised Spoil Sediments

In order to map the area of influence of the mobilised sediment and show how it evolves over the one-year run-on period, sequences of snapshots of sedimentation thickness throughout the simulation period were plotted. Figure 4.1 and Figure 4.2 show example two-hourly snapshot sequences of predicted bottom thickness over successive tidal cycles on 16 and 17 November 2019, to illustrate how the sedimentation changes over the short term (12 hours). The snapshots clearly show the deposition of sediment at slack tide and the resuspension of the deposited sediment on the following tide. These sequences were selected early in the run-on period to show the dispersion of the finer sediment as it is resuspended and moved on each tidal cycle progressively further away from the spoil ground.

Figure 4.3 shows progressive snapshots of bottom thickness at the start of the run-on period, half a week, one week, two weeks and three weeks into the run-on period, and at the end of the run-on period to present the evolution of the area of influence over time. In the longer term, significant sedimentation is shown to generally be limited to the vicinity of the spoil ground (within 9-10 km), while sediment that has dispersed and settled further away has typically been subsequently resuspended and dispersed to very low thicknesses (<1 mm). Some isolated patches of longer-term sedimentation are predicted in the shallows around the Vernon Islands and Glyde Point. These patches may be attributable to the combined effects of model bathymetry and hydrodynamics, representing sediments that are transported into the shallowest possible grid cells and then trapped upon reversal of the tide. While it is clear that there is potential for sediments released at the spoil ground to be found in the indicated areas, the persistence of material remaining at the water-land boundary in these locations may be overstated.

The maximum bottom thickness within the spoil ground over the simulation period was predicted to be approximately 400 mm during the disposal operations period, with the maximum longer-term bottom thickness being approximately 240 mm. The average bottom thickness over the spoil ground in the long term is approximately 50 mm.

Figure 4.1 Example two-hourly snapshots of modelled bottom thickness during a nominal spring tide cycle (based on 16 November 2019 1pm to 11pm, top-left panel to bottom-right panel). Periods of slack tide occur at approximately 2pm and 7pm. Note the trenching area widths shown on this and other Figures in this report are exaggerated to aid visual clarity.
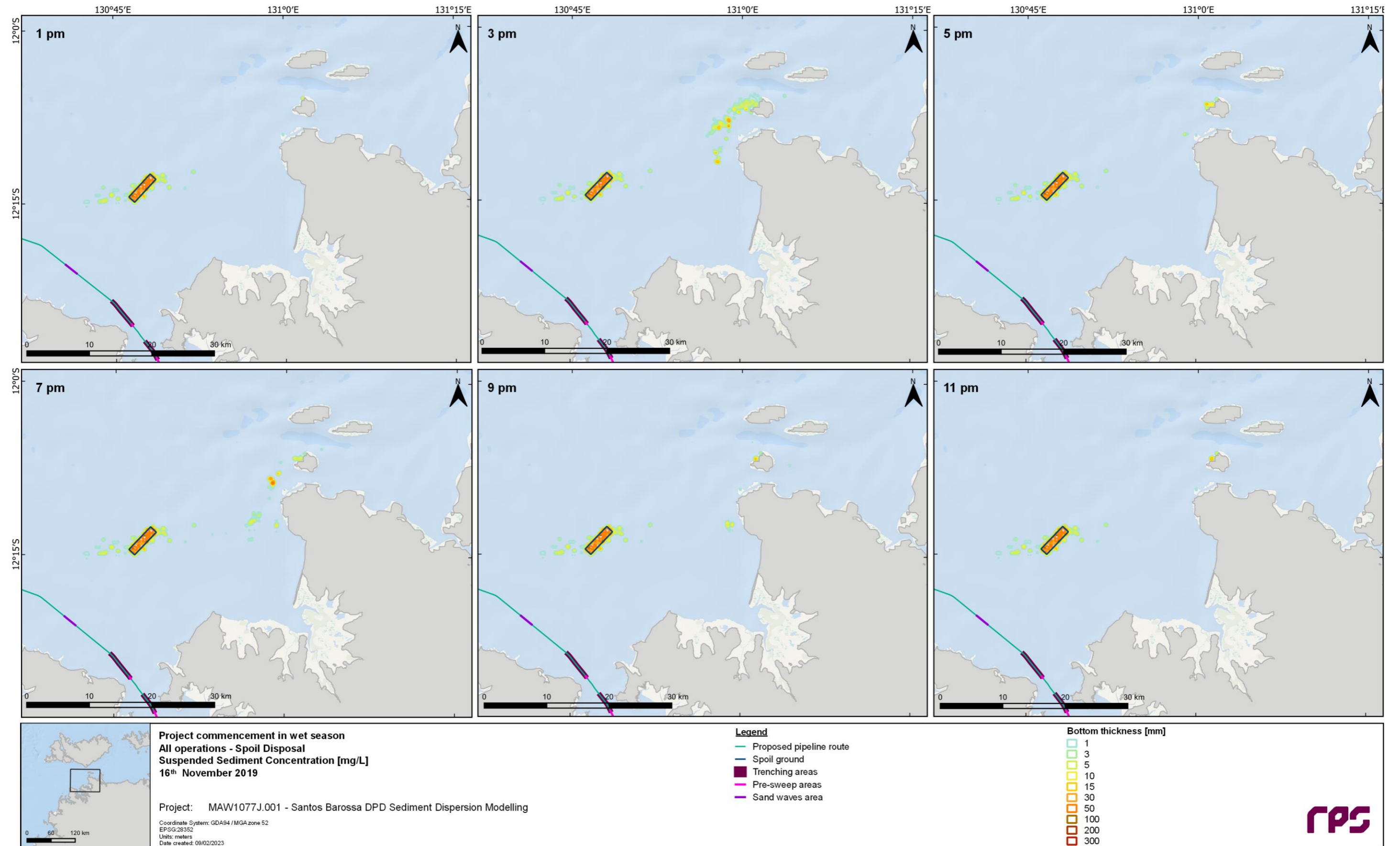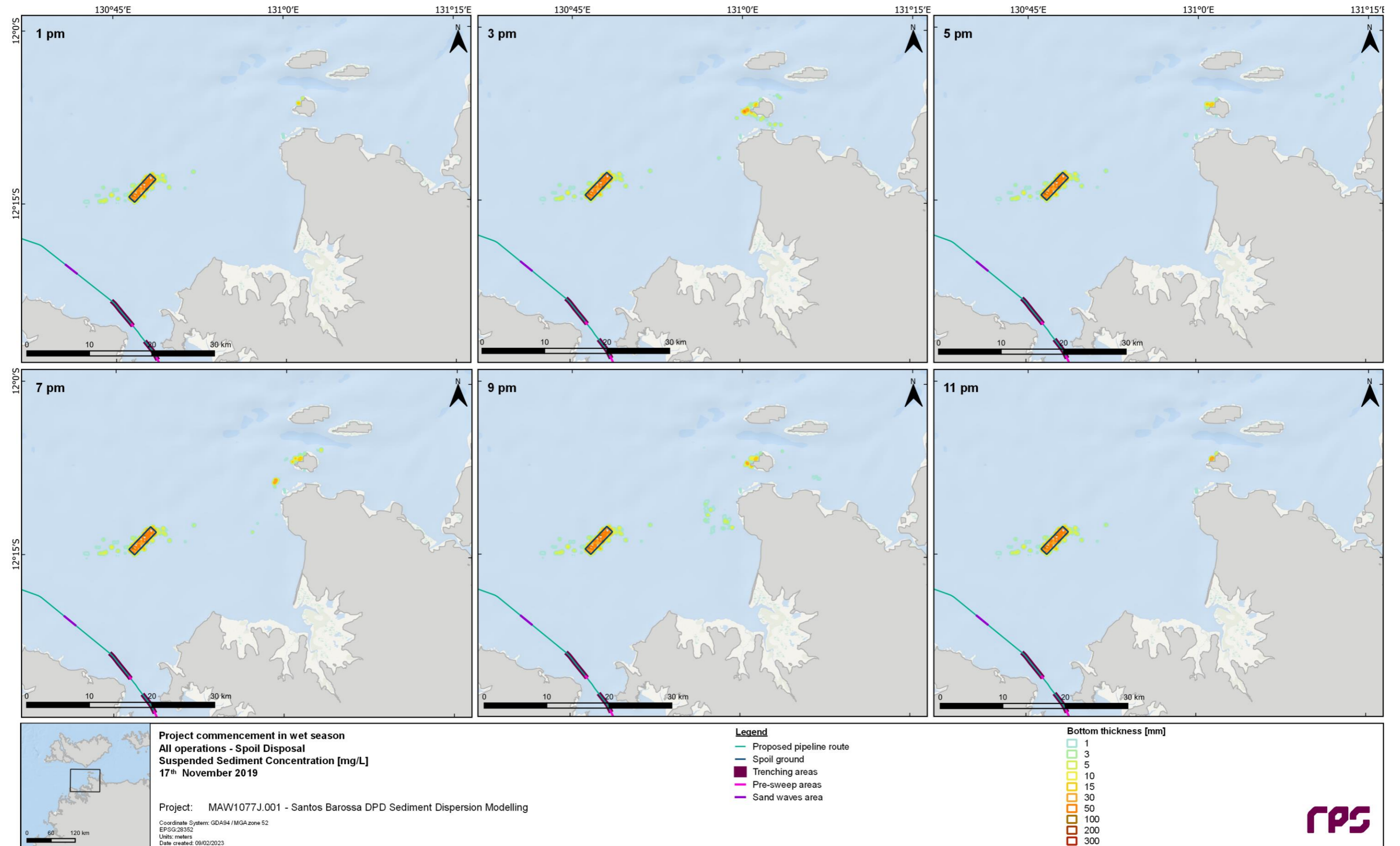
Figure 4.2 Example two-hourly snapshots of modelled bottom thickness during a nominal spring tide cycle (based on 17 November 2019 1pm to 11pm, top-left panel to bottom-right panel). Periods of slack tide occur at approximately 2pm and 7pm. Note the trenching area widths shown on this and other Figures in this report are exaggerated to aid visual clarity.

Figure 4.3 Progressive snapshots of modelled bottom thickness at the start of the run-on period, half a week, one week, two weeks and three weeks into the run-on period, and at the end of the run-on period (top-left panel to bottom-right panel). Note the trenching area widths shown on this and other Figures in this report are exaggerated to aid visual clarity.

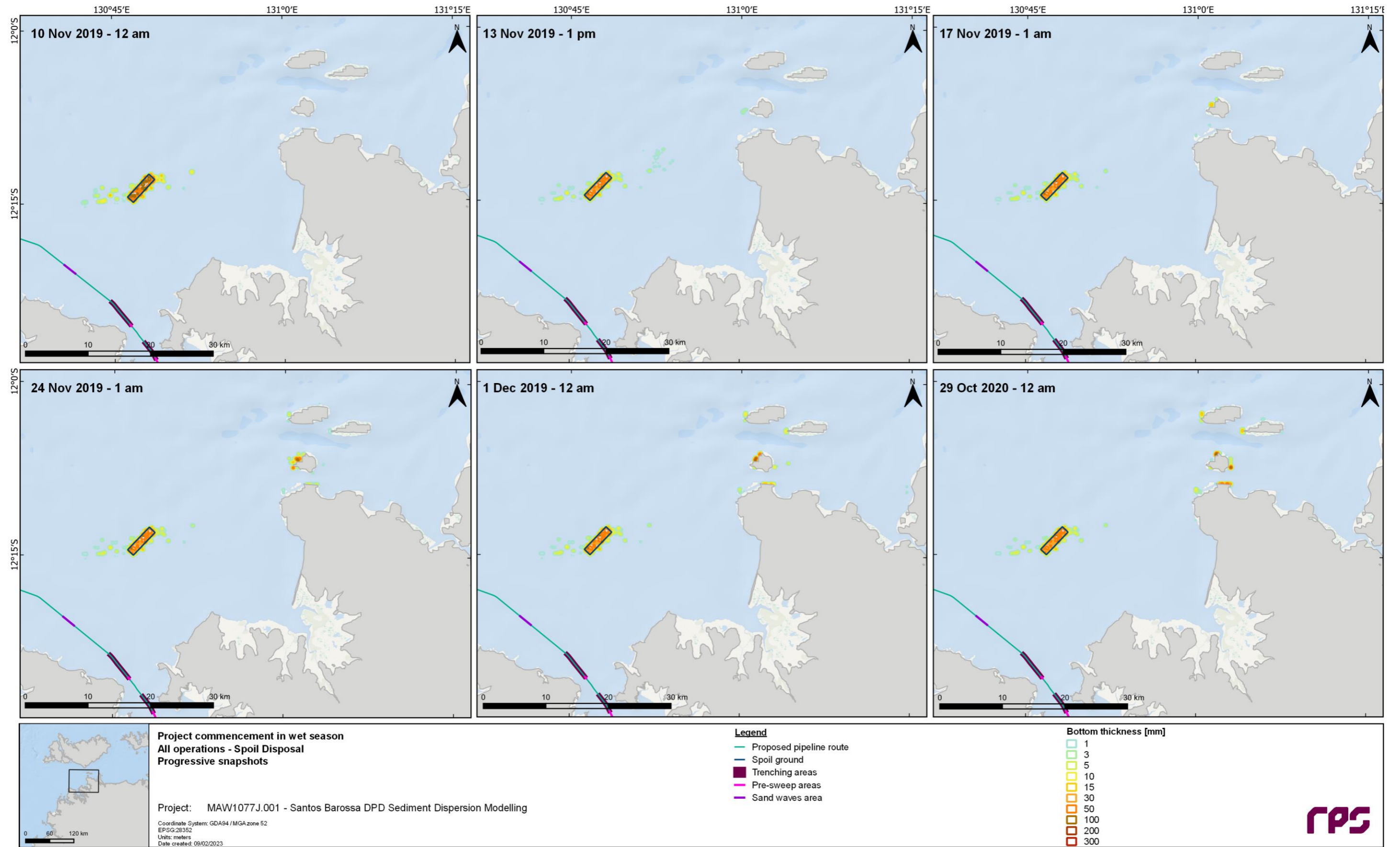## 4.2   Temporal Variability in Spoil Stability at the Spoil Ground

To explore the temporal variability of spoil stability at the proposed spoil ground, time series analysis of the predicted SSC and sedimentation at a set of locations previously defined at the proposed offshore disposal area (RPS, 2022) has been conducted. Table 4.1 presents the locations of the time series points used. Time series plots showing predicted depth-averaged and maximum-in-water-column disposal-excess SSC for each of the selected locations are presented in Figure 4.4 and Figure 4.5. The sedimentation time series plots for these points have not been included as they show very little change over the majority of the simulated period at the scales required to plot the thickness. In place of plots, Table 4.2 shows the median, maximum and last-time-step sedimentation values for each point.

Table 4.1   Time series analysis point locations.

Point Name	Point Abbreviation	Longitude (°)	Latitude (°)
Offshore Disposal Area Point 1	OD1	130.7553	-12.26529
Offshore Disposal Area Point 2	OD2	130.7814	-12.23756
Offshore Disposal Area Point 3	OD3	130.7904	-12.22830
Offshore Disposal Area Point 4	OD4	130.8001	-12.21846
Offshore Disposal Area Point 5	OD5	130.8253	-12.19286
Offshore Disposal Area Point 6	OD6	130.7773	-12.21576
Offshore Disposal Area Point 7	OD7	130.7869	-12.22465
Offshore Disposal Area Point 8	OD8	130.7952	-12.23249
Offshore Disposal Area Point 9	OD9	130.8036	-12.23999

The time series analysis indicated that there will be significant temporal variability in the distribution of SSC at the proposed spoil ground during disposal operations and in the initial 1-2 weeks following the end of disposal operations. This is due to resuspension of the available finer material within the spoil. Following this, the SSC in the vicinity of the spoil ground reduces significantly with only patchy short-lived spikes evident throughout the remaining run-on period. Additionally, the sedimentation values after the first 1-2 weeks of the run-on period at all points assessed show very little change, indicating that significant resuspension of the material in the mound at the disposal site has mostly ceased to occur.

Sediment thicknesses at the points within the spoil ground are predicted to range from 24 mm up to a maximum of 140 mm during the disposal operations period, with the long-term thickness ranging up to 96 mm.

The time series analysis shows no significant change in SSC or sedimentation at the proposed spoil ground during the four identified storm periods (refer Section 2.4). This indicates that once the finer proportions of the spoil material have dispersed away from the spoil ground in the initial 1-2 weeks after disposal operations cease, the mound is predicted to be relatively stable.

Table 4.2 **Median, maximum and last-time-step bottom thickness values at each time series analysis point throughout the disposal program and one-year run-on period.**

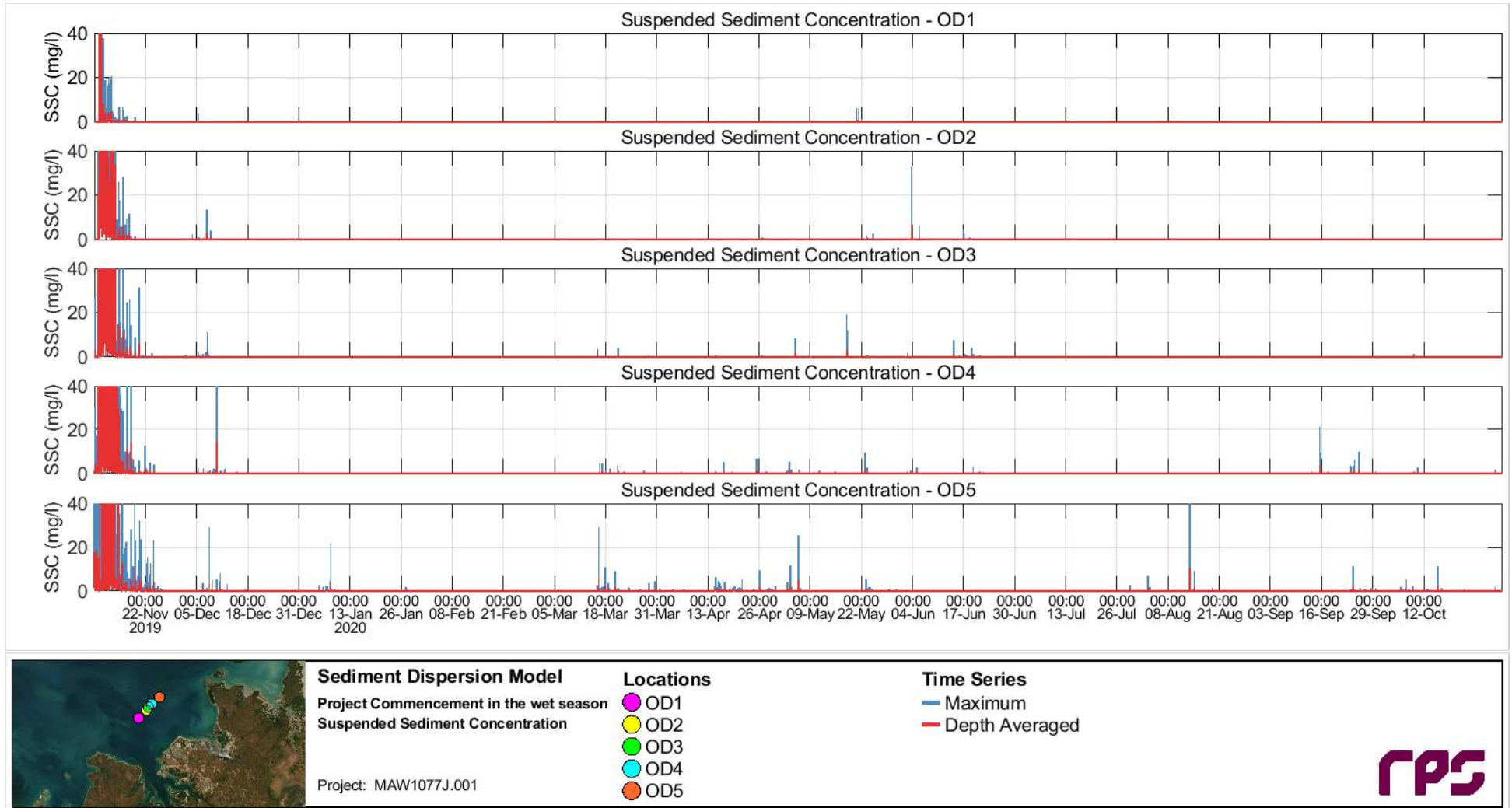| Point	Median Sedimentation (mm)	Maximum Sedimentation (mm)	Sedimentation at Last Time Step (mm)
OD1	0	0.01	0
OD2	47	101	47
OD3	41	68	41
OD4	96	139	96
OD5	0	0.2	0
OD6	0	3	0
OD7	52	66	52
OD8	24	42	24
OD9	0	9	0

Figure 4.4   Time series of predicted disposal-excess SSC at the *OD1* to *OD5* sites throughout the one-year run-on period.
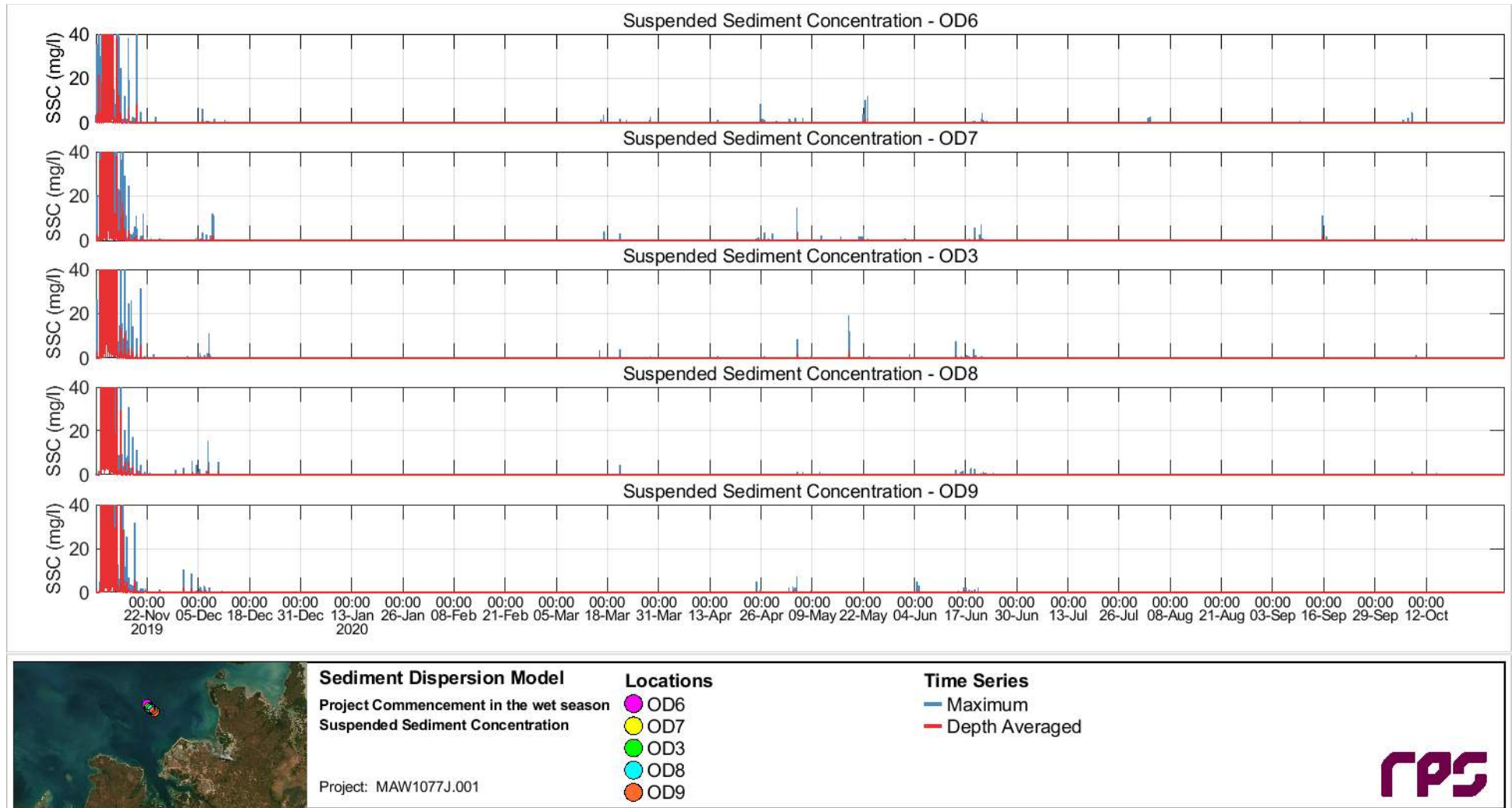
Figure 4.5 Time series of predicted disposal-excess SSC at the *OD6* to *OD9* (via *OD3*) sites throughout the one-year run-on period.

4.3 Cumulative Mass in Spoil Ground

The model results were assessed at the end of each simulated week to calculate the predicted mass inside the proposed spoil ground, and the percentages of the disposed mass remaining were used to assess the stability over time. Table 4.3 presents the cumulative mass remaining in the proposed spoil ground throughout the disposal operation and one-year run-on period. From the cumulative masses remaining, it is evident that a significant proportion of the spoil material has the potential to be dispersed away from the spoil ground during disposal operations and within the initial 1-2 weeks following the end of disposal operations. After the available finer proportion of the spoil material has been dispersed away from the spoil ground, the mass remaining becomes stable and is predicted to change very little, even during the non-cyclonic storm conditions which occur during the simulation period (refer Section 2.4).

It should be noted that the proportion of the spoil material that is available for resuspension, and hence dispersed away from the spoil ground, is overestimated in the model as the natural sediment capping that will occur in the mound is not precisely accounted for. Therefore, in reality the volumes of spoil material lost from the spoil ground are expected to be less than quoted in this addendum. However, this does not change the finding that once the mound surface layer has lost the finer material that is available to resuspend – within the first 1-2 weeks after cessation of disposal operations – it will be relatively stable during ambient and non-cyclonic storm conditions.

Table 4.3 Cumulative mass remaining in spoil ground over the disposal and one-year run-on period.

Weeks from Start of Disposal Operations	Cumulative Mass Remaining (% of Disposal Mass)
1	11.3
2	23.1
3	40.2
4	54.4
5	66.0
6 (disposal operations have finished)	50.1
7	50.1
8	50.1
12	50.1
16	50.1
56	50.1

4.4 Potential for Remobilisation of Deposited Spoil Material

Given the predicted rapid dispersion of the finer proportion of the material from the spoil ground and the predicted volume of spoil lost, a cross-check of the model findings against the calculated potential for resuspension due to the metocean conditions experienced at the spoil ground was conducted.

The effect that the wave and current forcings have on sediment dynamics/resuspension is through the friction that they exert on the seabed, which is expressed as the bed shear stress (frictional force exerted by the flow per unit area). A time series of bed shear stress due to predicted waves and currents, as extracted at the spoil ground, was calculated. To determine an estimate of the potential for remobilisation of spoil material under ambient and non-cyclonic storm conditions at the site, the time series data was compared to the critical bed shear stress required to mobilise the range of grain sizes modelled for the spoil material (Soulsby, 1997; van Rijn, 2005).

The calculations showed that the ambient currents at the spoil ground were strong enough to potentially resuspend material of up to 1.5 mm grain size, and to potentially resuspend the proportions of the sediments in the finer three modelled size classes for 60%, 38% and 27% of the time, respectively. The wave orbital velocities were calculated to rarely be large enough to resuspend sediments within the spoil ground, with the critical shear stress exceeded less than 1% of the time even for the finest material class modelled. This is due

to the depth of the spoil ground, the relatively small magnitude of the wave heights, and the relatively short wave periods resulting in low orbital velocities at the seabed – predicted to be always less than 0.18 m/s even during the modelled storm events. Note that during tropical cyclone events – which have not been modelled in this study – wave heights and wave periods may be larger, resulting in larger orbital velocities that have greater potential to resuspend material.

The calculations showed that tidal currents are the main force driving resuspension at the spoil ground and confirmed that the current magnitudes are strong enough for a significant proportion of the time to resuspend the finer proportions of the material from the spoil ground. This confirms the model findings that dispersion/loss of the available finer components of the spoil material will be rapid, that there is potential to resuspend a large proportion of the spoil material if it is available, and that once the finer proportions of the spoil material are dispersed away from the spoil ground the mound will be relatively stable during non-cyclonic storm events.

5   REFERENCES

Nicholas, WA, Smit, N, Siwabessy, PJW, Nanson, R, Radke, L, Li, J, Brinkman, R, Atkinson, R, Dando, N, Falster, G, Harries, S, Howard, FJF, Huang, Z, Picard, K, Tran, M & Williams, D 2019, *Characterising marine abiotic patterns in the Darwin-Bynoe Harbour region: Summary report, physical environments, Darwin Harbour mapping project*, Department of Environment and Natural Resources, Darwin, NT, Australia (http://pid.geoscience.gov.au/dataset/ga/127386).

RPS 2022, *Santos Barossa DPD studies: Sediment dispersion modelling* [MAW1077J.001 Rev. 2], prepared by RPS, Perth, WA, Australia for Santos Ltd, Perth, WA, Australia.

Soulsby, R 1997, *Dynamics of marine sands: A manual for practical applications*, Thomas Telford Publications, London, UK, 249 pp.

van Rijn, LC 2005, *Principles of sedimentation and erosion engineering in rivers, estuaries and coastal seas*, Aqua Publications, Blokzijl, The Netherlands, 623 pp.